Cell death processes in immune cells of the shore crab, *Carcinus maenas*.

Calum Turnbull Robb

A thesis submitted for the degree of

Doctor of Philosophy

School of Life Sciences

Heriot-Watt University

Edinburgh, Scotland, UK

January 2015

Abstract

This thesis aimed to investigate programmed cell death processes and their role in invertebrate host defence, using the shore crab, *Carcinus maenas* as the main experimental model. Effort was focussed on two: namely apoptosis and ETosis; the latter being the controlled release of chromatin from the nucleus. Comparison of methods showed that for apoptosis, flow cytometry with bovine lactadherin-FITC and propidium iodide staining was the most effective for quantification *in vitro* for both mixed and separated haemocytes. By this method, different patterns of cell death were observed in different haemocyte populations and under different life conditions. Additionally, ETosis was demonstrated in two haemocyte types, specifically the hyaline cells and semi-granular cells. The process was found not only to entrap bacteria but also to aid defence by providing the scaffold upon which intact haemocytes assemble during encapsulation; a major cellular process that sequesters non-self particles from the circulation. Importantly, defence cells from the mussel, *Mytilus edulis*, and the sea anemone, *Actinia equina*, were also found to exhibit ETotic-like behaviour. As sea anemones lack a dedicated coelomic system, ETosis must predate the evolution of the coelom, showing that it has an evolutionary ancient origin.

To my family.

Acknowledgements

Firstly I would like to thank my primary supervisor, Dr Elisabeth A Dyrynda (Heriot Watt University), for her help and unconditional support throughout this entire PhD, which has been integral to its completion. I also thank Dr Dyrynda for inspiring me to follow this research path and making this period of research as smooth as possible.

Secondly I would like to thank my secondary supervisors, Dr Valerie J Smith (University of St Andrews) and Professor Adriano G Rossi (University of Edinburgh) for their expertise and guidance throughout this PhD. This has been greatly appreciated and essential to the successful completion of this research. My gratitude also goes to Dr Smith and Professor Rossi for their kindness in allowing me to carry out research in their laboratories, namely the Gatty Marine Laboratory and the Queen's Medical Research Institute respectively. Without such kindness, many sections of this thesis would not have materialised.

Thirdly I would like to thank my research colleagues at Heriot-Watt University, namely Dr Lionel Jouvet, Dr John Tinsley and Dr Ashtavinayak Paradh for their help in the laboratory over the years. I would also like to thank my research colleague and late friend Dr Maia Strachan for her help in the aquarium facility over the years of my study. Dr Strachan, thank you for all the great memories, personally and professionally. A wonderful friend and you are sorely missed.

I also acknowledge the help and support I have received from many members of the academic and technical staff at Heriot-Watt University. Special thanks go to Mrs Margaret Stobie for regular help in maintenance of the aquarium facility, Mr Paul Cyphus for assistance with flow cytometry, Dr Stephen Euston for assistance with confocal microscopy, Dr Dawn Austin for assistance in bacteria preparation and Miss Marian Millar and Mr James Buchanan for their assistance in scanning electron microscopy. I also thank James Buchanan for assisting in the regular supply of crabs.

Extended thanks go to Fiona Rossi (for all the lovely food and flow cytometry expertise), Martina Rossi (for assistance with the collection of sea anemones) as well as Dr Andrew Leitch, Dr Rodger Duffin, Dr Robert Gray, Dr Chris Lucas, Dr David Dorward, Mr Duncan Humphries, Miss Jennifer Felton, Miss Melanie MacMillan and Mr Stephen Mitchell, for their assistance in experiments carried out at the University of Edinburgh. I would also like to thank Miss Karen Nicol (Heriot Watt University) and Miss Charlotte Gibout (University Institute of Technology La Rochelle) for assistance with confocal microscopy during mussel and sea anemone investigations respectively. I am also grateful for the Fees-Only Scholarship and Sports Scholarship I received for every year of my study at Heriot-Watt University, awarded to me by the School of Life Sciences Department and Centre for Sport and Exercise Department respectively. Specifically, I would like to thank Mr Mike Fitchett and Mr Ross Campbell for the unconditional support and guidance given to me throughout my sports scholarship. I also express my sincere gratitude to the Principal and Vice-Chancellor of Heriot-Watt University, Professor Steve Chapman, for his kindness in awarding me a Principal's Sports Award Grant for the last three experimental years of my PhD.

Lastly I would like to thank my mother Sheila, and father Robert, for their unconditional love and constant support, as well as my brothers Zander and Ewan and the respective members of their immediate families. Additionally, I wholeheartedly thank my parents for their huge financial contribution made to myself, and the sacrifices that they have had to make in life in order to do so. Without their huge financial kindness, I would never have been able to undertake this PhD.

Declaration

I, Calum Turnbull Robb, herby declare that I am the sole author of this thesis. All of the work described in this thesis is my own, except where stated in the text. The work presented here has not been accepted in any previous application for a higher degree. Additionally, all sources of information have been consulted by myself and are acknowledged by means of reference.

Calum Turnbull Robb

ACADEMIC REGISTRY
Research Thesis Submission

Name*:*	**Calum Turnbull Robb**		
School/PGI:	**School of Life Sciences**		
Version: *(i.e. First, Resubmission, Final)*	**Final submission**	Degree Sought (Award **and** Subject area)	**Doctor of Philosophy (PhD)**

Declaration

In accordance with the appropriate regulations I hereby submit my thesis and I declare that:

1) the thesis embodies the results of my own work and has been composed by myself
2) where appropriate, I have made acknowledgement of the work of others and have made reference to work carried out in collaboration with other persons
3) the thesis is the correct version of the thesis for submission and is the same version as any electronic versions submitted*.
4) my thesis for the award referred to, deposited in the Heriot-Watt University Library, should be made available for loan or photocopying and be available via the Institutional Repository, subject to such conditions as the Librarian may require
5) I understand that as a student of the University I am required to abide by the Regulations of the University and to conform to its discipline.

* *Please note that it is the responsibility of the candidate to ensure that the correct version of the thesis is submitted.*

Signature of Candidate*:*		Date:	

Submission

Submitted By *(name in capitals):*	**CALUM TURNBULL ROBB**
Signature of Individual Submitting:	
Date Submitted:	

For Completion in the Student Service Centre (SSC)

Received in the SSC by *(name in capitals):*			
Method of Submission *(Handed in to SSC; posted through internal/external mail):*			
*E-thesis Submitted (**mandatory for final theses)***			
Signature:		Date:	

Table of contents

Abstract i

Dedication ii

Acknowledgments iii

Declaration v

Research thesis submission vi

Table of contents vii

List of Tables xiv

List of Figures xv

List of Abbreviations and symbols xx

Publications and presentations xxiii

Chapter 1. General Introduction 1

1.1. Importance of cell death 2

1.2. Apoptosis 3

1.3. Apoptotic pathways 6

1.3.1. Intrinsic pathway 7

1.3.2. Extrinsic pathway 7

1.3.3. Inhibition of apoptosis 9

1.3.4. Apoptosis in invertebrates 9

1.4. Apoptotic-like cell death processes 11

1.5. Extracellular trap formation (ETosis) 13

1.6. *Carcinus maenas* as an experimental model for the study of cell death in invertebrates 18

1.7. Host defence reactions of *C. maenas* 19

1.7.1. Haemocyte types 19

1.7.2. Pathogen recognition 21

1.7.3. Immune defence reactions 21

1.7.4. Soluble immune effectors 25

1.8. Hypothesis and scientific aims 27

Chapter 2. Validation of apoptosis and comparison of methods 28

2.1. Introduction 29

2.2. Materials and methods 33

2.2.1. Reagents and solutions 33

2.2.2. Crabs 33

2.2.3. Haemolymph sampling 33

2.2.4. *In vitro* haemocyte culture 34

2.2.5. Detection of apoptosis 35

2.2.5.1. Light microscopy 35

2.2.5.2. Fluorescence microscopy 35

2.2.5.3. Confocal microscopy 37

2.2.5.4. Transmission electron microscopy 37

2.2.5.5. DNA fragmentation 38

2.2.6. Quantification of apoptosis 39

2.2.6.1. Microscopy 39

2.2.6.2. Flow cytometry with bovine lactadherin-FITC and PI staining 39

2.2.6.3. Flow cytometry – hypodiploid peak assay 40

2.2.7. Statistical analyses 41

2.3. Results 42

2.3.1. Detection of apoptosis 42

2.3.1.1. Light microscopy 42

2.3.1.2. Fluorescence microscopy 42

2.3.1.3. Confocal microscopy 46

2.3.1.4. Transmission electron microscopy 49

2.3.1.5. DNA fragmentation 52

2.3.2. Quantification of apoptosis 55

2.3.2.1. Microscopy 55

2.3.2.2. Flow cytometry with bovine lactadherin-FITC and PI staining 58

2.3.2.3. Hypodiploid peak assay 62

2.4. Discussion 66

Chapter 3. Quantification of apoptosis using flow cytometry 72

3.1. Introduction 73

3.2. Materials and methods 75

3.2.1. Preparation of mixed and separated haemocytes 75

3.2.2. Measurement of apoptosis under varying conditions 76

3.2.2.1. Temperature 76

3.2.2.2. Effect of repeated haemolymph sampling: mimic of injury/natural infection 76

3.2.3. Apoptosis in different haemocyte populations 77

3.2.4. Apoptosis in HCs after treatment with non-self agents 77

3.2.4.1. Lipopolysaccharide 78

3.2.4.2. Listonella anguillarum 78

3.2.5. Statistical analyses 79

3.3. Results 80

3.3.1. Apoptosis in haemocytes under varying life conditions 80

3.3.1.1. Temperature 80

3.2.2.2. Effect of repeated haemolymph sampling: mimic of injury/natural infection……..86

3.3.2. Apoptosis in different haemocytes populations.....90

3.3.3. Apoptosis in separated HCs after treatment with non-self agents ...98

3.3.3.1. Lipopolysaccharide.....98

3.3.3.2. Listonella anguillarum.....98

3.4. Discussion.....104

3.4.1. Effect of temperature 104

3.4.2. Variation in cell death among haemocyte types 106

3.4.3. Haemolymph loss and haemocytopenia.....108

3.4.4. Effect of LPS.....108

3.4.5. Response to *L. anguillarum* 109

Chapter 4. Characterisation of ETosis.....111

4.1. Introduction.....112

4.2. Materials and methods 114

4.2.1. Crabs 114

4.2.2. Preparation of monolayer hyaline haemocyte cultures.....114

4.2.3. Extracellular chromatin release assays *in vitro*.....114

4.2.4. Confirmation of NADPH-oxidase dependent ROS generation by HCs.....115

4.2.5. Ultrastructural morphology.....116

4.2.6. Extracellular chromatin decoration *in vitro* 117

4.2.7. Inhibition of extracellular chromatin release *in vitro* 118

4.2.8. Statistical analyses 118

4.3. Results.....119

4.3.1. Extracellular chromatin release.....119

4.3.2. Digestion of extracellular chromatin 126
4.3.3. Confirmation of ROS generation by HCs 129
4.3.4. Ultrastructural analysis 130
4.3.5. Extracellular chromatin decoration 134
4.3.6. Inhibition of extracellular chromatin release 136
4.4. Discussion 139

Chapter 5. Role of ETosis during host immune defence 142
5.1. Introduction 143
5.2. Materials and methods 145
5.2.1. Separation of haemocyte populations 145
5.2.2. Preparation of monolayer haemocyte cultures 145
5.2.3. Extracellular chromatin release assays *in vitro* 145
5.2.3.1. Different haemocyte types 145
5.2.3.2. LPS and Listonella anguillarum (non-self agents) 146
5.2.4. Inhibition of extracellular chromatin release *in vitro* 146
5.2.5. Entrapment of L. anguillarum by extracellular chromatin traps *in vitro* 147
5.2.6. Stimulation of extracellular chromatin release *in vivo* 147
5.2.7. ETosis in encapsulation reactions *in vitro* 150
5.2.8. Statistical analyses 151
5.3. Results 152
5.3.1. Extracellular chromatin release from other haemocyte types 152
5.3.2. ETosis following stimulation with LPS or *L. anguillarum* 155
5.3.3. Participation of ETosis in encapsulation reactions *in vivo* 159
5.3.4. ETosis in encapsulation reactions *in vitro* 163
5.4. Discussion 171

Chapter 6. Demonstration of ETosis in other invertebrates 175

6.1. Introduction 176

6.2. Materials and methods 179

6.2.1. Mussels and sea anemones 179

6.2.2. Haemolymph sampling from the mussel 179

6.2.3. Collection of amoebocytes from the sea anemone 179

6.2.4. Cyto-centrifuge preparations 180

6.2.5. Preparation of monolayer cell cultures 180

6.2.6. Extracellular chromatin release assays *in vitro* 180

6.2.7. Inhibition assays *in vitro* 181

6.2.8. Statistical analyses 181

6.3. Results 182

6.3.1. Mussel haemocytes 182

6.3.2. Sea anemone amoebocytes 186

6.4. Discussion 194

Chapter 7. General Discussion 197

7.1. General Discussion 198

Appendices 1-9 208

Appendix 1 209

Appendix 2 210

Appendix 3 211

Appendix 4 212

Appendix 5 213

Appendix 6 214

Appendix 7 216

Appendix 8 217

Appendix 9 218

Appendix 10: Published Paper 219

References 235

List of Tables

Table 1.1. Cell death processes. 12

Table 1.2. Comparison of haemocyte types in *C. maenas*. 20

Table 2.1. Summary of apoptosis-related proteins identified from crustaceans 31

Table 2.2. Summary of methods used in the present study 32

Table 2.3. Evaluation of apoptosis detection methods used in the present study 71

Table 4.1. Ultrastructural comparison of ETs released from *C. maenas* HCs and human NETs, assessed using high resolution scanning electron microscopy 132

.

List of Figures

Figure 1.1. Constitutively apoptotic human neutrophils after 20 h *in vitro* culture (37°C) 4

Figure 1.2. Constitutively necrotic human neutrophils after 24 h *in vitro* culture (37°C) 5

Figure 1.3. Simplified schematic representation of the intrinsic and extrinsic pathways of apoptosis initiation, modified from Elmore (2007)….. 8

Figure 1.4. Human NETs stained with Sytox Green after 3 h culture (37°C), stimulated with 0.1 μM PMA.……..…...14

Figure 1.5. Schematic representation of the mechanisms of NET release, modified from Zawrotniak and Rapala-Kozik, (2013)……..…….16

Figure 1.6. Generalised representation of the respiratory burst mechanism, modified from Parihar *et al*. (2008)…….……...22

Figure 1.7. An overview of the cellular immune responses in C. maenas, modified from Smith *et al*. (2003), during which degranulation plays a central role……..…...23

Figure 1.8. A simplified representation of the prophenoloxidase activating system in crustaceans.……..…….26

Figure 2.1. Light microscopy analysis of cyto-centrifuge preparations showing mixed haemocytes from *C. maenas* after 6 h suspension culture *in vitro* ……..…….....43

Figure 2.2. Light microscopy analysis of cyto-centrifuge preparations showing mixed haemocytes from *C. maenas* after 24 h suspension culture *in vitro* ……..…….....44

Figure 2.3. Fluorescence microscopy analysis showing DAPI stained mixed haemocytes from *C. maenas* after 6 h monolayer culture *in vitro*…….……45

Figure 2.4. Confocal microscopy showing apoptosis in mixed haemocytes from *C. maenas* throughout 6 h monolayer culture (15°C) *in vitro*……..……...……...47

Figure 2.5. Transmission electron microscopy of temperature-induced apoptotic mixed haemocytes from C. maenas after 24 h suspension culture (20°C) *in vitro*……..……....50

Figure 2.6. DNA fragmentation occurs as a result of temperature-induced apoptosis in mixed haemocytes from C. maenas after 24 h suspension culture (20°C) *in vitro*……..53

Figure 2.7. Efficacy of different inducers of apoptosis in mixed haemocytes from *C. maenas* after 6 h and 24 h suspension culture *in vitro*……..56

Figure 2.8. Fluorescence microscopy counts from DAPI stained *C. maenas* mixed haemocytes after monolayer culture *in vitro*…….……..…57

Figure 2.9. Flow cytometry assessment of temperature-induced apoptosis and apoptosis inhibition in mixed haemocytes after suspension culture *in vitro*.……...59

Figure 2.10. Flow cytometry assessment of temperature-induced apoptosis in mixed haemocytes after suspension culture *in vitro*, carried out using the hypodiploid peak assay…….....63

Figure 3.1. *C. maenas* mixed haemocytes counts after suspension culture *in vitro* at different incubation temperatures ……...…..…82

Figure 3.2. Morphological evidence of apoptosis and necrosis in *C. maenas* mixed haemocytes after suspension culture *in vitro* at different incubation temperatures. …….…..….83

Figure 3.3. Percentages of viable, early apoptotic and late apoptotic/necrotic *C. maenas* haemocytes after suspension culture *in vitro* at different incubation temperatures…….....84

Figure 3.4. Viable, early apoptotic and late apoptotic/necrotic *C. maenas* mixed haemocytes after suspension culture *in vitro,* obtained from crabs subject to repeated haemolymph sampling…….....87

Figure 3.5. Separated *C. maenas* haemocyte counts after suspension culture *in vitro*…….……...92

Figure 3.6. Morphological evidence of apoptosis and necrosis in separated *C. maenas* haemocytes after suspension culture *in vitro*…….93

Figure 3.7. Constitutive percentages of viable, early apoptotic and late apoptotic/necrotic separated *C. maenas* haemocytes after suspension culture *in vitro*…….……..……...94

Figure 3.8. Temperature-induced apoptosis and apoptosis inhibition in separated HCs and GCs after suspension culture *in* vitro…….……96

Figure 3.9. Lipopolysaccharide has a pro-survival effect upon separated *C. maenas* HCs after suspension culture *in vitro*……...…...100

Figure 3.10. Both viable and heat-killed *Listonella anguillarum* induce high levels of late apoptotis/necrosis in separated *C. maenas* HCs after suspension culture *in vitro*……..…….……102

Figure 4.1. Different forms of chromatin discharged by sperated HCs from *C. maeans in vitro*……...……..…...121

Figure 4.2. Concentration-time analysis *in vitro* of the effect of PMA on separated HCs from *C. maenas*……...……..…...122

Figure 4.3. Changes in percentages of chromatin extrusion over time in separated HCs from *C. maenas* treated with PMA *in vitro*…..…...123

Figure 4.4. Representative confocal images of Sytox Green stained 0.1 µM PMA treated HCs over a 24 h culturing period *in vitro*…...124

Figure 4.5. Representative confocal images of Sytox Green stained untreated (control) HCs over a 24 h culturing period *in vitro*…....125

Figure 4.6. DNAse digestion of extracellular chromatin released from *C. maenas* HCs *in vitro*…….....127

Figure 4.7. Scanning electron microscopy of extracellular chromatin release from HCs *in vitro* …….....131

Figure 4.8. Transmission electron microscopy showing extracellular chromatin release from HCs *in vitro*…….....133

Figure 4.9. Immunocytochemical analysis of extracellular chromatin released from HCs *in vitro*……..…….....135

Figure 4.10. Inhibition of extracellular chromatin release from *C. maenas* HCs *in vitro*……..…….....137

Figure 4.11. Representative confocal images after 24 h culture showing the inhibition of extracellular chromatin release in HCs *in vitro* by Sytox Green staining……..……...138

Figure 5.1. Rates of chromatin extrusion *in vitro* in different haemocyte types after PMA treatment ……...153

Figure 5.2. Morphological examination of extracellular chromatin release *in vitro* in different haemocyte type of *C. maenas*……....154

Figure 5.3. Stimulation/inhibition of chromatin extrusion in HCs *in* vitro…….156

Figure 5.4. Extracellular chromatin released from HCs successfully traps bacteria *in vitro*.…….158

Figure 5.5. *In vivo* demonstration of extracellular chromatin release and association of extracellular chromatin with haemocyte capsules.….160

Figure 5.6. *In vivo* ETosis: Immunohistochemical analysis revealing the distribution of DNA, PXN and H2A during the early stages of encapsulation.……..…162

Figure 5.7. ETosis in encapsulation reactions *in vitro*…...…….……...…….165

Figure 5.8. Quantification of haemocyte clump size and frequency during suspension culture *in vitro*……..…...167

Figure 5.9. Impairment of extracellular chromatin release affects the formation of haemocyte clumps during suspension culture *in vitro*…….……...…….....169

Figure 5.10. Viability of mixed haemocytes during *in vitro* suspension culture.....…….…….170

Figure 6.1. Charles Darwin's phylogenetic tree of life diagram…….…….....177

Figure 6.2. PMA-stimulated chromatin extrusion from *M. edulis* haemocytes *in vitro*…….……...…….....183

Figure 6.3. Representative confocal images of Sytox Green stained extracellular chromatin release from PMA-stimulated *M. edulis* haemocytes …….……...…….……....185

Figure 6.4. Morphology of *A. equina* crude mesogleal extracts and visualisation of extracellular chromatin release *in vitro*…….…….188

Figure 6.5. PMA-stimulated chromatin extrusion from *A. equina* enriched amoebocytes *in vitro*…….……...189

Figure 6.6. Representative confocal images of Sytox Green stained extracellular chromatin release from PMA-stimulated enriched *A. equina* amoebocytes …….…….…….191

Figure 6.7. DNAse digestion of extracellular chromatin released from *A. equina* enriched amoebocytes *in vitro*…….……192

List of abbreviations and symbols

‰	parts per thousand
Ø	diameter
™	trademark
x g	multiples of gravity
AMPs	antimicrobial peptides
AV	annexin V
ANOVA	analysis of variance
BIR	baculoviral IAP repeat
BIRC(s)	baculoviral IAP repeat-containing protein(s)
B. lactadherin	bovine lactadherin
BLAST	basic logical alignment search tool
bp	base pairs
BSA	bovine serum albumin
CDK	cyclin-dependent kinase
CS	*Carcinus* saline
DAPI	4',6-diamidino-2-phenylindole
DHR 123	dihydrorhodamine 123
DNA	deoxyribonucleic acid
DPI	diphenyleneiodonium chloride
EDTA	ethylenediaminetetraacetic acid
ET(s)	extracellular trap(s)
excitation/emission	ex/em
F(ab')2	a portion of an IgG molecule
FACS	fluorescence-activated cell sorting
FCS	fetal calf serum
FITC	fluorescein isothiocyanate
FL1	FITC or rhodamine 123 fluorescence
FL3	PI fluorescence
FoV	fields of view
FSC	forward scatter
G1	gap1 phase
GC(s)	granular cell(s)

H2A	histone H2A
HBSS	Hank’s balanced salt solution
HC(s)	hyaline cell(s)
IAP(s)	inhibitor of apoptosis protein(s)
Ig	immunoglobulin
kbp	kilobase pair
LPS	lipopolysaccharide
MAC	marine anticoagulant
ML-15	salt-modified Leibovitz’s L-15 medium
MPO	myeloperoxidase
n	number of replicates
NET(s)	neutrophil extracellular trap(s)
NFκB	nuclear factor kappa-light-chain-enhancer of activated B cells
NO	nitric oxide
NOS	nitric oxide synthase
OD	optical density
P	probability
PAP(s)	pro-apoptotic proteins(s)
PBS	phosphate buffered saline
PCR	polymerase chain reaction
Pen/Strep	penicillin/streptomycin
PFA	paraformaldehyde
pH	potential of Hydrogen
PI	propidium iodide
PKC	protein kinase C
PMA	phorbol 12-myristate 13-acetate
ProH(s)	pro-haemocyte(s)
proPO	prophenoloxidase
PS	phosphatidylserine
PXN	peroxinectin
Q-VD-OPh	N-(2-quinolyl)-L-valyl-L-aspartyl-(2,6- difluorophenoxy)-methylketone
ROS	reactive oxygen species
SEM	standard error of the mean

SGC(s)	semi-granular cell(s)
SOD	superoxide dismutase
SSC	side scatter
THCs	total haemocyte counts
TSA	tryptic soy agar
TSB	tryptic soy broth
v	voltage

Publications and presentations

Publications

Robb, C.T., Dyrynda, E.A., Gray, R.D., Rossi, A.G., Smith, V.J. (2014). Invertebrate extracellular phagocyte traps show that chromatin is an ancient defence weapon. *Nat. Commun* **5**, 4627.

Poster presentations

Robb, C.T., Rossi, A.G., Smith, V.J., Dyrynda, E.A. (2009). Demonstration of apoptosis in hyaline and granular haemocytes of the shore crab, *Carcinus maenas*. 11th International Society for Developmental and Comparative Immunology Congress, Prague, Czech Republic, June 28th-July 4th.

Smith, V.J., Robb, C.T., Constance, W., Dyrynda, E.A. (2012). Characterisation of prohaemocytes from crab, *Carcinus maenas*, and their survival *in vitro*. 12th International Society for Developmental and Comparative Immunology Congress, Fukuoka, Japan, July 9th-13th.

Oral presentations

Robb, C.T., Rossi, A.G., Dyrynda, E.A., Smith, V.J. (2013). Extracellular chromatin traps are an evolutionary conserved host defence process. Heriot-Watt University Distinctly Diverse PhD Conference, Scotland, December 13th.
(**Awarded best oral presentation**)

Chapter 1

General Introduction

1.1. Importance of cell death

Although appearing contradictory, cell death is the prerequisite for life. Cell population numbers are controlled by differentiation, proliferation, senescence and death, all of which are tightly regulated processes (Raff, 1992). Although cells can die from unpredictable traumatic events, most cell death in multicellular animals is part of normal physiological processes, such as tissue turnover. Every day, billions of cells are produced by mitosis (Singh, 2007), however, similar numbers die via different cell death pathways to maintain tissue homeostasis. Cell death processes are crucial for development and morphogenesis, maintaining constant cell numbers, balancing cell proliferation of newly produced cells and eliminating damaged cells (Penaloza *et al*., 2006).

Cell death processes are also essential in immunity by removing infected cells, thus preventing pathogen replication (Griffith and Ferguson, 2011). Additionally, the same cell death processes are required to control the number of cells generated during an immune response to infection, and to eliminate the majority of them once the pathogen is cleared (Pellegrini *et al*., 2003; Barreiro *et al*., 2004; Parish *et al*., 2009). In the mammalian system, cell death processes are critical in the development and deletion of autoimmune B and T lymphocytes. However, disordered cell death results in drastic consequences for the host and can result in unwanted survival of injurious cells, inappropriate death of viable cells and loss of tissue homeostasis, all of which are responsible for the onset of many human diseases.

It is now well established that different cell death processes occur in multicellular animals, with each cell death process encompassing its own specific stimuli, characteristics and importance to the host. Until recently, apoptosis (programmed cell death) and necrosis (uncontrolled/traumatic cell death) were thought to be the two main cell death pathways.

1.2. Apoptosis

The discovery of apoptosis by Kerr, Wyllie and Currie in 1972 challenged the perceptions of cell death processes. From initial observations in the 19th century (Vogt, 1842) until the early 1970s, necrosis was used to describe all types of cell death. Apoptosis is a carefully regulated mechanism of cellular suicide (orchestrated collapse of the cell) that avoids loss of cell membrane integrity (apart from late stage apoptosis) or an inflammatory response. Morphological changes during apoptosis have been accurately characterized by light and electron microscopy, with the latter the best way to describe definitive apoptotic cell morphology (Hacker, 2000). Features consistent with early apoptosis include cell shrinkage and karyopyknosis (irreversible condensation of chromatin in the nucleus) which are visible by light microscopy (Kerr *et al*., 1972), with karyopyknosis classed as the most characteristic feature of apoptosis. Early apoptotic cells can also exhibit membrane blebbing, irregular shaped nuclei and chromatin margination. Furthermore, early apoptosis is characterised by trademark membrane changes such as the translocation of the phospholipid phosphatidylserine (PS) from the inner to the outer membrane leaflet, and alteration/loss of mitochondrial transmembrane potential (Chaurio *et al*., 2009).

Morphological features consistent with later stages of apoptosis include cytoplasmic vacuolation, mitochondrial swelling and further condensation of nuclear chromatin, which is followed by nuclear fragmentation inside the cell, a feature described as karyorrhexis (Majno and Joris, 1995). After karyorrhexis, the separation of cell fragments into apoptotic bodies occurs during a process called ‘budding’. These membrane-bound apoptotic bodies contain organelles, cytosol and nuclear fragments. Even though late apoptotic cells lose membrane integrity, they do not release their cellular constituents into the extracellular environment as these apoptotic bodies/cells are quickly and efficiently removed by adjacent phagocytes, hence there is essentially no inflammatory reaction (Savill and Fadok, 2000; Kurosaka *et al*., 2003). Characteristic features of apoptotic cells can be seen in Figure 1.1.

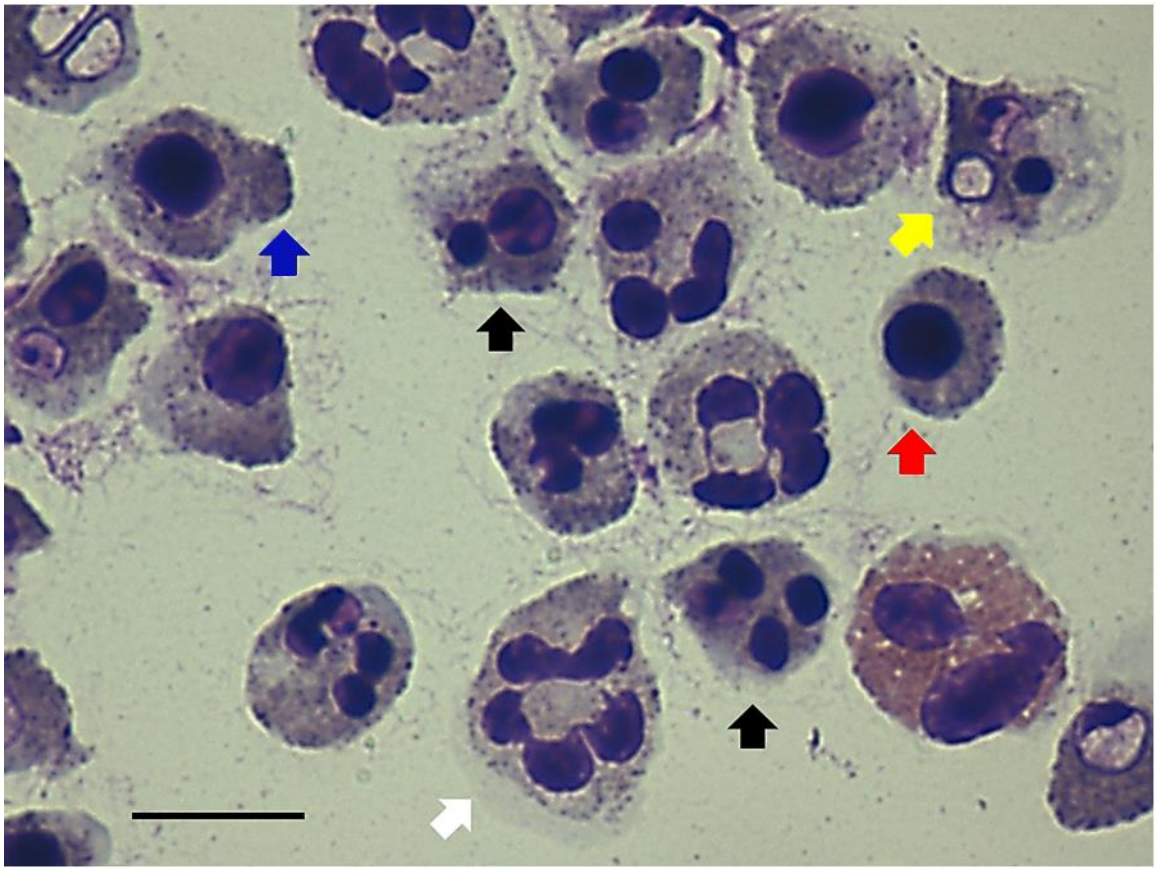

Figure 1.1. Constitutively apoptotic human neutrophils after 20 h *in vitro* culture (37°C). Neutrophils exhibit trademark nuclear fragmentation (karyorrhexis, black arrows), chromatin condensation (karyopyknosis, red arrow), cytoplasmic vacuolation (yellow arrow) and membrane blebbing (blue arrow). A viable neutrophil is also visible (white arrow), scale bar = 15 μm. Images produced by Mr Calum T. Robb.

In contrast, necrosis is a form of premature/uncontrolled (traumatic) cell death entailing the unregulated digestion and release of cellular and nuclear components due to loss of membrane integrity. Necrosis typically occurs in response to many types of insults associated with pathological processes (Rock and Kono, 2008). Features consistent with necrosis include cell swelling and complete dissolution of chromatin due to the activity of DNAse (Figure 1.2). This response is usually described as karyolysis (Elmore, 2007). The term secondary necrosis is applied to cells that have become late apoptotic, but have failed to be engulfed by phagocytes or neighbouring cells (Majno and Joris, 1995), hence secondary necrosis is a post-apoptotic event. Necrotic cell death often leads to an inflammatory response within the host organism (as chemotactic signals are sent) and

widespread damage to the immediate vicinity (Majno *et al*., 1960). Therefore, necrosis is almost always detrimental and in some instances can be fatal to the host organism (Walker *et al*., 1988; Zong and Thompson, 2006).

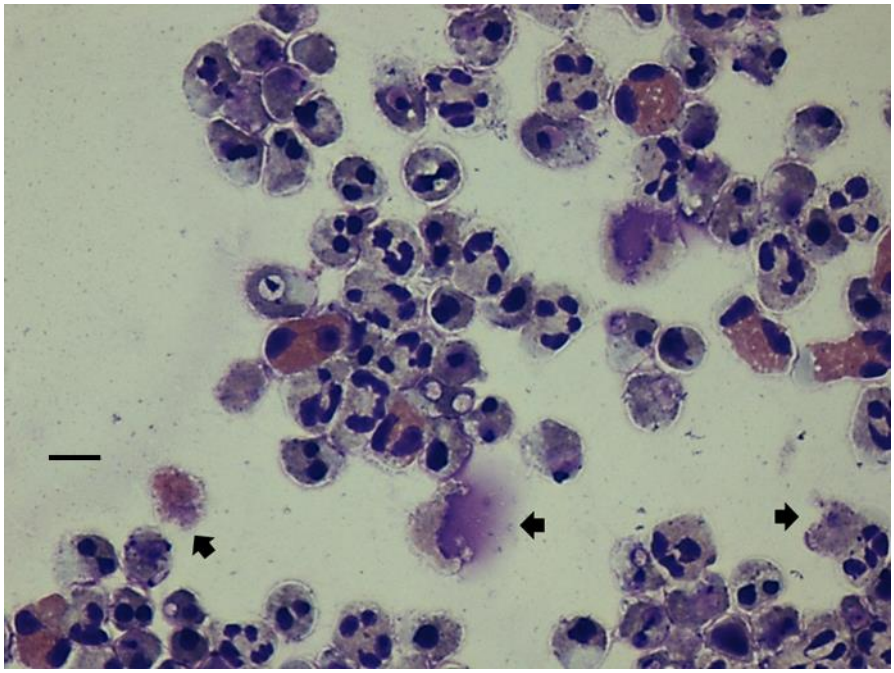

Figure 1.2. Constitutively necrotic human neutrophils after 24 h *in vitro* culture (37°C). Arrows indicate complete dissolution of nuclear chromatin (karyolysis) and loss of membrane integrity, scale bar = 15 µm. Images produced by Mr Calum T. Robb.

Apoptosis is vital in immunity, playing a crucial role in the destruction and clearance of diseased or injurious cells. Apoptosis also plays a central role in pathogenesis of diseases as the genes controlling apoptosis are suppressed, over-expressed or altered by mutation (Thatte and Dahanukar, 1997). Research interest in apoptosis has significantly increased since the link between apoptosis and cancer was established, when it was demonstrated that the Bcl-2 gene specifically blocks death of B lymphocytes in follicular lymphoma, (Vaux *et al*., 1988). In general, tumour formation results if there are decreased levels of apoptosis and cells grow faster and live longer than would normally be expected, in fact, it is this unexpected cell survival that is a key factor for the survival of a malignant cell. In addition, deficiencies in apoptosis signalling contribute to drug resistance of tumour cells, as many existing treatments such as non-steroidal, anti-inflammatories, and

anticancer treatments act through apoptotic cell death (Renehan *et al*., 2001). The main framework for this type of oncology research centralises around connecting failed apoptosis and cancer, harnessing apoptosis to destroy cancer cells and triggering apoptosis with new cancer drugs (Lowe and Lin, 1999). The exciting challenge in oncology is to translate the growing knowledge of apoptotic pathways into clinical applications (Schulze-Bergkamen and Krammer, 2004).

Disordered or un-regulated apoptosis is implicated in a variety of other human diseases (Kam and Ferch, 2000). Increased levels of apoptotic death in the central nervous system can lead to neurodegenerative diseases such as Alzheimer's or Parkinson's disease and cerebral ischaemia, with increased numbers of apoptotic lymphocytes tending to lead to sepsis (septicaemia) and/or human immunodeficiency virus (HIV) infection (Kam and Ferch, 2000). On the other hand decreased levels of apoptosis can lead to carcinogenesis, autoimmune disorders and leukaemia and/or lymphomas (Kam and Ferch, 2000). Additionally, aberrant surviving cells are implicated in the neoplastic process (Wyllie, 1987).

1.3. Apoptotic pathways

Caspases, a large family of cysteine proteases, play essential roles in apoptosis, necrosis and inflammation (Alnemri *et al*., 1996). Caspases, which are located intracellularly, are dubbed 'executioner proteins' as they are the chief proteins involved in apoptosis initiation (Elmore, 2007). Caspases can be activated through the intrinsic or extrinsic apoptotic pathways (Figure 1.3). Both pathways involve caspase 3 activity immediately before apoptosis is initiated, but are differentiated from each other by involvement of different caspases earlier in the cascade (for review see Elmore, 2007). In humans, 11 caspases including caspases 1-10 and caspase-14 have been identified (for review see Sakamaki and Satou, 2009).

1.3.1. Intrinsic pathway

The intrinsic signalling pathway is mediated through mitochondrial events, where a broad range of non-receptor-mediated stimuli produce and emit intracellular signals that act directly on targets within the cell (Elmore, 2007). The intrinsic pathway is characterised by mitochondrial outer membrane permeabilisation (MOMP) and release of cytochrome c into the surrounding cytoplasm (Tait and Green, 2010). From here the cytochrome c forms a multi-protein complex commonly referred to as an 'apoptosome', which in turn initiates activation of the caspase cascade via caspase 9 activity (Danial and Korsmeyer, 2004). MOMP is regulated by balance of opposing actions of pro-apoptotic and anti-apoptotic Bcl-2 gene family members (Bax, Bak, Bcl-2, Bcl-XL and Mcl-1) (Ghavami *et al*., 2009). Following MOMP, mitochondrial pro-apoptotic proteins such as cytochrome c, DIABLO/Smac and HTRA2/Omi (caspase dependent), as well as apoptosis-inducing factor (AIF) and endonuclease G (non-caspase-dependent) are released via transmembrane channels across the mitochondrial outer membrane (Ghavami *et al*., 2009).

1.3.2. Extrinsic pathway

The extrinsic signalling pathway is mediated by death receptors located on the plasma membrane (Tait and Green, 2010). Transmembrane receptor-mediated interactions are involved in initiating apoptosis through involvement of death receptors that are members of the tumour necrosis factor (TNF) receptor gene superfamily (Locksley *et al*., 2001). Death receptors located on the plasma membrane such as TNF receptor 1 and TNF receptor superfamily member 6, also referred to as Fas/CD95, activate apoptosis (Guicciardi and Gores, 2009). Death ligands then bind to these death receptors and, in doing so, form the death-inducing signalling complex (DISC) that via caspase 8 initiates the caspase cascade (Danial and Korsmeyer, 2004). Death receptors can activate caspases within seconds of death ligand binding thus initiating programmed death of a cell within hours (Kühnel *et al*., 2000). These death receptors transmit apoptotic signals initiated by specific ligands such as TNF alpha, TNF-related apoptosis-inducing ligand (TRAIL) and Fas ligand (de Jong *et al*., 2001). In the penultimate stage of the extrinsic apoptotic pathway, through the action of caspase activated DNAse (CAD), the DNA of the cell nucleus is fragmented into nucleosomal units (for review see Nagata, 2005).

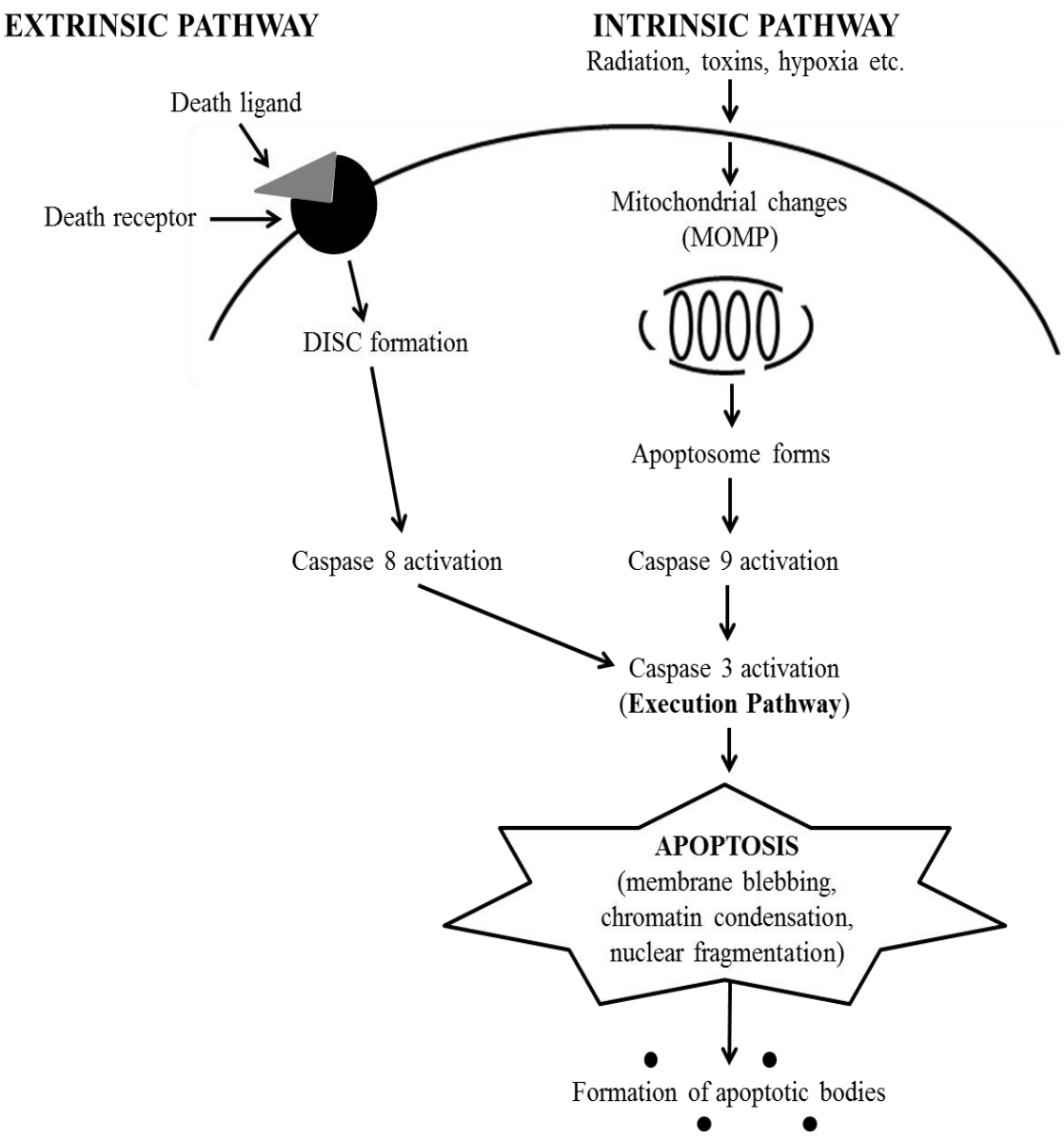

Figure 1.3. Simplified schematic representation of the intrinsic and extrinsic pathways of apoptosis initiation, modified from Elmore (2007). DISC = death-inducing signalling complex, MOMP = mitochondrial outer membrane permeabilisation.

1.3.3. Inhibition of apoptosis

The inhibitor of apoptosis proteins (IAPs) are the chief proteins involved in apoptosis inhibition (for review see Deveraux and Reed, 1999). The IAP family of proteins contain at least one baculoviral IAP repeat (BIR) domain, through which they interact with caspases, and suppress their activity (Srinivasula and Ashwell, 2008). Hence, IAPs are also known as BIR-containing proteins (BIRCs) (Dubrez-Daloz *et al*., 2008). IAPs contain characteristic structural motif domains such as BIR (BIR 1, BIR 2 and BIR 3), a really interesting new gene (RING) domain, a caspase recruitment domain (CARD) and a ubiquitin-conjugating (UBC) domain (Leu *et al.*, 2008). The BIR domain is essential for the inhibitory activity of an IAP. Overexpression of IAPs can ultimately protect cells against apoptotic stimuli (Marivin *et al*., 2012), while deletion or inhibition of IAPs can sensitise cancer cells to various treatments, such as chemotherapy, radiotherapy or cell death agonistic treatment (Fulda and Vucic, 2012).

1.3.4. Apoptosis in invertebrates

Landmark molecular studies of apoptosis using the invertebrate models, the nematode worm, *Caenorhabditis elegans* (Hengartner and Horvitz, 1994; Conradt and Horvitz, 1999; Liu and Hengartner, 1999) and the fruit fly, *Drosophila melanogaster*, (Abrams *et al*., 1993; Kumar and Doumanis, 2000) helped lay the foundation for the study of apoptosis in vertebrates. Caspase genes have been identified in several invertebrates, such as the sponges *Geodia cydonium* and *Hydra vulgaris*, sea anemone *Aiptasia pallida*, nematode worm *C. elegans*, fruitfly *D. melanogaster*, sea urchin *Strongylocentrotus purpuratus* and the ascidians *Ciona intestinalis* and *Ciona savignyi* (Shaham, 1998; Cikala *et al*., 1999; Lamkanfi *et al*., 2002; Terajima *et al*., 2003; Wiens *et al*., 2003; Weill *et al*., 2005; Dunn *et al*., 2006; Robertson *et al*., 2006; Kumar, 2007). Moreover, several caspases in these organisms are orthologues to caspases in vertebrates (Sakamaki and Satou, 2009). A short form of sponge caspases show highest sequence similarity to human caspase-3 and was confirmed to have caspase-3-like enzyme activity (Wiens *et al*., 2003). Therefore, it is fair to suggest that the functionality of caspases is conserved through evolution.

With the exception of the model organisms, *D. melanogaster* and *C. elegans*, apoptosis remains poorly characterised in invertebrates, particularly at the cellular/functional levels. Moreover, a large proportion of what is known in invertebrates is based on assumption. Studies of apoptosis in invertebrates are commonly carried out using mammalian methodologies not optimised for use with invertebrates, and although apoptosis is essential for the maintenance of homeostasis in the vertebrate immune system, few studies have explored its role in invertebrate immunity. Furthermore, methods for the detection and quantification of apoptosis in invertebrate haemocytes (immune cells) have rarely been validated, an area which needs more work. Previous studies attempting to quantify apoptosis in invertebrate haemocytes have largely focussed on the use of pooled haemolymph in order to obtain enough haemolymph for experimental assays, e.g. the mussel, *Mytilus galloprovincialis*, (Romero *et al*., 2011), oyster, *Crassostrea gigas*, (Lacoste *et al*., 2001; Terahara *et al*., 2005) and fruit fly, *D. melanogaster* (Bidla *et al*., 2007). However, pooling of haemolymph often causes non-self activation as part of the invertebrate immune response, such as initiation of coagulation cascades.

There are additional studies which have attempted to quantify apoptosis in invertebrate haemocytes from un-pooled haemolymph, however such studies have focussed only on mixed haemocytes as previously carried out for shrimp (Hameed *et al*., 2006; Xian *et al*., 2012; Wang and Zhang, 2008; Chang *et al*., 2009). There is a complete lack of apoptosis research regarding separated invertebrate haemocytes, with many studies failing to even consider them. The main reason for this dearth is because haemocyte separation procedures for invertebrates are often problematic. It can be difficult to obtain enough haemolymph for successful cell separations, to control the rapid and efficient haemolymph coagulation, and to manage the high cellular reactivity. Quantification of apoptosis in both mixed and separated haemocytes is essential for a comprehensive understanding of apoptosis in the invertebrate immune system, as well as in invertebrate pathophysiology.

1.4. Apoptotic-like cell death processes

Since the discovery of apoptosis, several apoptotic-like cell death processes have been described in humans, e.g. anoikis (Frisch and Francis, 1994), paraptosis (Sperandio *et al*., 2000), pyroptosis (Cookson and Brennan, 2001) and parthanatos (Andrabi *et al*., 2008) (Table 1.1). These processes represent slight variations to the generalised theme of apoptosis, with many displaying features similar to apoptosis, unlike non-apoptotic forms of cell death such as autophagy (Deter and De Duve, 1967) and ferroptosis (Dixon *et al*., 2012). Anoikis protects tissues from inappropriate colonisation by non-adherent cells (McFall *et al*., 2001) and in adult organisms is commonly observed during skin regeneration or involution of the mammary gland (Hall *et al*., 1994; Polakowska *et al*., 1994; Boudreau *et al*., 1995). Moreover, resistance to anoikis is implicated in cancer cell survival (Kim *et al*., 2012), whereas paraptosis is implicated in overcoming apoptosis-resistance during colon cancer (Gandin *et al*., 2012; Zhang *et al*., 2013).

Pyroptosis does not involve classical apoptotic caspases such as caspase-3 and caspase-8, and is instead (in contrast to apoptosis) mediated by a caspase-1-dependent pathway (Cookson and Brennan, 2001). Although apoptosis was previously proposed as a key mechanism of cell death during HIV-1 infection, caspase-1-dependent pyroptosis has been shown to drive over 95% of quiescent lymphoid CD4-positive T cell death in HIV-1 infected hosts (Doitsh *et al*., 2014). Furthermore, observed caspase-1 activation or dependence during cell death in the immune (Chen *et al*., 1996), central nervous (Liu *et al*., 1999), and cardiovascular systems (Kolodgie *et al*., 2000; Frantz *et al*., 2003) indicates that pyroptosis plays an important role in a variety of biological systems (Fink and Cookson, 2005). Lastly, the role of parthanatos has been widely implicated principally in neurologic diseases (Wang *et al*., 2009). To date however, there is little known of any apoptotic-like cell death processes in invertebrates, and it is unclear which markers of such processes might be expected to be observed and under which conditions (Kaczanowski *et al*., 2011).

Table 1.1. Cell death processes.

Cell death process/Key reference	Features
Necrosis Vogt, 1842	Cell swelling, complete dissolution of chromatin, loss of membrane integrity, un-regulated release of cellular and nuclear components, inflammatory response generated.
Apoptosis Kerr *et al*., 1972	Cell shrinkage, chromatin condensation, membrane blebbing, DNA fragmentation, membrane integrity retained, programmed cell death, no inflammatory response generated.
Anoikis Frisch & Francis, 1994	Stimulated by anchorage-dependent cells, due to loss of cell-matrix interactions. Also known as suspension-induced apoptosis.
Paraptosis Sperandio *et al*., 2000	Vacuolation occurs in the cytoplasm and the mitochondria swell in size. No nuclear fragmentation, chromatin condensation or apoptotic body formation.
Pyroptosis Cookson & Brennan, 2001	Caspase-1-dependent cell death that occurs during inflammation associated with antimicrobial responses. Features include DNA fragmentation, membrane blebbing, cell swelling, cell lysis and release of inflammatory cellular contents.
Parthanatos Andrabi *et al*., 2008	Process culminating in apoptosis-inducing factor mediated cell death. Features include chromatin condensation, DNA fragmentation and the absence of apoptotic bodies.
Extracellular Trap formation (ETosis) Brinkmann *et al*., 2004	Controlled extrusion of nuclear chromatin which forms extracellular traps studded with antimicrobial peptides (AMPs) that serve to entrap and kill pathogens.

1.5. Extracellular trap formation (ETosis)

A completely novel cell death process, separate to necrosis, apoptosis and apoptotic-like cell death, was discovered in 2004 by Volker Brinkmann and Arturo Zychlinsky (Brinkmann *et al*., 2004). This process was first observed in human neutrophils and entails the controlled discharge of chromatin from the nucleus following stimulation with phorbol 12-myristate 13-acetate (PMA) (Figure 1.4), H_2O_2 (generated exogenously using glucose oxidase), lipopolysaccharide (LPS), platelet activating factor or calcium ionophore ionomycin (Brinkmann *et al*., 2004; Fuchs *et al*., 2007, 2010; Parker *et al*., 2012a). The extruded chromatin entraps bacteria, leading the discoverers to designate them as neutrophil extracellular traps (NETs) (Brinkmann *et al*., 2004), with the pathway termed NETosis (Steinberg and Grinstein, 2007). More recently, however, the process has come to be known as ETosis (Wartha and Henriques-Normark, 2008). ETosis may be induced by various agents, including bacteria (Fuchs *et al*., 2007; Papayannopoulos and Zychlinsky, 2009), fungi (Bruns *et al*., 2010; Bianchi *et al*., 2011), viruses such as HIV-1 (Saitoh *et al*., 2012) and influenza A (Narasaraju *et al*., 2011), haem (Chen *et al*., 2014) and even exercise (Beiter *et al*., 2014). Pro-inflammatory stimuli, such as interleukin 1β (IL-1β), IL-8 and tumour necrosis factor alpha (TNFα) may, in addition, induce ETosis in a similar way (Keshari *et al*., 2012). Recently, silver nanoparticles as well as ionic silver have also been demonstrated to trigger the release of NETs (Haase *et al*., 2014), which are capable of entrapping and degrading single-walled carbon nanotubes (Farrera *et al*., 2014). Interestingly, impaired NET formation is observed in older individuals (65-75 years old) (Hazeldine *et al*., 2014).

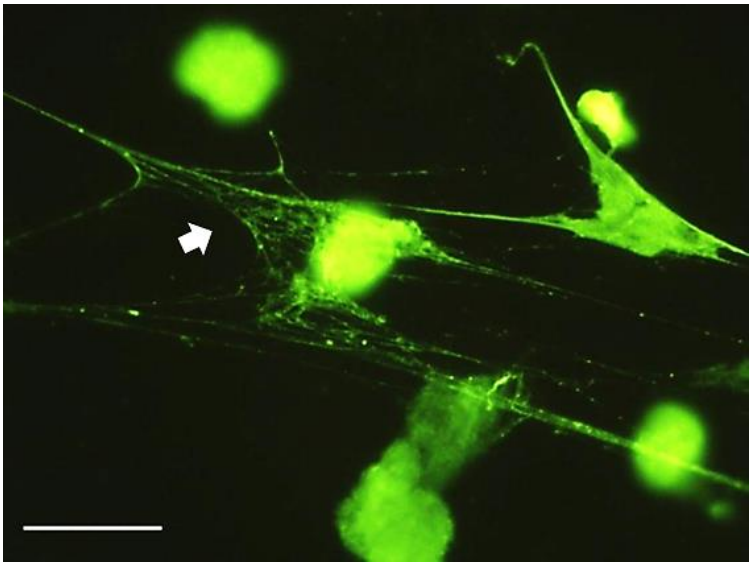

Figure 1.4. Human NETs stained with Sytox Green after 3 h culture (37°C), stimulated with 0. 1 µM PMA. Arrow indicates a fine web of extracellular chromatin being released from an ETotic neutrophil. Image courtesy of Dr Robert Gray (University of Edinburgh). Scale bar = 25 µm.

In neutrophils, the NETs are composed of decondensed nuclear chromatin (Papayannopoulos *et al*., 2010). Since treatment with DNAse leads to disintegration of the NETs, it was established that DNA was the main structural component of NETs (Brinkmann *et al*., 2004). Studded on the DNA backbone of NETs are nuclear, granule and cytosolic proteins. Such nuclear proteins include citrullinated histones and antimicrobial peptides (AMPs) such as the cathelicidin, LL37, azurophilic (primary) granule proteins such as neutrophil elastase (NE), cathespin G, myeloperoxidase (MPO) and α-defensins, specific proteins from secondary and tertiary granules such as lactoferrin and gelatinase respectively, or cytosolic proteins such as the cytosolic protein complex, calprotectin (Brinkmann *et al*., 2004; Urban *et al*., 2009). Using a proteomic approach, 24 NET-associated proteins have been identified with a protein:DNA ratio of 1.67 (Urban *et al*., 2009). The core histones H2A, H2B, H3 and H4, were the most abundant proteins and account for 70% of all NET-associated proteins (Urban *et al*., 2009). Histones are highly conserved nuclear proteins with potent antimicrobial activities (Hirsch, 1958), and ETosis is the only known mechanism by which they are exposed to infective agents. Indeed, histone decoration of chromatin on NETs is a diagnostic feature of the phenomenon for

mammals (Fuchs *et al*., 2010), with histone hypercitrullination mediated via peptidylarginine deiminase 4 (PAD4) (Neeli and Radic, 2012).

ETosis is dependent upon the generation of reactive oxygen species (ROS) by nicotinamide adenine dinucleotide phosphate (NADPH) oxidase (Fuchs *et al*., 2007). Such is the dependency of NETs on ROS generation, pre-treatment of human neutrophils with the NADPH oxidase inhibitor diphenylene iodonium chloride (DPI) completely obliterates NET formation even when the NET stimulator PMA is present in the same cell sample (Fuchs *et al*., 2007). Furthermore, cytochalasin D, an inhibitor of actin filamentation, severely diminished the ability of neutrophils to respond to LPS by releasing chromatin from the cells (Neeli *et al*., 2009). ETosis is characterised by the nuclear membrane being entirely fragmented with most of the granules being dissolved thus allowing direct contact and mixing of nuclear, cytoplasmic and granular components, such as granular proteins, (Fuchs *et al*., 2007). The discharged chromatin forms complex meshes that entrap microorganisms (Brinkmann *et al.,* 2004). Extracellular killing which is the penultimate function of NETs, is then achieved through potent antimicrobial activities, e.g. from histones and MPO, studded on the chromatin (Papayannopoulos and Zychlinsky, 2009). A schematic representation of the mechanism of NET release can be seen in Figure 1.5. These ETs have the ability to trap and/or disarm and kill both Gram-positive and Gram–negative bacteria, fungi (Urban *et al*., 2006; Fuchs *et al*., 2007; Ma and Kubes, 2008), and larger parasites such as sporozoites of *Eimeria bovis* (Hermosilla *et al*., 2014). The role of NETs in fighting viral infections remains to be fully characterised, although NETs can promote lung injury following influenza infection (Wardini *et al*., 2010; Hemmers *et al*., 2011; Narasaraju *et al*., 2011). Additionally, NETs can capture HIV and promote its elimination through MPO and α-defensins (Saitoh *et al*., 2012). The ultrastructure of NETs is unusual, NETs consist of smooth filaments with a diameter of 15-17 nm (Brinkmann *et al*., 2004), with these filaments composed of stacked, and probably modified, nucleosomes (Urban *et al*., 2009). This backbone is punctured with globular domains with a diameter of 25 nm which are made of granule proteins that aggregate into larger threads with diameters up to 50 nm (Brinkmann *et al*., 2004). This unique NET morphology, when analysed by high resolution scanning electron microscopy, enables easy differentiation of NETs from other fibrous structures such as fibrin.

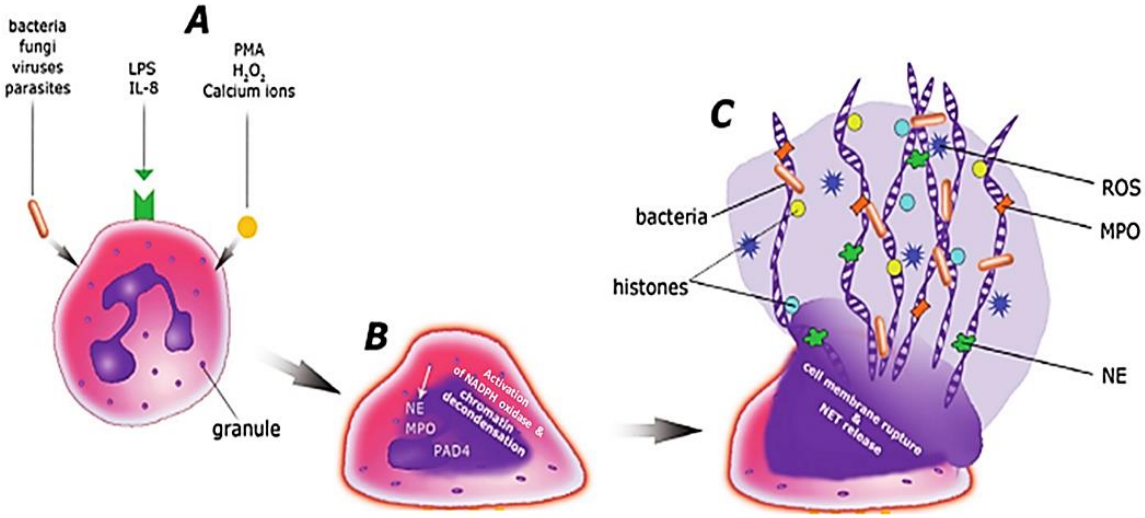

Figure 1.5. Schematic representation of the mechanism of NET release, modified from Zawrotniak and Rapala-Kozik, (2013). Neutrophils can be induced to form NETs by various stimuli (**A**), including bacteria, fungi, viruses, parasites and chemical factors such as PMA. This leads to activation of NADPH oxidase and chromatin decondensation due to histone cleavage by NE and MPO and histone hypercitrullination by PAD4 (**B**). Penultimately, the cell membrane ruptures and NETs are released that entrap and kill microorganisms via action of various antimicrobial factors such as histones, NE and MPO (**C**). LPS = lipopolysaccharide, IL-8 = interleukin-8, PMA = phorbol 12-myristate 13-acetate, H_2O_2 = hydrogen peroxide, NADPH = nicotinamide adenine dinucleotide phosphate, NE = neutrophil elastase, MPO = myeloperoxidase, PAD4 = peptidylarginine deiminase 4, ROS = reactive oxygen species.

Importantly the phenomenon is not confined to neutrophils as ETosis has further been shown to occur in eosinophils (Ueki *et al*., 2013), mast cells (von Köckritz-Blickwede *et al*., 2008), monocytes (Webster *et al*., 2010) macrophages (Aulik *et al*., 2012) and HL60 cells (Kawakami *et al*., 2014). ETosis has also been reported for bovine (Lippolis *et al*., 2006), murine (Ermert *et al*., 2009) feline (Wardini *et al*., 2010), equine (Galvão *et al*., 2012), porcine (Bréa *et al*., 2012) and caprine (Silva *et al*., 2014) inflammatory cells, leading ETosis to be regarded as an integral part of the mammalian inflammatory repertoire. Furthermore, ETosis is not confined to mammals as it also occurs in the cells of other vertebrates including chicken heterophils (Chuammitri *et al*., 2009), and fish

neutrophils, specifically the fathead minnow (Palic *et al*., 2007a), zebrafish (Palic *et al*., 2007b) and carp (Pijanowski *et al*., 2013).

The confinement of pathogens to a local site of infection may be an important function of NETs (Urban *et al*., 2006). However, it has been suggested that the antimicrobial mechanism of NET formation occurs at the expense of injury to the host (Clark *et al*., 2007), i.e. if not effectively cleared by the action of nucleases such as plasma DNAse and/or macrophage phagocytosis of the NET/neutrophil complex (Farrera and Fadeel, 2013). Certainly, ETosis-associated pathologies/clinical conditions e.g. thrombosis, appendicitis, pneumonia, pre-eclampsia, tuberculosis, mastitis, cystic fibrosis, promotion of cancer metastasis, abdominal sepsis, type 2 diabetes, atherosclerotic plaques and autoimmune diseases including systemic lupus erythematosus (SLE) and rheumatoid arthritis occur in mammals (Fuchs *et al*., 2010; Remijsen *et al*., 2011; Brinkmann and Zychlinsky, 2012; Cools-Lartigue *et al*., 2013; Khandpur *et al*., 2013; Yu and Su, 2013; Luo *et al*., 2014; Menegazzo *et al*., 2014; Oklu *et al*., 2014). Exposure of NET-associated proteases and other granular proteins to the extracellular environment has also been shown to damage endothelial cells *in vitro* (Clark *et al*., 2007; Villanueva *et al*., 2011). Moreover, extracellular histones released from NETs are implicated as key effectors of inflammation in rat and mice models of acute lung injury (Bosmann *et al*., 2013). Although the role of NETs has been detected during infection, inflammation and sepsis, their role *in vivo* remains unclear, and it remains uncertain whether cell death itself is required for the release of NETs *in vivo* (Remijsen *et al*., 2011). Intriguingly, Yousefi *et al*. (2008, 2009) claim that viable eosinophils and neutrophils can release mitochondrial DNA to form extracellular traps (ETs) in an ROS-dependent manner. However, mitochondrial DNA is 100,000 times less abundant in ETs than nuclear DNA (Pilsczek *et al*., 2010), hence, the significance of this finding awaits further investigation, and the steps of this process remain poorly understood. For an overview of the different pathways of ETosis refer to Phillipson and Kubes, (2011).

At present there are no published reports of ETotic cell death in the haemocytes of any invertebrate, so it remains unknown if the process is confined to inflammatory cells of vertebrates or has a more ancient origin. Some observations of extracellular structures that may have been discharged from the circulating blood cells (haemocytes or coelomocytes) of invertebrates such as *Drosophila melanogaster* and *Galleria mellonella* have occasionally appeared in the literature (Theopold *et al*., 2004; Altincicek *et al*., 2008; Wang *et al*., 2010). As yet however no further evidence has been presented confirming that the extruded material observed in these studies is chromatin that is expelled through an ROS-dependent pathway, which also shares other important similarities to ETosis in higher vertebrates. Interestingly, extracellular DNA in root-cap slime of the pea plant, *Pisum sativum*, has been shown to confer protection against fungal infections (Wen *et al.*, 2009). However this is yet to be confirmed as an ETotic response.

Invertebrates have strong dependence on the inflammatory activities of circulating blood cells, and for those with open circulatory systems, ETosis could represent a powerful way to restrict the spread of invasive or opportunistic microorganisms gaining entry to the coelomic cavity. The present investigation therefore included work to test the hypothesis that ETosis is a primordial defence strategy that exists with functional immunological value in invertebrates. If ETosis is an ancient cell death phenomenon, the process should occur in invertebrates, and importantly share key structural and biochemical similarities in its initiating mechanism(s) as that shown by inflammatory cells of higher vertebrates.

1.6. *Carcinus maenas* as an experimental model for the study of cell death in invertebrates

The shore crab, *Carcinus maenas,* was chosen as the main experimental invertebrate to investigate apoptotic and ETotic cell death. This animal has the advantage of being readily available, easy to maintain in aquaria, has no ethical constraints, and possesses a large volume of cell-rich haemolymph. Its haemocytes have been well characterised

with protocols for quick separation (10 min) of the different types well established (Söderhäll and Smith, 1983), unlike other crustaceans such as shrimp and prawns where cell separations are commonly problematic. Moreover, methodologies for medium term *in vitro* culture of crab haemocytes have been developed (Walton and Smith, 1999; Sperstad *et al*., 2010).

1.7. Host defence reactions of *C. maenas*

C. maenas, like all other invertebrates, lack adaptive immunity (specific immunity with immunological memory) dependent upon clonal selection of lymphocyte subsets, isotype switching and variation in reception diversity through recombination-activating genes. Instead, invertebrates rely only on innate immune responses for host protection. The success of invertebrate animals, which comprise around 97% of the total number of extant animal species on earth, shows that their ability to defend themselves against a diverse range of pathogens through only innate immunity is quite remarkable. Key effectors of immunity in crustaceans are the haemocytes that are present within the haemolymph. These carry out the various inflammatory responses, synthesize and store immunologically active proteins as well as executing a number of other physiological processes, such as tanning of the new cuticle after molting. What follows is a short overview of the different haemocyte types in *C. maenas* and their roles in host protection.

1.7.1. Haemocyte types

There are four haemocyte types in *C. maenas*, namely the pro-haemocytes (ProHs), hyaline cells (HCs), semi-granular cells (SGCs) and the granular cells (GCs). HCs comprise ca. 80% of the haemocyte population in *C. maenas*, whereas GCs (and to a lesser extent SGCs) comprise ca. 20% (Smith and Ratcliffe, 1978). A comparison of the different haemocyte types found in *C. maenas* can be seen in Table 1.2.

Table 1.2. Comparison of haemocyte types in *C. maenas*.

Haemocyte Type	Morphology	Functions
Pro-haemocyte 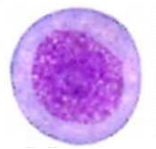	Large nucleus, small cytoplasmic rim (Roulston and Smith, 2011). Size: 8-20 µm diameter	Highly proliferative. Maturation and differentiation into other haemocyte types.
Hyaline cell 	No/few refractive granules in cytoplasm. Variable no. of small (<1 µm) non-refractive granules (Smith and Ratcliffe, 1978). Size: 10-17 µm diameter	Phagocytosis and generation of ROS.
Semi-granular cell 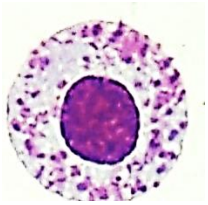 Granular cell 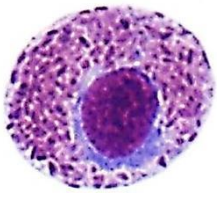	Cytoplasm moderately (semi-granular cells) or densely packed (granular cells) with intracellular refractive granules ca. 1 µm diameter (Smith and Ratcliffe, 1978). Size: 12-20 µm diameter	Release of immune proteins such as AMPs, proPO and peroxinectin via degranulation.

Abbreviations: ROS = reactive oxygen species, AMPs = antimicrobial peptides, ProPO = prophenoloxidase. Images produced by Mr Calum T. Robb.

1.7.2. Pathogen recognition

In general, pathogen recognition is mediated through the binding of particular molecules on the microbial surface known as pathogen associated molecular patterns (PAMPs) to pattern recognition receptors (PRRs), which are either on the blood cell surface or free in the plasma (Janeway and Medzhitov, 2002; Medzhitov and Janeway, 2002). Examples of PAMPs include fungal β-1,3-glucans, peptidoglycans, as well as bacterial LPS on Gram-negative bacteria or lipoteichoic acid on Gram-positive bacteria (Janeway and Medzhitov, 2002; Iwanaga and Lee, 2005). Amongst the known PRRs on crustacean haemocytes are β-1,3-glucan binding proteins (βGBP), LPS-binding proteins and peptidoglycan-binding proteins (Cheng *et al*., 2005). Binding of PAMPs by PRRs constitutes immunological recognition and is essential for activation of both cell-mediated and humoral (non-cellular-mediated) immune defence reactions in crustaceans.

1.7.3. Immune defence reactions

In crab, the HCs are the only haemocyte type known to be phagocytic (Smith and Ratcliffe, 1978) although in other crustaceans such as shrimp and crayfish, the SGCs are phagocytic. Phagocytosis is important for all animals, because it plays an integral role in the surveillance and defence against non-self particles, and subsequent removal of microorganisms from haemolymph or body fluids (Bayne, 1990). Surprisingly however, only around 2-15% of *C. maenas* HCs and crayfish SGCs phagocytose bacteria *in vitro* (Smith and Ratcliffe, 1978; Söderhäll *et al*., 1986), with similar low rates of 3-16% phagocytosis observed in haemocytes of the black tiger shrimp, *Penaeus monodon in vitro* (Rengpipat *et al*., 2000). Few decapods show phagocytic rates as high as in bivalve molluscs, where around 70% or more of the circulating haemocytes undergo phagocytosis (Wootton *et al*., 2003). The relatively low level of phagocytosis in *C. maenas* and other decapods remains enigmatic. Whilst it is generally thought that measurements of phagocytic rates *in vitro* are poorly indicative of the levels *in vivo*, no alternative satisfactory explanation has been forthcoming. It is therefore possible that the HCs may deal with invasive micro-organisms in other ways.

Following recognition and the induction of phagocytosis, various killing mechanisms are brought into play. Phagocytes frequently synthesize and store a variety of AMPs, which are released into the phagosome or released into the vicinity of the infective agents (Janeway *et al*., 2001). In this regard, *C. maenas* is unusual, in that the HCs do not seem to express AMPs, at least as indicated by the lack of strong antibacterial activity of HC lysate supernatants *in vitro* (Chisholm and Smith, 1992). Instead, crab HCs probably use reactive oxygen species (ROS), such as superoxide anion (O_2^-) and hydrogen peroxide (H_2O_2), released from the cells through a respiratory burst (Bell and Smith, 1993). The ROS may be released intracellularly within the phagocytic vacuole or extracellularly into the surrounding milieu. Extracellular ROS may contribute to the killing of bacteria by intact *C. maenas* HCs *in vitro*, reported by Bell (1994), although further confirmation of this is yet to be forthcoming. A simplified diagram of the respiratory burst mechanism can be seen below in Figure 1.6.

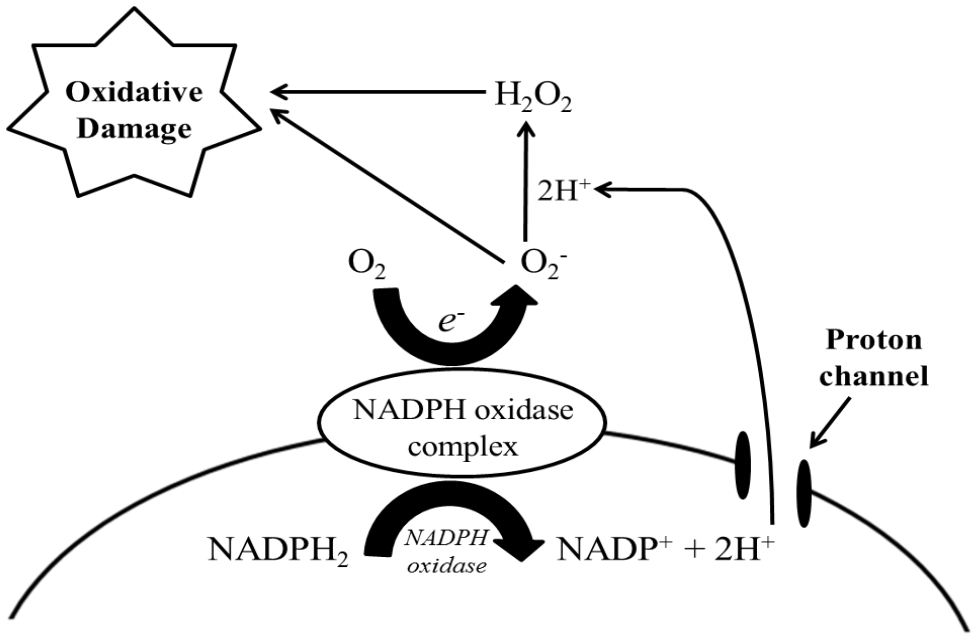

Figure 1.6. Generalised representation of the respiratory burst mechanism, modified from Parihar *et al*. (2008). NADPH oxidase is located in the cell membrane and transports electrons across the membrane to produce large amounts of reactive oxygen species. NADPH = nicotinamide adenine dinucleotide phosphate, e^- = electrons, O_2 = oxygen, O_2^- = superoxide anion, H_2O_2 = hydrogen peroxide.

The SGCs and GCs contribute to the majority of the crab's innate immune responses through a process of regulated exocytosis, commonly termed degranulation. A generalised scheme of the central role that degranulation plays in the immune responses of the crab is shown below in Figure 1.7.

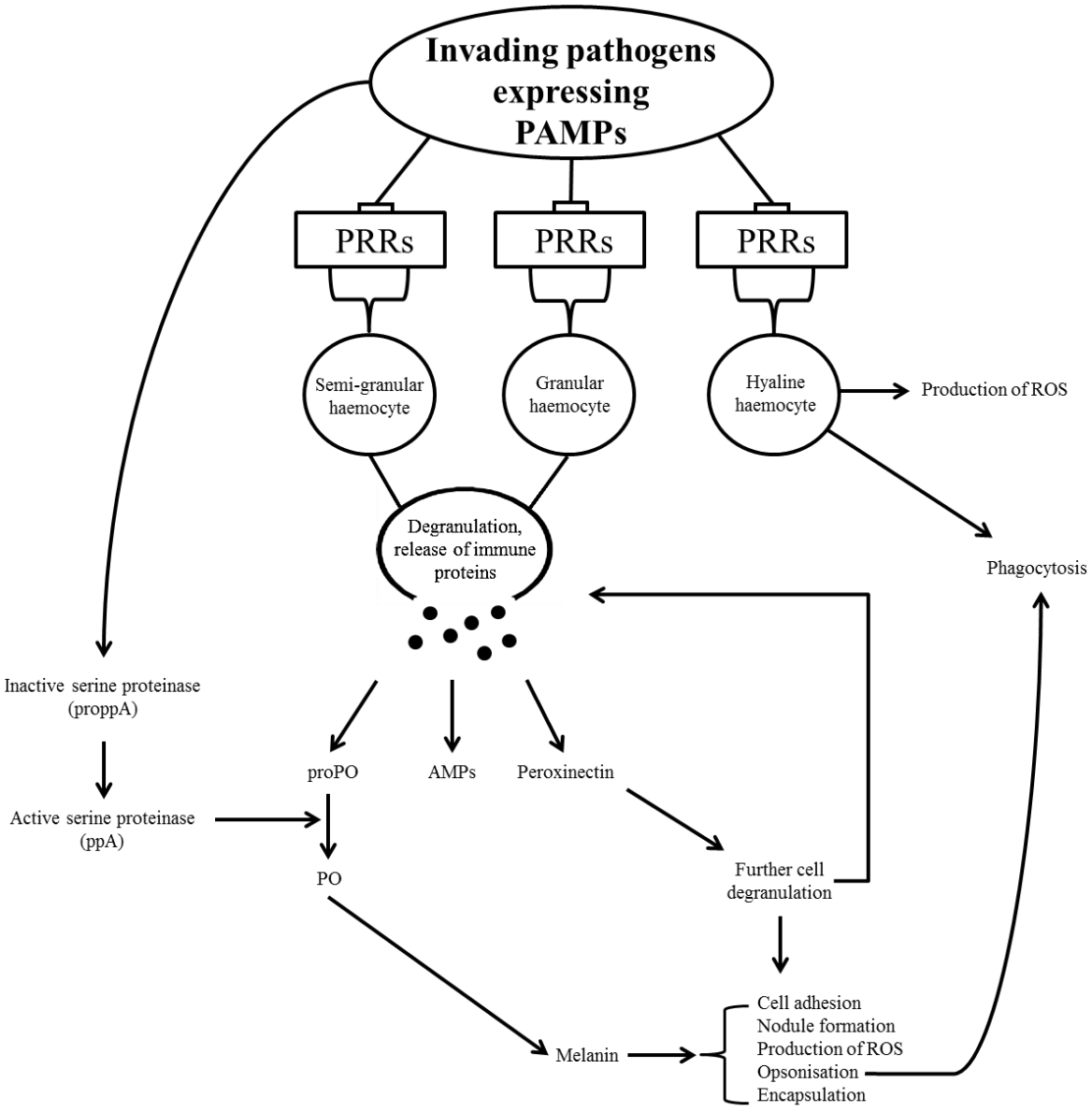

Figure 1.7. An overview of the cellular immune responses in *C. maenas*, modified from Smith *et al*. (2003), during which degranulation plays a central role.
PAMPs = pathogen associated molecular patterns, PRRs = pattern recognition receptors, ROS = reactive oxygen species, proPO = prophenoloxidase, PO = phenoloxidase, AMPs = antimicrobial peptides.

Haemocytes containing intracellular refractive granules are extremely labile, rapidly undergoing degranulation or lysis *in vitro* (Smith and Ratcliffe, 1978), with degranulation occurring at an overall much higher rate than HC phagocytosis. The SGCs invariably die (Söderhäll and Smith, 1983) but the GCs may survive in a degranulated form for at least a short while (Söderhäll and Smith, 1983). The release of peroxinectin (PXN) (which facilitates encapsulation responses), AMPs and prophenoloxidase (proPO) (pro-enzyme required for initiation of the proPO system) from the SGCs and GCs is achieved through degranulation.

A key mechanism in which decapods deal with bacteria or other infective agents is by encapsulation reactions. These reactions are mediated by the release of the cell adhesion peroxidase protein, PXN. PXN is a crustacean homologue of human myeloperoxidase, which is released from the haemocytes and enables the haemocytes within the capsule to stick together (Johansson *et al*., 1995). Briefly, encapsulation entails the migration and adherence of haemocytes to a focus of infection, forming layers of cells around the foreign material. As the layers build up the capsule forms and the matrix material becomes blackened due to the deposition of melanin. In *C. maenas*, the HCs, SGCs and GCs all participate in encapsulation/clumping (adhesion) reactions (Smith and Ratcliffe, 1980a). In crustaceans, capsules usually lodge in the haemal sinuses, for example the gill filaments, from where they are cast with the gills at the moult (Smith and Ratcliffe, 1980a, 1980b; Smith *et al*., 1984). The formation of capsules/clumps is usually accompanied by a reduction in the number of circulating haemocytes, a condition known as haemocytopenia (Smith, 2010). Haemocyte numbers then re-enter circulation from either the haematopoietic tissue (where new haemocytes are produced during haematopoiesis), mobilisation from blood sinuses or by proliferation of ProHs within the haemolymph itself (Hammond and Smith, 2002; Söderhäll *et al*., 2003). It has long been assumed that the death of the haemocytes within the capsule is necrotic. No studies have been carried out to ascertain whether the encapsulation response involves apoptosis, apoptotic-like phenomena or ETosis.

1.7.4. Soluble immune effectors

AMPs can be synthesized at low metabolic cost and rapidly diffuse to the point of infection (Zasloff, 1992) where they aid in the killing of microbial pathogens. In *C. maenas*, antibacterial activity resides exclusively in the SGCs and GCs (Chisholm and Smith, 1992) and the AMPs are synthesized and stored within the intracellular refractive secretory granules. The SGCs and GCs contribute AMPs (primarily proline-rich or cysteine-rich peptides) to the capsule matrix where they help to kill pathogens localised within the matrix and in the close vicinity (Smith, 2010). AMPs active against Gram-positive and/or Gram-negative bacteria have been isolated from GCs of *C. maenas*. The first was a proline-rich 6.5 kDa peptide (Schnapp *et al*., 1996), followed by the first crustin (a family of AMPs confined to Crustacea). This crustin is an cysteine-rich 11.5 kDa AMP active against Gram-positive bacteria only (Relf *et al*., 1999) and later designated carcinin (Smith and Chisholm, 2001). Additionally, proline rich AMPs have also been isolated from the spider crab, *Hyas araneus*, namely arasin (Stensvag *et al*., 2008), hyasin-1 and hyasin-2 (Sperstad *et al*., 2009a) as well as the glycine rich AMP hyastatin (Sperstad *et al*., 2009b). Currently, over 50 crustin sequences have been reported for a variety of marine decapod crustacean species (Smith *et al*., 2008), including shrimp such as *Litopenaeus vannamei* and *L. setiferus* (Bartlett *et al*., 2002), *Marsupenaeus japonicas* (Ratanachai *et al*., 2004), *Fenneropenaeus chinensis* (Zhang *et al*., 2007) and *Penaeus monodon* (Supungul *et al*., 2004; Amparyup *et al*., 2008), as well as the European lobster, *Homarus gammarus* (Hauton *et al*., 2006) and the signal crayfish, *Pacifastacus leniusculus* (Jiravanichpaisal *et al*., 2007).

The SGCs and GCs also release enzymes and other proteinaceous factors (via degranulation) that lead to melanisation (Smith and Ratcliffe, 1980a, 1980b; Smith *et al*., 1984). These molecules are collectively known as the proPO activating system because they lead to the activation of the pro-enzyme proPO that through a series of steps converts quinones into insoluble melanin (Smith and Söderhäll, 1991, 1983a; Söderhäll, 1982; Söderhäll *et al*., 1994). In *C. maenas*, this complex enzyme system is present only in the granular haemocytes (Söderhäll and Smith, 1983). A key component generated through proPO activation is PXN, which acts as an opsonin

during phagocytosis and in promotion of haemocyte encapsulation of foreign material (Thörnqvist *et al*., 1994). A simplified summary of the proPO system is shown below in Figure 1.8.

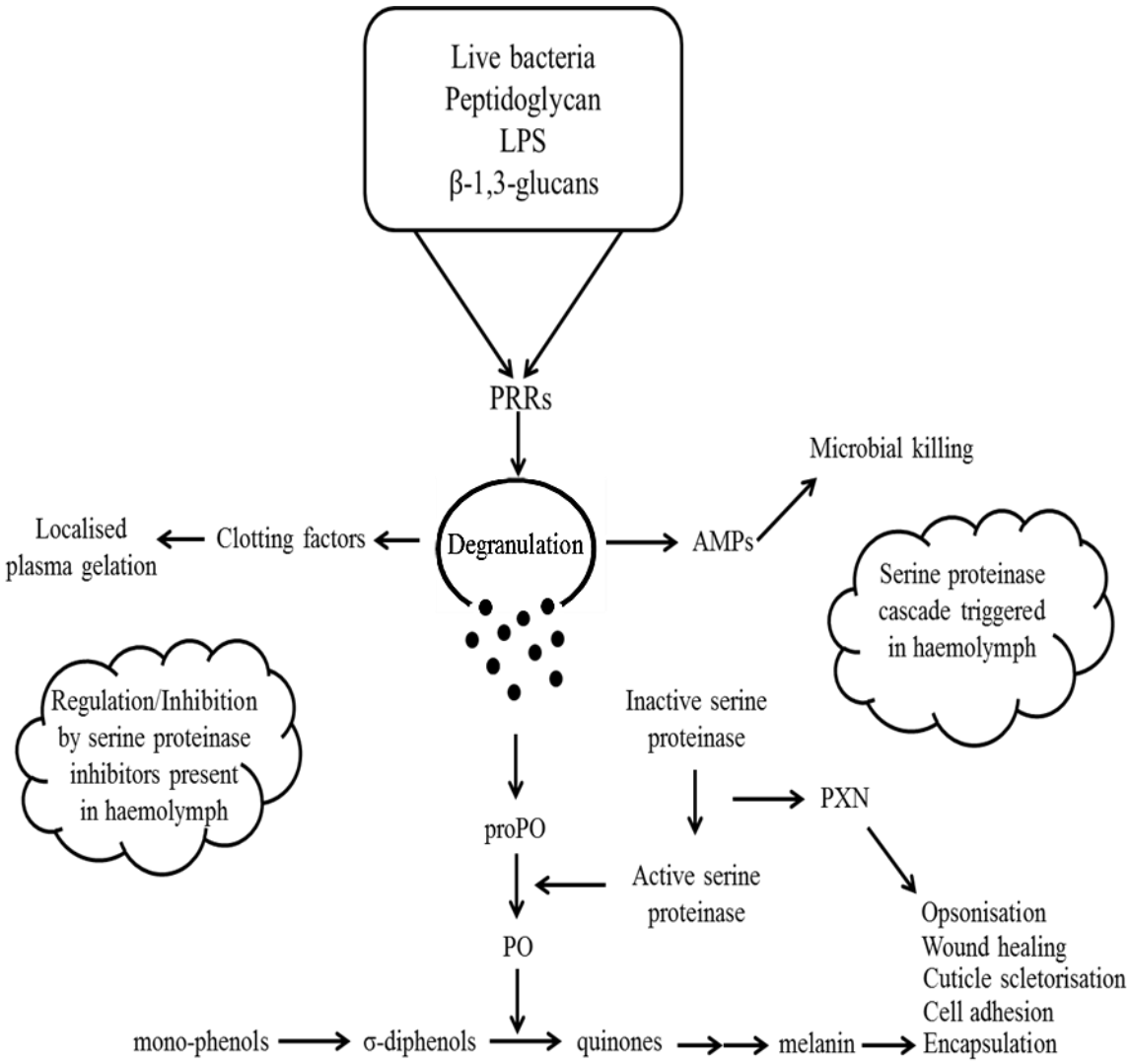

Figure 1.8. A simplified representation of the prophenoloxidase activating system in crustaceans. PRRs = pattern recognition receptors, AMPs = antimicrobial peptides, proPO = prophenoloxidase, PO = phenoloxidase, PXN = peroxinectin.

1.8. Hypothesis and scientific aims

Given the lack of knowledge and detailed information upon apoptosis and ETosis in invertebrates, the shore crab, *C. maenas* was used as an experimental model to investigate these cell death phenomena.

The hypothesis of this study is that haemocytes from *C. maenas* undergo evolutionary conserved regulated apoptotic and ETotic cell death. The broad aims of this study are to identify and describe at least two cell death processes in the shore crab, *C. maenas*, and investigate their role(s) in the immune response of this animal.

Specifically the objectives are:

1. To compare standard methods for the detection and validation of apoptosis in washed mixed haemocyte populations from *C. maenas*.

2. To investigate the role of apoptosis in host protection by quantifying apoptosis in washed mixed haemocyte and separated haemocyte populations from *C. maenas* under various life conditions, such as temperature and natural infection using flow cytometry.

3. To characterise ETosis in separated hyaline haemocytes from *C. maenas* thus demonstrating ETosis for the first time in any invertebrate.

4. To investigate the role of ETosis as part of the immune response in *C. maenas*, and to implicate its role with regard to host protection *in vivo*.

5. To gain insight into the phylogeny of ETosis by undertaking preliminary investigations into ETotic-type phenomenon in immune cells from other invertebrates, specifically in the blue mussel, *Mytilus edulis*, and the sea anemone, *Actinia equina*.

Chapter 2

Validation of apoptosis and comparison of methods

2.1. Introduction

Since the discovery of apoptosis by Kerr *et al*. (1972), a multitude of studies elucidating the role of apoptosis in immunity have transpired, with many methods for its detection established. Surprisingly however, there has been a paucity of invertebrate studies investigating the role of apoptosis in immunity until recently. With regard to 'shrimp apoptosis', between the years 1990-1999 there were just 3 publications, whereas between the years 2000-2009 and 2010-2015 there were 76 and 132 publications respectively (Web of Science, January, 2015). Such recent publication increases, many of which were gene-related studies, were likely influenced by the severe impact viral diseases such as the white spot syndrome virus (WSSV) have upon shrimp aquaculture (Smith *et al*., 2010).

The majority of cellular investigations in crustaceans have been observational, with only a relatively small number including quantification of apoptosis (e.g. Hameed *et al*., 2006; Hernroth *et al*., 2012). Furthermore, most have avoided the validation regarded as essential in mammalian immunology or endeavoured to test experimental or natural inducers/inhibitors of apoptosis (Smith *et al*., 2010). Lately, studies at the molecular level have increased, with several genes relating to apoptosis and its' regulation identified in shrimp that have homology with mammalian genes (Table 2.1). These include those involved in the execution pathway of apoptosis (e.g. caspase-3) as well as those contributing to regulation (e.g. fortilin). However, there are limitations to the 'boom' of apoptosis-related gene studies in shrimp which have emerged since 2010. The majority of gene expression studies are based on short sequences and, *in vivo*, a great deal remains unknown as these studies did not relate gene expression to true functionality *in vivo*. Therefore, such gene expression studies are not overly informative.

As apoptosis is a complex, multi-stage process, it is widely acknowledged in mainstream immunology that before any quantification is attempted, it is essential that apoptosis is validated using at least two different assays, ideally based on different aspects of apoptosis (Elmore, 2007). However, some crustacean studies claim to have validated apoptosis in mixed haemocyte populations yet use only one assay (Granja *et al*., 2003; De

Guise *et al*., 2005; Wang and Zhang, 2008; Hernroth *et al*., 2012) or investigate a single aspect with two assays (Sahtout *et al*., 2001; Hameed *et al*., 2006; Oweson *et al*., 2006). One example where more than one aspect of apoptosis was investigated using more than two detection methods is Khanobdee *et al*. (2002) who observed histological, cytochemical and ultrastructural changes during apoptosis in the haemocytes, lymphoid organs and gills of *P. monodon*. Here, apoptosis was validated by the use of TUNEL, DAPI staining, DNA laddering and transmission electron microscopy. However, such an approach has been rare in crustacean research.

It is therefore important to thoroughly validate apoptosis in a crustacean model before any subsequent quantification attempts in a novel species, and also to distinguish apoptosis from other separate cell death processes, such as necrosis, autophagy and ETosis (Smith *et al*., 2010). Therefore, to increase knowledge about apoptosis at the cellular level in decapod crustaceans, an investigation was undertaken in an attempt to validate apoptosis in haemocytes from the shore crab *C. maenas*, using several methods of detection, based on different aspects (summarized in Table 2.2).

The hypothesis is that haemocytes from *C. maenas* undergo classical caspase-dependent apoptosis that can be detected using numerous methods.

Specifically the objectives of this chapter are:

1. To validate apoptosis in *C. maenas* haemocytes testing various detection methods based on different aspects, which include microscopy (such as light, fluorescence, confocal and electron microscopy), DNA fragmentation and flow cytometry.

2. To assess and compare the applicability of each apoptosis detection method for quantification purposes.

3. To test different inducers of apoptosis commonly used with mammalian cells and to confirm caspase-dependent cell death using the pan-caspase inhibitor, Q-VD-OPh.

Table 2.1. Summary of apoptosis-related genes identified from crustaceans.

Species	Apoptosis-related genes
Penaeus monodon (black tiger shrimp)	**Fortilin** (Li *et al*., 2001; Graidist *et al*., 2006) **Alix/AIP** (Sangsuriya *et al*., 2007) **Caspase-3** (Wongprasert *et al*., 2007) ***P. monodon* inhibitor of apoptosis protein** (Leu *et al*., 2008) **Ribophorin I** (Molthathong *et al*., 2008a) **DAD1** (Molthathong *et al*., 2008b) **Cathepsin C** (Qiu *et al*., 2008) **Programmed cell death 6-interacting protein** (Rajesh *et al*., 2012) **Cathepsin B & Endonuclease G** (Kuruthika *et al*., 2013)
Litopenaeus vannamei (Pacific white shrimp)	**Caspase-3** (Chang *et al*., 2008, 2009) ***L. vannamei* inhibitor of apoptosis protein 1** (Leu *et al*., 2012) **Caspase-3 & Cathepsin B** (Guo *et al*., 2013)
Penaeus japonicus (kuruma prawn)	**Caspase-3** (Pan *et al*., 2005, Wang *et al*., 2008) **Cellular apoptosis susceptibility protein** (Pan *et al*., 2005)
Penaeus merguiensis (banana shrimp)	**Caspase-3** (Phongdara *et al*., 2006)
Fenneropenaeus chinensis (Chinese shrimp)	***Fenneropenaeus chinensis* caspase** (Wang *et al*., 2011a)
Eriocheir sinensis (Chinese mitten crab)	**Cathepsin C & Cathepsin L** (Li *et al*., 2010a,b) ***Eriocheir sinensis* caspase** (Jin *et al*., 2011) **nm23** (Jin *et al*., 2011) **p53** (Hou and Yang, 2013)
Cherax quadricarinatus (red claw crayfish)	**Apoptosis-linked gene 2** (Liu *et al*., 2011)

Table 2.2. Summary of methods used in the present study.

Detection method	**Features**	**Key reference(s)**
Brightfield microscopy	Stains such as Diff-Quik™ used to visualize early apoptosis (membrane blebbing, irregular shaped nuclei) and late apoptosis (cytoplasmic vacuolation, nuclear fragmentation and apoptotic body formation).	Savill *et al*., 1989
Fluorescence microscopy	Stains such as DAPI reveal irregular shaped nuclei in early apoptotic cells.	Jurisicova *et al*., 1996
Transmission electron microscopy	Features of early and late apoptosis visualized in detail at the ultrastructural level, including chromatin condensation.	Kerr *et al*., 1972
DNA fragmentation	Separated DNA fragments revealed by staining on agarose gel. Indicates late stage apoptosis resulting from activity of endogenous endonucleases and subsequent cleavage of DNA into inter-nucleosomal fragments.	Wyllie, 1980
MitoCapture assay	Identifies alterations in mitochondrial transmembrane potential associated with early apoptotic cells.	Ogawa *et al*., 2001
AV-FITC/B-lactadherin-FITC and PI staining	AV and B-lactadherin bind to PS after translocation to outer membrane leaflet, characteristic of early apoptotic cells (FITC +ve and PI –ve). Identifies late apoptotic/necrotic cells as FITC +ve and PI +ve, when cell membrane integrity lost, thus PI penetrates and stains nucleus. Can be visualized and counted by fluorescence/confocal microscopy or objectively quantified by flow cytometry.	Koopman *et al*., 1994 Shi *et al*., 2006
Hypodiploid peak assay	Detects cells exhibiting low DNA content (hypodiploid cells) arising from DNA fragmentation (late stage apoptosis). Quantified by flow cytometry.	Nicoletti *et al*., 1991

Abbreviations: AV-FITC = annexin V-fluorescein isothiocyanate, B-lactadherin-FITC = bovine lactadherin-fluorescein isothiocyanate, DAPI = 4′,6′-diamidino-2-phenylindole dihydrocholride, PI = propidium iodide.

2.2. Materials and methods

2.2.1. Reagents and solutions

Unless otherwise specified, all reagents throughout this study were purchased from Sigma Aldrich (Poole, Dorset, UK) with solutions prepared under sterile conditions and filtered through a 0.22 µm cellulose nitrate membrane filter.

2.2.2. Crabs

Specimens of *C. maenas* were collected from the Firth of Forth estuary (Edinburgh, Scotland). The crabs were maintained in an aerated re-circulating seawater system (~32‰) at a temperature of 12 ± 2°C. All crabs were acclimated for 2 weeks and during this time were fed twice per week with trout feed pellets. Only healthy intermoult adult crabs (carapace widths between 60-90 mm), with no missing limbs, carapace lesions or gross signs of disease were chosen for experimental purposes.

2.2.3. Haemolymph sampling

Prior to bleeding, *C. maenas* individuals were pre-chilled for 10 min and the area to be bled swabbed with 96% ethanol. Using a 23G 1.25" needle, approximately 1 mL haemolymph was withdrawn from the unsclerotised membrane between the merus and the carpus of a cheliped into a 2.5 ml sterile syringe containing 1.5 mL ice-cold marine anticoagulant (MAC: 0.45 M NaCl, 0.1 M glucose, 30 mM trisodium citrate, 26 mM citric acid, 10mM EDTA; pH 4.6; Söderhäll and Smith, 1983). The diluted haemolymph was then centrifuged (5 min at 500 x g, 4°C) and the supernatant discarded, with the haemocytes either used immediately or washed twice (5 min at 500 x g, 4°C) with 3.2% NaCl and resuspended in salt-modified Leibovitz's L-15 medium (ML-15), (pH 7.4), supplemented with 0.4 M NaCl + 1 % penicillin-streptomycin (100 U/100 µg mL^{-1}). For some experiments, haemocytes were resuspended in *Carcinus* saline (CS: 0.58 M NaCl, 13 mM KCl, 13 mM $CaCl_2.6H_2O$, 26 mM $MgCl_2.6H_2O$, 0.5 mM $Na_2HPO_4.12H_2O$, 50 mM TRIS; pH 7.4; Smith and Ratcliffe, 1978).

2.2.4. *In vitro* haemocyte culture

Assays were performed using mixed haemocytes cultured in suspension in sterile 15 mL plastic Falcon tubes. Approximately 2 mL mixed haemocytes (2 x 10^6 mL^{-1} final concentration, with haemocytes counted using an improved Neubauer chamber) were used with ML-15 as the culture medium, and cultured at 10°C unless otherwise stated. These conditions have previously been shown to be suitable for short/medium term culture of crab haemocytes *in vitro* (Walton and Smith, 1999; Sperstad *et al*., 2010). Moreover, this temperature is comparable to both the aquarium temperature and the middle of the crabs' physiological tolerated range (Cohen *et al*., 1995).

For some experiments, haemocyte monolayers were used instead of suspension cultures following the approach first described for crab haemocytes by Smith and Ratcliffe, (1978). In the present study 10 mm diameter circular glass coverslips were placed in wells of 24-well flat bottomed tissue-culture plates (Costar) for fluorescence microscopy. Alternatively, 42 mm diameter circular glass coverslips were placed in a secure cell chamber system (45 mm) (Helmut Saur, Laborbedarf) for confocal microscopy. When using 24-well plates, 1 mL freshly harvested and washed haemocytes resuspended in ML-15 or CS were added to each well at a final concentration of 5 x 10^4/well. The haemocytes were then left for 1 h at 10°C to allow attachment to the coverslips. After 1 h, ML-15 or CS was removed and the haemocytes washed twice in 1 mL of 3.2% NaCl. Next, 500 µL of fresh ML-15 or CS was added to the haemocyte monolayers which were incubated at 10°C or 20°C. When using the secure cell chamber, approximately 2 mL freshly harvested and washed haemocytes were resuspended in CS at a concentration of 5 x 10^4 mL^{-1}, and added to the coverslip at a total concentration of 1 x 10^5 haemocytes. The haemocytes were then left for 1 h at 10°C (as above) after which the CS was removed and the haemocytes washed twice in 2 mL of 3.2% NaCl, before the addition of 2 mL fresh CS.

2.2.5. Detection of apoptosis

2.2.5.1. Light microscopy

A 200 µL haemocyte sample (*ca*. 4 x 10^5 cells) plus 200 µL MAC was added per funnel of a Shandon Cytospin 3 cyto-centrifuge. Samples were centrifuged at 7 x g for 3 min (low acceleration) then left at room temperature to dry. The haemocytes were fixed/permeabilised with absolute methanol for 1 min and then stained with Diff-Quik™ (Gamidor, Didcot, UK) red for 1.5 min, then blue for 1 min, (Romanowsky stain variant), or with Wright's stain for 1.5 min. Each slide was mounted in DePeX mounting medium and examined with a light microscope (Olympus, BX40) to discern characteristic features of apoptotic cells such as karyorrhexis (nuclear fragmentation), irregular shaped nuclei and membrane blebbing.

2.2.5.2. Fluorescence microscopy

DAPI staining

Monolayer haemocyte cultures were set up on 10 mm diameter circular glass coverslips in wells of a 24-well plate as above (Section 2.2.4) and stained with 4′,6-diamidino-2-phenylindole dihydrochloride (DAPI). After culture for 6 h in ML-15 (10°C) on coverslips, haemocytes were fixed in 4% paraformaldehyde (PFA) in 2% NaCl for 30 min and then washed twice in phosphate buffered saline (PBS). The fixed haemocytes were then permeabilised with 0.01% Triton X-100 for 30 min and washed twice again in PBS before staining with 1 µg mL^{-1} DAPI (30 min) to allow detection of apoptotic irregular shaped nuclei (Jurisicova *et al*., 1996). Lastly, the haemocytes were washed twice in PBS and each coverslip mounted onto a glass slide with 1.5 µL Vectasheild™ mounting media (Vector Laboratories, Peterborough, UK). The slides were then examined under short wave length light (excitation 358 nm and emission 461 nm) with a Zeiss Axiophot fluorescence microscope. One crab was sampled per experimental run with duplicate coverslips mounted after culture.

MitoCapture Apoptosis Detection Kit

Monolayer haemocyte cultures were set up on 10 mm diameter circular glass coverslips in wells of a 24-well plate as above (Section 2.2.4) and stained according to manufacturer's instructions using the MitoCapture Apoptosis Detection Kit (Millipore). The MitoCapture Apoptosis Detection Kit was used in an attempt to assess apoptosis initiated via the intrinsic pathway (Ogawa *et al*., 2001). This kit utilises a cationic dye that exhibits distinct fluorescence in viable cells versus apoptosis cells. In viable cells, the dye accumulates and aggregates in the mitochondria, giving off a bright red/orange fluorescence. This is due to an un-altered mitochondrial transmembrane potential (i.e. $\Delta\Psi_{m\ stable}$ cells). In apoptotic cells, the dye cannot aggregate in the mitochondria due to the altered mitochondrial transmembrane potential (i.e. $\Delta\Psi_{m\ unstable}$ cells), and thus remains in the cytoplasm in its monomer form, generating a green fluorescence. Alteration and disruption of the mitochondrial transmembrane potential is one of the earliest intracellular events that occur following the induction of apoptosis.

Haemocytes were cultured for 24 h in CS at 10°C (control) or room temperature (*ca*. 18-20°C) to maximise cell death. After culture haemocytes were stained for 20 min (20°C) with MitoCapture dye, made up as appropriate according to manufacturer's instructions (1 µL dye added to 1 mL pre-warmed incubation buffer). After incubation with the dye, each coverslip was mounted onto a glass slide with 1.5 µL Vectasheild™ mounting media. The slides were then examined immediately using a Zeiss Axiophot fluorescence microscope as above. The fluorescein isothiocyanate (FITC) channel was used for the detection of green monomers (apoptotic cells) (excitation 488 nm and emission 518 nm) whereas the propidium iodide (PI) channel was used for the detection of red aggregates (viable cells) (excitation 540 nm and emission 617 nm). One crab was sampled per experimental run with duplicate coverslips mounted after culture.

2.2.5.3. Confocal microscopy

To visualise apoptosis in real time, a monolayer culture of mixed haemocytes obtained from a single crab were subject to live cell imaging using a Leica (DMIRE2) TCS2 confocal microscope (Leica Microsystems, Milton Keynes, UK). Approximately 2 mL freshly isolated and washed haemocytes resuspended in CS were added to a sterile 42 mm diameter circular glass coverslip held in a secure cell chamber system as above (Section 2.2.4) to give a concentration of 1 x 10^5 haemocytes on the coverslip. After 1 h (10°C) to allow the haemocytes to attach to the glass slide, the media was removed and the haemocytes washed as above (Section 2.2.4). Next, after the addition of 2 mL fresh CS, 10 µL of stock bovine lactadherin (1.6 µM) conjugated with FITC (Cambridge Bioscience) (excitation 488 nm and emission 518 nm) was added to the haemocytes and left for a further 10 min on ice protected from light. Immediately before confocal examination, 4 µL of PI (1 mg mL^{-1}) (excitation 540 nm and emission 617 nm) was also added to the haemocytes. The haemocytes in the cell chamber were then examined by a confocal microscope set on time-lapse mode to take still images every 90 sec with phase contrast transmission overlay for a total of 3 h 30 min at 15°C (temperature in microscopy suite). The image sequence was then imported to ImageJ™ (National Institutes of Health) and converted to video format (avi) and un-cropped (supplementary video 1) and cropped (supplementary video 2) time-lapse videos produced to show, in real-time, the progression of viable haemocytes (FITC-negative and PI-negative) into early apoptosis (FITC-positive and PI-negative) and late apoptosis/necrosis (FITC-positive and PI-positive). After 6 h total culture, additional snapshot images were taken at different areas of the cell chamber with/without phase contrast transmission in order to show the proportions of viable, early apoptotic, and late apoptotic/necrotic haemocytes judged from differences in fluorescent FITC and PI staining patterns (Vermes *et al*., 1995; Chiruvella *et al*., 2008).

2.2.5.4. Transmission electron microscopy

After 24 h culture at room temperature (*ca*. 18-20°C) to maximise cell death, haemocytes from a single crab were fixed in an equal volume of 2.5% glutaraldehyde in 0.1 M sodium cacodylate buffer (pH 7.2) for 24 h. The cells were then centrifuged for 10 min at 800 x g and the haemocyte pellet resuspended in 2 mL of 0.1 M sodium cacodylate

buffer. The sample was then processed for transmission electron microscopy by Mr Stephen Mitchell (Bio-imaging Facility, Edinburgh University). Briefly, after 3 x 10 min washes in fresh buffer, the cells were post-fixed in 1% osmium tetroxide in 0.1 M sodium cacodylate (45 min) and washed thrice as before. The samples were then dehydrated in 50%, 70%, 90% and 100% normal grade acetone for 10 min each, followed by a further 2 x 10 min washes in analar acetone before embedding in araldite resin. Sections of 1 μm thickness were cut with a Reichert OMU4 ultramicrotome (Leica Microsystems, Milton Keynes, UK), stained with toluidine blue and viewed under a light microscope (Olympus, BX40) to select suitable areas for investigation. Ultrathin sections (60 nm thickness) were stained in uranyl acetate and lead citrate modified from the procedure described by Reynolds (1963), and the apoptotic haemocytes viewed using a Phillips CM120 transmission electron microscope (FEI, Cambridge, UK).

2.2.5.5. DNA fragmentation

Following 24 h suspension culture at room temperature (*ca*. 18-20°C), 1 mL from the haemocyte sample was removed from the suspension culture and transferred to an Eppendorf tube for DNA extraction and further processing using a commercial 'Apoptosis DNA Ladder Kit' (Roche, Burgess Hill, UK) following the manufacturer's instructions. As a control, DNA was extracted from haemocytes at 0 h. After DNA isolation, 10 μL of the haemocyte DNA was mixed with 10 μL gel loading buffer and added to the appropriate wells of a 1 % agarose gel. An extra well was set up as a positive control using fragmented DNA supplied from the kit. In addition, 5 μL HyperLadder I (Bioline) was added to another well to enable DNA fragment sizes to be determined. The gel was then subjected to electrophoresis at 75 v for 1.5 h, and after staining with ethidium bromide, was viewed under transmitted UV light. Duplicate cyto-centrifuge preparations (Section 2.2.6) were also made from the haemocyte suspensions at 0 h and after 24 h culture to compare viable and apoptotic haemocytes by microscopy.

2.2.6. Quantification of apoptosis

2.2.6.1. Microscopy

To quantify apoptosis with different stimuli, haemocytes were incubated either at 20^{o}C, (a high temperature at the upper limit of the shore crabs' physiological range) or at 10^{o}C with two biochemical apoptosis inducers commonly used with mammalian neutrophils. The inducers were the fungal metabolite and nuclear factor kappa-light-chain-enhancer of activated B cells (NFκB) inhibitor, gliotoxin (Ward *et al*., 1999), and the cyclin-dependent kinase (CDK) inhibitor, R-roscovitine (Rossi *et al*., 2006; Leitch *et al*., 2010, 2012), used in the present study at final concentrations of 10 µg mL^{-1} and 10 µM, respectively. One crab was sampled per experimental run with triplicate preparations made at 0 h, 6 h and 24 h. Controls were incubated at 10^{o}C with ML-15 substituted for gliotoxin or roscovitine.

Using either Diff-Quik™ stained cyto-centrifuge preparations or DAPI stained monolayer cultures, percentages of viable and apoptotic haemocytes were calculated from counts of a minimum of 200 haemocytes counted over a minimum of 3 fields of view (FoV).

2.2.6.2. Flow cytometry with bovine lactadherin-FITC and PI staining

Apoptosis was stimulated in suspension cultures (2 mL) of washed mixed haemocytes (2 x 10^{6} mL^{-1}) at 20°C as above (Section 2.2.6.1). To confirm that the apoptosis was caspase-dependent, haemocytes were pre-treated for 1 h (20°C) with the pan-caspase inhibitor, N-(2-quinolyl)-L-valyl-L-aspartyl-(2,6-difluorophenoxy)-methylketone (Q-VD-OPh) at a final concentration of 10 µM (Caserta *et al*., 2003). The haemocytes were then cultured for 6 h and values for viable, early apoptotic and late apoptotic/necrotic haemocytes determined by flow cytometry. For analysis, after gentle re-suspension, 200 µL haemocytes from each suspension culture were added to 800 µL of ML-15 in a flow-cytometry tube (Sarstedt) and kept on ice. Next, 4 µL of stock bovine lactadherin-FITC (1.6 µM) (Shi *et al*., 2006) was added to the samples and allowed to stand on ice for 10 min protected from the light. Immediately before running the haemocyte sample through the flow cytometer (Partec, CyFlow), 2 µL of PI (1 mg mL^{-1})

was added. Gating was used to distinguish percentages of viable (FITC-negative and PI-negative), early apoptotic (FITC-positive and PI-negative) and late apoptotic/necrotic haemocytes (FITC-positive and PI-positive) (Koopman *et al*., 1994; Homburg *et al*., 1995; Vermes *et al*., 1995). Throughout this study, FITC-negative and PI-positive events were not considered routinely as this staining pattern can represent either cellular debris or bare nuclei in the very late stages of necrosis (Zali *et al*., 2008; Wang *et al*., 2011b) with destroyed cell membranes (Bauriedel *et al*., 1999), hence making discrimination of cellular nuclei from cellular debris very difficult. Moreover, throughout this study, percentages of FITC-negative and PI-positive events were persistently very low (normally between 1-2% and at most <5%). The FITC fluorescence signal was measured at 520 nm (FL1) and the PI fluorescence signal measured at 630 nm (FL3). The data were analysed using FloMax™ software integral to the machine. One crab was sampled per experimental run with triplicate flow samples carried out after culture.

2.2.6.3. Flow cytometry - hypodiploid peak assay

A second flow cytometric assay, the hypodiploid peak assay (Nicoletti *et al*., 1991), was assessed for evaluating apoptosis by crab haemocytes in suspension culture (2 mL). Apoptosis was stimulated in washed haemocytes (2×10^6 mL^{-1}) by incubation at 20°C as above (Section 2.2.6.1) and percentages of apoptosis determined from PI staining by flow cytometry after 0 h (control) and 24 h culture. After gentle re-suspension, 200 µL of *C. maenas* haemocytes, cultured in ML-15, were added to a flow cytometer tube containing 800 µL of PI solution (50 µg mL^{-1} PI; 0.1% sodium citrate; 0.1% Triton X-100) (Lee *et al*., 2013) and incubated in the dark at 4°C for 20 min. Fragmented DNA in apoptotic haemocytes appeared as a broad hypodiploid peak (Nicoletti *et al*., 1991; Riccardi and Nicoletti, 2006) before the narrow peak of viable haemocytes with normal DNA content (diploid haemocytes), and were gated to measure apoptosis as a percentage. One crab was sampled per experimental run with triplicate flow samples and duplicate cyto-centrifuge preparations (Section 2.2.6) carried out after culture.

2.2.7. Statistical analyses

All values were calculated as mean percentage ± standard error of the mean (SEM), and percentage values arc sine transformed before statistical analysis. Statistical differences were determined using either one-way ANOVA or a paired *t* test via InStat™ statistical software (GraphPad, San Diego, USA). Significance was accepted at $P<0.05$. Where ANOVA revealed a probability of $P<0.05$ a Student-Newman-Keuls multiple comparison *post-hoc* test was subsequently applied.

2.3. Results

2.3.1. Detection of apoptosis

2.3.1.1. Light microscopy

Characteristic features of apoptosis such as karyorrhexis, cytoplasmic vacuolation, irregular shaped nuclei and membrane blebbing were observed in haemocytes after 6 h (Figure 2.1, A-D) and 24 h (Figure 2.2, A-D) culture, predominantly in the hyaline haemocytes. These morphological changes were observed in haemocytes cultured at room temperature (*ca*. 18-20°C) overnight (Figures 2.1 and 2.2, B), and in the presence of gliotoxin (Figures 2.1 and 2.2, C) or R-roscovitine, where the haemocytes were cultured at 10°C (Figures 2.1 and 2.2, D). Control haemocytes cultured at 10°C appeared morphologically viable after 6 h (Figure 2.1, A) and 24 h culture (Figure 2.2, A).

2.3.1.2. Fluorescence microscopy

DAPI staining

Viable control haemocytes exhibited circular shaped (intact) nuclei (Figure 2.3, A and B). Characteristic irregular shaped nuclei were observed in gliotoxin-induced apoptotic haemocytes (Figure 2.3, C and D).

MitoCapture Apoptosis Detection Kit

Using this kit very few viable or early apoptotic haemocytes were detectable at the PI or FITC emission wavelengths respectively. Moreover, in haemocytes that were detected, staining was poorly localised in the mitochondria of viable haemocytes or the cytoplasm of early apoptotic haemocytes, and as a result were barely visible. Therefore, data was not shown.

Figure 2.1.

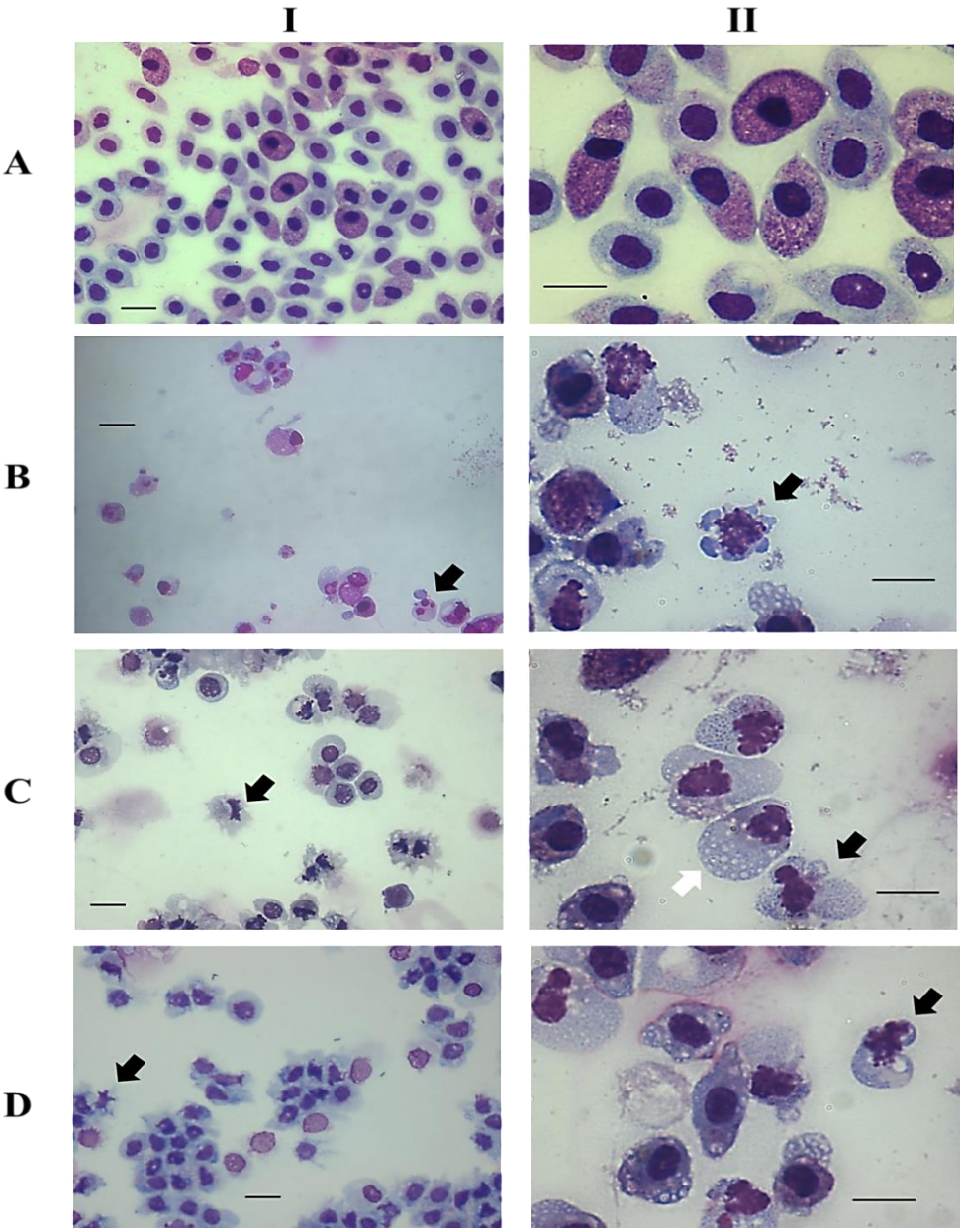

Figure 2.1. Light microscopy analysis of cyto-centrifuge preparations showing mixed haemocytes from *C. maenas* after 6 h suspension culture *in vitro*.
Haemocytes were either stained with Diff-Quik™ (**B**, **I**) or Wright's stain (all other images). (**A**): 10°C (control); (**B**): 20°C; (**C**): 10 µg mL^{-1} gliotoxin (10°C); (**D**): 10 µM R-roscovitine (10°C). Arrows indicate characteristic features of apoptosis such as karyorrhexis (**B, I**), cytoplasmic vacuolation (**C, II,** white arrow), irregular shaped nuclei (**C, D, I**), and membrane blebbing (**B, C, D, II,** black arrows). Cyto-centrifuge preparations at 200x total mag (**I**) or 630x total mag (**II**) and are representative of n=3 experiments. Scale bars = 15 µm.

Figure 2.2.

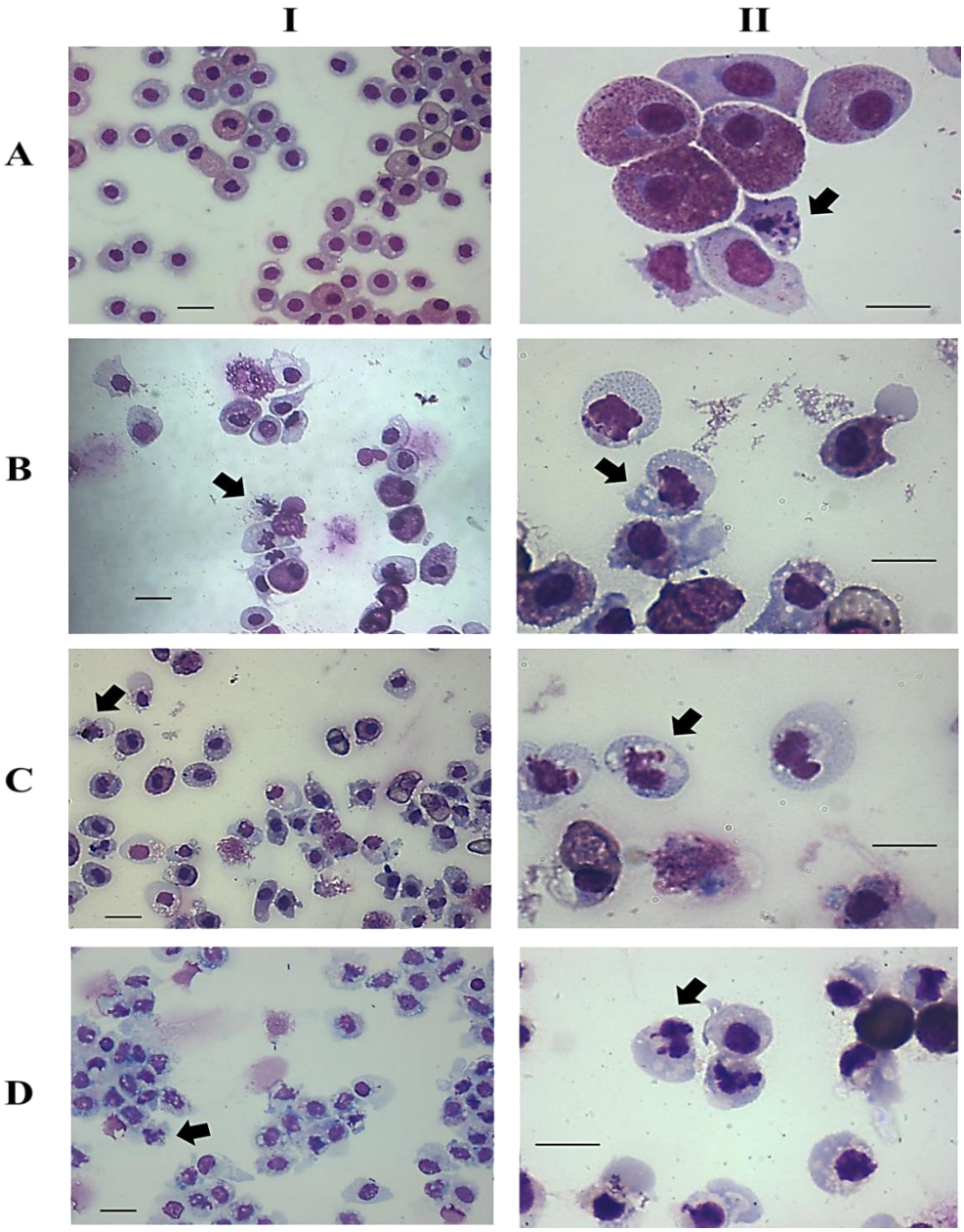

Figure 2.2. Light microscopy analysis of cyto-centrifuge preparations showing mixed haemocytes from *C. maenas* after 24 h suspension culture *in vitro*.
Mixed haemocytes were either stained with Diff-Quik™ (**A**) or Wright's stain (all other images). (**A**): 10°C (control); (**B**): 20°C; (**C**): 10 µg mL^{-1} gliotoxin (10°C); (**D**): 10 µM R-roscovitine (10°C). Arrows indicate karyorrhexis (**A, C, D, II**), irregular shaped nuclei (**B, D, I**), and membrane blebbing (**B, II, C, I**). Cyto-centrifuge preparations at 200x total mag (**I**) or 630x total mag (**II**) and are representative of n=3 experiments. Scale bars = 15 µm.

Figure 2.3.

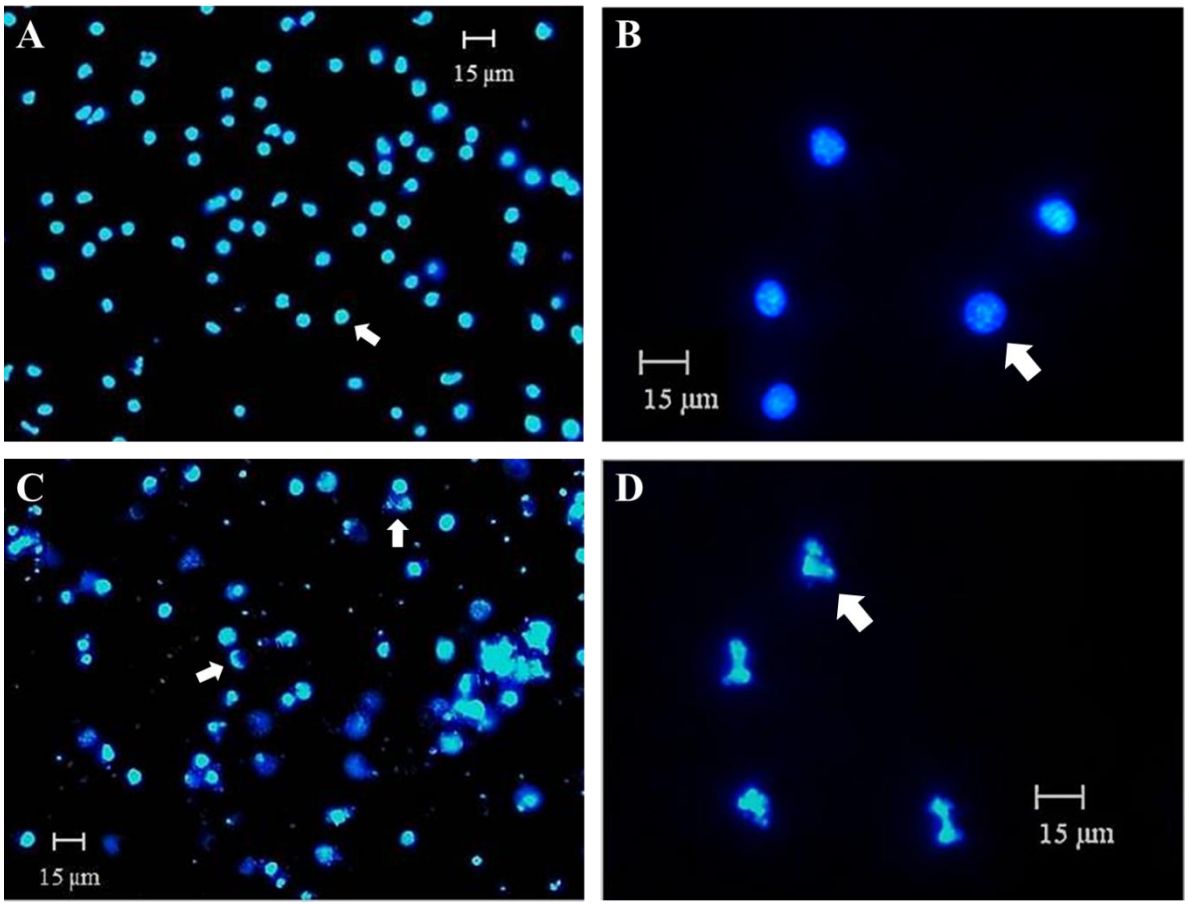

Figure 2.3. Fluorescence microscopy analysis showing DAPI stained mixed haemocytes from *C. maenas* after 6 h monolayer culture *in vitro*. (**A-B**)**:** Representative control haemocyte nuclei, 200x total mag (**A**) and 630x total mag (**B**); (**C-D**)**:** Representative gliotoxin-treated haemocyte nuclei, 200x total mag (**C**) and 630x (**D**). Viable haemocytes displayed circular (intact) nuclear morphology (arrows **A, B**), whereas apoptotic haemocytes displayed irregular shaped nuclei (arrows **C, D**), a hallmark feature of apoptosis. Scale bars =15 µm.

2.3.1.3. Confocal microscopy

Confocal microscopy using FITC and PI staining enabled the visualisation of apoptosis in real-time. Time-lapse videography revealed that over the course of a 3 h 30 min (210 min) culture period (15°C), viable haemocytes (FITC-negative and PI-negative) progressed into states of early apoptosis (FITC-positive and PI-negative) and late apoptosis/necrosis (FITC-positive and PI-positive) (supplementary videos 1 and 2). Snapshot images were taken from supplementary video 2 (cropped video) to show the different staining patterns exhibited by a viable, early apoptotic and late apoptotic/necrotic haemocyte (Figure 2.4, A). After 6 h culture, numerous early apoptotic and late apoptotic/necrotic haemocytes were observed at different areas of the cell chamber (Figure 2.4, B, C).

Figure 2.4.

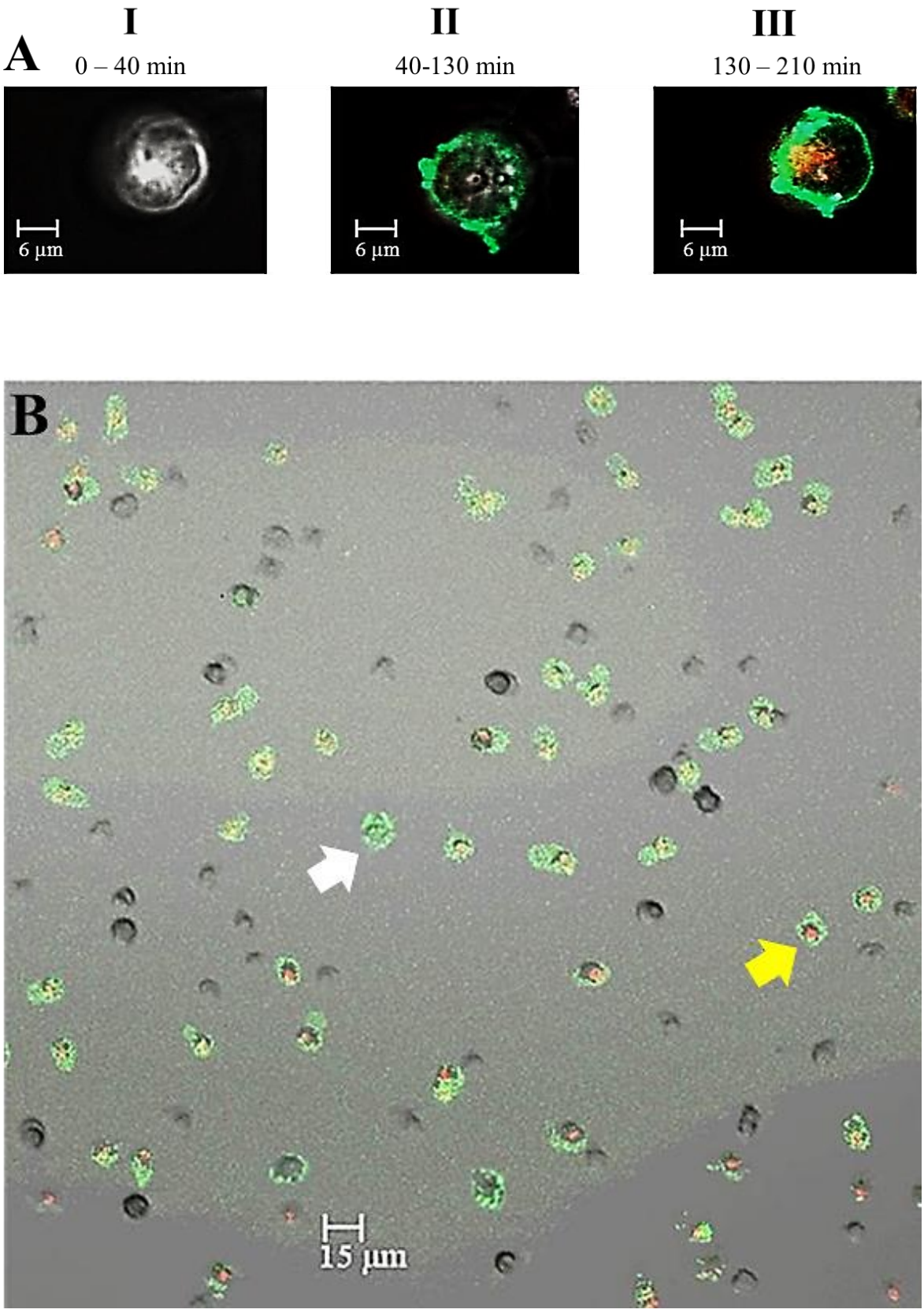

Figure 2.4 continued.

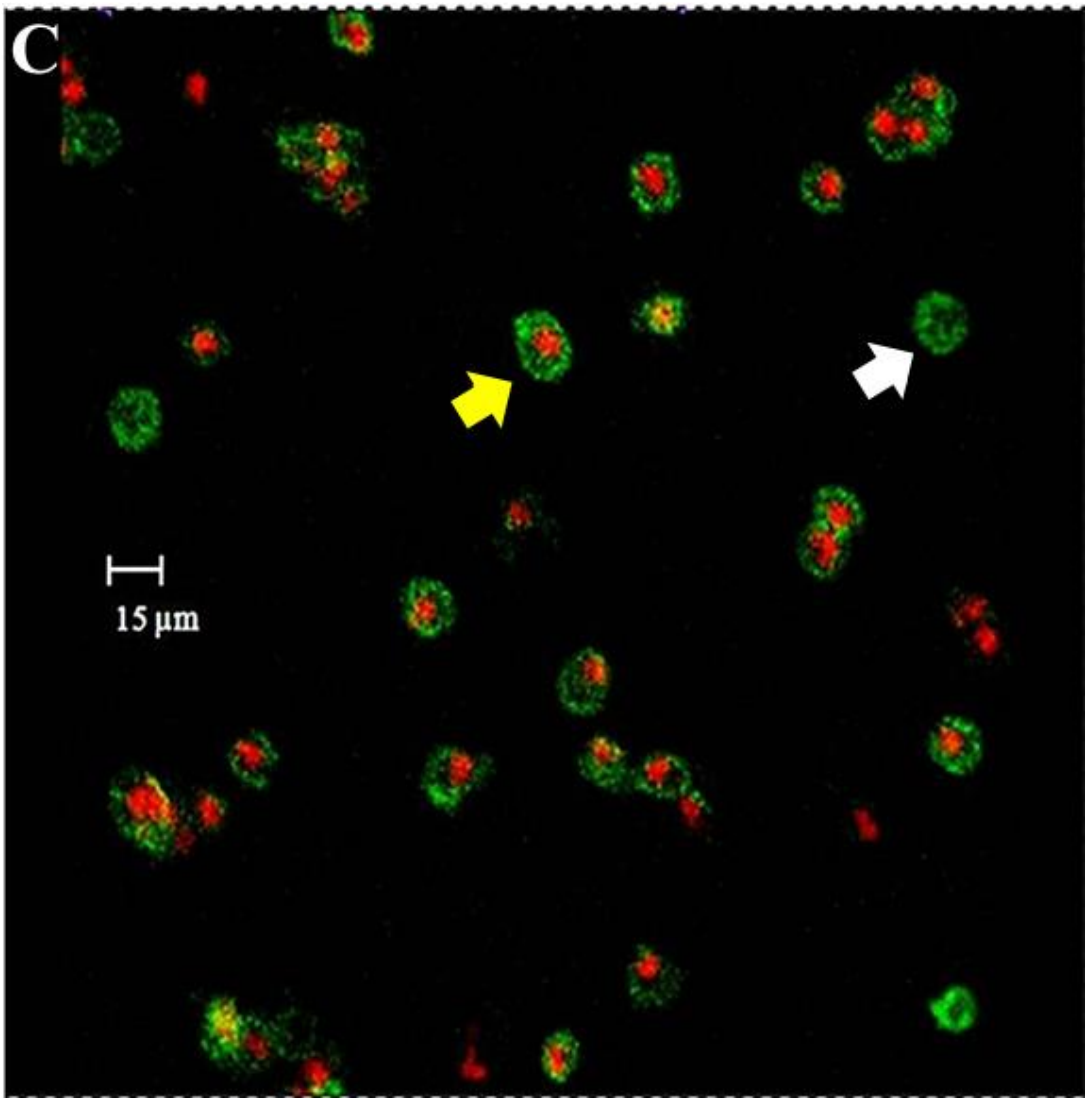

Figure 2.4. Confocal microscopy showing apoptosis in mixed haemocytes from *C. maenas* throughout 6 h monolayer culture (15°C) *in vitro*. Haemocytes stained with bovine lactadherin-FITC and PI. (**A**): Representative snapshot images (from supplementary video 2) at the indicated time interval ranges during 3 h 30 min culture period showing progression of a viable haemocyte (FITC-negative/PI-negative) (**I**) into early apoptosis (FITC-positive/PI–negative) (**II**) and late apoptosis/necrosis (FITC-positive/PI-positive) (**III**); (**B-C**): Representative images of haemocytes at different areas of the cell chamber after 6 h culture with phase contrast transmission overlay at 100x total mag, zoom 2 (**B**), or minus phase contrast transmission at 100x total mag, zoom 4 (**C**). Numerous early apoptotic (**B, C,** white arrows) and late apoptotic/necrotic haemocytes were observed (**B, C,** yellow arrows). Scale bars = 6 µm (**A**) and 15 µm (**B** and **C**).

2.3.1.4. Transmission electron microscopy

Ultrastructural visualization of apoptotic mixed haemocytes from *C. maenas* by transmission electron microscopy enabled clear identification of hallmark features of apoptosis. Within the nucleus of an apoptotic hyaline haemocyte, nuclear chromatin appeared marginated and formed crescent bodies (Figure 2.5, A, I and B, arrow). Additionally, nuclear fragmentation (karyorrhexis) was also observed in a semi-granular haemocyte (Figure 2.5, A, II and C, arrows). Both chromatin margination and nuclear fragmentation are classed as early events of apoptosis as cell membrane integrity is still retained (Figures 2.5, B and C), whereas during late apoptosis/necrosis membrane integrity is lost, as is shown in a semi granular haemocyte (Figure 2.5, A, arrow). Conversely, in a viable hyaline haemocyte (Figure 2.5, D) the organelles are clearly visible and appear intact, as does the cell and nuclear membrane.

Figure 2.5.

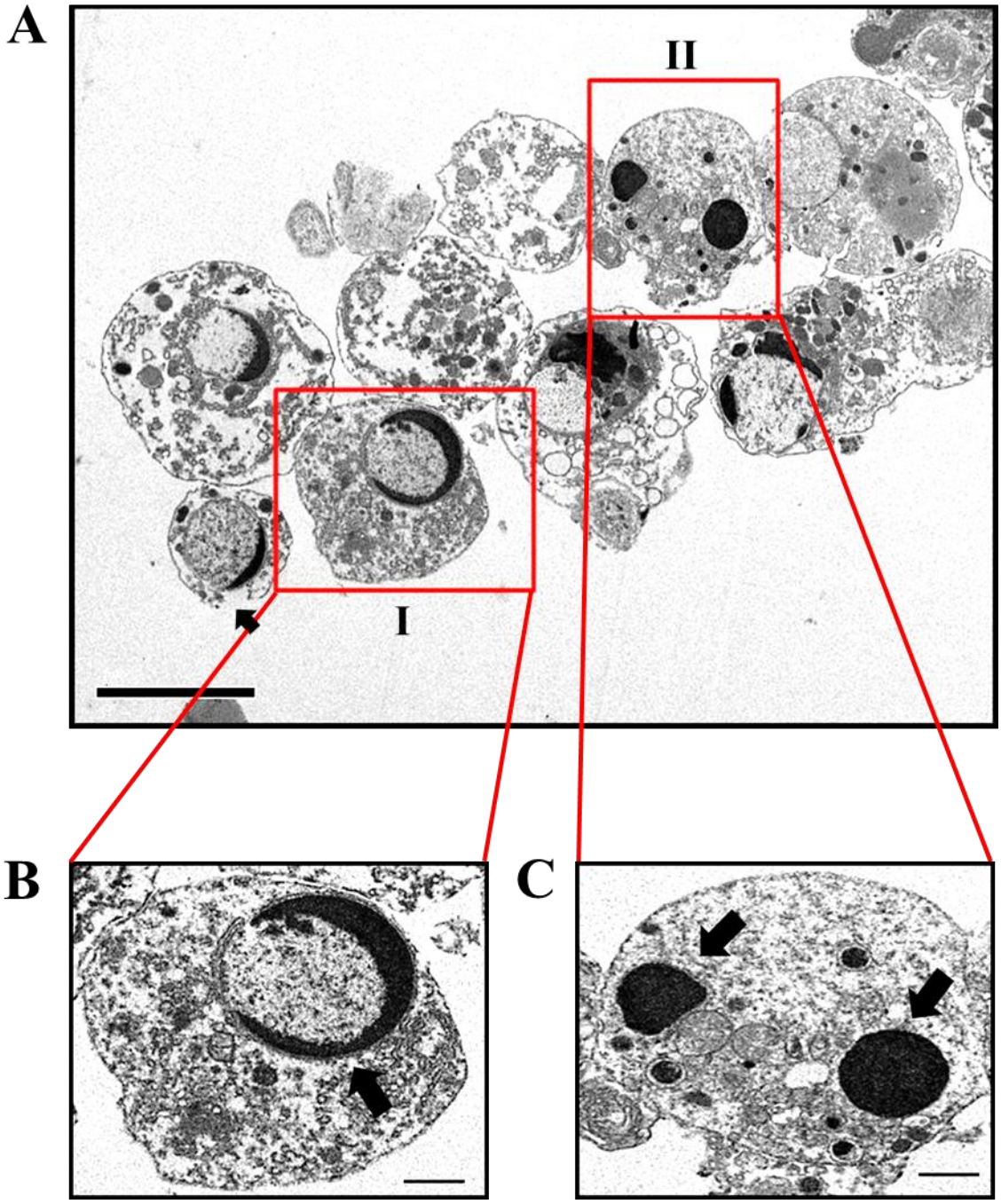

Figure 2.5 continued.

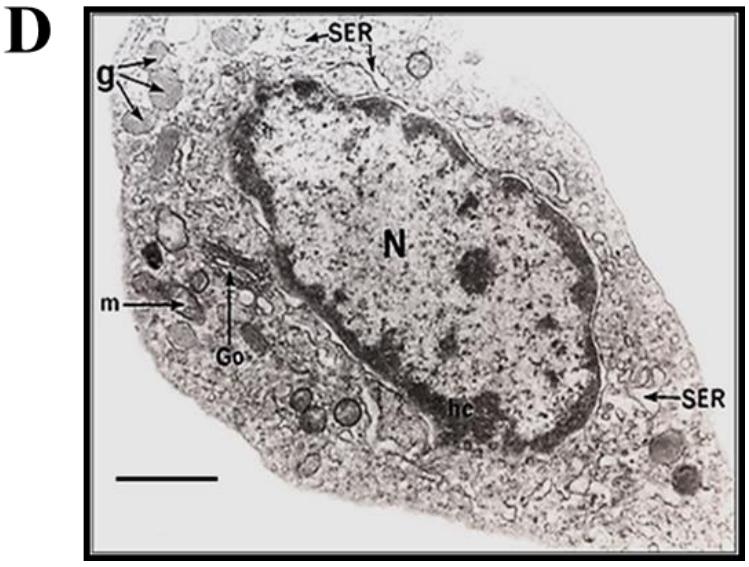

Figure 2.5. Transmission electron microscopy of temperature-induced apoptotic mixed haemocytes from *C. maenas* after 24 h suspension culture (20°C) *in vitro*. (**A**): A collection of apoptotic haemocytes exhibiting distinctive features of apoptosis including chromatin margination (**I**) and nuclear fragmentation (karyorrhexis) (**II**). A late apoptotic/necrotic semi granular haemocyte which has lost its membrane integrity can also be seen (arrow); (**B-C**): Enlarged images of highlighted regions (**A**), which depict chromatin margination in an apoptotic hyaline haemocyte (**B**, arrow) and nuclear fragmentation in an apoptotic semi-granular haemocyte (**C**, arrows) in better detail. (**D**): A viable hyaline haemocyte (0 h) exhibiting intact organelles, where g = intracellular granules (<1 µm), Go = Golgi apparatus, m = mitochondria, SER = smooth endoplasmic reticulum, hc = condensed chromatin in the nucleoplasm and N = nucleus, image courtesy of Dr Valerie J. Smith (St Andrews University). Scale bars = 5 µm (**A**), 1 µm (**B, C**) or 2.5 µm (**D**).

2.3.1.5. DNA fragmentation

Viable haemocyte DNA isolated at 0 h (control) appeared as a single band absent of fragmentation (Figure 2.6, A, Lane II), whereas apoptotic haemocyte DNA after 24 h culture exhibited characteristic DNA fragmentation with fragments ranging from 1000-2000 bp (Figure 2.6, A, Lane III). Cyto-centrifuge preparations carried out upon the remaining haemocyte suspensions further confirmed apoptosis in haemocytes after 24 h culture (Figure 2.6, C), whereas viable haemocytes were observed at 0 h (control) as expected (Figure 2.6, B).

Figure 2.6.

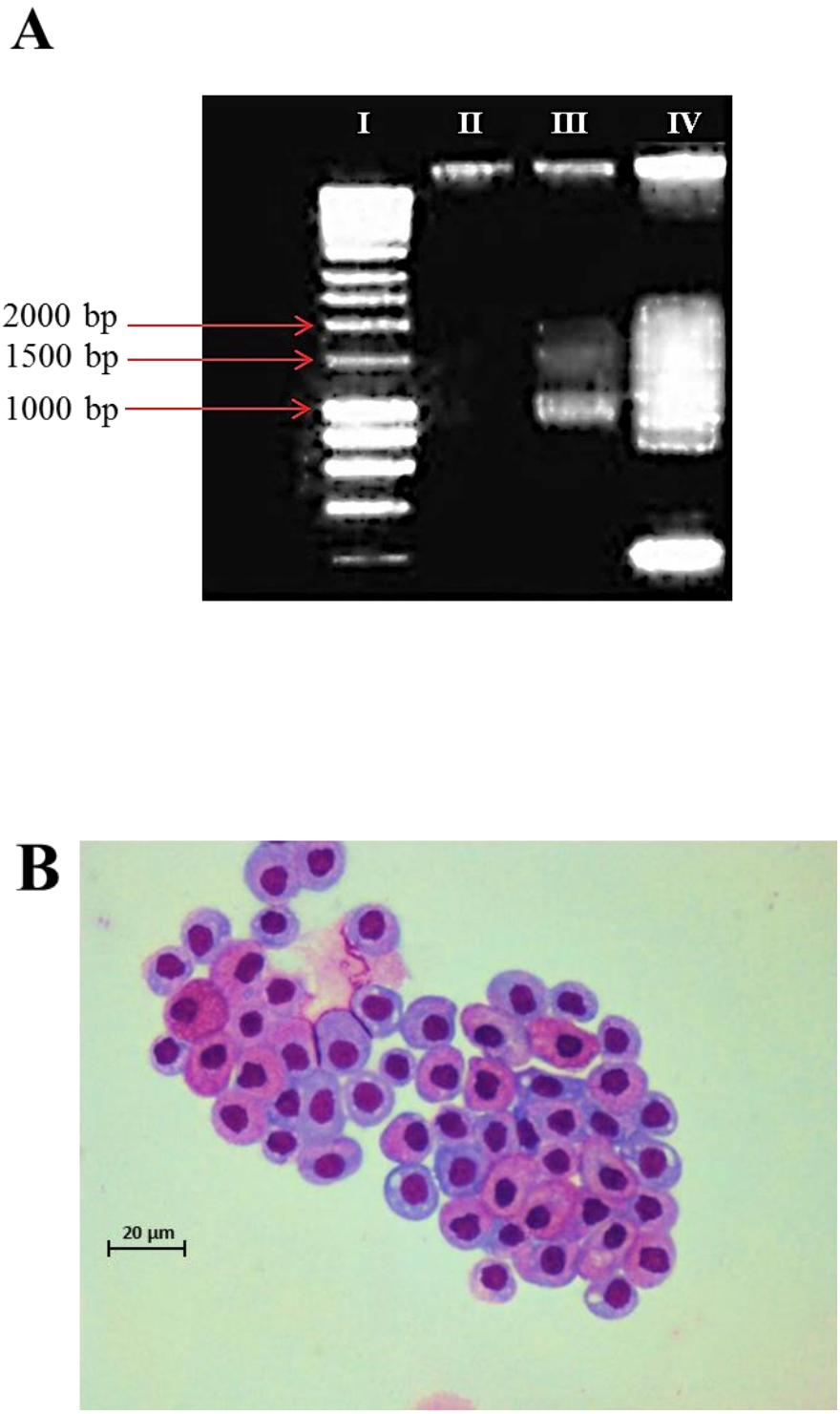

Figure 2.6 continued.

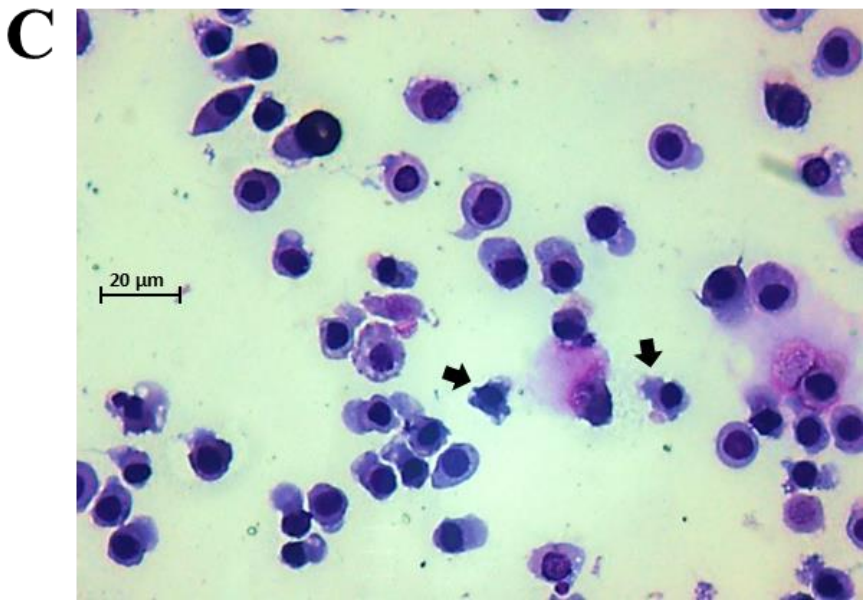

Figure 2.6. DNA fragmentation occurs as a result of temperature-induced apoptosis in mixed haemocytes from *C. maenas* after 24 h suspension culture (20°C) *in vitro*. (**A**): DNA ladder, where (**I**) = HyperLadder I; (**II**) = 0 h cultured haemocyte DNA (control); (**III**) = 24 h cultured apoptotic haemocyte DNA; (**IV**) = apoptotic DNA supplied from DNA ladder kit (Roche) (positive control). (**B-C**): Representative Diff-Quik™ stained cyto-centrifuge preparations of 0 h viable control haemocytes (**B**) and 24 h cultured apoptotic haemocytes (**C**). Arrows indicate membrane blebbing indicative of apoptosis. Images at 200x total mag, scale bars = 20 µm.

2.3.2. Quantification of apoptosis

2.3.2.1 Microscopy

From counts of apoptotic haemocytes from Diff-Quik™ cyto-centrifuge preparations, significantly higher values ($P<0.001$; n=3) of apoptosis were observed after 6 h (49.2% ± 4.2% SEM) and 24 h (59.7% ± 3.0% SEM) culture at 20°C, compared to constitutive apoptosis in controls at 10°C after 6 h (12.4% ± 3.6% SEM) and 24 h culture (10.4% ± 2.5% SEM) (Figure 2.7). Similarly, significantly higher apoptosis ($P<0.001$; n=3) in haemocytes treated with 10 µg mL^{-1} gliotoxin was observed after 6 h (41.9% ± 1.5% SEM) and 24 h (74.4% ± 3.3% SEM) culture (Figure 2.7) compared with controls. Significantly higher values of apoptosis were also observed after 6 h (33.7% ± 4.5% SEM) ($P<0.01$; n=3) and 24 h (55.1% ± 4.3% SEM) ($P<0.001$; n=3) culture of haemocytes with 10 µM R-roscovitine (Figure 2.7).

Figure 2.7.

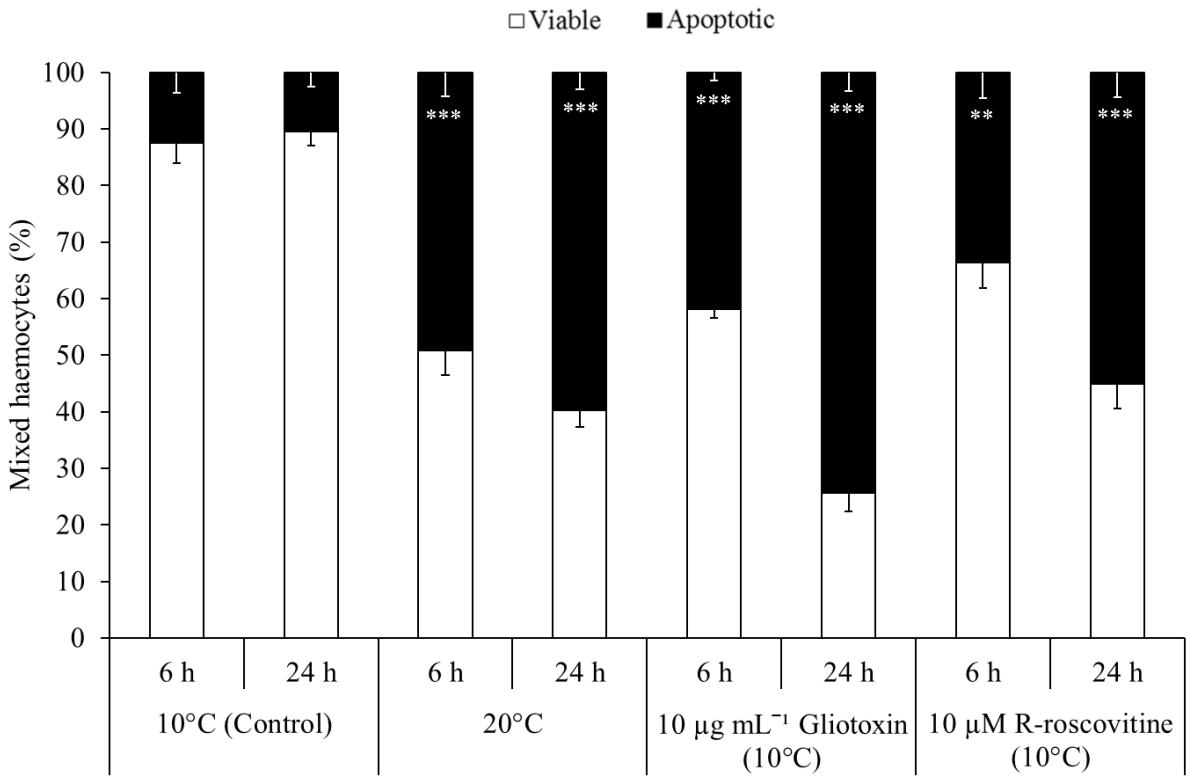

Figure 2.7. Efficacy of different inducers of apoptosis in mixed haemocytes from *C. maenas* after 6 h and 24 h suspension culture *in vitro*. Apoptosis was stimulated in haemocytes by temperature (20°C), or with 10 µg mL^{-1} gliotoxin or 10 µM R-roscovitine (10°C). Otherwise untreated haemocytes incubated at 10°C served as controls to assess constitutive apoptosis. Apoptosis was analysed from cyto-centrifuge preparations using light microscopy. Data are expressed as means ± SEM, n=3, with a different crab used on each occasion. Statistical analysis was performed upon arc sine transformed data using one-way ANOVA with a Student Newman-Keuls multiple comparison *post hoc* test. ** $P<0.01$, *** $P<0.001$ *vs.* control (untreated) apoptosis at the corresponding timepoint.

Apoptosis was further confirmed by counts of DAPI stained irregular shaped nuclei, a characteristic feature of apoptotic cells. Values in mixed haemocytes from *C. maenas* after 6 h culture (10°C) with 10 µg mL^{-1} gliotoxin were significantly higher (50.6% ± 4.1% SEM; $P<0.001$; n=3) compared to controls (4.6% ± 2.3% SEM), (Figure 2.8).

Figure 2.8.

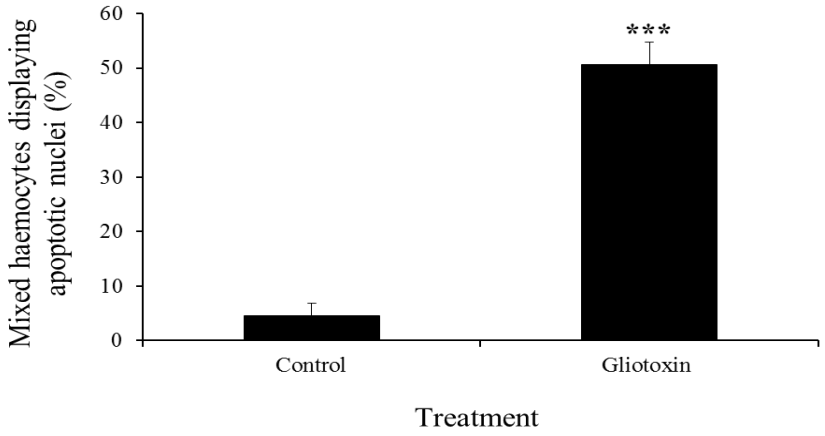

Figure 2.8. Fluorescence microscopy counts from DAPI stained *C. maenas* mixed haemocytes after monolayer culture *in vitro*. (**A**): Percentages of apoptosis after 6 h culture (10°C) ± 10 µg mL^{-1} gliotoxin. Data are expressed as means ± SEM, n=3, with a different crab used on each occasion. Statistical analysis was performed upon arc sine transformed data using a paired *t* test and the two-tailed *P* value considered. *** $P<0.001$ *vs.* control (untreated) apoptosis.

2.3.2.2. Flow cytometry with bovine lactadherin-FITC and PI staining

Using bovine lactadherin-FITC and PI staining, significantly higher values of early apoptosis (21.0% ± 1.4% SEM; $P<0.01$; n=3) and late apoptosis/necrosis (31.3 ± 6.7% SEM; $P<0.001$; n=3) were produced in control haemocytes after 6 h culture at 20°C (Figure 2.9, A) compared to Q-VD-OPh treated haemocytes at the same temperature. Haemocytes treated with the pan-caspase inhibitor Q-VD-OPh retained significantly higher viability (92.1% ± 1.1% SEM; $P<0.001$; n=3) compared to control haemocytes, and exhibited minimal percentages of early apoptosis (4.7% ± 1.6% SEM) and late apoptosis/necrosis (2.8% ± 0.6% SEM) (Figure 2.9, A). Representative flow cytometry dotplots of untreated haemocytes indicate early apoptotic and late apoptotic/necrotic haemocytes which appear in the lower right quadrant (FITC-positive and PI-negative) and upper right quadrant (FITC-positive and PI-positive) respectively (Figure 2.9, B), whereas Q-VD-OPh treated viable haemocytes remain in the lower left quadrant (FITC-negative and PI-negative) (Figure 2.9, C). Analysis of cyto-centrifuge preparations further confirmed that thermally induced apoptotic haemocytes exhibited morphological features consistent with apoptosis such as trademark membrane blebbing (Figure 2.9, D, arrows), whereas Q-VD-OPh treated haemocytes displayed characteristic viable morphology (Figure 2.9, E).

Figure 2.9.

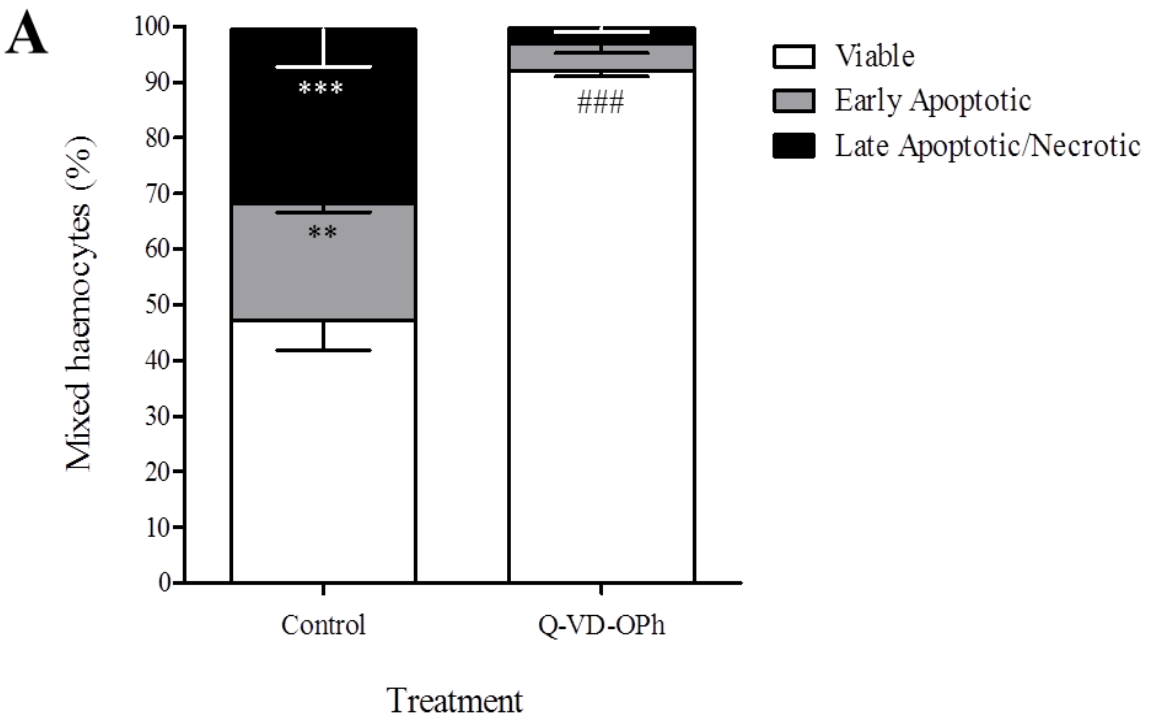
A
Mixed haemocytes (%)
100
90
80
70
60
50
40
30
20
10
0
***
**
###
Control
Q-VD-OPh
Treatment
Viable
Early Apoptotic
Late Apoptotic/Necrotic

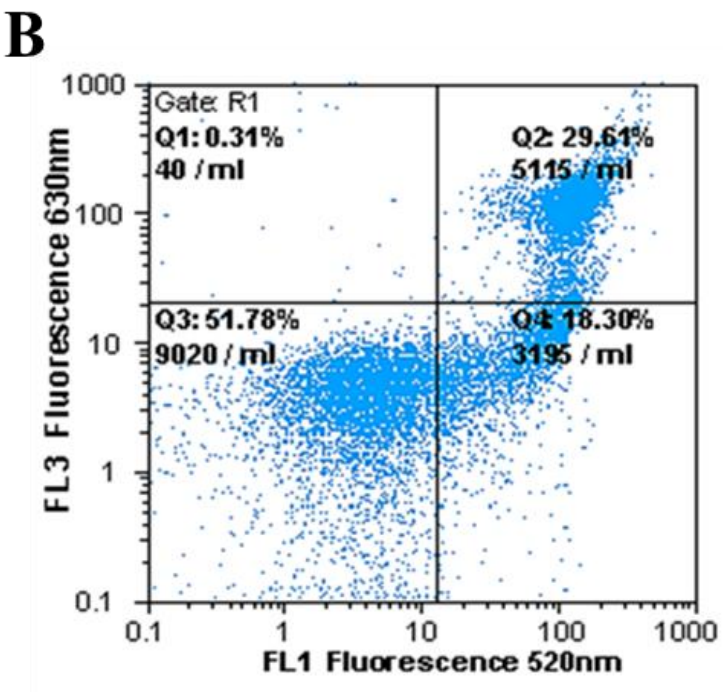
B
Gate: R1
Q1: 0.31%
40 / ml
Q2: 29.61%
5115 / ml
Q3: 51.78%
9020 / ml
Q4: 18.30%
3195 / ml
FL3 Fluorescence 630nm
1000
100
10
1
0.1
0.1
1
10
100
1000
FL1 Fluorescence 520nm

Figure 2.9 continued.

C

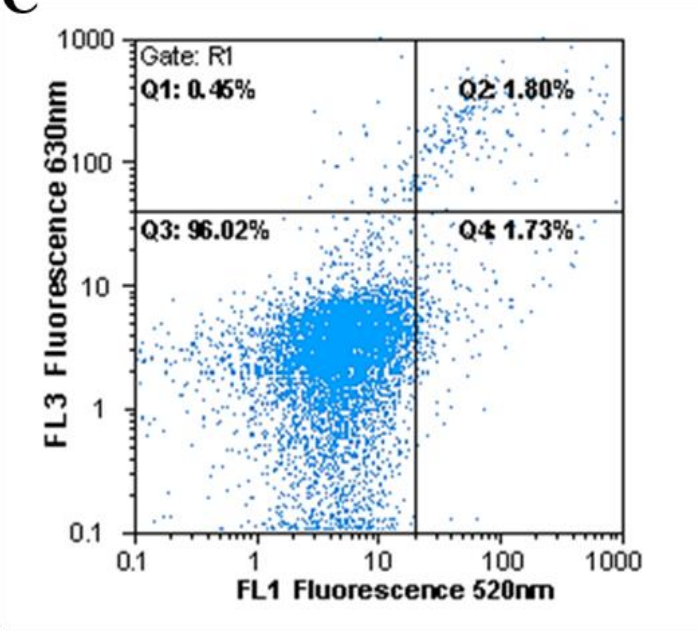

D

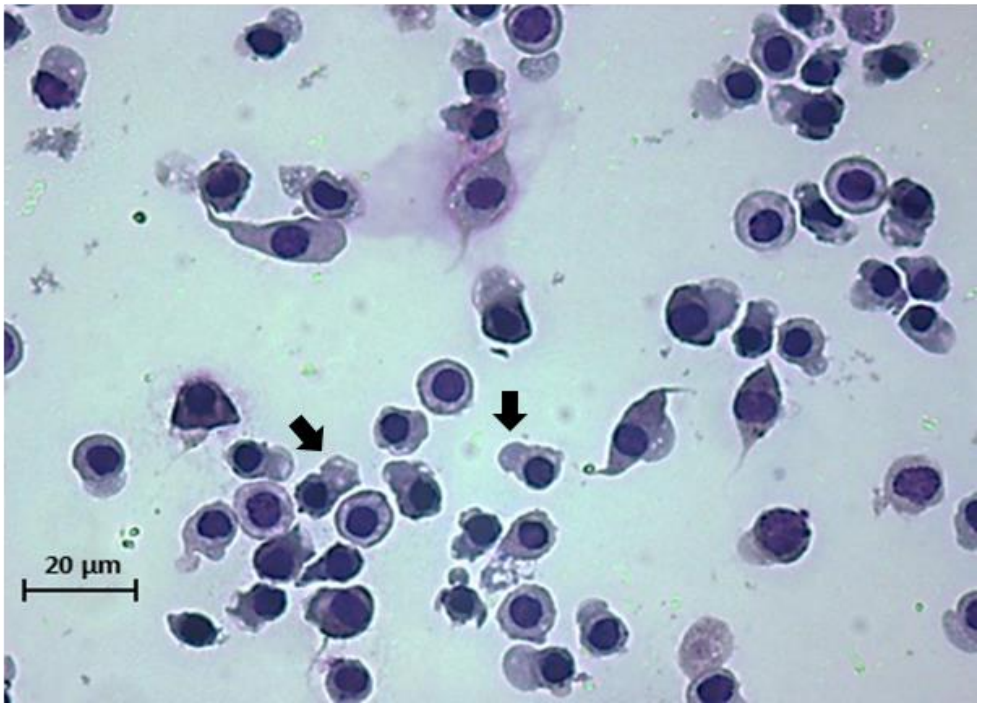

Figure 2.9 continued.

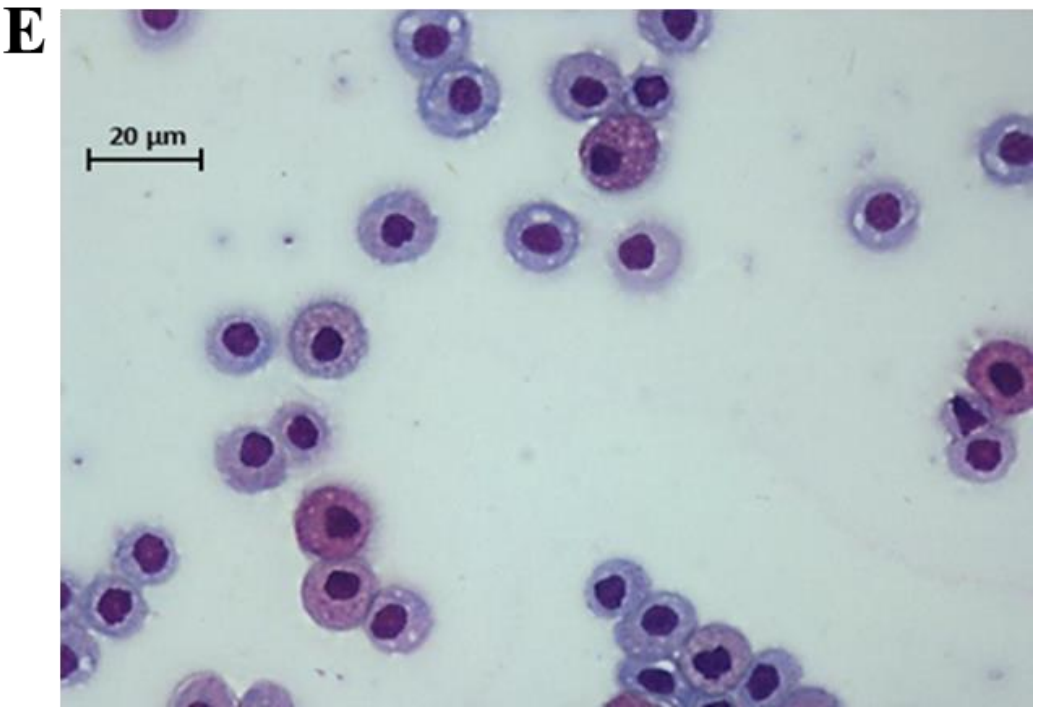

Figure 2.9. Flow cytometry assessment of temperature-induced apoptosis and apoptosis inhibition in mixed haemocytes after suspension culture *in vitro*.
Apoptosis was quantified using bovine lactadherin-FITC and PI staining. (**A**): Values of apoptosis after 6 h culture (20°C) ± 10 µM of the pan-caspase inhibitor Q-VD-OPh. Data expressed as means ± SEM, n=3, with a different crab used on each occasion. Statistical analysis was performed upon arc sine transformed data using one-way ANOVA with a Student Newman-Keuls multiple comparison *post hoc* test. ** $P<0.01$ *vs.* matching Q-VD-OPh treated early apoptotic haemocytes; *** $P<0.001$ *vs.* matching Q-VD-OPh treated late apoptotic/necrotic haemocytes; ### $P<0.001$ *vs.* matching control (untreated) viable haemocytes. (**B**-**C**): Representative flow cytometry dotplots of apoptotic haemocytes cultured at 20°C (**B**) and viable Q-VD-OPH treated haemocytes (**C**); (**D**-**E**): Representative cyto-centrifuge preparations (Wright's stain) at 200x total mag of apoptotic haemocytes cultured at 20°C (**D**) exhibiting membrane blebbing (arrows) and viable Q-VD-OPh treated haemocytes (**E**). Scale bars = 20 µm.

2.3.2.3. Hypodiploid peak assay

Temperature-induced apoptosis levels in mixed haemocytes from *C. maenas* were also quantified using the hypodiploid peak assay. Using this method, significantly higher apoptosis ($P<0.001$; n=3) was detected in haemocytes after 24 h culture (20°C) (50.2% ± 3.2% SEM) compared to levels of apoptosis at 0 h (2.2% ± 0.2% SEM) (Figure 2.10, A). Haemocytes cultured at 20°C exhibited hypodiploid DNA (fragmented/disordered DNA) indicative of apoptosis which appear as broad hypodiploid peaks before the narrow peak of viable haemocyte DNA (Figure 2.10, C). Moreover, cyto-centrifuge preparation analysis enabled further confirmation of temperature-induced apoptosis by identification of irregular shaped haemocyte nuclei (Figure 2.10, E). Conversely, hypodiploid DNA was minimal in viable haemocytes at 0 h (Figure 2.10, B) as expected, with viable haemocyte morphology further confirmed from cyto-centrifuge preparation analysis (Figure 2.10, D).

Figure 2.10.

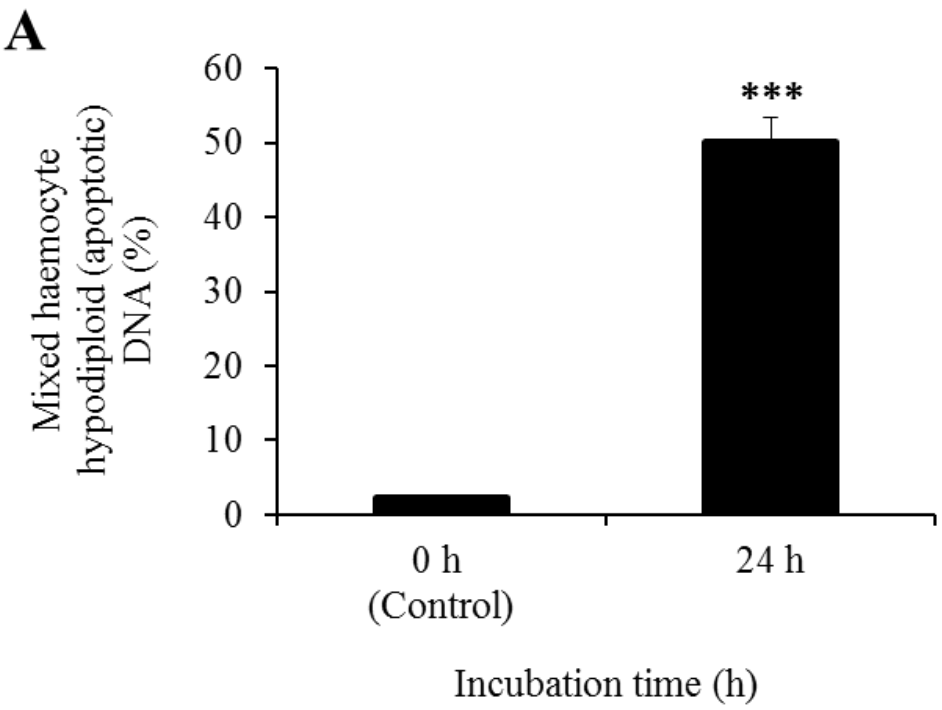
A
Mixed haemocyte hypodiploid (apoptotic) DNA (%)
60
50
40
30
20
10
0
***
0 h (Control)
24 h
Incubation time (h)

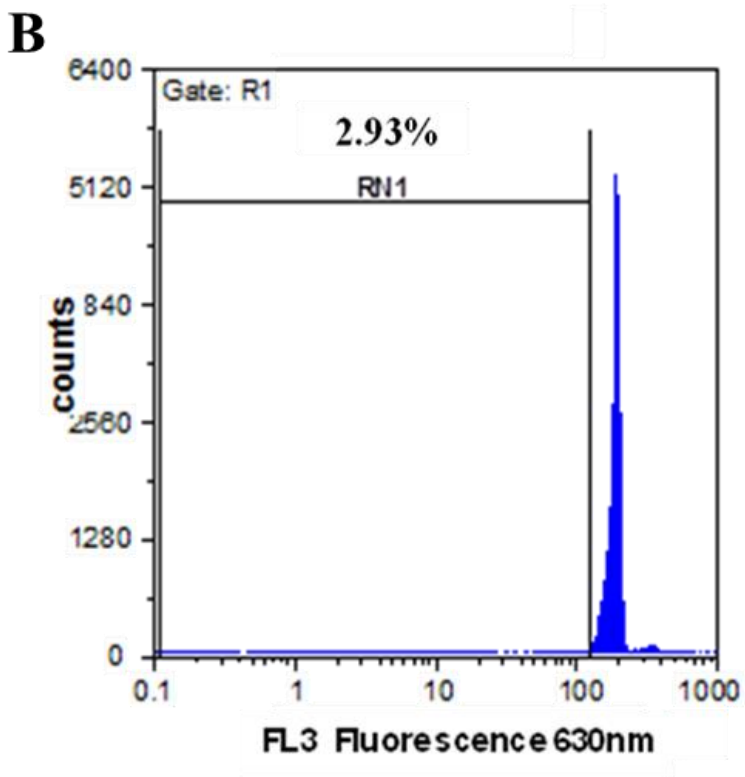
B
6400
5120
840
2560
1280
0
counts
Gate: R1
2.93%
R1
0.1
1
10
100
1000
FL3 Fluorescence 630nm

Figure 2.10 continued.

C

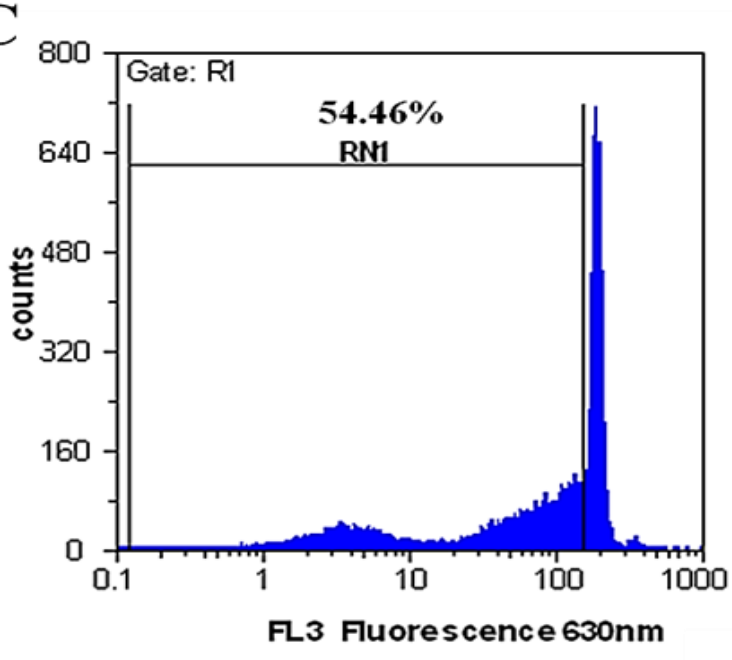

D

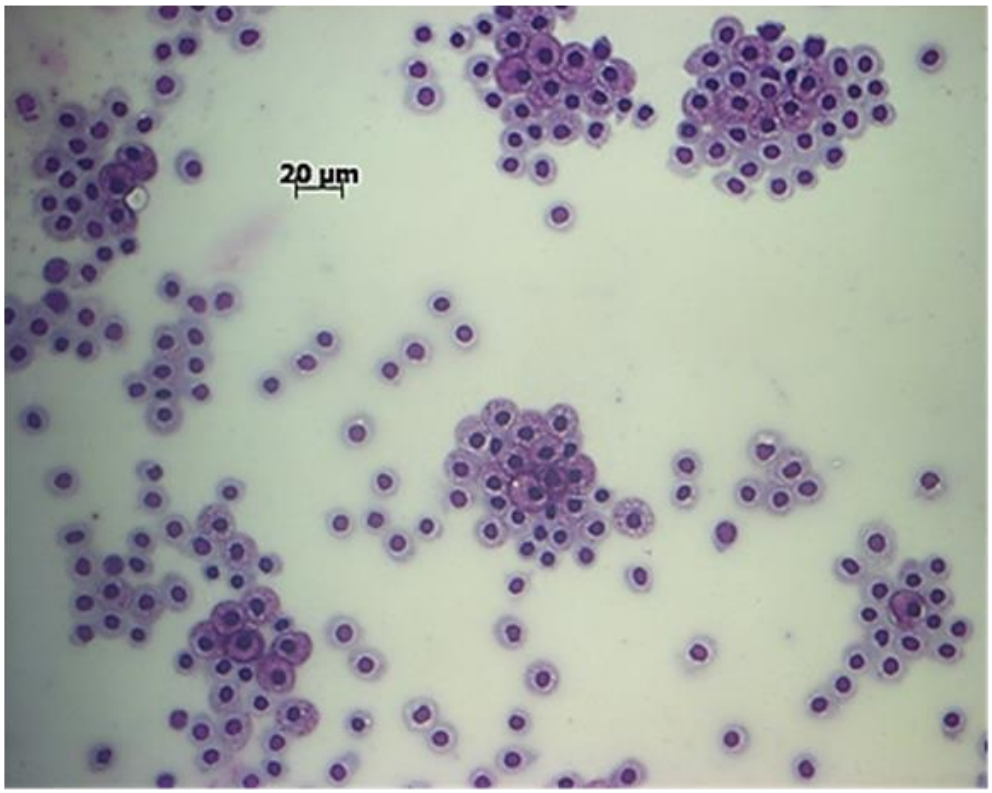

Figure 2.10 continued.

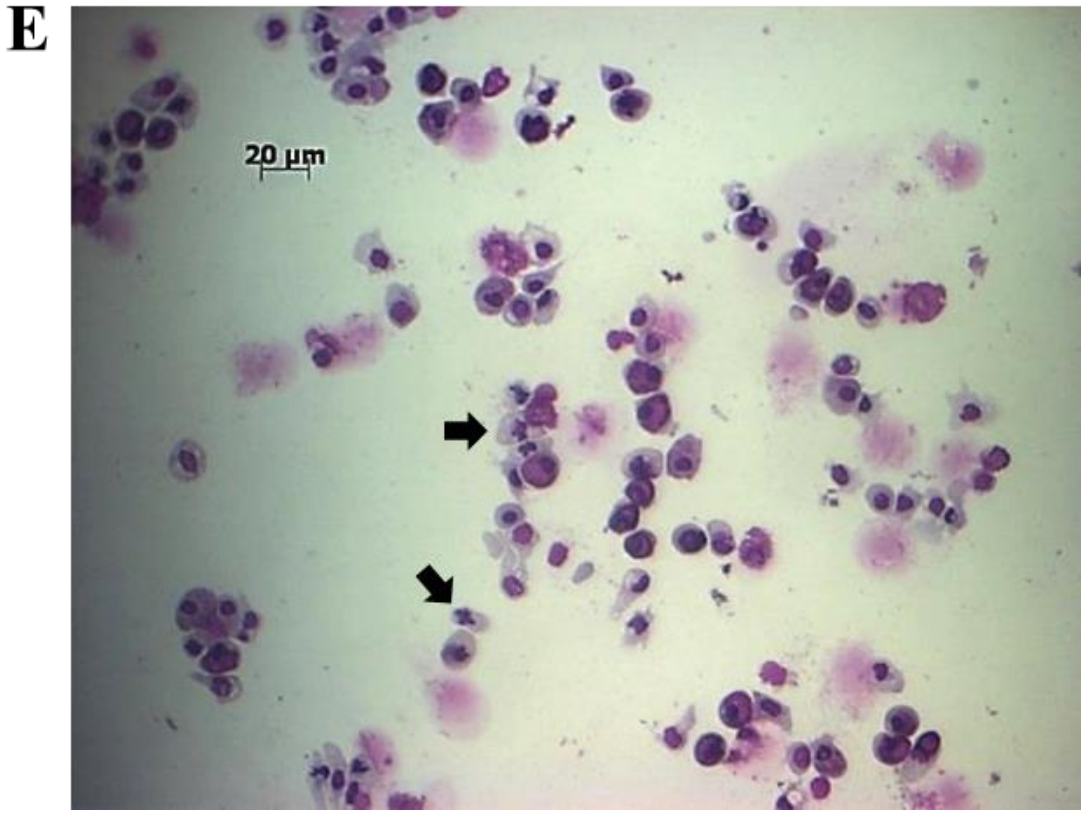

Figure 2.10. Flow cytometry assessment of temperature-induced apoptosis in mixed haemocytes after suspension culture *in vitro*, carried out using the hypodiploid peak assay. (**A**): Percentages of hypodiploid (apoptotic) DNA exhibited by haemocytes at 0 h (control) and after 24 h culture (20°C). Data expressed as means ± SEM, n=3, with a different crab used on each occasion. Statistical analysis was performed upon arc sine transformed data using a paired *t* test and the two-tailed *P* value considered. *** $P<0.0001$ *vs.* 0 h (control) apoptosis. (**B-C**): Representative flow cytometry dotplots of 0 h viable haemocytes (no hypodiploid peak) (**B**) and 24 h cultured apoptotic haemocytes which exhibit characteristic broad hypodiploid peaks of DNA (**C**); (**D-E**): Representative cyto-centrifuge preparations (Diff-Quik™ stain) at 100x total mag of 0 h viable haemocytes (**D**) and 24 h cultured apoptotic haemocytes (**E**) exhibiting irregular shaped nuclei indicative of apoptosis (arrows). Scale bars = 20 µm.

2.4. Discussion

Most of the detection and quantification methods tested on crab haemocytes were successful and confirmed that the main hallmark features of apoptosis were identifiable and similar to those observed in mammalian cell types.

Percentages of constitutive apoptosis in *C. maenas* mixed haemocytes at 10°C were found to be consistently low, at around 10-12% up to 24 h culture. Such low values are similarly to constitutive apoptosis values in shrimp mixed haemocytes (Wang *et al*., 2004; Hameed *et al*., 2006; Guo *et al*., 2013; Xian *et al*., 2010, 2012, 2013). However, such shrimp studies are not strictly comparable to the crab since the shrimp species in question are tropical and inhabit waters with temperatures between 25-30°C. Keeping *C. maenas* haemocytes at room temperature compared with their optimum temperature of 10°C provided an easy and convenient method of inducing high levels of apoptosis when comparing and assessing detection methods. When quantifying apoptosis via microscope counts and flow cytometry, comparable values were obtained between the two methods, with 50-60% of haemocytes detectably apoptotic after 6 and 24 h culture at room temperature.

FITC conjugated annexin V (AV) is frequently used in flow cytometry and confocal/fluorescence microscopy for the detection of apoptosis. However, preliminary experiments showed no difference between AV and B. lactadherin when assessing apoptosis via these methods. One of the earliest events during the biological mechanism of apoptosis in mammals is PS translocation from the inner to the outer membrane leaflet (Martin *et al*., 1995). AV binding to PS is dependent upon the presence of Ca^{2+} (Vermes *et al*., 1995). However, as many buffers for invertebrate systems frequently contain EDTA which chelates Ca^{2} (such as *C. maenas* MAC), several modifications were required when using this method for the detection of apoptosis in *C. maenas*. Conversely, B. lactadherin, a cow glycoprotein secreted by macrophages has high affinity for negatively charged PS and functions independently of Ca^{2+} (Shi *et al*., 2006). Therefore, B. lactadherin was substituted for the more commonly used AV. This decision was made because not only does B. lactadherin bind to PS independently of Ca^{2+}, but also, in

various competitive binding experiments, B. lactadherin has been shown to detect PS expression and bind to PS quicker than AV in different cell types undergoing early apoptosis (Dasgupta *et al*., 2006; Shi *et al*., 2006; Waehrens *et al*., 2009). Therefore, the earliest detection of apoptosis in *C. maenas* mixed haemocytes was ensured using this method. Additionally, B. lactadherin-FITC is substantially cheaper than AV-FITC. Thus, the reasons above justify why B. lactadherin-FITC was selected for apoptosis assessment.

The MitoCapture Apoptosis Detection Kit is a standard one used for the detection of apoptosis initiated via the intrinsic pathway (Ogawa *et al*., 2001). However, even after numerous optimizations and various titrations of the MitoCapture dye, very poor fluorescence was consistently observed in *C. maenas* haemocytes. This made it impossible to accurately identify and distinguish viable haemocytes from apoptotic haemocytes, even after 24 h culture at room temperature when substantial apoptosis was occurring, as confirmed via various other detection methods. A possible reason for these difficulties may be the high salt content present in the haemolymph of marine crustaceans. Many standard kits for the detection of apoptosis in mammalian cells remain poorly optimized for use in marine crustaceans, with many investigations failing to take into account the effect of salt when assessing apoptosis. Another commonly used mammalian kit for the detection of apoptosis is terminal deoxynucleotidyl transferase dUTP nice end labelling (TUNEL). TUNEL staining for the detection of apoptosis is commonly used in freshwater crustacean species where salt is not an issue, such as the giant fresh water prawn, *Macrobrachium rosenbergii*, (Hsu *et al*., 2005) and the freshwater crayfish, *Procambarus clarkii*, (Wu *et al*., 2012). However, as a result of the problems encountered using the MitoCapture Apoptosis Detection Kit, and also due to time and budgetary constraints, the TUNEL assay was not considered for apoptosis assessment in *C. maenas* haemocytes. Additionally, the TUNEL assay is by no means the most accurate assay for the detection of apoptosis because false positives can frequently arise from necrosis and cells undergoing DNA repair or gene transcription (Elmore, 2007).

Apoptosis was successfully induced in haemocytes from *C. maenas* using gliotoxin and R-roscovitine, albeit to a lesser extent than in human neutrophils. Gliotoxin at final concentrations ranging from 0.1-30 µg mL^{-1} induced 100 % neutrophil apoptosis *in vitro* after both 6 h and 20 h *in vitro* culture, where apoptotic neutrophil counts were quantified via light microscopy from cyto-centrifuge preparations (Ward *et al*., 1999). Using the same method of quantification in *C. maenas* haemocytes, percentages of apoptosis remained lower, with 41% and 74% apoptosis after 6 h and 24 h culture respectively with 10 µg mL^{-1} gliotoxin. R-roscovitine at a final concentration of 20 µM induced 75% early apoptosis in human neutrophils after 8 h culture *in vitro*, quantified using flow cytometry via AV-FITC and PI staining (Leitch *et al*., 2012). Lower levels of apoptosis were achieved in *C. maenas* haemocytes after 6 h (33%) and 24 h (55%) culture with a slightly lover concentration of 10 µM R-roscovitine. Here however, apoptosis was quantified using a different method i.e. via light microscopy from cyto-centrifuge preparations. Even so, using R-roscovitine as the stimulator, far less apoptosis was observed in *C. maenas* haemocytes after 24 h as opposed to human neutrophils after just 8 h. Nonetheless, the results do imply that apoptosis induction in *C. maenas* mixed haemocytes does occur via similar inhibitory pathways as described in mammals. However, further research is required to elucidate the exact roles that NFκB transcription factors and CDK inhibitors play in crustacean haemocyte apoptosis. Ultimately, the percentages of gliotoxin and R-roscovitine-induced apoptosis were markedly higher in human neutrophils compared to unseparated haemocytes from *C. maenas*. Such differences are likely due to the fact that in this chapter only unseparated haemocytes were considered for investigation, whereas neutrophils are a highly specialized sub-population of cells which were isolated in great proportion before apoptosis assessment. Additional factors which are likely contributors to the variances in apoptosis levels observed are differences in culturing temperatures, different doses of gliotoxin and R-roscovitine used, and the obvious difference between crabs and humans in terms of evolutionary distance.

Apoptosis in crab haemocytes was almost completely abrogated after 6 h culture (<10% total cell death) with the pan-caspase inhibitor Q-VD-OPh. This is comparable to human neutrophils where Q-VD-OPh abolishes apoptosis and greatly increases viability

compared to control cultures after 6 h, 18 h, 20 h and 24 h culture (Wardle *et al.*, 2011; Lucas *et al*., 2013). Additionally, Q-VD-OPh attenuates human Jurkat T cells and mouse immature B cell apoptosis (Caserta *et al*., 2003). Therefore, it can be confirmed that haemocytes of the shore crab do undergo classical caspase-dependent apoptosis. Similar apoptosis inhibition has been demonstrated in *P. japonicus* mixed haemocytes by the use of another pan-caspase inhibitor, namely z-VAD-FMK (Wang and Zhang, 2008). However, in both instances, because broad-spectrum caspase inhibitors have been used, inhibition of apoptosis cannot be pinpointed to a specific caspase(s). As yet, no caspase genes have been identified from *C. maenas* haemocytes, nevertheless, expressed sequence tag (EST) hits (GeneBank accession numbers DV944907, DV944626, DV111415, DN738966 and DY656150) were found after mining the nucleotide query of the *Eriocheir sinensis* (Chinese mitten crab) caspase gene (GeneBank accession number HM483599) against the *C. maenas* EST library (Mount Desert Island Biological Laboratory).

Regulatory proteins present in un-separated haemolymph released from circulating haemocytes may contribute to the high levels of survival and low levels of constitutive apoptosis observed in haemocytes after 6 h and 24 h culture at 10°C. Although very little is known about possible apoptosis regulators in crustacean haemolymph, astakines (crustacean cytokine-like proteins) from haemocytes of the signal crayfish, *Pacifastacus leniusculus*, stimulate haemocyte survival in the haematopoietic tissue (Watthanasurorot *et al*., 2011). Certainly in humans, soluble inflammatory mediators present in whole blood and also secreted by other inflammatory cells do promote cell survival and inhibit apoptosis. Inflammatory mediators such as granulocyte macrophage colony stimulating factor (GM-CSF) secreted by macrophages as well as interleukin 6 (IL-6) and IL-15 (survival cytokines) do inhibit constitutive neutrophil apoptosis (Lee *et al*., 1993; Ottonello *et al*., 2002). Additionally, other pro-inflammatory mediators such as IL-5, IL-1β, complement component 5a (C5a), interferon gamma (IFNγ) and leukotriene B_4 (LTB_4) inhibit constitutive granulocyte apoptosis (Her *et al*., 1991; Colotta *et al*., 1992; Stern *et al*., 1992; Lee *et al*., 1993; Murray *et al*., 1997).

Understandably, each method of apoptosis detection used in this study has its own distinct advantages and disadvantages which are summarised in Table 2.3. Overall, flow cytometry analysis via bovine lactadherin-FITC and PI staining has several advantages over the other methods. It is a relatively quick assay, is computerised so avoids much of the subjectivity and human error inherent in microscopy when quantifying apoptosis from cell counts (Sequeira *et al.,* 1995), and also generates robust and reproducible data. Moreover, using bovine lactadherin-FITC and PI staining can also distinguish between early apoptosis and late apoptosis/necrosis, therefore providing a more thorough assessment of apoptosis. However, morphological assessment via microscopy on cyto-centrifuge preparations is still an ideal way to define morphological apoptosis and confirm flow cytometric results (Majno and Joris, 1995; Darzynkiewicz *et al.*, 1997, 2004; Ziegler and Groscurth, 2004). Cyto-centrifuge preparations can be produced cheaply and quickly, are highly reproducible and easily performed in tandem with flow cytometry, unlike analysis of apoptotic cells using fluorescence or transmission electron microscopy which prove more expensive and time-consuming.

In conclusion, this chapter reports the successful validation of apoptosis in haemocytes from *C. maenas* for the first time, and compares the advantages and disadvantages of methodologies for routine measurement of the phenomenon. It was established that *C. maenas* haemocytes do undergo gliotoxin, R-roscovitine and temperature-induced apoptosis, with the latter subsequently confirmed as classical caspase-dependent apoptosis. Therefore, it is likely that *C. maenas* haemocytes do undergo apoptosis via similar pathways to mammalian cells.

Table 2.3. Evaluation of apoptosis detection methods used in the present study.

Detection method	Advantages	Disadvantages
Brightfield microscopy	Quick, cheap and reproducible, requires small cell number. Easy to discriminate between viable/ apoptotic/necrotic cells. Long-term storage of slides possible. Quantifiable and can be performed in concert with other apoptosis assays.	Quantification can be slow and labour-intensive. Human error and subjectivity possible.
Fluorescence microscopy	Easy to discriminate early apoptotic and viable cell nuclei. Long-term storage of slides possible in the dark coupled with use of anti-fade mounting media.	As above. Can be expensive.
Confocal microscopy (B. lact-FITC and PI staining)	Allows analysis of apoptosis in real-time via time-lapse videography which enables discrimination between viable/early apoptotic/late apoptotic and necrotic cells, quantifiable.	More specialized equipment needed than for routine microscopy.
Transmission electron microscopy	Classic assessment method for confirming apoptotic cell ultrastructure, easy to discriminate between viable/early apoptotic and late apoptotic/necrotic cells.	Time-consuming, needs specialized preparation & examination. Not practical for quantification. Can be expensive.
DNA fragmentation	Allows clear visualisation of apoptotic DNA fragments, can be used to accurately determine fragment size.	DNA fragments can also be produced by necrotic cells, not practical for quantification.
Flow cytometry (B. lact-FITC and PI staining)	Computerised, multi-parametric analysis upon gated cell populations. Discriminates between viable/ early apoptotic and late apoptotic/necrotic cells. Quick processing time per sample, reproducible, small cell volume required. Easily and objectively quantifiable, thus can avoid human error and subjectivity which may occur in microscopy.	Requires specialised, expensive equipment, cannot discriminate between late apoptotic and necrotic cells.
Flow cytometry Hypodiploid peak assay (PI staining only)	As above, enables discrimination of viable and apoptotic cells.	As above. Necrotic cells can appear within hypodiploid peak.

Abbreviations: AV-FITC = annexin V-fluorescein isothiocyanate, B. lact-FITC = bovine lactadherin-fluorescein isothiocyanate, PI = propidium iodide.

Chapter 3

Quantification of apoptosis using flow cytometry

3.1. Introduction

Having tested various methods of apoptosis detection and quantification in mixed haemocytes from *C. maenas* (Chapter 2), subsequent investigations were undertaken to quantify apoptosis *in vitro* under different conditions. Based on the previous results, flow cytometry using bovine lactadherin-FITC and PI staining was selected as the main quantification method. The experiments were carried out to consider the role of apoptosis in host protection under various conditions that would be naturally experienced by the animal, such as temperature or natural exposure to non-self agents. Recent studies on tropical shrimp have focussed more on expression of apoptosis-related genes in response to viral pathogens (mainly WSSV) or water quality variants, rather than considering how cell death might change in response to commonly encountered life conditions.

Although different haemocyte populations in several crustacean species are well-characterized, to date, investigations of apoptosis have overlooked any variations in the process among cell types. It is essential that apoptosis is quantified in both mixed and separated haemocytes, not only to provide more comprehensive knowledge of apoptosis in relation to the immune system and pathophysiology, but also to consider apoptosis in the absence of humoral factors present in haemolymph. Cell separations in shrimp species can be challenging, particularly with respect to controlling haemolymph coagulation (Vargas-Albores *et al*., 2005). Despite this, however, reports have been published detailing successful separation of different cell types (Rodriguez *et al*., 1995; Perazzolo and Barracco, 1997; Sritunyalucksana *et al*., 2001; Vargas-Albores *et al*., 2005), although in these reports, apoptosis was not one of the parameters considered for investigation.

Undoubtedly apoptosis in *C. maenas* haemocytes will vary according to treatment and concentration. It is anticipated that apoptosis will be the primary response to stress to limit potential damage, but at times of shock or strong infection, apoptosis will be overridden by necrosis. The general hypothesis is that high levels of apoptosis/necrosis will occur in haemocytes obtained from crabs subject to repeated haemolymph sampling

(mimic of injury/natural infection), after incubation at high temperature (20°C), or in response to non-self agents (LPS and bacteria).

Specifically the objectives of this chapter are:

1. To compare apoptosis in haemocytes *in vitro* under conditions representing stressful life events to the animal, including temperature and haemocytopenia (mimic of injury/natural infection).

2. To compare apoptosis between mixed haemocytes and enriched cell populations (HCs, GCs and ProHs) to test whether all cell types respond in the same way.

3. To measure apoptosis in haemocytes after exposure to non-self agents, including *E. coli* derived LPS or the bacterium, *Listonella anguillarum* (a mild shellfish pathogen).

3.2. Materials and methods

3.2.1. Preparation of mixed and separated haemocytes

C. maenas were collected and maintained as described in Chapter 2 (Section 2.2.2). Haemocytes were withdrawn from *C. maenas* and washed as described above (Chapter 2, Section 2.2.3). Separated, enriched HC and GC populations were obtained following the separation procedure of Söderhäll and Smith, (1983). Briefly, 60% Percoll (GE Healthcare, Buckinghamshire, UK) was made up using a combination of 32% and 3.2% NaCl solutions, and 60% continuous Percoll gradients prepared by centrifugation for 22 min at 25, 000 x g (4°C). Approximately 4 mL freshly extracted haemolymph diluted in MAC was layered onto the gradient and the cells were separated by centrifugation for 10 min at 3, 000 x g (4°C). The enriched HC and GC bands were then removed from the gradient in 1 mL fractions. The SGCs were not considered at this point in the investigation. Tait and Gunn, (1918) demonstrated that SGCs of decapods are extremely sensitive to contact with foreign substances and rapidly release their intracellular contents *in vitro*. As a result these haemocytes were distinguished as 'explosive corpuscles' (Tait and Gunn, 1918).

Cells were counted using an improved Neubauer chamber. Approximately 2 mL mixed haemocytes (2 x 10^6 mL^{-1}) or separated HCs/GCs (5 x 10^5 mL^{-1}) were cultured in suspension in ML-15 containing 1 % penicillin-streptomycin (100 U/100 µg mL^{-1}) as described above (Chapter 2, Section 2.2.4). ML-15 without penicillin-streptomycin was used for experiments involving the bacterium, *Listonella anguillarum*.

To obtain enriched populations of ProHs (immature, proliferative haemocytes), a two-step density gradient centrifugation procedure was used (Roulston and Smith, 2011). Firstly, an initial removal of 2 mL haemolymph from each crab was made, which stimulates release of immature cells into circulation. Twenty-four hours later, a second 2 mL haemolymph sample was taken (from the same crabs bled 24 h previous), which was layered onto 60% continuous Percoll and centrifuged as above. Following this first separation, only the very top layer of the HC band was removed from the gradient and

layered onto a fresh 40% continuous Percoll gradient, (made up accordingly using a combination of 32% and 3.2% NaCl solutions and prepared by centrifugation exactly as above), and subject to a second separation (10 min at 3,000 x g, 4°C). After this, the enriched ProHs (apparent as a separate layer above the HC band) were removed from the gradient in 1 mL fractions. The separated ProHs (2×10^5 mL^{-1}) were then cultured in suspension in ML-15 containing 1 % penicillin-streptomycin (100 U/100 µg mL^{-1}) as described above (Chapter 2, Section 2.2.4).

3.2.2. Measurement of apoptosis under varying conditions

Apoptosis was measured by flow cytometry using bovine lactadherin-FITC and PI staining as described in Chapter 2 (Section 2.2.6.2). Where appropriate, sub-samples of cells were also used for cyto-centrifugation and stained using Diff-Quik™ or Wright's stain, as described above (Chapter 2, Section 2.2.5.1).

3.2.2.1. Temperature

Suspension cultures (2 mL) of mixed haemocytes (2×10^6 mL^{-1}) set up in Falcon tubes and cultured in ML-15 (Chapter 2, Section 2.2.4) were incubated at 4°C, 10°C or 20°C for a total of 24 h. Temperatures of 4°C and 20°C represented the extremes that crabs are likely to experience under natural conditions, while 10°C had previously been found to be suitable for haemocyte culture (Chapter 2, Section 2.3.2.1, Figure 2.7). At 6 and 24 h, haemocyte samples (200 µL) were taken for flow cytometry as described earlier (Chapter 2, Section 2.2.6.2). One crab was sampled per experimental run with triplicate flow samples and duplicate cyto-centrifuge preparations carried out per timepoint. Haemocyte counts were made at each incubation temperature and time-point using an improved Neubauer chamber.

3.2.2.2. Effect of repeated haemolymph sampling: mimic of injury/natural infection

To mimic injury/natural infection and also to examine the effect of homeostatic disturbance, haemolymph was repeatedly sampled from crabs to induce states of haemocytopenia. Crabs may experience haemocytopenia as a result of injury or natural

infections. For this, crabs were bled by withdrawing 2 mL of haemolymph (Chapter 2, Section 2.2.3) three times per week over a period of 2 weeks. The crabs were bled again in the third week but this time the mixed haemocytes were harvested, washed (Chapter 2, Section 2.2.3), and cultured in suspension (2 mL) in ML-15 in Falcon tubes at a concentration of 5×10^5 mL^{-1} (lower cell concentration due to haemocytopenia) as above (Chapter 2, Section 2.2.4). The haemocytes were incubated for 24 h at 10°C with sub-samples taken from each after 6 h and at the end of the incubation period. The samples were subjected to flow cytometric analysis to ascertain the percentage of viable, early apoptotic and late apoptotic/necrotic haemocytes (Chapter 2, Section 2.2.6.2). One crab was sampled per experimental run with triplicate flow samples and duplicate cyto-centrifuge preparations (Chapter 2, Section 2.2.5.1) carried out per timepoint (1×10^5 haemocytes/cyto-centrifuge preparation).

3.2.3. Apoptosis in different haemocyte populations

To compare apoptosis in different haemocyte types, suspension cultures (2 mL) of separated HCs and GCs (5×10^5 mL^{-1}) or ProHs (2×10^5 mL^{-1}) in ML-15 were prepared and maintained as above (Section 3.2.1). As ProHs are less numerous than the other cell types, even under enforced haemocytopenia, their starting concentration was lower. At 6 and 24 h (10°C), sub-samples were taken from the cultures for counting, flow cytometry and cyto-centrifugation. The percentage of viable, early apoptotic or late apoptotic/necrotic haemocytes were then determined for each haemocyte type, following the procedures described in Chapter 2 (Section 2.2.6.2). For each haemocyte type, one crab was sampled per experimental run, with triplicate flow samples and duplicate cyto-centrifuge preparations (Chapter 2, Section 2.2.5.1) carried out per time-point. To confirm that temperature-induced apoptosis in HCs and GCs was caspase-dependent, the pan-caspase inhibitor Q-VD-OPh was used as above (Chapter 2, Section 2.2.6.2).

3.2.4. Apoptosis in HCs after treatment with non-self agents

Following the results from the above experiment (Section 3.2.3), the HCs were the only cell type used in the experiments with non-self agents, specifically LPS or the bacterium, *Listonella anguillarum*.

3.2.4.1. Lipopolysaccharide

Triplicate suspension cultures (2 mL) of HCs (5 x 10^5 mL^{-1}) in ML-15 were set up in Falcon tubes (Section 3.2.3). The HCs were incubated with either 0.1 or 1 µg mL^{-1} of LPS from *Escherichia coli* serotype 0111:B4, or ML-15 only (control). All tubes were incubated at 10^{o}C for 6 h and 24h. At both intervals, the percentages of viable, early apoptotic or late apoptotic/necrotic cells were determined by flow cytometry as described in Chapter 2 (Section 2.2.6.2). One crab was sampled per experimental run with triplicate flow samples carried out per timepoint on each treatment.

3.2.4.2. Listonella anguillarum

Suspension cultures (2 mL) of freshly isolated HCs (5 x 10^5 mL^{-1}) were set up as described above (Section 3.2.3), but using ML-15 without penicillin-streptomycin. The HCs were subsequently challenged with different concentrations of either viable or heat-killed suspension cultures of the marine Gram negative bacterium, *L. anguillarum* (ATCC 43305). The bacteria were grown to log phase (ca. 24 h) in tryptic soy broth (TSB) (Oxoid) supplemented with 1% NaCl at room temperature. After harvesting, the bacteria were washed once in TSB (4, 000 x g for 5 min) and resuspended in 10 mL 0.9% sterile NaCl before assessing viable plate counts on tryptic soy agar (TSA) (Oxoid) supplemented with 1% NaCl. Approximately 200 µL of the viable bacteria resuspended in 0.9% NaCl were then added to the HC suspension cultures to give final bacteria concentrations of 3 x 10^4 mL^{-1}, 3 x 10^5 mL^{-1}, 3 x 10^6 mL^{-1}, 3 x 10^7 mL^{-1} and 3 x 10^8 mL^{-1} in a final volume of 2 mL. Control HCs received an equal volume of 0.9% NaCl only. All HC suspension cultures were incubated at 10°C, with sub-samples taken at 6 and 24 h intervals. The percentages of viable, early apoptotic or late apoptotic/necrotic cells were then determined by flow cytometry as described above (Chapter 2, Section 2.2.6.2). One crab was sampled per experimental run with triplicate flow samples carried out per timepoint on each treatment.

In separate experiments, suspension cultures (2 mL) of HCs (5 x 10^5 mL^{-1}) were set up, as above, except that after washing in broth, the bacteria were heat-killed (95^{o}C, 25 min). To confirm the bacteria were dead the bacteria were plated out on TSA plates supplemented with 1% NaCl to ensure no colony growth occurred. Approximately

200 µL of heat-killed bacteria resuspended in 0.9% NaCl were then added to the HC suspension cultures to give the same final concentrations of bacteria as above in a final volume of 2 mL. Again, control HCs received an equal volume of 0.9% NaCl only. The experimental and control HC cultures were then incubated at 10°C with sub-samples taken at 6 h and 24 h for flow cytometric analysis (Chapter 2, Section 2.2.6.2). One crab was sampled per experimental run with triplicate flow samples carried out per timepoint on each treatment.

3.2.5. Statistical analyses

All values were calculated as mean ± SEM. Percentage values were arc sine transformed and cell count data square root transformed before statistical analysis. Statistical differences were then determined as described in Chapter 2 (Section 2.2.7). Significance was accepted at $P<0.05$.

3.3. Results

3.3.1. Apoptosis in haemocytes under varying life conditions

3.3.1.1. Temperature

Haemocyte numbers were significantly reduced at both 6 and 24 h timepoints at 20°C (P<0.001; n=3), compared to controls (Figure 3.1). After 6 h culture at 20°C, the haemocyte numbers dropped to 7.8 x 10^5 mL^{-1} ± 1.2 x 10^5 mL^{-1} SEM (P<0.001; n=3), representing >50% of total haemocyte loss from original concentration at 0 h (2 x 10^6 mL^{-1}). A further decrease representing >70% was observed after 24 h at 20°C (5.2 x 10^5 mL^{-1} ± 1 x 10^5 mL^{-1} SEM; P<0.001; n=3). After 6 h culture at 4°C and 10°C (control), haemocyte numbers remained high at 1.4 x 10^6 mL^{-1} ± 1.2 x 10^5 mL^{-1} SEM and 1.5 x 10^6 mL^{-1} ± 7.2 x 10^4 mL^{-1} SEM respectively (Figure 3.1). After 24 h culture at 4°C and 10°C only slight additional decreases in haemocyte numbers were observed, with haemocyte numbers of 1.1 x 10^6 mL^{-1} ± 7.7 x 10^4 mL^{-1} SEM and 1.3 x 10^6 mL^{-1} ± 6.1 x 10^4 mL^{-1} SEM respectively at this timepoint (Figure 3.1). In terms of total percentage loss, haemocyte numbers only decreased by *ca.* 35% and 30% after 24 h culture at 4°C and 10°C respectively, and no significant difference was found between these two temperatures (Figure 3.1). Numerous necrotic haemocytes were observed after 6 h culture at 20°C (Figure 3.2, C, I, arrows) and after 24 h culture, haemocytes exhibited membrane blebbing, indicative of apoptotic cells (Figure 3.2, C, II, arrows). There appeared far less morphological evidence of cell death in haemocytes cultured at 4°C (Figure 3.2, A) or 10°C (Figure 3.2, B) after both 6 h (I) and 24 h (II) culture. At 4°C and 10°C, the majority of haemocytes appeared viable, although small numbers of haemocytes did exhibit characteristic apoptotic irregular shaped nuclei (Figure 3.2, A, B, I, II, arrows).

Flow cytometry confirmed that haemocytes cultured at 20°C exhibited lower viability and higher levels of cell death compared with 4 or 10°C at both time intervals (Figure 3.3, A, B). Optimal viability was observed at 10°C where haemocyte viability remained high after 6 h (73.1% ± 3.1% SEM) and 24 h (80.2% ± 2.4% SEM) (Figure 3.3, A). At 20°C, percentages of viability were significantly less after 6 h (40.8% ± 7.4% SEM; P<0.05; n=3) and 24 h (43.3% ± 4.5% SEM; P<0.01; n=3) compared to control haemocytes cultured at 10°C (Figure 3.3, A). Significantly higher levels of late apoptosis/necrosis were

obtained after 6 h culture at 20°C (46.2% ± 5.8% SEM; $P<0.05$; n=3) compared to late apoptotic/necrotic control haemocytes cultured at 10°C (16.4% ± 5.2% SEM) (Figure 3.3, B). After 24 h at 20°C, a significant increase in early apoptosis was observed (35.5% ± 3.1% SEM; $P<0.001$; n=3) compared to early apoptotic control haemocytes cultured at 10°C (4.1% ± 1.7% SEM) (Figure 3.3, B). Additionally, significant levels of late apoptosis/necrosis were exhibited after 24 h culture at 4°C (27.5% ± 7.6% SEM) compared to late apoptotic/necrotic control haemocytes at the same timepoint (Figure 3.3, B).

Representative flow cytometry dotplots illustrate that after 6 h culture (20°C), the majority of events appear in the upper right quadrant indicative of late apoptotic/necrotic haemocytes (Appendix 1, C, I). Conversely, after 24 h culture (20°C) a larger proportion of events appear in the lower right quadrant indicative of higher levels of early apoptosis (Appendix 1, C, II). Flow cytometry dotplots representative of haemocytes cultured at 4°C (Appendix 1, A) and 10°C (Appendix 1, B) show that after 6 h (I) and 24 h (II) the majority of events remain in the lower left quadrant, indicative of viable haemocytes.

Figure 3.1.

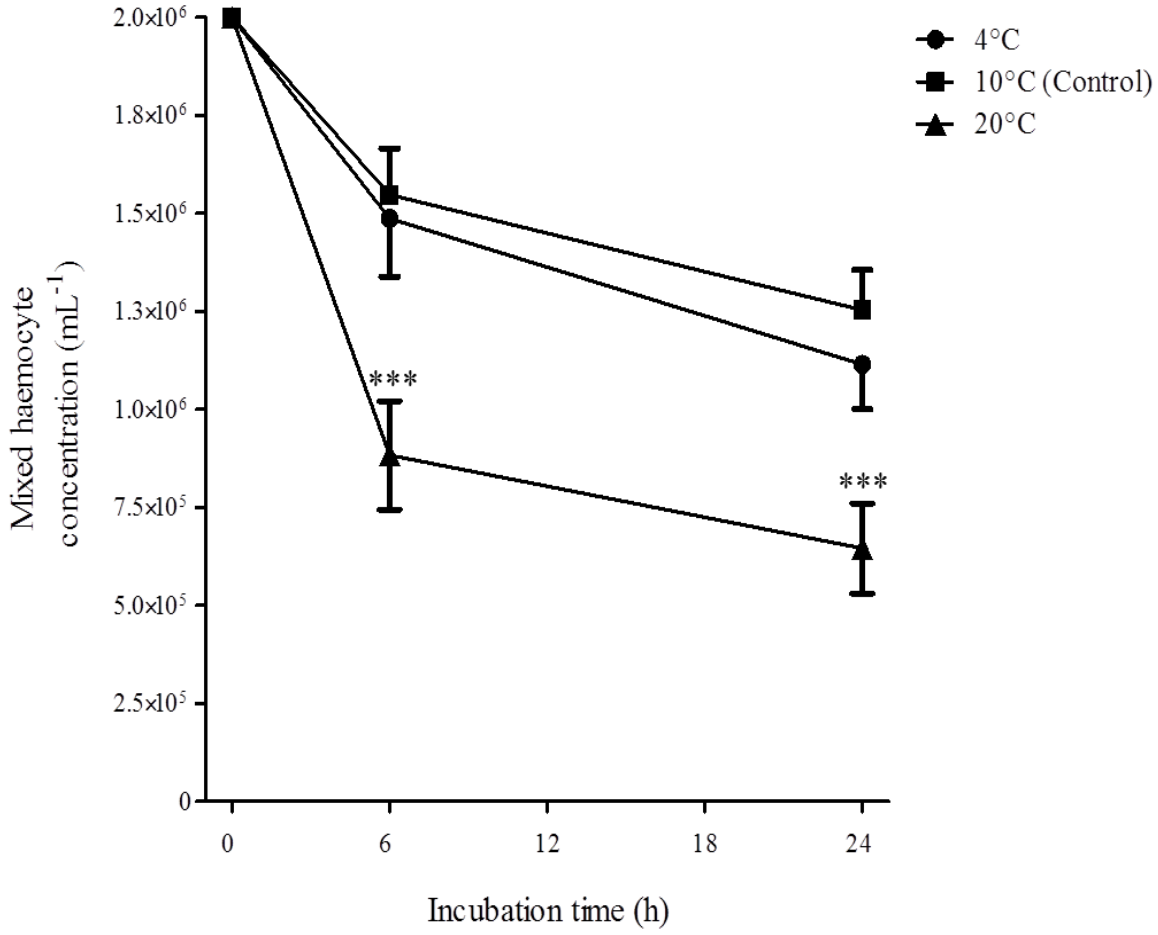

Figure 3.1. *C. maenas* mixed haemocytes counts after suspension culture *in vitro* at different incubation temperatures. Mixed haemocytes (2 x 10^6 mL^{-1} at 0 h) were cultured at 4°C, 10°C (control) or 20°C and haemocytometer counts made after 6 h and 24 h. Data are expressed as means ± SEM, n=3, with a different crab used on each occasion. Statistical analysis was performed upon square root transformed data using one-way ANOVA with a Student Newman-Keuls multiple comparison *post hoc* test. *** $P<0.001$ *vs.* 10°C (control) mixed haemocyte concentration at the corresponding timepoint.

Figure 3.2.

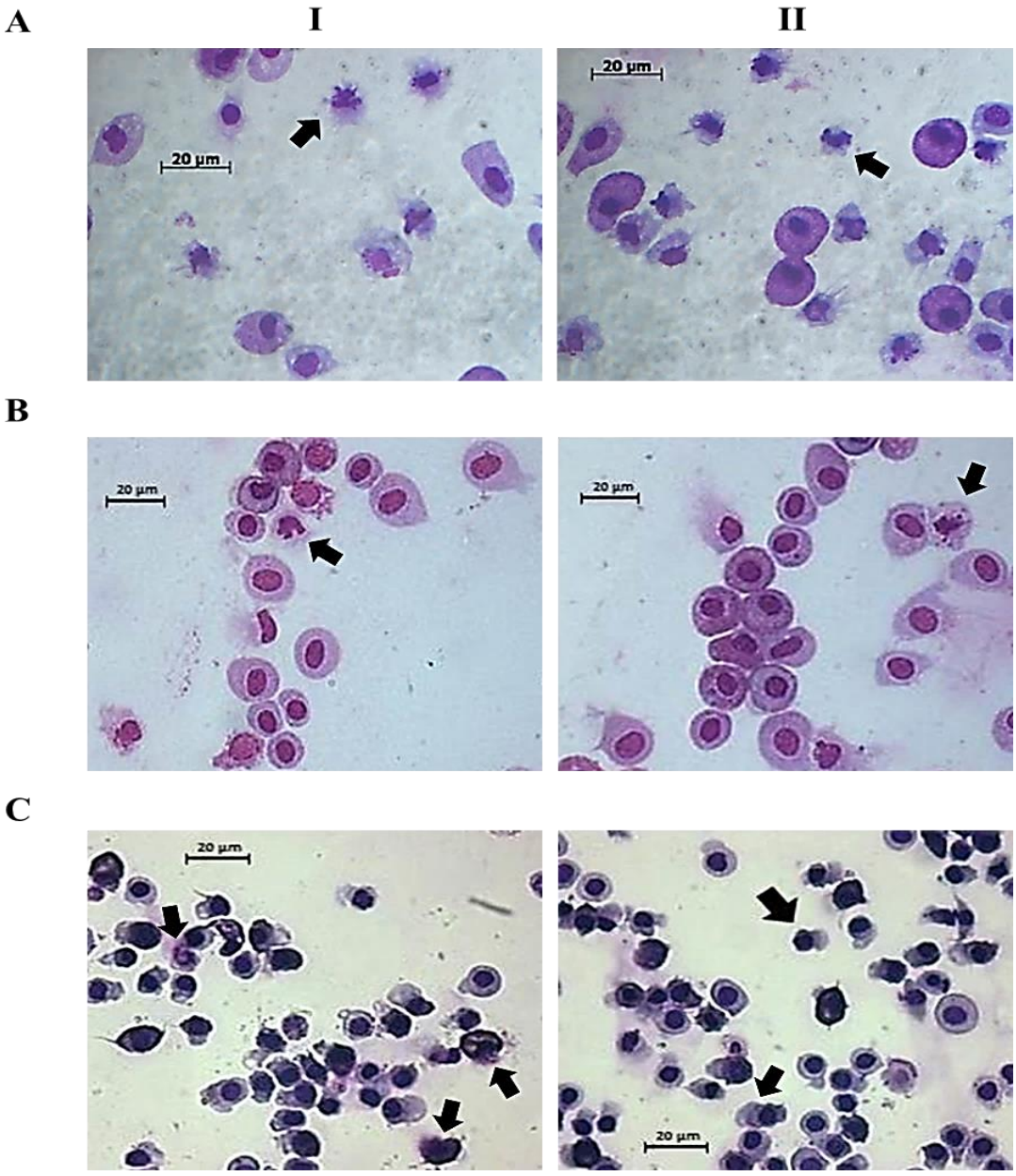

Figure 3.2. Morphological evidence of apoptosis and necrosis in *C. maenas* mixed haemocytes after suspension culture *in vitro* at different incubation temperatures. Representative Diff-Quik™ stained (**A, B**) and Wright's stained (**C**) cyto-centrifuge preparations after 6 h (**I**) and 24 h (**II**) culture at 4°C (**A**), 10°C (**B**, control) or 20°C (**C**). Arrows indicate characteristic features of apoptosis such as irregular shaped nuclei (**A, B**) and membrane blebbing (**C, II**), whereas loss of membrane integrity, a trademark feature of necrosis was observed after 6 h culture at 20°C (**C, I**). Moreover, cell shrinkage was evident at 20°C, providing further evidence of apoptosis (**C**). Cyto-centrifuge preparations at 200x total mag and are representative of n=3 experiments. Scale bars = 20 µm.

Figure 3.3.

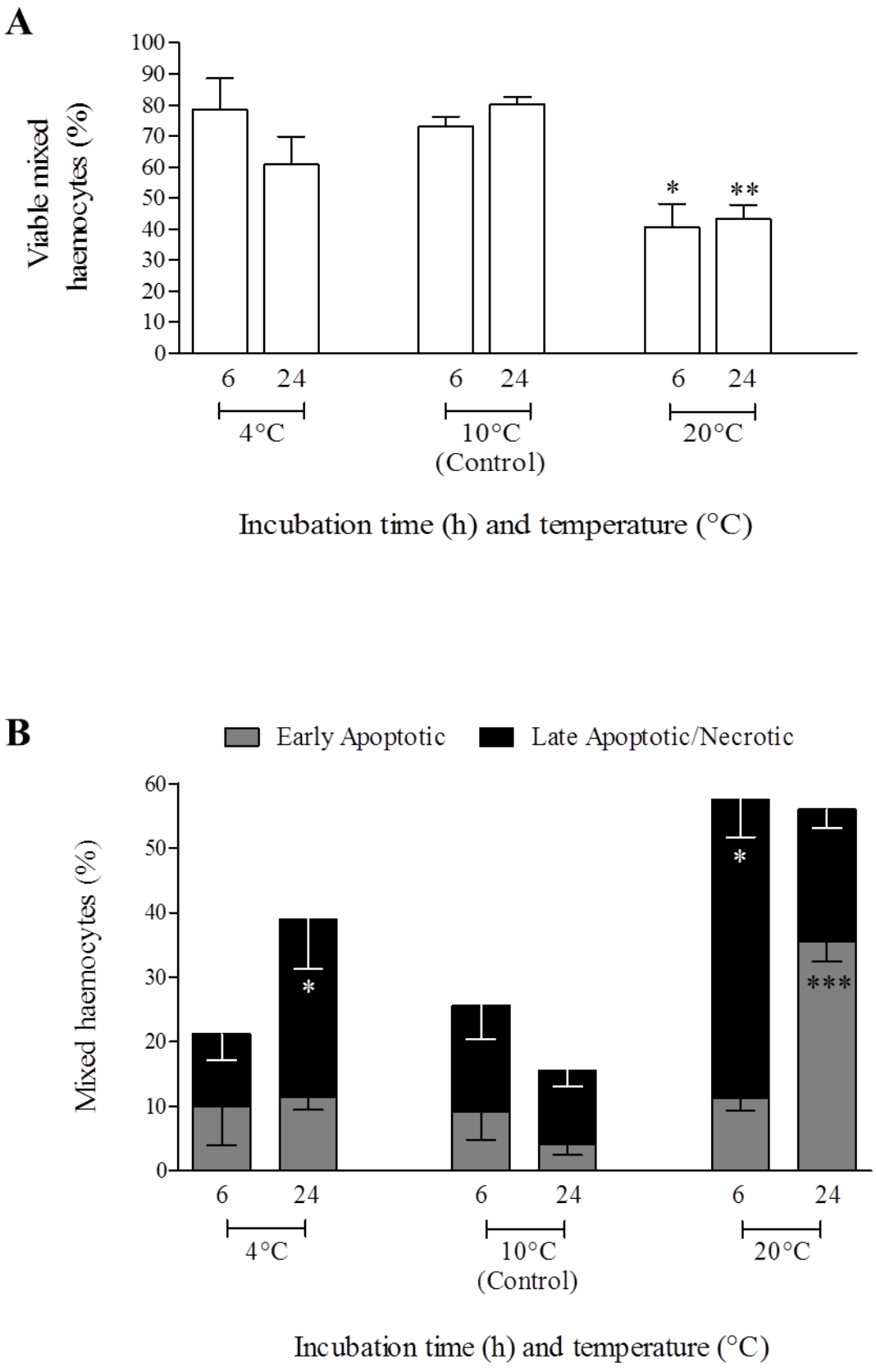
A
Viable mixed haemocytes (%)
100
90
80
70
60
50
40
30
20
10
0
*
**
6
24
6
24
6
24
4°C
10°C
(Control)
20°C
Incubation time (h) and temperature (°C)
B
Early Apoptotic
Late Apoptotic/Necrotic
Mixed haemocytes (%)
60
50
40
30
20
10
0
*
*
***
6
24
6
24
6
24
4°C
10°C
(Control)
20°C
Incubation time (h) and temperature (°C)

Figure 3.3. Percentages of viable, early apoptotic and late apoptotic/necrotic *C. maenas* haemocytes after suspension culture *in vitro* at different incubation temperatures. (**A**-**B**): Quantified percentages of viability (**A**) and apoptosis/necrosis (**B**) in mixed haemocytes after 6 h and 24 h culture at 4°C, 10°C (control) or 20°C. Values were quantified using flow cytometry via bovine lactadherin-FITC and PI staining. Data are expressed as means ± SEM, n=3, with a different crab used on each occasion**.** Refer to Appendix 1 for representative flow cytometry dot plots**.** Statistical analysis was performed upon arc sine transformed data using one-way ANOVA with a Student Newman-Keuls multiple comparison *post hoc* test. * $P<0.05$ *vs.* matching viable control mixed haemocytes or late apoptotic/necrotic control mixed haemocytes at the corresponding timepoint; ** $P<0.01$ *vs.* matching viable control mixed haemocytes at the corresponding timepoint; *** $P<0.001$ *vs.* matching early apoptotic control mixed haemocytes at the corresponding timepoint.

3.3.1.2. Effect of repeated haemolymph sampling: mimic of injury/natural infection

Haemocytes obtained from crabs subject to repeated haemolymph sampling exhibited abundant apoptotic and necrotic cell morphology (Figure 3.4, A). Numerous apoptotic irregular shaped nuclei were apparent after 6 h (Figure 3.4, A, I, arrows) whereas, after 24 h many of the granular haemocytes within the mixed haemocyte pool were necrotic, evidenced by the large abundance of extracellular granules due to loss of membrane integrity (Figure 3.4, A, II, arrows). Flow cytometry analysis revealed a significant reduction in the percentage of viable haemocytes obtained from crabs subjected to repeated haemolymph sampling after 6 h (48.7% ± 7.9% SEM; $P<0.05$; n=3) and 24 h (36.8% ± 5.9% SEM; $P<0.001$; n=3) compared to haemocytes obtained from previously un-bled (control) crabs (Figure 3.4, B; Appendix 2). Haemocyte viability remained high in control crabs after 6 and 24 h culture, with percentages of 73.1% ± 3.1% SEM and 80.2% ± 2.4% SEM respectively (Figure 3.4, B). Haemocytes obtained from crabs subjected to repeated haemolymph sampling also exhibited significant increases in percentages of late apoptosis/necrosis after both 6 h (37.4% ± 5% SEM; $P<0.05$; n=3) and 24 h (44.1% ± 5.1% SEM; $P<0.001$; n=3), as well as a significant increase in early apoptosis after 24 h (18.7% ± 3.3% SEM; $P<0.01$; n=3) compared to haemocytes obtained from control crabs (Figure 3.4, C; Appendix 2). Conversely, percentages of late apoptosis/necrosis remained low in haemocytes obtained from control crabs, with percentages of 16.4% ± 5.2% SEM and 11.4% ± 2.5% SEM after 6 and 24 h culture respectively (Figure 3.4, C). Similarly, percentages of early apoptosis also remained low in haemocytes obtained from control crabs, with percentages of 9.1% ± 4.3% SEM and 4.1% ± 1.7% SEM after 6 and 24 h culture respectively (Figure 3.4, C). In crabs subject to repeated bleeding, the maximum attainable concentration of mixed haemocytes (mL^{-1}) for experimental culture was 4x less (5×10^5 mL^{-1}) than the concentration obtained from un-bled (control) crabs (2×10^6 mL^{-1}).

Figure 3.4.

A

I

II

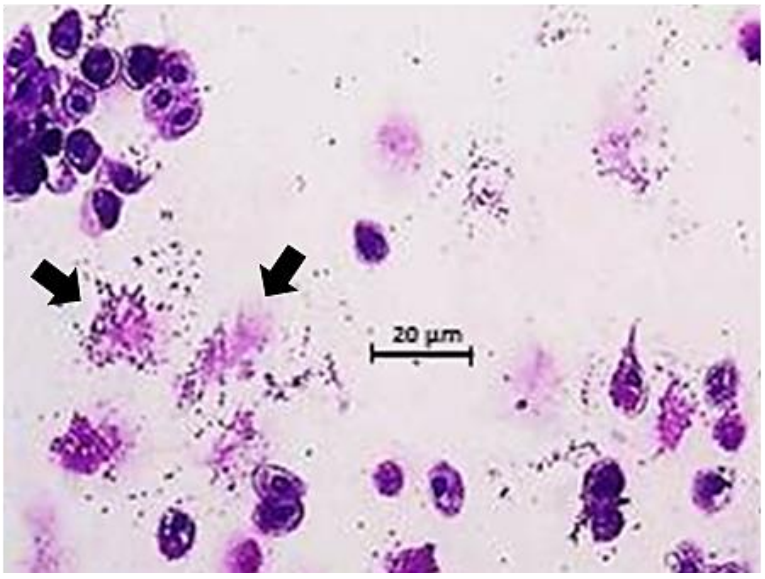

Figure 3.4 continued.

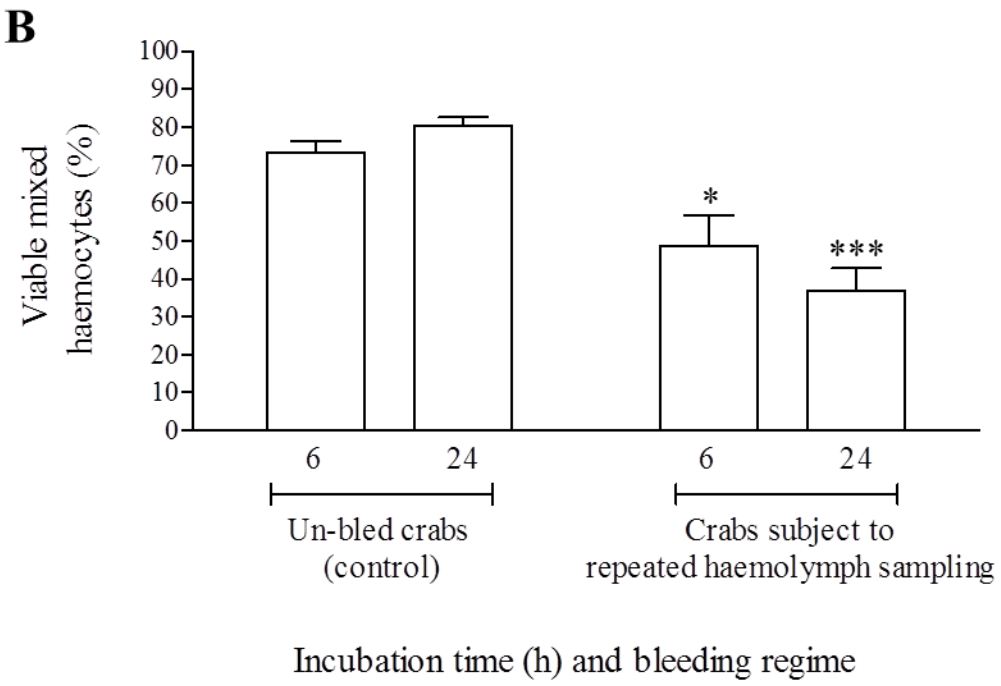

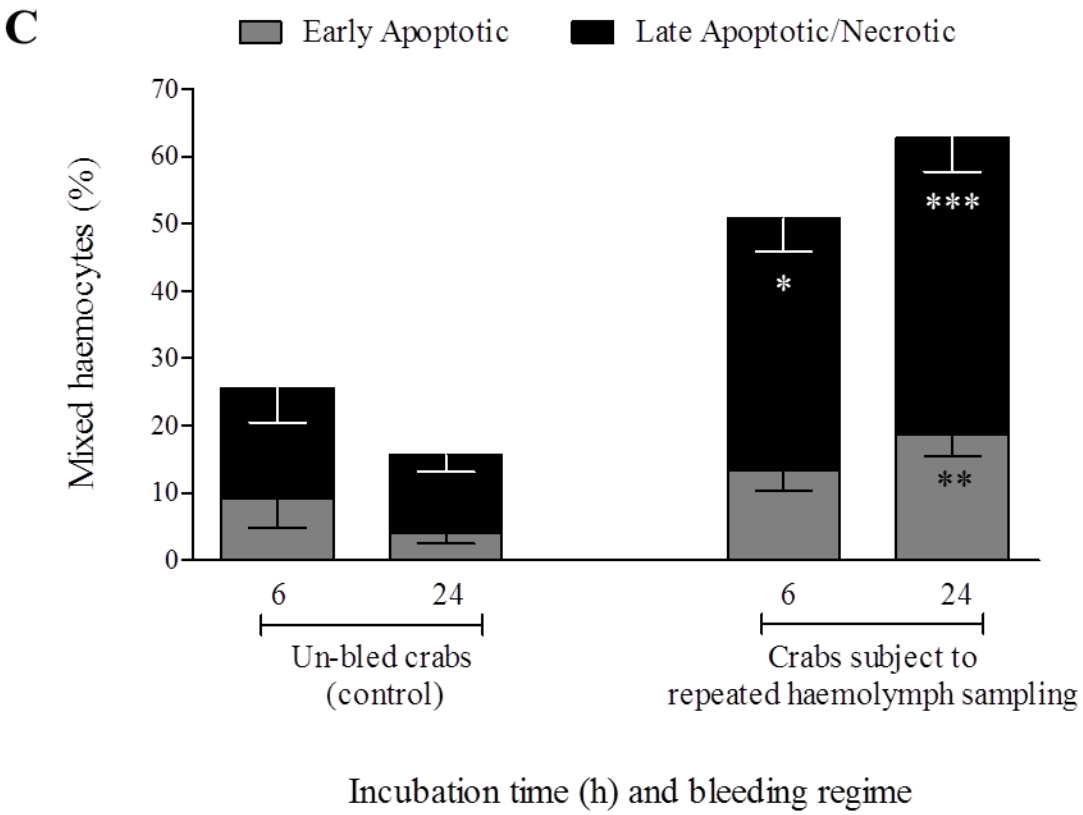

Figure 3.4. Viable, early apoptotic and late apoptotic/necrotic *C. maenas* mixed haemocytes after suspension culture *in vitro*, obtained from crabs subject to repeated haemolymph sampling. (**A**): Representative (n=3 experiments) Diff-Quik™ stained cyto-centrifuge preparations of haemocytes after 6 h (**I**) and 24 h (**II**) culture (10°C), obtained from crabs bleed three times per week for two weeks. Arrows indicate characteristic features of cell death, such as apoptotic irregular shaped nuclei (**A, I**) and loss of membrane integrity as a result of necrosis, evidenced by extracellular granules (**A, II**). Cyto-centrifuge preparations at 200x total mag, scale bars = 20 µm. (**B-C**): Quantified percentages of viability (**B**) and apoptosis/necrosis (**C**) in mixed haemocytes after 6 h and 24 h culture (10°C), obtained from previously un-bled crabs (control) or crabs subject to repeated haemolymph sampling. Quantification using flow cytometry with bovine lactadherin-FITC and PI staining. Data are expressed as means ± SEM, n=3, with a different crab used on each occasion. Refer to Appendix 2 for representative flow cytometry dot plots. Statistical analysis was performed upon arc sine transformed data using one-way ANOVA with a Student Newman-Keuls multiple comparison *post hoc* test. * $P<0.05$, *** $P<0.001$ *vs.* matching viable control mixed haemocytes or late apoptotic/necrotic control mixed haemocytes at the corresponding timepoint; ** $P<0.01$ *vs.* matching early apoptotic control mixed haemocytes at the corresponding timepoint.

3.3.2. Apoptosis in different haemocyte populations

Significant reductions in HC numbers were observed after 6 h (3.3×10^5 mL^{-1} ± 0.19×10^5 mL^{-1} SEM; $P<0.01$; n=3) and 24 h (1.4×10^5 mL^{-1} ± 0.18×10^5 mL^{-1} SEM; $P<0.001$; n=3) compared with the GCs (Figure 3.5). GCs numbers declined far more gradually, with higher cell numbers retained after 6 h (4.2×10^5 mL^{-1} ± 0.08×10^5 mL^{-1} SEM) and 24 h (3.2×10^5 mL^{-1} ± 0.14×10^5 mL^{-1}) (Figure 3.5). A similar trend was observed in separated ProHs after 6 h (1.5×10^5 mL^{-1} ± 0.13×10^5 mL^{-1} SEM) and 24 h (1.1×10^5 mL^{-1} ± 0.9×10^5 mL^{-1} SEM) (Figure 3.5).

From analyses of cyto-centrifuge preparations it was evident that separated HCs exhibited characteristic apoptotic morphology, such as irregular shaped nuclei, karyorrhexis and/or membrane blebbing (Figure 3.6, A, I, II, arrows). There was also evidence of membrane rupture in a necrotic HC after 24 h (Figure 3.6, A, II, red arrow). Separated GCs remained largely viable after both 6 h and 24 h (Figure 3.6, B, I, II) with little evidence of cell death, although a degranulating GC was visible after 24 h (Figure 3.6, B, II, arrow). There was a marginally higher level of apoptosis in separated ProHs where haemocytes displayed karyorrhexis and membrane blebbing after 24 h (Figure 3.6, C, II, arrows).

Flow cytometry confirmed that HCs exhibited lower viability and more cell death (Figure 3.7, A, B; Appendix 3, A) over a 24 h incubation period. In contrast, higher viability and lower cell death values were obtained in separated GCs and ProHs (Figure 3.7, A, B; Appendix 3, B, C), with optimal viability observed in separated GCs after 24 h culture (Figure 3.7, A; Appendix 3, B). Viability of HCs was significantly less after 6 h (59.1% ± 1.8% SEM; $P<0.001$; n=3) and 24 h (44.3% ± 3.9% SEM; $P<0.05$; n=3) compared to GCs (Figure 3.7, A). High percentages of viability were retained after 24 h in separated GCs (77.9% ± 2.1% SEM) and in ProHs (70.1% ± 7.9% SEM) (Figure 3.7, A). After 6 h culture, HCs exhibited significant increases in both early (22.4% ± 2.1% SEM; $P<0.01$; n=3) and late apoptosis (18.5% ± 3.8% SEM; $P<0.05$; n=3) compared to GCs (Figure 3.7, B). After 24 h, the rate of HC early apoptosis was 19.1% ± 1.8% SEM and late apoptosis/necrosis was 36.6% ± 5.5% SEM (Figure 3.7, B), however, values were not

statistically significant compared to GCs. With regard to GCs and ProHs, low levels of early apoptosis and late apoptosis/necrosis were obtained in these haemocyte types after 6 h and 24 h, with lowest overall levels of cell death exhibited by GCs (Figure 3.7, B).

When tested with Q-VD-OPh, it was confirmed that both HCs and GCs underwent caspase-dependent apoptosis. After 6 h culture (20°C) with Q-VD-OPh, both HCs and GCs retained significant viability ($P<0.001$; n=3) compared to controls (Figure 3.8, A-D). Viability in Q-VD-OPh treated HCs remained high at 79.4% (± 3.4% SEM) whereas HCs minus Q-VD-OPh at the same temperature exhibited low viability (37.9% ± 4.7% SEM) (Figure 3.8, A, C). Similarly, Q-VD-OPh treated GCs also showed high viability (82.8% ± 2.8% SEM) compared to control GCs minus Q-VD-OPh (45.2% ± 1.9% SEM) (Figure 3.8, B, D). HCs at 20°C exhibited significant increases ($P<0.05$; n=3) in early apoptosis (20.7% ± 8.5% SEM) and late apoptosis/necrosis (39.2% ± 3.3% SEM) compared to Q-VD-OPh treated HCs (Figure 3.8, A, C). Conversely, Q-VD-OPh treated HCs exhibited <25% total cell death (Figure 3.8, A, C). GCs showed similar results, with GCs at 20°C exhibiting significantly higher values for early apoptosis (20.8% ± 3.3% SEM; $P<0.05$; n=3) and late apoptosis/necrosis (32.9% ± 3.6% SEM; $P<0.01$; n=3) compared to Q-VD-OPh treated GCs (Figure 3.8, B, D). In contrast, Q-VD-OPh treated GCs exhibited <20% total cell death (Figure 3.8, B, D).

Figure 3.5.

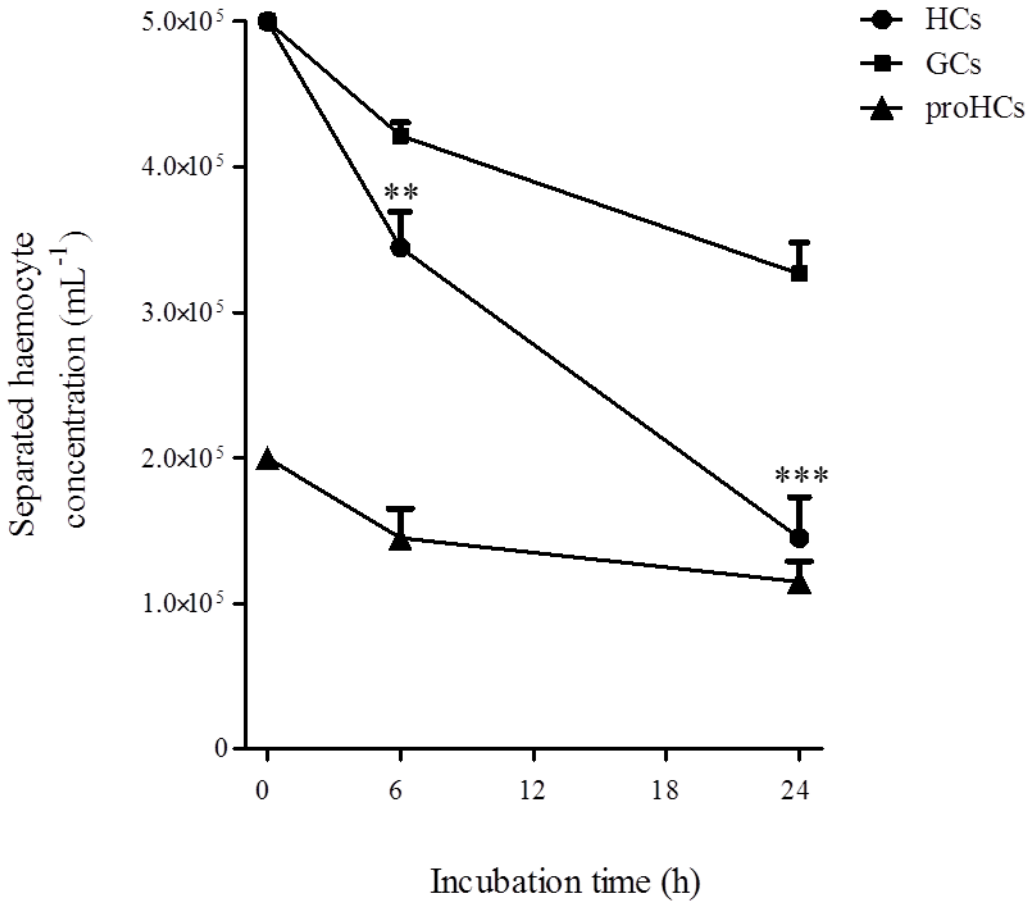

Figure 3.5. Separated *C. maenas* haemocyte counts after suspension culture *in vitro*. Separated HCs and GCs (5 x 10^5 mL^{-1} at 0 h) or ProHs (2 x 10^5 mL^{-1} at 0 h) were cultured at 10°C and haemocytometer counts made after 6 h and 24 h. Data are expressed as means ± SEM, n=3, with a different crab used on each occasion. Statistical analysis was performed upon square root transformed data using one-way ANOVA with a Student Newman-Keuls multiple comparison *post hoc* test. ** $P<0.01$, *** $P<0.001$ *vs.* granular cell concentration at the corresponding timepoint.

Figure 3.6.

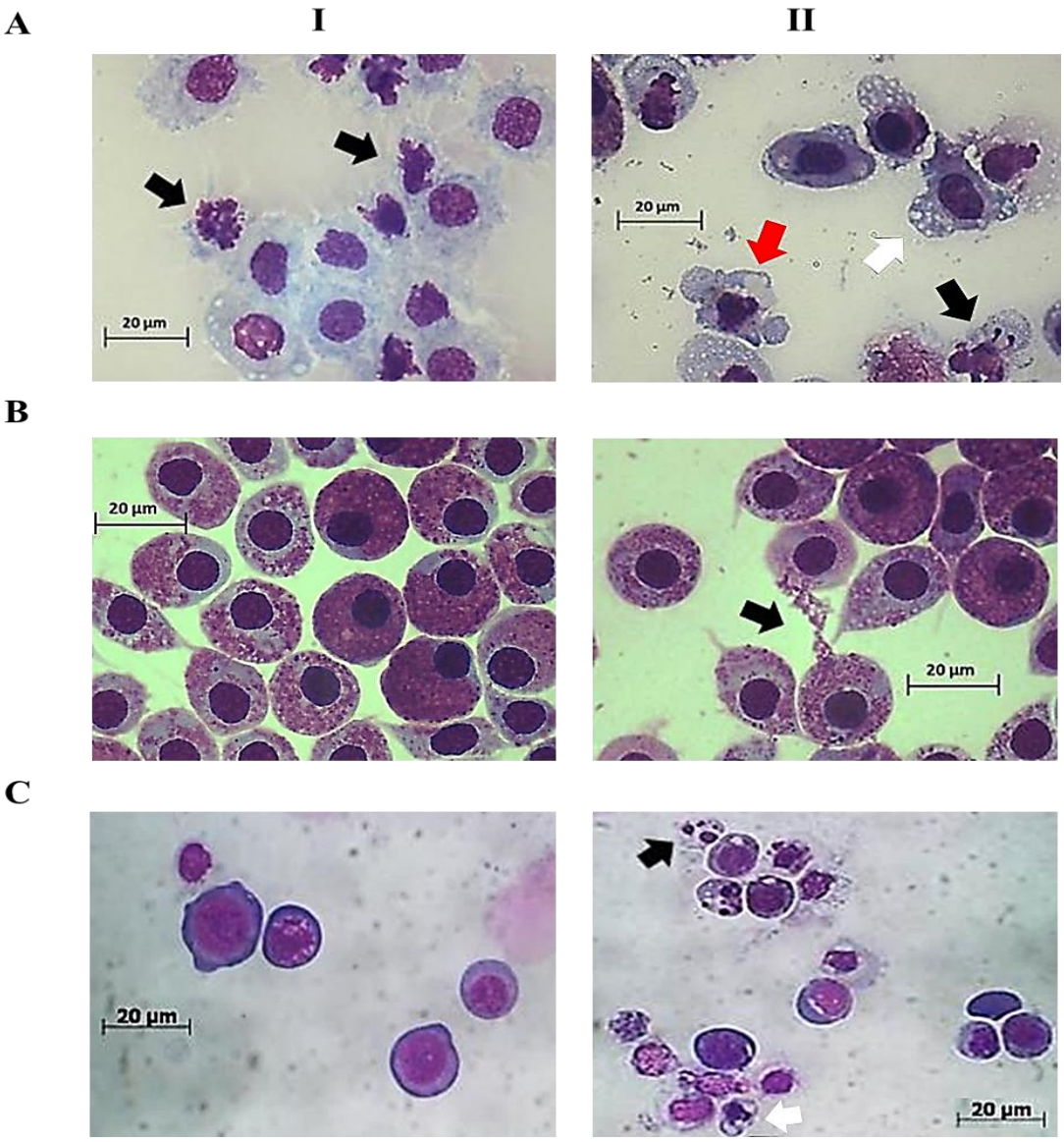

Figure 3.6. Morphological evidence of apoptosis and necrosis in separated *C. maenas* haemocytes after suspension culture *in vitro*. Representative Wright's stained (**A**) and Diff-Quik™ stained (**B, C**) cyto-centrifuge preparations of separated HCs (**A**), GCs (**B**) or ProHs (**C**) after 6 h (**I**) and 24 h (**II**) culture (10°C). Arrows indicate characteristic features of apoptosis such as irregular shaped nuclei (**A, I**), membrane blebbing (**A, C, II** white arrows), and karyorrhexis (**A, C, II** black arrows). Cell shrinkage is also apparent in apoptotic ProHs after 24 h culture (**C, II**). Membrane rupture in a necrotic hyaline cell (**A, II** red arrow) and degranulation in a granular cell (**B, II**) can also be seen. Cyto-centrifuge preparations at 630x total mag (**A, B**) or 200x total mag (**C**) and are representative of n=3 experiments. Scale bars = 20 µm, images representative of n=3 experiments.

Figure 3.7.

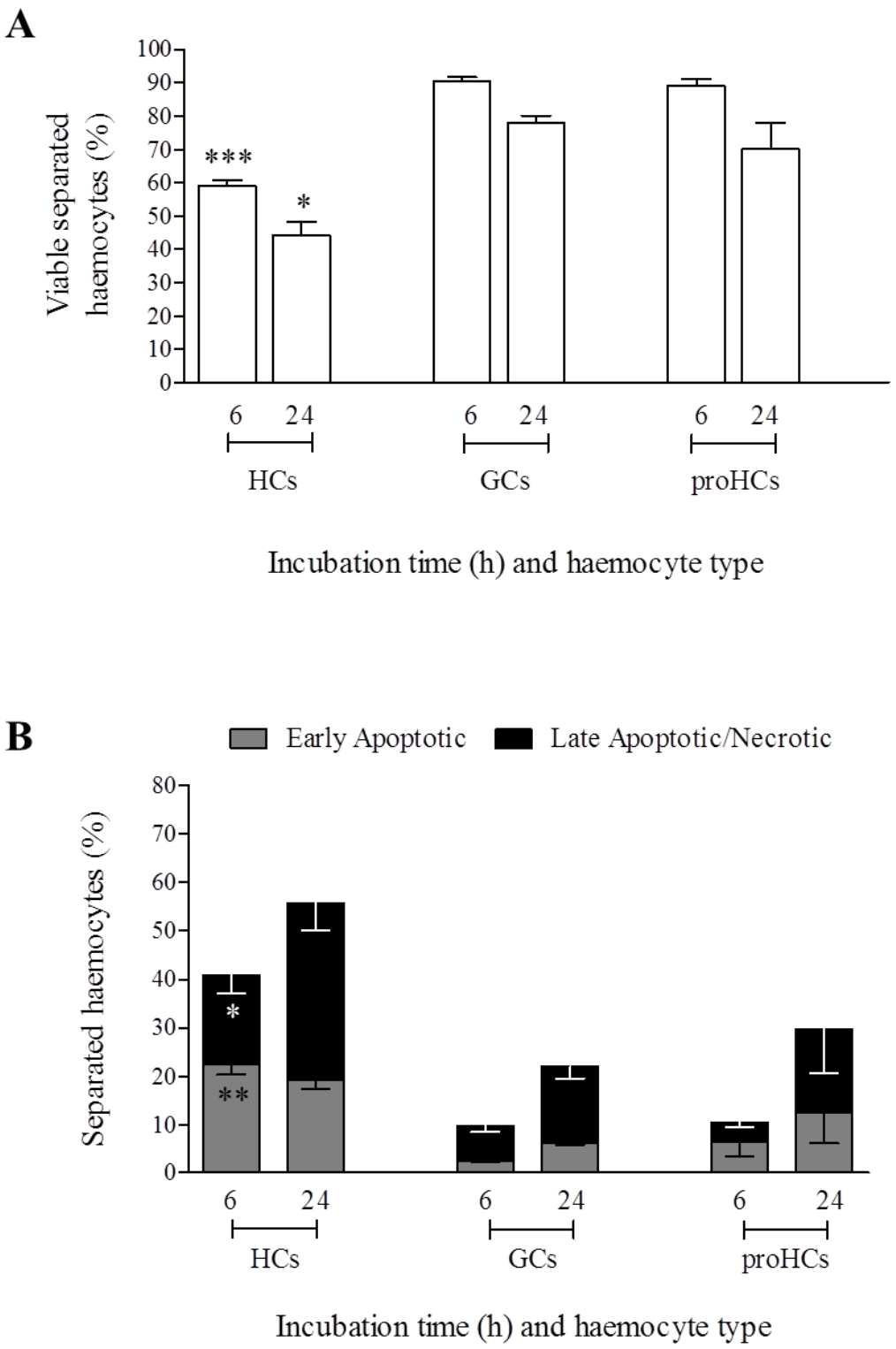
A
Viable separated haemocytes (%)
100
90
80
70
60
50
40
30
20
10
0
***
*
6
24
6
24
6
24
HCs
GCs
proHCs
Incubation time (h) and haemocyte type
B
Early Apoptotic
Late Apoptotic/Necrotic
Separated haemocytes (%)
80
70
60
50
40
30
20
10
0
*
**
6
24
6
24
6
24
HCs
GCs
proHCs
Incubation time (h) and haemocyte type

Figure 3.7. Constitutive percentages of viable, early apoptotic and late apoptotic/necrotic separated *C. maenas* haemocytes after suspension culture *in vitro*. (**A-B**): Viability (**A**) and apoptosis/necrosis (**B**) in HCs, GCs or ProHs after 6 h and 24 h culture (10°C). Values were quantified using flow cytometry via bovine lactadherin-FITC and PI staining. Data are expressed as means ± SEM, n=3, with a different crab used on each occasion. Refer to Appendix 3 for representative flow cytometry dot plots. Statistical analysis was performed upon arc sine transformed data using one-way ANOVA with a Student Newman-Keuls multiple comparison *post hoc* test. * $P<0.05$, *** $P<0.001$ *vs.* matching viable GCs or late apoptotic/necrotic GCs at the corresponding timepoint; ** $P<0.01$ *vs.* matching early apoptotic GCs at the corresponding timepoint.

Figure 3.8.

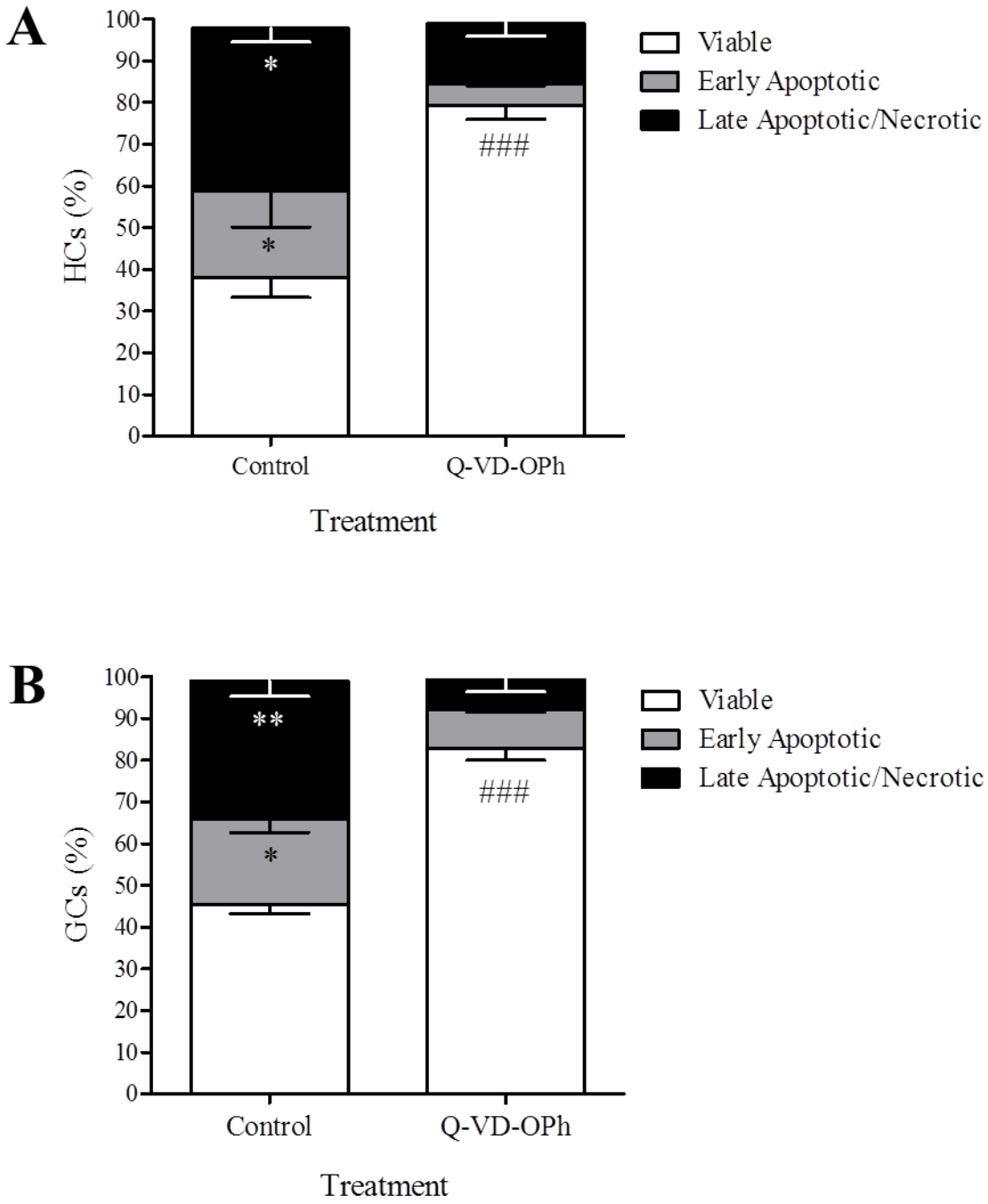
A
100
90
80
70
60
50
40
30
20
10
0
HCs (%)
*
*
###
Control
Q-VD-OPh
Treatment
Viable
Early Apoptotic
Late Apoptotic/Necrotic
B
100
90
80
70
60
50
40
30
20
10
0
GCs (%)
**
*
###
Control
Q-VD-OPh
Treatment
Viable
Early Apoptotic
Late Apoptotic/Necrotic

Figure 3.8 continued.

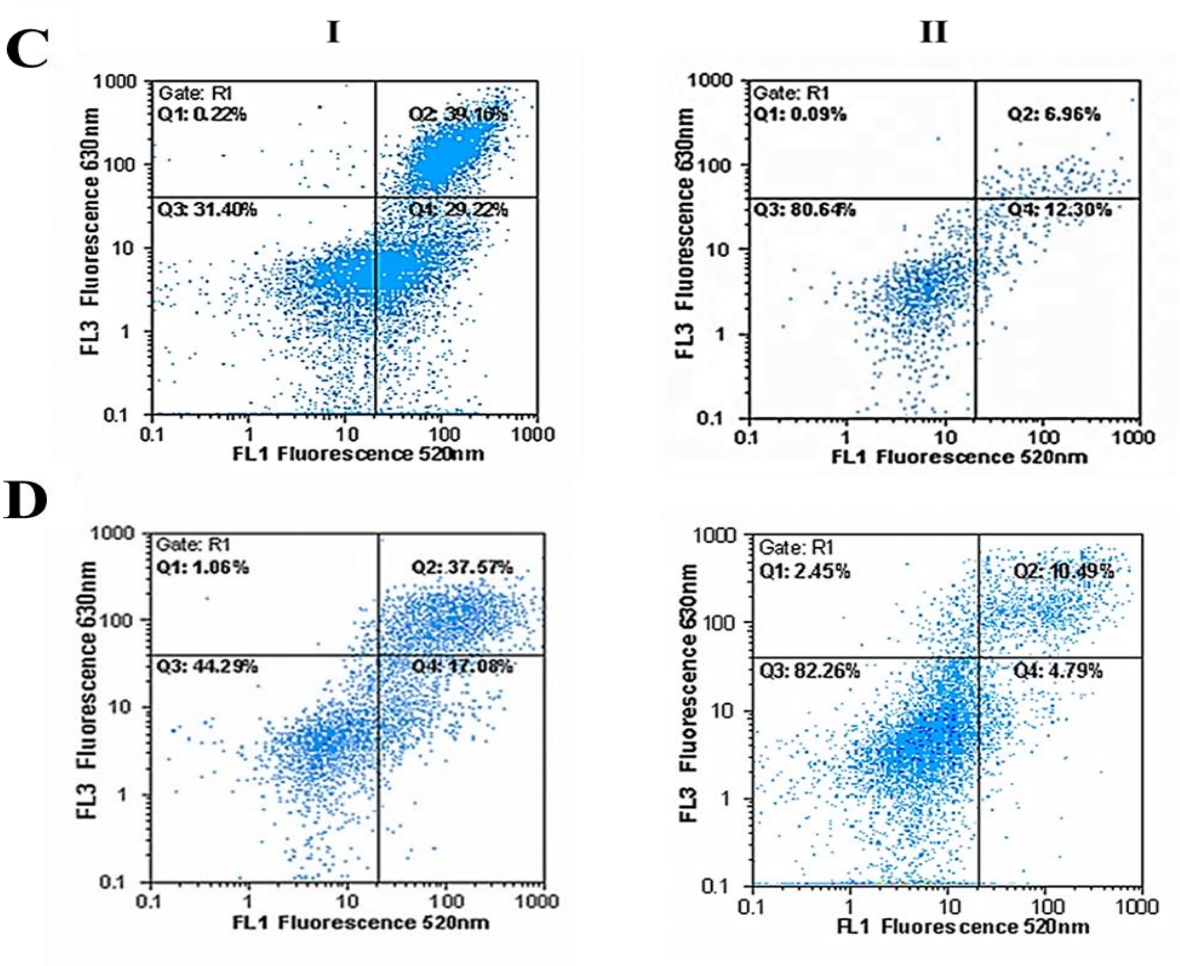

Figure 3.8. Temperature-induced apoptosis and apoptosis inhibition in separated HCs and GCs after suspension culture *in vitro*. Apoptosis was quantified with flow cytometry using bovine lactadherin-FITC and PI staining. (**A-B**): Apoptosis after 6 h culture (20°C) in separated HCs (**A**) and separated GCs (**B**) ±10 µM of the pan-caspase inhibitor Q-VD-OPh. Apoptosis is minimal in Q-VD-OPh treated HCs and GCs. Data expressed as mean ± SEM, n=3, with a different crab used on each occasion. Statistical analysis was performed upon arc sine transformed data using one-way ANOVA with a Student Newman-Keuls multiple comparison *post hoc* test. * $P<0.05$ *vs.* matching Q-VD-OPh treated early apoptotic HCs or GCs, or Q-VD-OPh treated late apoptotic/necrotic HCs; ** $P<0.01$ *vs.* matching Q-VD-OPh treated late apoptotic/necrotic GCs; ### $P<0.001$ *vs.* matching control viable HCs or GCs. (**C-D**): Representative flow cytometry dotplots of separated HCs (**C**) and GCs (**D**) showing thermally induced apoptotic HCs (**C, I**) and GCs (**D, I**) in contrast to viable Q-VD-OPh treated HCs (**C, II**) and GCs (**D, II**).

3.3.3. Apoptosis in separated HCs after treatment with non-self agents

3.3.3.1. Lipopolysaccharide

After 6 and 24 h culture at 10°C, viability in HCs treated with 0.1 or 1 µg mL^{-1} LPS remained comparable with values obtained from control HCs (Figure 3.9, A; Appendix 4). After 24 h, significantly higher viability was observed in HCs treated with 1 µg mL^{-1} LPS (59.8% ± 1.4% SEM; $P<0.05$; n=3) compared to control HCs (39.1% ± 3.9% SEM) (Figure 3.9, A; Appendix 4, A, C, II). Similarly, early apoptosis and late apoptosis/necrosis exhibited by control and LPS treated HCs remained relatively similar after 6 h (Figure 3.9, B; Appendix 4, A-C, I). After 24 h, significantly lower late apoptosis/necrosis was found in HCs treated with 1 µg mL^{-1} LPS (22.8% ± 0.9% SEM; $P<0.01$; n=3) compared to the control (46.5% ± 1.6% SEM) (Figure 3.9, B; Appendix 4, A, C, II).

3.3.3.2. Listonella anguillarum

HC viability decreased in a concentration-time dependent manner with increasing concentration of viable or heat-killed *L. anguillarum* over a 24 h incubation period (Figure 3.10, A; Appendix 5). Significant reductions in HC viability were observed after 6 h culture with viable bacteria at concentrations of $3x10^7$ mL^{-1} (32.1% ± 7.2% SEM; $P<0.05$; n=5) and $3x10^8$ mL^{-1} (12.7% ± 2.5% SEM; $P<0.001$; n=5) compared to untreated (control) HCs (54.2% ± 2.9% SEM) (Figure 3.10, A; Appendix 5, A, B, I). With regard to heat-killed bacteria over 6 h, a similar pattern was observed but the results were not statistically significant compared to controls (Figure 3.10, A). After 24 h culture, HCs showed significant decreases in viability when cultured with live bacteria at concentrations of $3x10^4$ mL^{-1} ($P<0.01$; n=5) and $3x10^5$ mL^{-1} - $3x10^8$ mL^{-1} ($P<0.001$; n=5) (Figure 3.10, A). After 24 h, viability was lowest in HCs cultured with $3x10^8$ mL^{-1} viable bacteria (3.6% ± 0.5% SEM; $P<0.001$; n=5), whereas control viability was 41.2% (± 4.9% SEM) (Figure 3.10, A; Appendix 5, A, B, II). Also over 24 h, viability in HCs cultured with heat-killed bacteria remained higher than values obtained from HCs cultured with viable bacteria at every concentration (Figure 3.10, A). Nonetheless, significant decreases in viability were still observed in HCs cultured with heat-killed bacteria at concentrations of $3x10^6$ mL^{-1} - $3x10^8$ mL^{-1} ($P<0.05$; n=3) (Figure 3.10, A). Viability remained lowest in HCs cultured with $3x10^7$ mL^{-1} heat-killed bacteria

(23.8% ± 3.9% SEM; $P<0.05$; n=3) whereas control HC viability remained highest (47.6% ± 3.2% SEM) (Figure 3.9, A).

No significant differences in early apoptosis values were seen between control HCs and HCs treated with either viable or heat-killed *L. anguillarum* after 6 h and 24 h culture (Figure 3.10, B). In fact, the majority of early apoptosis in HCs treated with viable or heat-killed bacteria remained lower than values obtained from control (untreated) HCs after culture (Figure 3.10, B).

A significant increase in late apoptosis/necrosis was observed after 6 h culture with viable bacteria at a concentration of $3x10^8$ mL^{-1} (66.7% ± 11.1% SEM; $P<0.001$; n=5) compared to control HCs (18.7% ± 3.1% SEM) (Figure 3.10, C; Appendix 5, A, B, I), as well as with heat-killed bacteria at the same timepoint (51.2% ± 1.3% SEM; $P<0.05$; n=3) compared to control HCs (16.4% ± 2.3% SEM) (Figure 3.10, C; Appendix 5, A, C, I). Over 24 h culture, late apoptosis/necrosis in HCs increased with bacterial concentration and time with both viable and heat-killed *L. anguillarum* (Figure 3.10, C; Appendix 5, B, C, II). After 24 h, significant increases in late apoptosis ($P<0.001$; n=5) were observed in HCs cultured with viable bacteria at all concentrations used ($3x10^4$ mL^{-1} - $3x10^8$ mL^{-1}) (Figure 3.10, C). With heat-killed bacteria, late apoptosis/necrosis in HCs remained lower compared with values from HCs cultured with viable bacteria at every concentration (Figure 3.10, C). Significant increases in late apoptosis/necrosis were still observed in HCs cultured with heat-killed bacteria at concentrations of $3x10^5$ mL^{-1} ($P<0.05$; n=3) and $3x10^6$ mL^{-1}- $3x10^8$ mL^{-1} ($P<0.01$; n=3) compared to control HCs (Figure 3.10, C). In summary, levels of viability decreased whilst levels of late apoptosis/necrosis increased in HCs in a concentration-time dependent manner, with increasing concentrations of viable or heat-killed bacteria.

Figure 3.9.

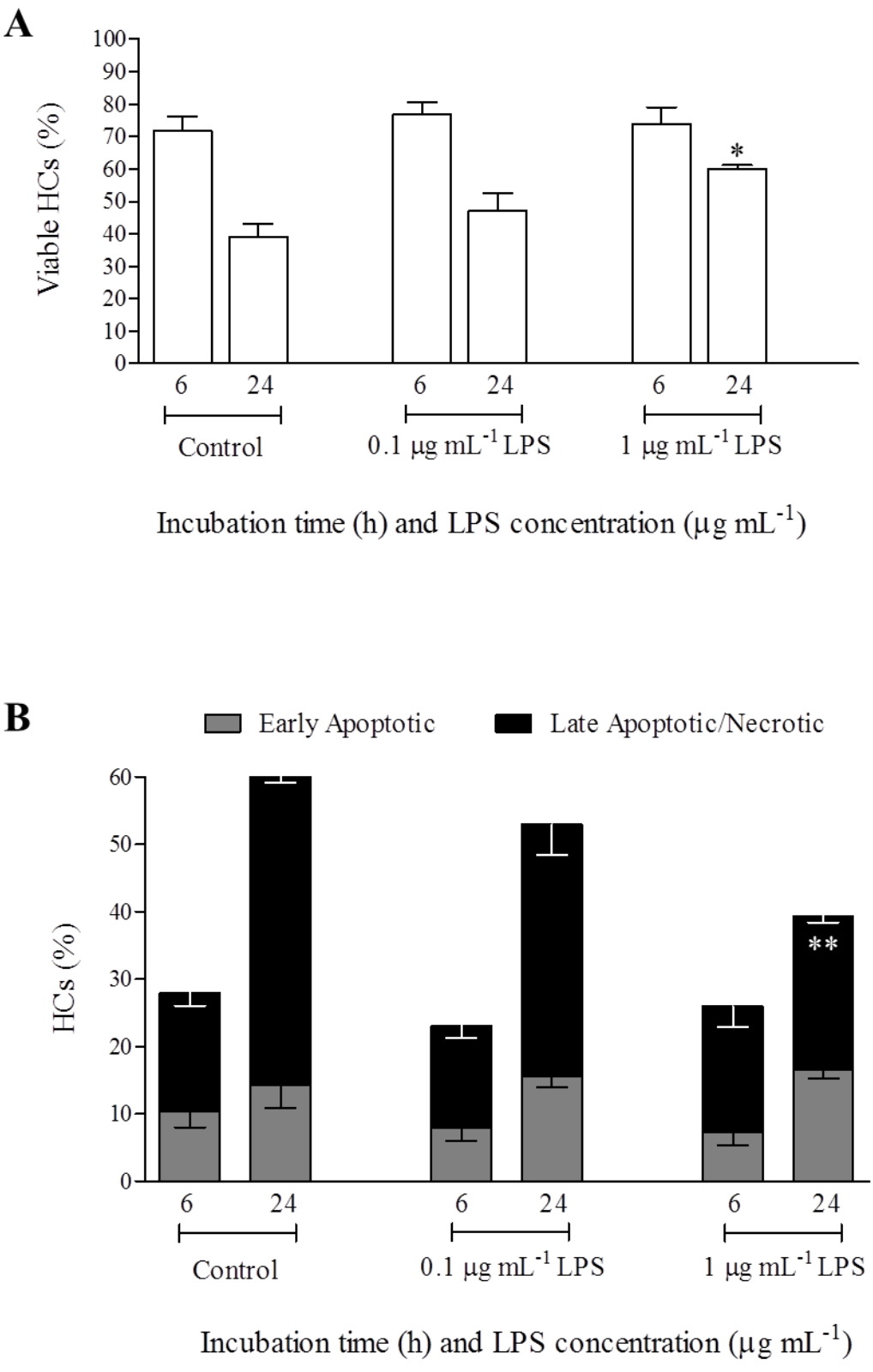
A
Viable HCs (%)
100
90
80
70
60
50
40
30
20
10
0
*
6
24
6
24
6
24
Control
0.1 µg mL-1 LPS
1 µg mL-1 LPS
Incubation time (h) and LPS concentration (µg mL-1)
B
Early Apoptotic
Late Apoptotic/Necrotic
HCs (%)
60
50
40
30
20
10
0
**
6
24
6
24
6
24
Control
0.1 µg mL-1 LPS
1 µg mL-1 LPS
Incubation time (h) and LPS concentration (µg mL-1)

Figure 3.9. Lipopolysaccharide has a pro-survival effect upon separated *C. maenas* HCs after suspension culture *in vitro*. (**A-B**): Quantified percentages of viability (**A**) and apoptosis/necrosis (**B**) in untreated HCs (control) or HCs treated with 0.1 mg mL^{-1} or 1 mg mL^{-1} LPS after 6 h and 24 h culture (10°C). Values were quantified using flow cytometry via bovine lactadherin-FITC and PI staining. Data are expressed as means ± SEM, n=3, with a different crab used on each occasion. Refer to Appendix 4 for representative flow cytometry dot plots. Statistical analysis was performed upon arc sine transformed data using one-way ANOVA with a Student Newman-Keuls multiple comparison *post hoc* test. * $P<0.05$ *vs.* matching viable control (untreated) HCs at the corresponding timepoint; ** $P<0.01$ *vs.* matching late apoptotic/necrotic control (untreated) HCs at the corresponding timepoint.

Figure 3.10.

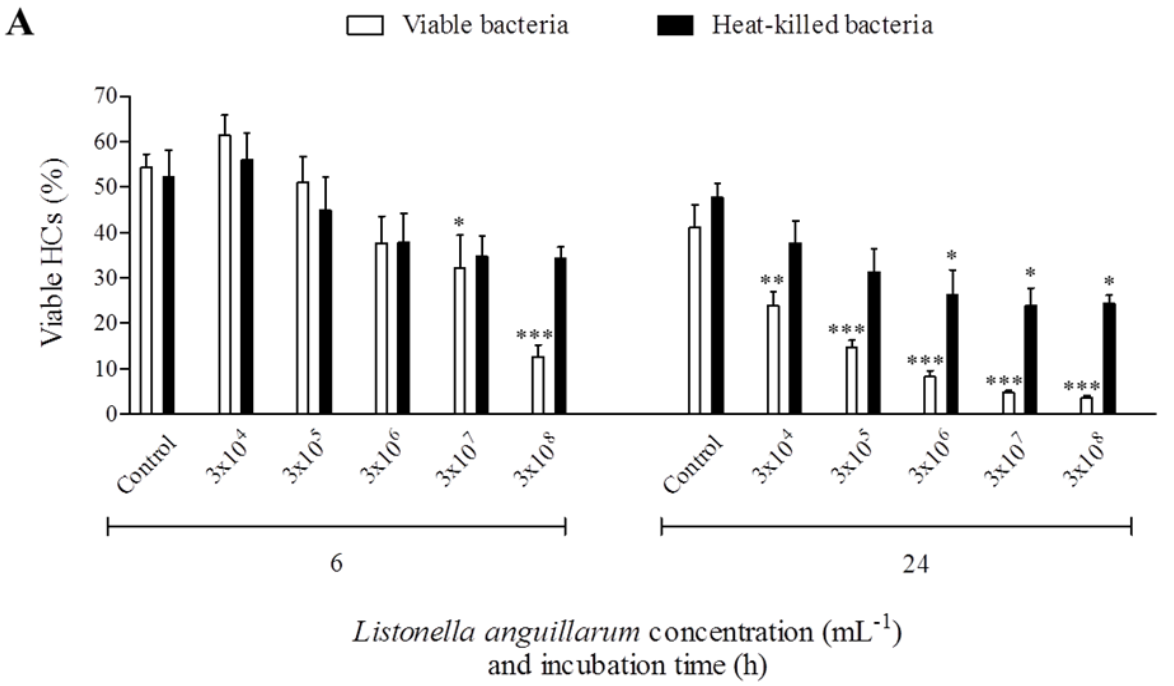
A
Viable bacteria
Heat-killed bacteria
Viable HCs (%)
70
60
50
40
30
20
10
0
Control
3x10^4
3x10^5
3x10^6
3x10^7
3x10^8
6
24
Listonella anguillarum concentration (mL^-1)
and incubation time (h)

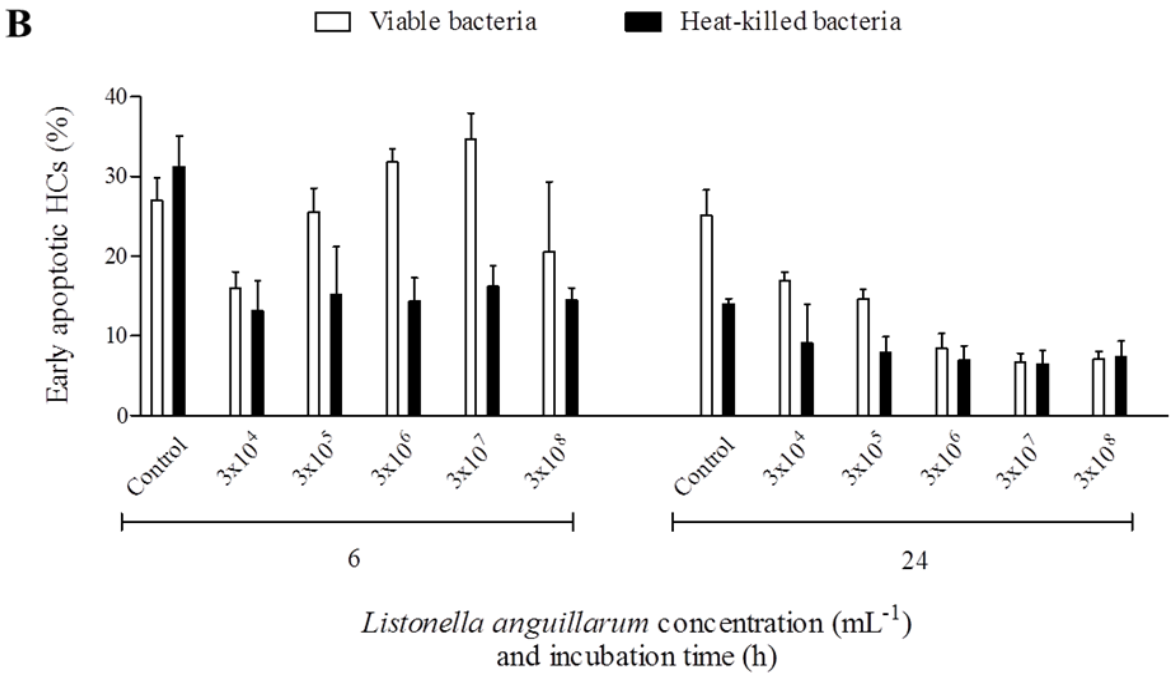
B
Viable bacteria
Heat-killed bacteria
Early apoptotic HCs (%)
40
30
20
10
0
Control
3x10^4
3x10^5
3x10^6
3x10^7
3x10^8
6
24
Listonella anguillarum concentration (mL^-1)
and incubation time (h)

Figure 3.10 continued.

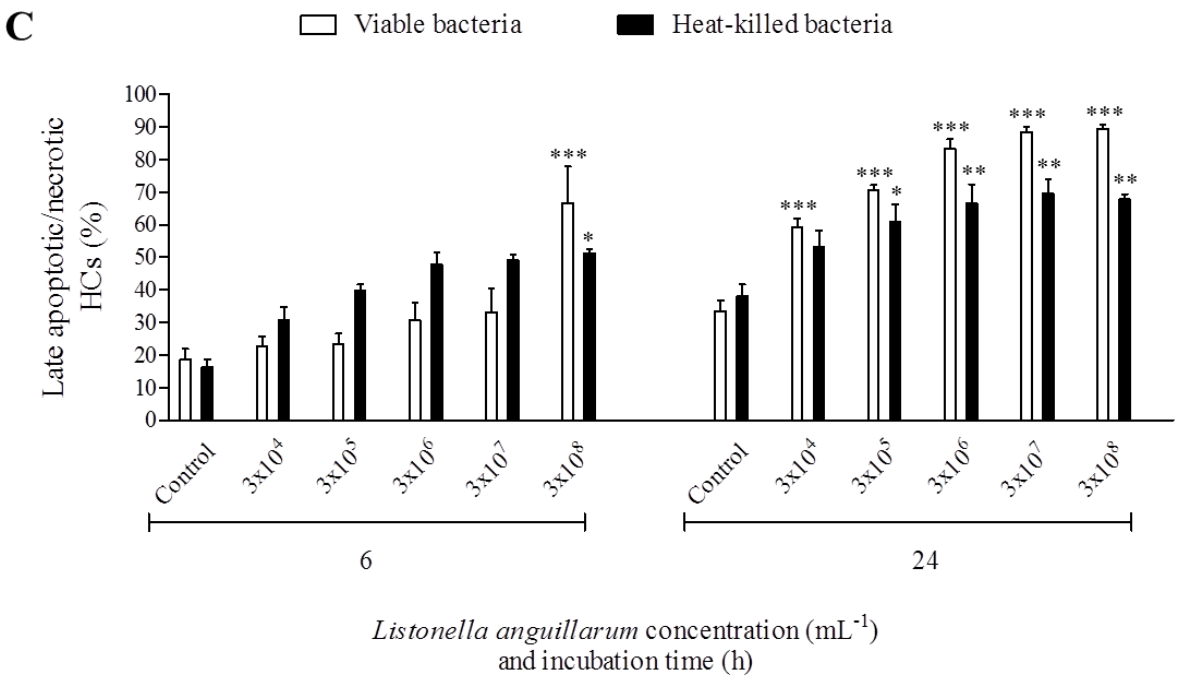

Figure 3.10. Both viable and heat-killed *Listonella anguillarum* induce high levels of late apoptotis/necrosis in separated *C. maenas* HCs after suspension culture *in vitro*. (**A-C**): Quantified percentages of viability (**A**), early apoptosis (**B**) or late apoptosis/necrosis (**C**) in untreated HCs (control) or HCs treated with different concentrations of viable or heat-killed *L. anguillarum* (3×10^4 mL^{-1} – 3×10^8 mL^{-1}) after 6 h and 24 h culture (10°C). Values were quantified using flow cytometry via bovine lactadherin-FITC and PI staining. Data are expressed as means ± SEM, (n=5 for viable bacteria data, n=3 for heat-killed bacteria data), with a different crab used on each occasion. Refer to Appendix 5 for representative flow cytometry dot plots. Statistical analysis was performed upon arc sine transformed data using one-way ANOVA with a Student Newman-Keuls multiple comparison *post hoc* test. * $P<0.05$, ** $P<0.01$, *** $P<0.001$ *vs.* matching viable control (untreated) HCs or late apoptotic/necrotic control (untreated) HCs at the corresponding timepoint.

3.4. Discussion

It is clear that levels of cell death can vary considerably under different conditions and even among different cell types. This emphasizes the importance of understanding both constitutive levels of immune cell death and also how it can vary under changing conditions that may be experienced as part of the animals' normal life and which are not necessarily representing extreme forms of stress.

3.4.1. Effect of temperature

'High' and 'low' evaluations of temperature are dependent on individual species and their natural environments. Apoptosis has not previously been extensively studied in cold water species of crustaceans. This study found that the optimum temperature for culturing *C. maenas* haemocytes was 10°C, with apoptosis percentages averaging around 10-12%. This agreed with the results obtained from counts of the mixed haemocyte population, which were most stable at 10°C. This also concurs with results from previous studies on antibacterial activity in the shore crab, where at temperatures of 10-15°C, total haemocyte counts were found to be at their maximum (Chisholm and Smith, 1994; Brockton and Smith, 2008). Constitutive apoptosis values in studies on tropical shrimp (temperatures of around 25°C) were comparable to those found in the present study, where flow cytometry was as also used for apoptosis detection, but instead AV-FITC and PI staining was used (Guo *et al*., 2013; Xian *et al*., 2010, 2012, 2013).

Overall, levels of cell death remained lower in mixed haemocytes after *in vitro* culture at a lower temperature (4°C). Certainly, low temperatures have been demonstrated to partially inhibit apoptosis in various cell types *in vitro*. A temperature of 4°C has been shown to inhibit mouse thymocyte apoptosis (Nicoletti *et al*., 1991), whilst arrest of human neutrophil apoptosis is achieved at a lower temperature of 15°C (Pryde *et al*., 2000) compared to an optimal culturing temperature of 37°C. In C. *maenas*, high temperature seems to speed up cell death in mixed and separated haemocytes, where after 6 h culture there is proportionally higher levels of late apoptosis/necrosis compared to early apoptosis. However the present study also indicates that lower temperature may also be stressful to haemocytes over time. After 24 h, mixed haemocytes cultured at 4°C

exhibited greater percentages of late apoptosis/necrosis compared to mixed haemocytes cultured at 20°C. These cell death trends exhibited by mixed haemocytes after 24 h culture at 4°C attributed to a *ca.* 35% total decrease in mixed haemocytes numbers.

As an intertidal species, *C. maenas* often experiences dramatic changes in its environment, which include daily and seasonal variations in temperature. In the wild, crabs subject to the lower temperature limits of their range would experience a reduction in metabolic rate. In turn, this would 'slow' physiological processes, including mitosis, tissue homeostasis, as well as levels of apoptosis. This reduction in metabolic rate would be of some biological value to the crab allowing it to survive for a transient time period when exposed to low temperature extremes. However, cell death processes are crucial for development and morphogenesis, tissue turnover, maintaining constant cell numbers, balancing cell proliferation of newly produced cells and eliminating damaged cells (Penaloza *et al*., 2006). Low levels of cell death might be of biological 'cost', and prolonged exposure to low temperature extremes in the wild could become detrimental with regard to physiology and immune regulation.

From the results of the present study, it appears that at 20°C a large proportion of haemocytes rapidly pass into late apoptosis/necrosis. In an *in vivo* scenario, if cell death were primarily necrotic, it could lead to leakage of intracellular components provoking widespread damage to the immediate vicinity, as in mammals (Majno *et al*., 1960). For the crab, necrotic cell death in the GCs and SGCs would lead to release of granular immune proteins, including carcinin (Smith and Chisholm, 2001; Brockton *et al*., 2007), the pro-enzyme proPO (Söderhäll and Smith, 1983) and the cell adhesion protein, peroxinectin, (Johansson *et al*., 1995). This would cause further degranulation, possible initiation of encapsulation responses due to the release of proPO and peroxinectin and potentially cause damage in the immediate extracellular vicinity. Therefore, necrosis is of severe biological cost, is almost always detrimental and in some instances can be fatal to the host organism (Walker *et al*., 1988; Zong and Thompson, 2006). In the present study, *in vitro* findings show that the majority of haemocytes are in early apoptosis after 24 h suspension culture at high temperature (20°C). *In vivo* this would be of biological value

as apoptosis is a carefully regulated mechanism of 'beneficial' cellular suicide that does not result in loss of cell membrane integrity or in an inflammatory response.

The importance of environmental factors, in particular temperature, with regard to immune capability, is of significance both to the shellfish aquaculture industry, and in terms of using immune parameters as biomarkers of environmental disturbance (Chisholm and Smith, 1994). The present study shows that cell death varies considerably with respect to temperature. In addition, antibacterial activity is lowest in haemocytes from crabs kept at low water temperature (~3°C) and highest in lysates obtained from crabs subjected to higher water temperatures (Chisholm and Smith, 1994). Other physiological responses to temperature variation in the shore crab include changes in ventilation, circulation, haemocyanin oxygen-binding properties and aerobic and anaerobic metabolism (Wachter *et al*., 1997).

3.4.2. Variation in cell death among haemocyte types

Many studies on invertebrate immunity either overlook the existence of different cell populations or assume that that the response of different cell types is broadly similar. The present study shows that constitutive apoptosis varies significantly among different cell types. The phagocytic HCs in isolation appear much more likely to undergo apoptosis than either the GCs or ProHs. In the present study, constitutive levels of mixed haemocyte total cell death remained low (~15%) after 24 h suspension culture. No differential cell counts were made as part of those experiments, so it is unclear whether numbers of HCs in those haemocyte populations may have been low. Alternatively, it is possible that pro-survival factors liberated from other cell types may help contribute to increased HC viability within the mixed haemocyte population.

In humans, soluble inflammatory mediators present in whole blood and also secreted by other inflammatory cells do promote cell survival and contribute to inhibition of cell death. Inflammatory mediators such GM-CSF secreted by macrophages, as well as interleukin 6 (IL-6) and IL-15 (survival cytokines) inhibit constitutive apoptosis in

separated neutrophils (Lee *et al*., 1993). Other examples include erythrocytes (red blood cells) which exert a pro-survival effect (due to catalase and glutathione metabolism) upon separated human neutrophils (Aoshiba *et al*., 1999), and mast cells which release GM-CSF to enhance separated eosinophil survival (Levi-Schaffer *et al*., 1998). It would therefore be interesting to co-culture separated HCs (in suspension) with separated GCs, SGCs or ProHs, or with addition of cell-free haemolymph to assess any pro-survival effect upon the HCs.

It is also possible that small-scale contamination of HC cultures with SGCs may contribute to higher values of apoptosis. The diffuse SGC layer lies immediately beneath the HCs after density gradient centrifugation (Söderhäll and Smith, 1983), therefore some SGCs could be taken up when removing the HC band from the gradient. The SGCs easily undergo lysis and release intracellular contents so could cause some HC activation during culture. This is less of a problem with respect to the GC band position, while ProHs are subject to two-step density gradient centrifugation, thus greatly reducing the risk of SGC contamination. Alternatively, assuming minimal SGC contamination in HC suspension cultures, the high levels of cell death and low viability observed in HCs may be a true representation of how the HCs die constitutively during *in vitro* suspension culture. Similar cell death trends are observed in separated human neutrophils where after 20 h *in vitro* culture (37°C) high percentages of constitutive apoptosis (40-65%) and lower percentages of viability (25-35%) are observed (Dorward *et al*., 2013). Certainly it would be relevant in future studies of apoptosis in crustacean haemocytes to routinely include differential cell counts to establish whether cell death genuinely changes or whether differences are reflective of varying proportions of different cell types.

3.4.3. Haemolymph loss and haemocytopenia

Repeated haemolymph sampling served as a 'tool' to mimic the loss of haemocytes that shore crabs would likely experience as a result of mechanical injury/natural infection, resulting in haemocytopenia, with a probable reduction in immunocompetence. In such instances, crabs would likely become highly susceptible to infection as there would be an overall lower number of circulating haemocytes to defend the crab from pathogenic insults. It is highly likely that in the wild, crabs experiencing mechanical injury would subsequently suffer from infection at the wound site arising from opportunistic pathogens. Haemocytopenia has also been demonstrated in the Atlantic blue crab, *Callinectes sapidus*, after injection of Gram-negative bacteria, specifically *Vibrio campbelli* and *L. anguillarum* (Johnson *et al*., 2011). Certainly in the shore crab, haemocytopenia is associated with the clearance of encapsulated bacterial pathogens from circulation, which is then rectified within 24-48 h post pathogen sequestration (Smith and Ratcliffe, 1980a). In crabs suffering haemocytopenia, such pathogenic insults may help to explain the high levels of cell death observed in mixed haemocytes during *in vitro* culture. Additionally, if crabs were suffering from infection, further haemocytopenia would most probably occur due to an elevation in apoptosis to help aid in the clearance of diseased cells. Aside from injury and infection, haemocyte numbers can also fluctuate during the moult cycle (ecdysis) (Hose *et al*., 1992), a stage in the life cycle of decapod crustaceans during which they are highly susceptible to infection. Therefore, using the shore crab as a model organism, it would be interesting to investigate trends in cell death and decipher mechanisms of cell death during ecdysis.

3.4.4. Effect of LPS

Treating separated HCs with *E. coli*-derived LPS removes the complication of the pathogenicity of *L. anguillarum*. Compared to HCs treated with viable and heat-killed bacteria, percentages of late apoptosis/necrosis in HCs treated with LPS are prominently reduced, even below levels exhibited by untreated (control) HCs. Surprisingly, a small-scale pro-survival effect was observed in separated HCs treated with 1 µg mL^{-1} LPS after 24 h suspension culture (*in vitro*). Similar LPS-induced survival trends have been demonstrated in human neutrophils (Ward *et al*., 2005), monocytes (Venet *et al*., 2006) and eosinophils (Takanaski *et al*., 1994) after *in vitro* culture, via production of pro-

inflammatory cytokines, such as IL-6, IL-8 and GM-CSF. However, the pro-survival effect of LPS upon separated HCs observed during this study contrasts with recent findings in mixed haemocytes from other decapod crustaceans, where LPS has been demonstrated to induce apoptosis in mixed haemocytes of shrimp, including *P. monodon* (Xian *et al*., 2013) and *L. vannamei* (Xian *et al*., 2009). In these studies, apoptosis was quantified by flow cytometry using the AV-FITC/PI (Xian *et al*., 2013) and hypodiploid peak assay (Xian *et al*., 2009). With regard to the hypodiploid peak assay, necrotic cells can sometime display some degrees of DNA degradation that may result in hypodiploid nuclei, therefore often exaggerating levels of apoptosis (Riccardi and Nicoletti, 2006). Additionally, in such instances, because LPS-induced apoptosis was assessed in mixed haemocytes, there are evidently more factors to consider (e.g. different cell types, humoral factors) and therefore attempt to control than there would be for separated haemocytes. Hence, it is reasonable to suggest that the LPS-induced apoptosis observed in mixed haemocytes of shrimp may have been exaggerated due to elevated levels of haemocyte activation (via ROS generation or release of AMPs during degranulation) caused by the different haemocyte types present. As a general comment, investigations frequently use different types/qualities of LPS, derived either from varying species of bacteria or alternative serotypes of the same species of bacteria. This in turn may have contributed to the differences in values of cell death obtained in crab HCs compared to shrimp haemocytes, after treatment with LPS.

3.4.5. Response to *L. anguillarum*

Since infection is likely to follow injury or mechanical trauma, the effects of *L. anguillarum* upon levels of cell death in separated HCs was investigated. It was clearly established that late apoptosis values were highest in the cells after 6 h and 24 h suspension culture with bacteria, where percentages increased in concentration-time dependent manner. Overall, unsurprisingly, higher values of late apoptosis/necrosis were obtained in HCs treated with viable bacteria compared to heat-killed bacteria. This increased level of cell death is likely due to the release of exotoxins from viable bacteria, a process which would be impaired in heat-killed bacteria as exotoxins are destroyed (denatured) at high temperatures (Smith and Ratcliffe, 1980a, b). Due to the low percentages of phagocytosis (~15%) exhibited by HCs in the presence of bacteria (Smith

and Ratcliffe, 1978), it is not unexpected that high levels of death were observed in bacteria treatments. *In vivo* work performed by Hauton *et al*. (1997) observed significant decreases in the number of circulating haemocytes that was maintained over a 7 day period in *C. maenas* individuals inoculated with 10^5 mL^{-1} viable *L. anguillarum*. Following infection, a significant reduction in the number of circulating haemocytes was observed which was attributed to preferential removal of phagocytic HCs from circulation which resulted in a substantially higher ratio of GCs to HCs in infected crabs after 7 days post incubation (Hauton *et al*., 1997). However, these authors did not establish how the HCs were lost from circulation, nor considered levels of viability. In the present study, based on the results presented here showing the cell death trends obtained in HCs after suspension culture, it would be reasonable to suggest that reductions in the numbers of circulating HCs observed by Hauton *et al*. (1997) *in vivo*, was likely due to necrotic cell death. Therefore, before subsequent *in vivo* studies are attempted, it is important that further *in vitro* studies are carried out in an attempt to decipher the exact mechanism(s) of pathogenicity exerted by *L. anguillarum* and other pathogens upon haemocytes of the shore crab.

To conclude, this chapter successfully quantifies constitutive and treatment-induced percentages of viability/apoptosis/necrosis after short term primary culture *in vitro* in both mixed and separated haemocytes from the shore crab, *C. maenas*. Quantification of apoptosis in both mixed and separated haemocytes is essential for comprehensive understanding of apoptosis in the invertebrate immune system. With regard to decapod crustaceans, no previous studies of this kind have considered the separated haemocytes for investigation. Therefore, this study provides first insight into the responses of separated haemocytes exposed to various life conditions and non-self agents during *in vitro* culture.

Chapter 4

Characterisation of ETosis

4.1. Introduction

Since the start of the PhD, a novel cell death process separate to apoptosis has become well established in mammalian immunology. This process involves the ROS-dependent controlled release of chromatin from vertebrate phagocytes to form extracellular traps and is now known as ETosis. It was first discovered in human neutrophils (Brinkmann *et al*., 2004) and represents an important mechanism of innate defence in mammals and non-mammalian vertebrates. During ETotic cell death the extruded chromatin elongates to form ETs studded with AMPs that serve to ensnare and kill invading microorganisms. ETosis is now widely regarded as an important part of the mammalian inflammatory repertoire. Surprisingly, the presence and role of ETosis in invertebrates (around 97% of all animal life) has never been explored, even though understanding the phylogeny of the process may help explain why it can have negative effects in mammals. These include thrombosis, mastitis, appendicitis, pre-eclampsia, arthritis and promotion of cancer metastasis (Fuchs *et al*., 2010; Brinkmann and Zychlinsky, 2012; Cools-Lartigue *et al*., 2013).

As invertebrates have strong dependence on the defensive activities of circulating haemocytes, and possess the key structures and protein homologues necessary to execute inflammation, it was hypothesised that ETosis is not confined to vertebrates, and is, in fact, an evolutionary conserved host defence process that exists in lower animals. The study in this chapter set out to characterise ETosis, using the shore crab, *Carcinus maenas* as the experimental organism. The HCs were chosen for initial experiments, as out of the four haemocyte types in *C. maenas* they are the only ones known to be both phagocytic (Smith and Ratcliffe, 1978) and able to produce ROS during a respiratory burst (Bell and Smith, 1993).

Specifically the objectives of this chapter are:

1. To determine if separated HCs release extracellular chromatin following activation of protein kinase C (PKC) and NADPH-oxidase, and to identify if this chromatin release is dependent upon actin filament polymerisation.

2. To analyse the general and ultrastructural morphology of separated HCs exhibiting extracellular chromatin release, and to investigate if the extruded chromatin is decorated with histone H2A and the cell adhesion protein, peroxinectin (PXN).

3. To quantify percentages of extracellular chromatin release and inhibition from separated HCs over various timepoints.

4.2. Materials and methods

4.2.1. Crabs

C. maenas specimens were collected and maintained as described in Chapter 2 (Section 2.2.2).

4.2.2. Preparation of monolayer hyaline haemocyte cultures

Haemolymph was sampled from crabs as described above (Chapter 2, Section 2.2.3) and separated HCs obtained after separation on a 60% continuous Percoll gradient via density gradient centrifugation, as described in Chapter 3 (Section 3.2.1). Approximately 1 mL of 3 x 10^4 mL^{-1} HCs resuspended in ML-15 (Chapter 2, Section 2.2.3) were added to wells of a 24-well flat bottomed tissue culture plate (Costar) and left for 1 h at 10°C (in the dark) to allow the HCs to adhere to the bottom of the well. One crab was sampled per experimental run with triplicate monolayer cultures set up per treatment per timepoint.

4.2.3. Extracellular chromatin release assays *in vitro*

After HCs had attached to the bottom of the wells, the supernatant was carefully removed. Next extracellular chromatin release was induced using the PKC activator, PMA (an established inducer of ETosis in vertebrates, Fuchs *et al*., 2007) at final concentrations ranging from 0.01 – 1 µM in a final volume of 500 uL fresh ML-15. Controls received equal volumes of ML-15 only. To induce necrosis (positive control), HCs were treated with 50% ethanol. An additional vehicle control in which HCs were treated with 0.1% DMSO only was run in parallel. The plates were then incubated at 10°C for 1-24 h (in the dark) before staining, unfixed, with Sytox Green (Invitrogen) for 20 min at a final concentration of 1 µM. The cells were examined using a Leica (DMIRE2) TCS2 confocal microscope (Leica Microsystems, Milton Keynes, UK) (excitation 504 nm; emission 523 nm), with images captured with and without phase contrast transmission. The total number of cells was counted from the appropriate phase contrast image and the corresponding image (fluorescence only) was used to count the number of Sytox Green-positive cells releasing extracellular chromatin (ETotic) or Sytox Green-positive cells exhibiting no extracellular chromatin release (intact dead). From these counts, the percentages of viable, chromatin extruding and

intact dead (non-chromatin extruding) HCs were calculated from a minimum of 300 cells counted from a minimum of 3 fields of view (FoV) using the image analysis software, ImageJ™ (National Institutes of Health).

To confirm that the released material was of nuclear origin, DNAse-1 (Fermentek) at a final concentration of 100 U mL^{-1} was added to HCs in monolayer cultures that had been previously induced for chromatin release with 0.1 µM PMA for 24 h (10°C) and stained, unfixed with 1 µM Sytox Green as above. Control treatments consisted of PMA-activated HCs minus DNAse-1. The HCs were then incubated for a total of 4 h 40 min (280 min) at 15°C (temperature in microscopy suite) until all extracellular chromatin had been dissolved. Changes were recorded by confocal time-lapse photo microscopy (10x objective with zoom 2) with images taken every 20 min. The image sequence was then imported into ImageJ™ and converted to video format (avi) to show the digestion of extracellular chromatin over time (supplementary video 3). DNAse-1 was made up in storage buffer (50% glycerol containing 10 mM Tris-HCl (pH 7.5), 10 mM $CaCl_2$ and 10 mM $MgCl_2$)) and added directly into monolayer cultures.

4.2.4. Confirmation of NADPH-oxidase dependent ROS generation by HCs

Bell and Smith, (1993) have previously demonstrated that HCs of the crab are able to undergo a respiratory burst. However, it was deemed appropriate to confirm NADPH-oxidase dependent respiratory burst generation from HCs when maximal generation of extracellular chromatin release was observed (24 h, 0.1 µM PMA, 10°C). This is especially important considering extracellular chromatin release in mammalian neutrophils is dependent upon generation of a respiratory burst (Fuchs *et al*., 2007). HCs were subjected to the dihydrorhodamine 123 (DHR 123) assay using flow cytometry (Nicoletti *et al*., 1991). DHR 123 used at a final concentration of 1 µM was added to 15 mL Falcon tubes containing 1 mL of HCs resuspended at 1 x 10^6 mL^{-1} in ML-15 medium. Next, HCs were incubated with the NADPH-oxidase inhibitor diphenyleneiodonium chloride (DPI) (2 µM final concentration) for 1 h (10°C) before the addition of PMA at a final concentration of 0.1 µM. HCs were then cultured in suspension *in vitro* for 24 h (10°C). Additional treatments consisted of PMA-activated

HCs minus DPI, non-activated HCs plus DPI or non-activated HCs in ML-15 only (control).

After culture, cells were gently resuspended and subjected to immediate flow cytometric analysis (Partec, CyFlow) (Leitch *et al*., 2010). During generation of ROS, non-fluorescent DHR 123 is oxidised to the highly fluorescent derivative rhodamine 123 which is detectable by flow cytometry. Therefore, HCs were gated according to levels of rhodamine 123 (FL1) fluorescence (excitation 488 nm; emission 525 nm) (Henderson and Chappell, 1993) measured on a FL1 fluorescence histogram. Mean channel FL1 fluorescence was recorded from the display statistics (FloMax™ software) and used to measure and quantify respiratory burst generation by the HCs. Additionally to create a fluorescence histogram overlay WinMDI™ flow cytometry software was used. One crab was sampled per experimental run with duplicate flow samples carried out per treatment.

4.2.5. Ultrastructural morphology

Both scanning and transmission electron microscopy was used to visualise the morphology of candidate ETotic HCs at the ultrastructural level. For scanning electron microscopy, 0.1 µM PMA was added to monolayer cultures of HCs (3×10^4 mL^{-1}) set up on 10 mm diameter circular glass coverslips in the plate wells, and left for 24 h (10°C). Controls received equal volumes of ML-15 only. After culture, the HCs were fixed (2 h, 10°C) in an equal volume of 2.5% glutaraldehyde in 0.1 M sodium cacodylate (CAC) buffer (pH 7.2). The cells were next washed 3x in PBS (5 min each) then dehydrated through ascending grades of ethanols (30%, 50%, 70%, 80%, 90%, 100%, 100%, 100%, 5 min per grade) before critical point drying (3 h) and sputter-coating with gold. A Quanta™ 3D FEGFEI scanning electron microscope (FEI, Cambridge, UK) was used to visualise the HCs. The diameters (nm) of globular domains and smooth fibres present on the extracellular chromatin released from crab HCs were measured from high resolution scanning electron microscopy using ImageJ™. The diameter of approximately 15 randomly selected globular domains or smooth fibres were measured and the average calculated. For transmission electron microscopy analysis, 1 mL of 3×10^4 mL^{-1} HCs resuspended in ML-15 were cultured in suspension with 0.1 µM PMA in a 2 mL

Eppendorf tube for 24 h (10°C). The HCs were then fixed (24 h, 10°C) in an equal volume of 2.5% glutaraldehyde in 0.1 M CAC buffer (pH 7.2) and processed for transmission electron microscopy analysis as described above (Chapter 2, Section 2.2.5.4). Visualisation of the HCs was achieved using a Phillips CM120 transmission electron microscope (FEI, Cambridge, UK).

4.2.6. Extracellular chromatin decoration *in vitro*

Immunocytochemical analyses was carried out to confirm extracellular chromatin released from crab HCs was decorated with histone H2A (H2A) and peroxinectin (PXN), a crustacean homologue of human myeloperoxidase (MPO). The primary antibodies, specifically monoclonal mouse anti-H2A IgG1 (New England Biolabs) and polyclonal rabbit anti-human MPO IgG (Dako) were used to recognise H2A and PXN respectively. The fluorescently conjugated secondary antibodies, specifically Alexa Fluor® 594F $(ab')_2$ goat anti-mouse IgG (excitation 590 nm; emission 617 nm) and Alexa Fluor® 488 goat anti-rabbit IgG (excitation 495 nm; emission 519 nm) (both from Invitrogen) were used to label H2A and PXN respectively. Monolayer HC cultures were set up on glass coverslips and stimulated for extracellular chromatin release with 0.1 µM PMA, as above. After 24 h culture (10°C), ML-15 was removed and the HCs fixed with 4% paraformaldehyde in 2% NaCl (30 min). The HCs were washed 3x with PBS, permeabilised with 0.1% TritonX-100 (5 min), then washed again, before blocking in 3% bovine serum albumin (BSA) in PBS for 1 h. After blocking, HCs were incubated for 1.5 h at room temperature with the relevant primary antibody (both diluted 1:200 in 3% BSA in PBS). The HCs were again washed as before then incubated for 1.5 h at room temperature (in the dark) with the relevant secondary antibody (both diluted 1:300 in 3% BSA in PBS). DNA and F-actin were localised, respectively, with 5 µM Draq-5 (Biostatus) (excitation 647 nm; emission 681 nm, pseudocoloured blue) or 0.15 µM rhodamine phalloidin (Invitrogen) (excitation 540 nm; emission 565 nm) plus the secondary antibodies. Controls included HCs minus primary and secondary antibodies, HCs incubated only with secondary antibodies and HCs plus mouse and rabbit sera instead of primary antibodies (isotype matched controls, both diluted 1:200 in 3% BSA in PBS). For each control, 3% BSA in PBS was substituted for the relevant antibody solution(s) and the DNA of HCs stained with Draq-5. After the secondary antibody

incubation, the HCs were washed as before, mounted onto sterile glass slides with Vectasheild™ (Vector Laboratories Ltd) and examined with a confocal microscope as before (Section 4.2.3).

4.2.7. Inhibition assays of extracellular chromatin release *in vitro*

In an attempt to inhibit extracellular chromatin release, fresh monolayer cultures of HCs were incubated for 1 h (10°C) with either DPI, apocynin (Calbiochem), cytochalasin D (cyto D) or Ro-31-8220, before addition of PMA as above (Section 4.2.3). These chemical agents have been demonstrated to inhibit ETosis in mammalian neutrophils (Fuchs *et al*., 2007; Neeli *et al*., 2009; Azevedo *et al*., 2012; Gray *et al*., 2013). DPI and apocynin are NADPH oxidase inhibitors, cyto D as an inhibitor of actin filament polymerisation as well as phagocytosis and Ro-31-8220 is a pan-PKC inhibitor. Controls consisted of PMA-activated HCs minus inhibitor and non-activated HCs plus inhibitor. For these experiments, inhibitors were used at final concentrations of 2 µM (DPI), 50 µM (apocynin), 10 µM (cyto D) or 1 µM (Ro-31-8220). Chromatin release was detected and the percentages of chromatin-extruding, intact dead and viable HCs quantified as above (Section 4.2.3).

4.2.8. Statistical analyses

All values were calculated as mean ± SEM, with percentage values arc sine transformed or fluorescence values (DHR assay) left un-transformed before statistical analysis. Statistical differences were then determined as described in Chapter 2 (Section 2.2.7). Significance was accepted at $P<0.05$.

4.3. Results

4.3.1. Extracellular chromatin release

Pre-formed monolayers of isolated HCs treated with PMA resulted in expulsion of material staining positively with the DNA stain, Sytox Green (Figure 4.1, A-F). Ejection of chromatin usually occurred between 2 and 24 h, and the extruded material takes the form of 'puff-ball'-like structures (Figure 4.1, A, B), 'comet'-like streaks (Figure 4.1, C, D, E) or extended strands that interlink across cells (Figure 4.1, F). As a general observation it was more common that longer streaks (Figure 4.1, C, D, E) and interconnected strands (Figure 4.1, F) of Sytox stained extracellular material formed at later incubation times. The 'puff-ball'-like and 'comet'-like extracellular structures released from crab HCs closely resembled those of diffuse and spread NETs respectively, with the terminology 'diffuse' and 'spread' now accepted to describe the different ETotic morphologies exhibited by neutrophils (Hakkim *et al*., 2011). Initial analysis revealed that after 4 h (10°C) a concentration of 0.1 µM PMA was optimum for extracellular chromatin release from crab HCs, combined with the overall lowest rate of intact dead (non-chromatin extruding) HCs (Figure 4.2, red arrow). After 4 h culture with 0.1 µM PMA, a significant (P<0.05; n=3) percentage of viable HCs remained (61.5% ± 1.1% SEM) compared to the percentage of viable HCs treated with 1 µM PMA (38.5% ± 2.5% SEM) at the same time point (Figure 4.2). Moreover, after 4 h culture, a significant (P<0.01; n=3) percentage of extracellular chromatin release was obtained from 0.1 µM PMA treated HCs (12.2% ± 1.7% SEM) compared to the percentage of extracellular chromatin release exhibited by control HCs (1.6% ± 0.7% SEM) (Figure 4.2).

The concentration of PMA selected for further investigation was 0.1 µM. With this concentration the percentage of chromatin extruding HCs rose significantly from 12.2% ± 1.7% SEM after 4h, to 33.3% ± 2.0% SEM after 14 h (P<0.01; n=5), reaching a maximal response of 63.4% ± 5.1% SEM after 24 h (P<0.001; n=5) (Figure 4.3 and Figure 4.4, A-D). After 4, 14 or 24 h, the rate of extracellular chromatin release from control HCs remained less than <5% (Figure 4.3 and Figure 4.5, A-C). Conversely, larger scale extracellular chromatin release was evident from 0.1 µM PMA treated HCs after 4, 14 and especially 24 h culture (Figure 4.4, A-D, arrows). To serve as a positive control to induce cell death, HCs were treated with 50% ethanol, and after 24 h, all cells were dead

and not extruding chromatin (Figure 4.3 and Figure 4.5, D). Furthermore, the vehicle control confirmed that DMSO was not cytotoxic to HCs. After 24 h culture with 0.1% DMSO (maximum concentration that HCs were exposed to) levels of HC viability remained at 56.0% ± 6.2% SEM, which was comparable to levels of viability exhibited by control (untreated) HCs at the same timepoint (47.3% ± 13.8% SEM) (Figure 4.3).

Figure 4.1.

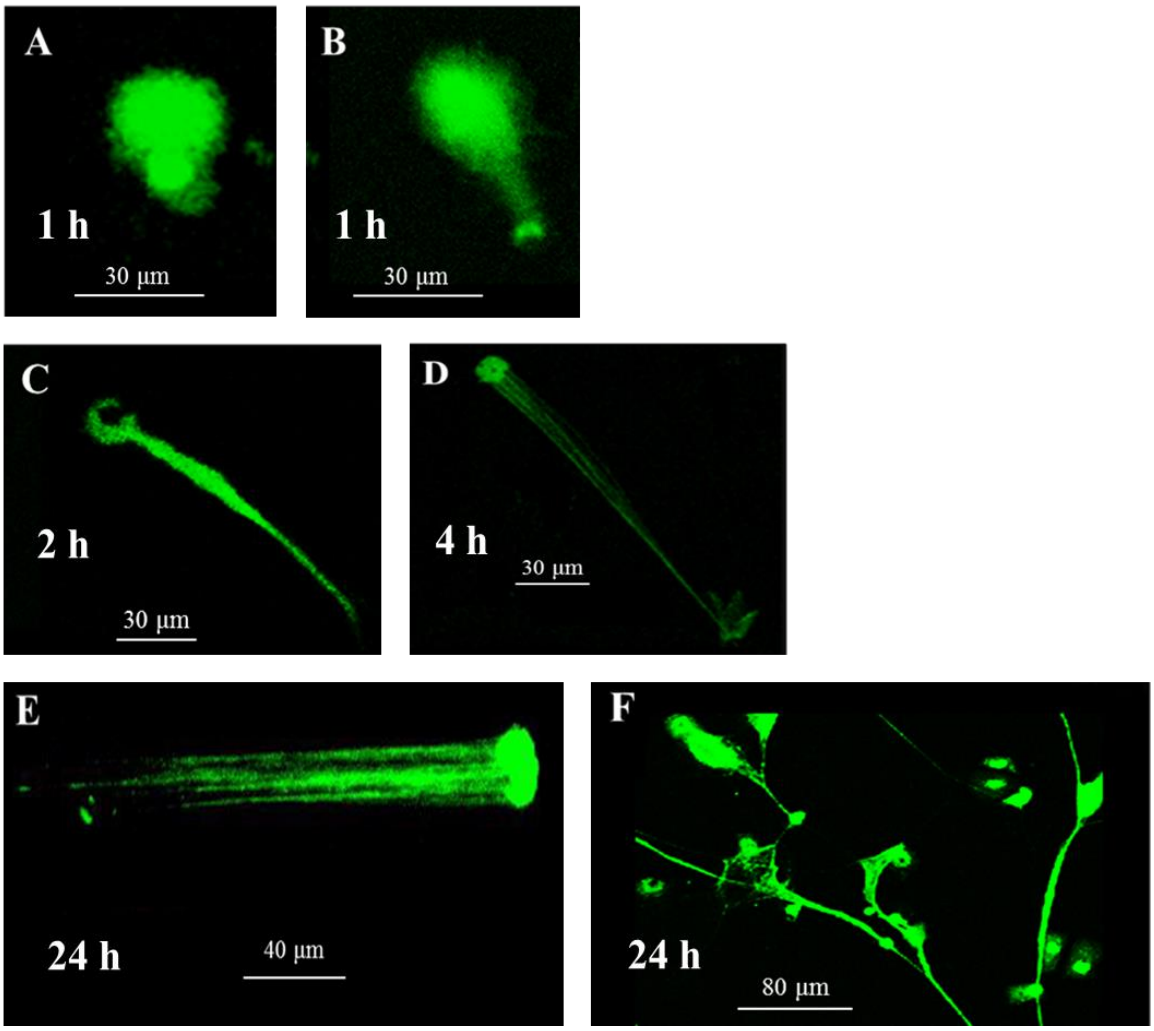

Figure 4.1. Different forms of chromatin discharged by sperated HCs from *C. maeans in vitro*. (**A-F**): Confocal images of Sytox Green stained chromatin extruding HCs observed after various incubation times with different concentrations of PMA. (**A-B**): 1 h, 1 µM PMA, HCs exhibit swollen 'puff-ball-like' nuclei indicative of early stages of chromatin extrusion; (**C-E**): Nuclear material extruded from HCs forms 'comet-like' streaks, which become longer and more prominent in a time-dependent manner. (**C**): 2 h, 0.1 µM PMA (**D**): 4 h, 0.1 µM PMA (**E**): 24 h, 0.1 µM PMA. (**F**): 24 h, 0.1 µM PMA, HCs exhibit long inter-connecting strands of extracellular nuclear material. Scale bars = 30 µm (**A-D**), 40 µm (**E**) or 80 µm (**F**).

Figure 4.2.

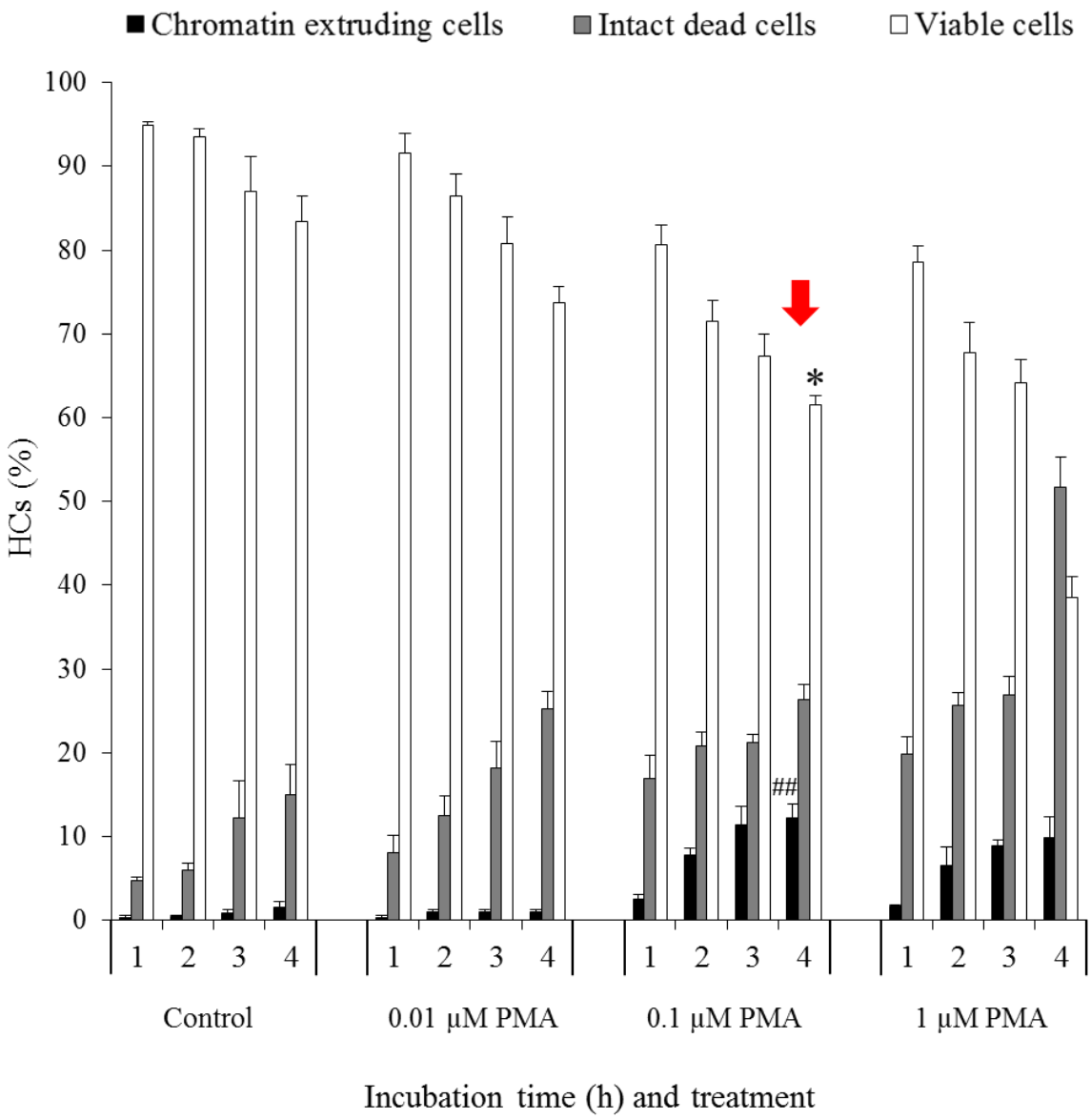

Figure 4.2. Concentration-time analysis *in vitro* of the effect of PMA on separated HCs from *C. maenas*. Percentage of viable, intact dead and chromatin extruding HCs treated with 0.01, 0.1 and 1 µM PMA over a 4 h incubation period. Red arrow indictaes the optimal concentration of PMA for chromatin extrusion (0.1 µM) combined with an overall lower percentage of dead, non-chromatin extruding, HCs. Data are expressed as means ± SEM, n=3, with a different crab used on each occasion**.** Statistical analysis was performed upon arc sine transformed data using one-way ANOVA with a Student Newman-Keuls multiple comparison *post hoc* test.
* $P<0.05$ *vs.* 4 h viable HCs treated with 1 µM PMA; ## $P<0.01$ *vs*. 4 h control (untreated) HCs.

Figure 4.3.

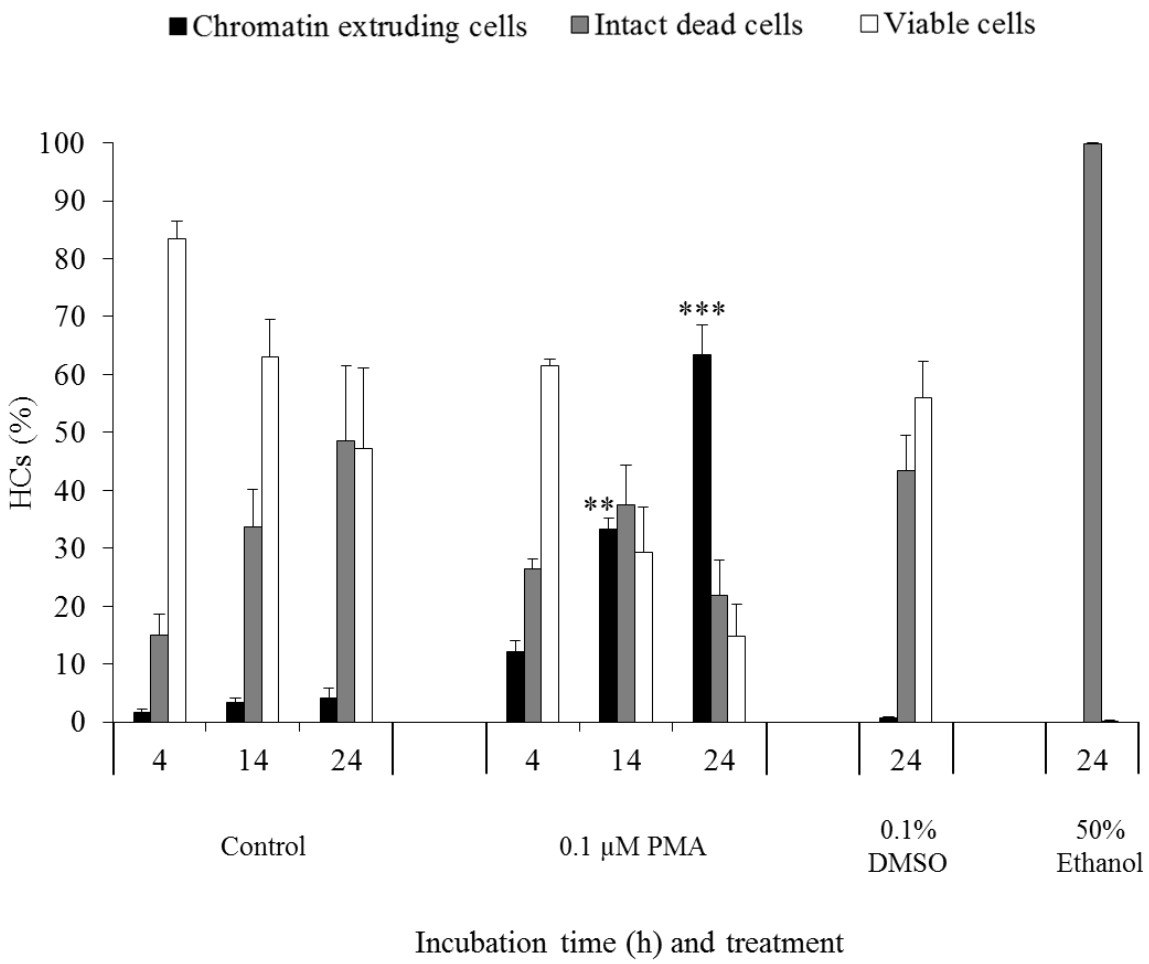

Figure 4.3. Changes in percentages of chromatin extrusion over time in separated HCs from *C. maenas* treated with PMA *in vitro*. Percentage of viable, intact dead and chromatin extruding HCs after 4, 14 and 24 h culture ± 0.1 µM PMA, or after 24 h culture with 0.1% DMSO or 50% ethanol. Data are expressed as means ± SEM, n=3 (4 h data, DMSO and ethanol treatments) or n=5 (all other data), with a different crab used on each occasion**.** Statistical analysis was performed upon arc sine transformed data using one-way ANOVA with a Student Newman-Keuls multiple comparison *post hoc* test. ***P*<0.01, *** *P*<0.001 *vs.* 4 h chromatin extruding HCs treated with 0.1 µM PMA.

Figure 4.4.

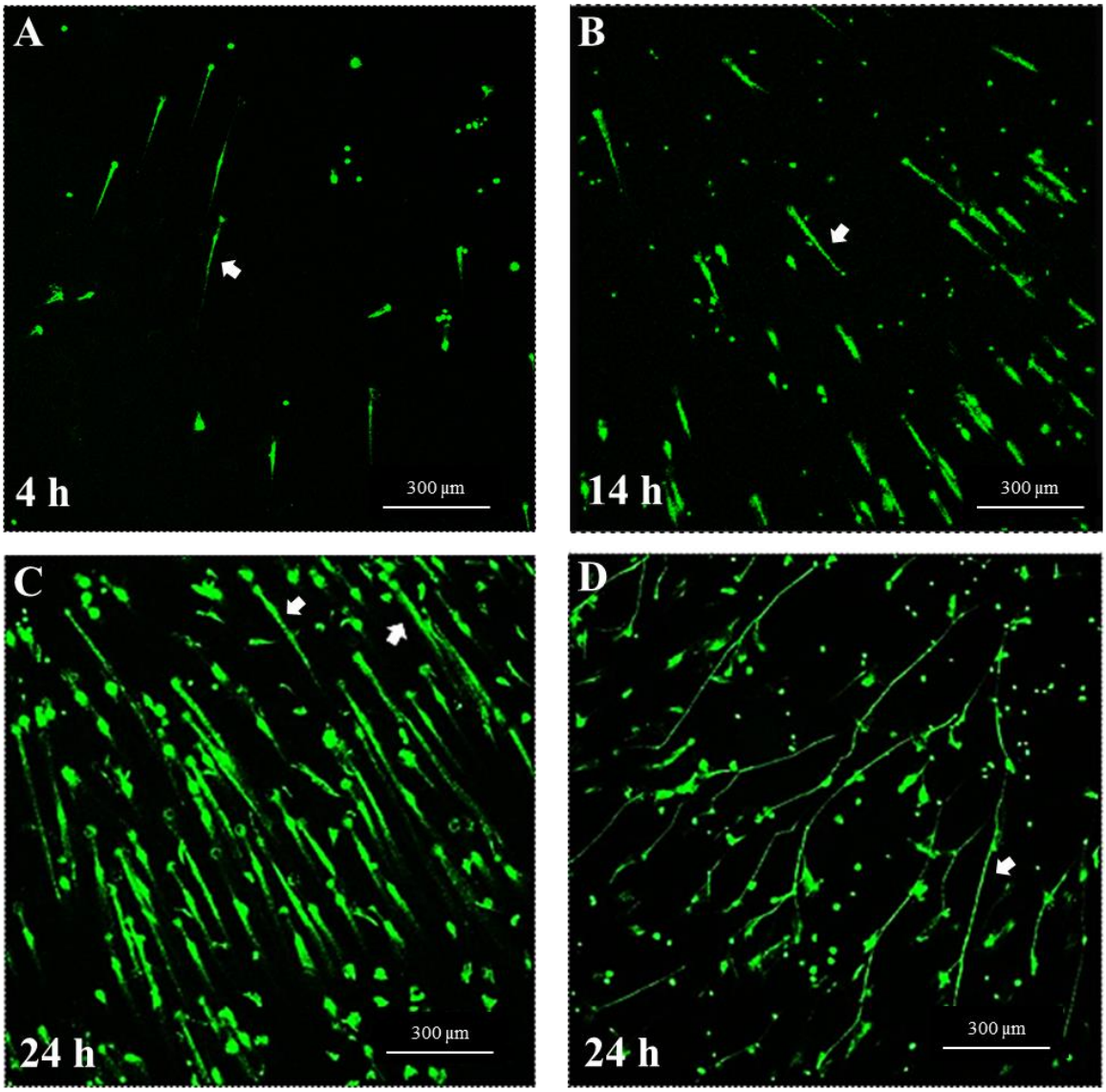

Figure 4.4. Representative confocal images of Sytox Green stained 0.1 µM PMA treated HCs over a 24 h culturing period *in vitro*. (**A-D**): HCs after 4 h (**A**), 14 h (**B**) and 24 h (**C and D**) co-culture with 0.1 µM PMA. Arrows indicate extracellular chromatin release, which is highly abundant in HCs after 24 h culture (**C** and **D**). All images representative of n=3 experiments (**A**) or n=5 experiments (all other images). Scale bars = 300 µm.

Figure 4.5.

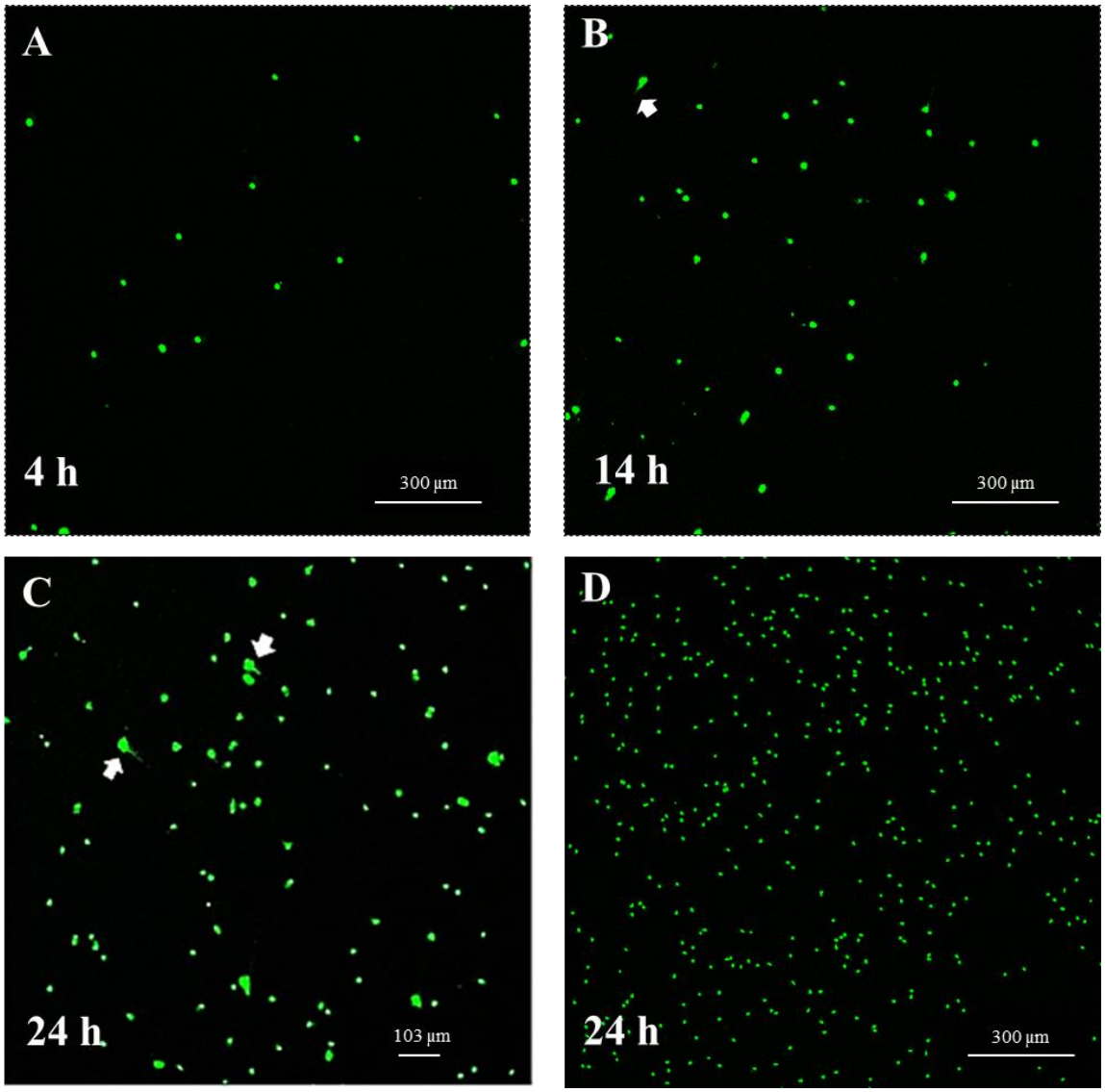

Figure 4.5. Representative confocal images of Sytox Green stained untreated (control) HCs over a 24 h culturing period *in vitro*. (**A**-**C**): Untreated (control) HCs after 4 h (**A**), 14 h (**B**) and 24 h (**C**) culture. Arrows indicate small-scale evidence of extracellular chromatin release. (**D**): HCs after 24 h culture in the presence of 50% ethanol (positive control to induce non-ETotic cell death). The majority of haemocytes are intact dead, i.e. non-chromatin extruding. All images representative of n=3 experiments (**A** and **D**) or n=5 experiments (**B** and **C**). Scale bars = 103 µm (**C**) or 300 µm (all other images).

4.3.2. Digestion of extracellular chromatin

Importantly, after stimulation with 0.1 µM PMA (24 h), addition of DNAse-1 completely dissolved the extracellular material released from HCs, confirming that the released material is chromatin (Figure 4.6, A; supplementary video 3). After 20 min post DNAse-1 treatment digestion of extracellular chromatin released from HCs was apparent (Figure 4.6, A, arrows). In total it took 4 h 40 min (280 min) for DNAse-1 to completely dissolve all the extracellular chromatin released from HCs (Figure 4.6, A; supplementary video 3). In HCs stimulated with 0.1 µM PMA (24 h) but which did not receive DNAse-1, the extracellular chromatin structures remained over the same time period (280 min) (Figure 4.6, B). Therefore, it can be confirmed the extracellular chromatin structures released from HCs do not readily dissolve, and do in fact persist for a considerable length of time once released.

Figure 4.6.

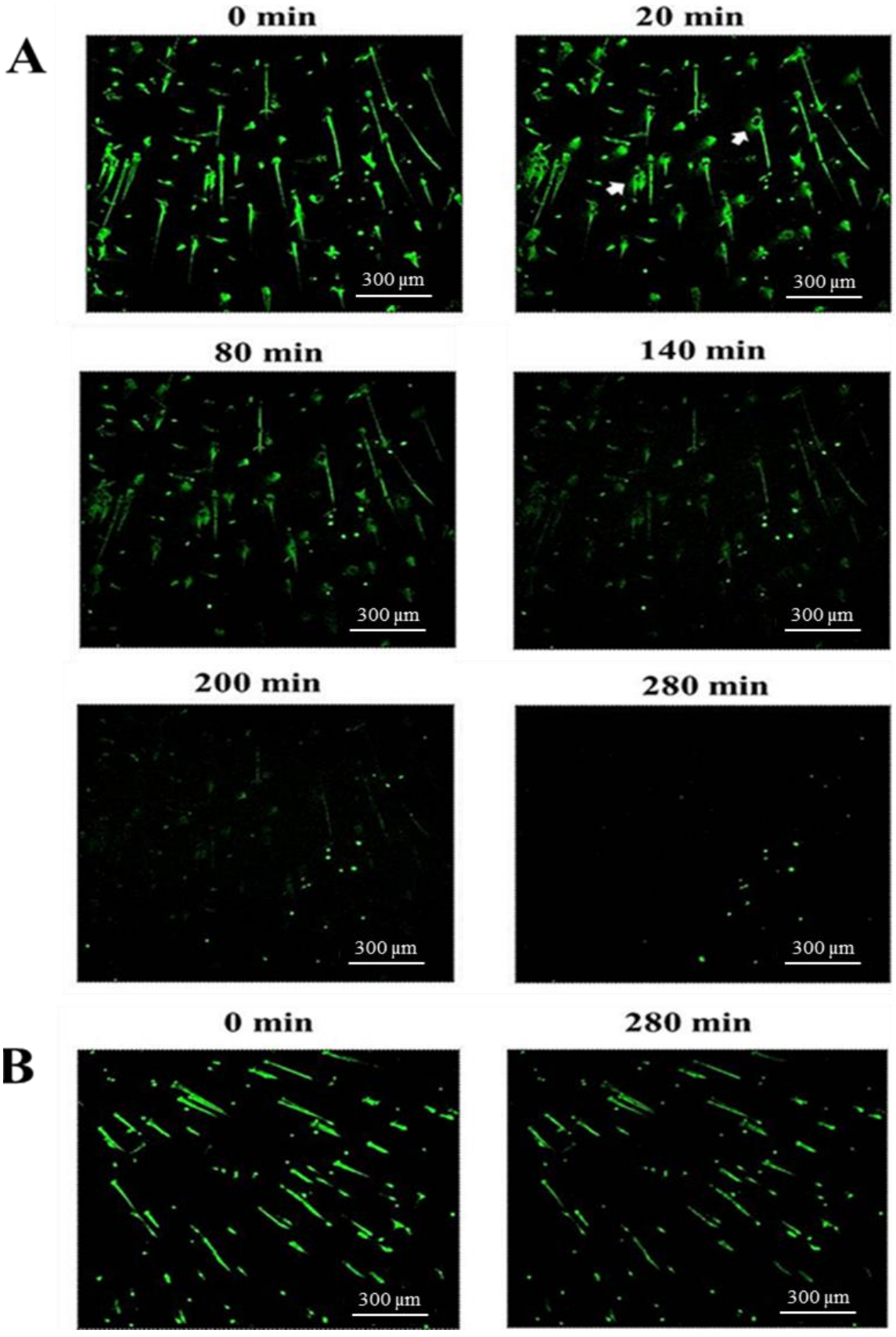
A
0 min
20 min
300 µm
300 µm
80 min
140 min
300 µm
300 µm
200 min
280 min
300 µm
300 µm
B
0 min
280 min
300 µm
300 µm

Figure 4.6. DNAse digestion of extracellular chromatin released from *C. maenas* HCs *in vitro*. Confocal time-lapse photo microscopy of Sytox Green stained HCs over a 280 min period. (**A**): Confocal images showing the digestion of extracellular chromatin 20, 80, 140, 200 and 280 min post addition of 100 U mL^{-1} DNAse-1 (refer to supplementary video 3), arrows indicate early digestion of extracellular chromatin by DNAse-1 after 20 min; (**B**): Confocal images of control HCs (no DNAse-1) taken at 0 and 280 min, which show that the released chromatin structures remain and do not readily dissolve over the same time period. Scale bars = 300 µm.

4.3.3. Confirmation of ROS generation by HCs

After 24 h culture, HCs treated with PMA exhibited a significant increase ($P<0.001$; n=3) in mean rhodamine 123 (FL1) fluorescence (146.9 nm ± 10.1 nm SEM) compared to control (untreated) HCs (2.6 nm ± 0.2 nm SEM), indicative of a strong respiratory burst (Appendix 6, A). Addition of the NADPH oxidase inhibitor DPI (2 µM) abrogated generation of ROS. Significantly low ($P<0.001$; n=3) mean FL1 fluorescence was exhibited from HCs cultured with PMA + DPI (0.96 nm ± 0.2 nm SEM) and DPI alone (0.97 nm ± 0.2 nm SEM) compared to PMA treated HCs (146.9 nm ± 10.1 nm SEM) (Appendix 6, A). A representative fluorescence histogram of PMA treated HCs shows the large rightward shift in fluorescence due to large-scale generation of a respiratory burst (Appendix 6, B, C). Conversely, only marginal shifts in mean FL1 fluorescence were observed in control (untreated) HCs, HCs treated with PMA + DPI or HCs treated with DPI only (Appendix 6, B, C), indicating very small-scale generation of a respiratory burst.

4.3.4. Ultrastructural analysis

Scanning electron microscopy revealed that unlike a viable (untreated) HC (Figure 4.7, A), extruded DNA from PMA-treated HCs forms large extracellular complex meshes (Figure 4.7, B), composed of smooth strand-like fibres (Figure 4.7, C, red arrow) that are studded with small globular domains (Figure 4.7, C, white arrow). The globular domains and smooth fibres of ETs released from crab HCs were slightly larger than those previously determined for human NETs (Brinkmann *et al*., 2004) (Table 4.1). Transmission electron microscopy further revealed that in contrast to a viable (untreated) HC (Figure 4.8, A) or an apoptotic HC which diplayed a characteristic thick rim of marginated chromatin (Figure 4.8, B, arrow), PMA-treated HCs exhibited no peripheral condensation of chromatin at the nuclear membrane (Figure 4.8, C). Furthermore, complete nuclear membrane breakdown and direct mixing of cytoplasmic and nuclear components preceeds chromatin release from a breach point (Figure 4.8, C, arrow), as is observed in ETotic neutrophils (Fuchs *et al*., 2007).

Figure 4.7.

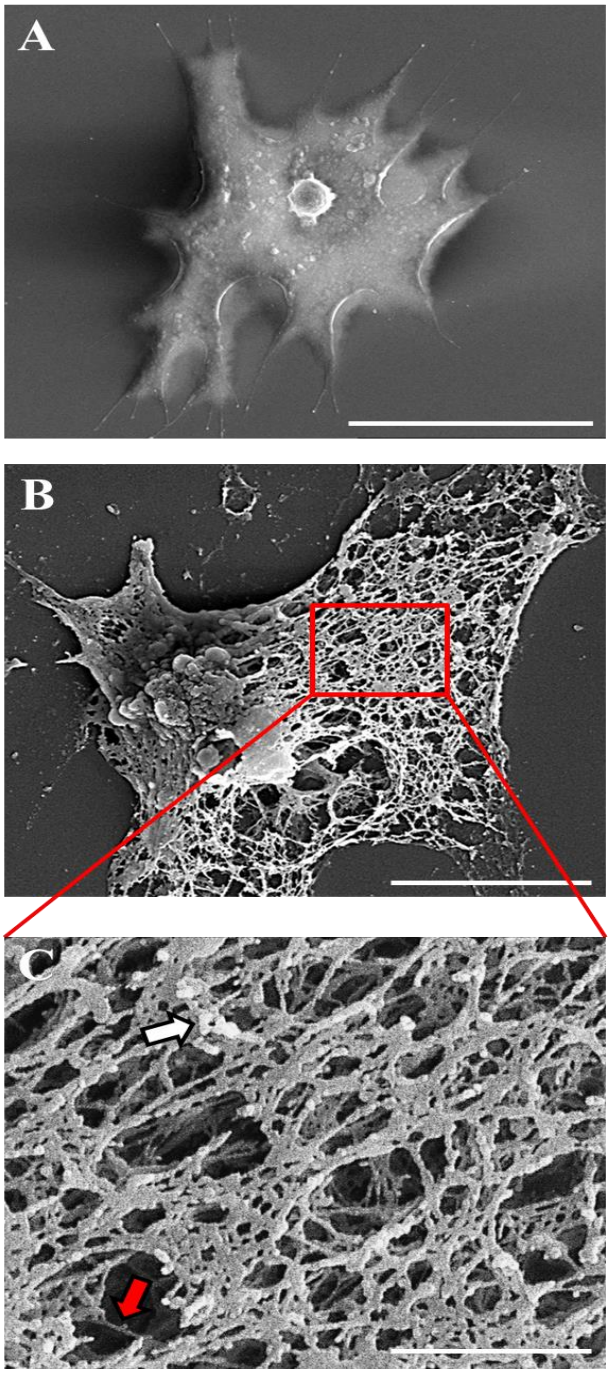

Figure 4.7. Scanning electron microscopy of extracellular chromatin release from HCs *in vitro*. HCs after 24 h culture ± 0.1 µM PMA (10°C). (**A**): Viable (untreated) HC spreading on the coverslip; (**B**): HC treated with PMA exhibiting extracellular chromtain release; (**C**): High magnification of red boxed region (B), where red arrow indicates the smooth fibral composition of the extracellular chromatin, and white arrow indicates globular domains studded throughout the extensive extracellular chromatin mesh. Scale bars = 20 µm (**A**), 5 µm (**B**) and 1 µm (**C**).

Table 4.1. Ultrastructural comparison of ETs released from *C. maenas* HCs and human NETs, assessed using high resolution scanning electron microscopy.

Ultrastructural feature measured	***C. maenas* ETs (nm)**	**Human NETs (nm)**
Diameter of globular domains	47.8 nm ± 3.4 SEM	25 nm but can aggregate into longer threads up to 50 nm (Brinkmann *et al*., 2004)
Diameter of smooth fibres	26.0 nm ± 1.75 SEM	15-17 nm (Brinkmann *et al*., 2004)

Abbreviations: ETs = extracellular traps, NETs = neutrophil extracellular traps

Figure 4.8.

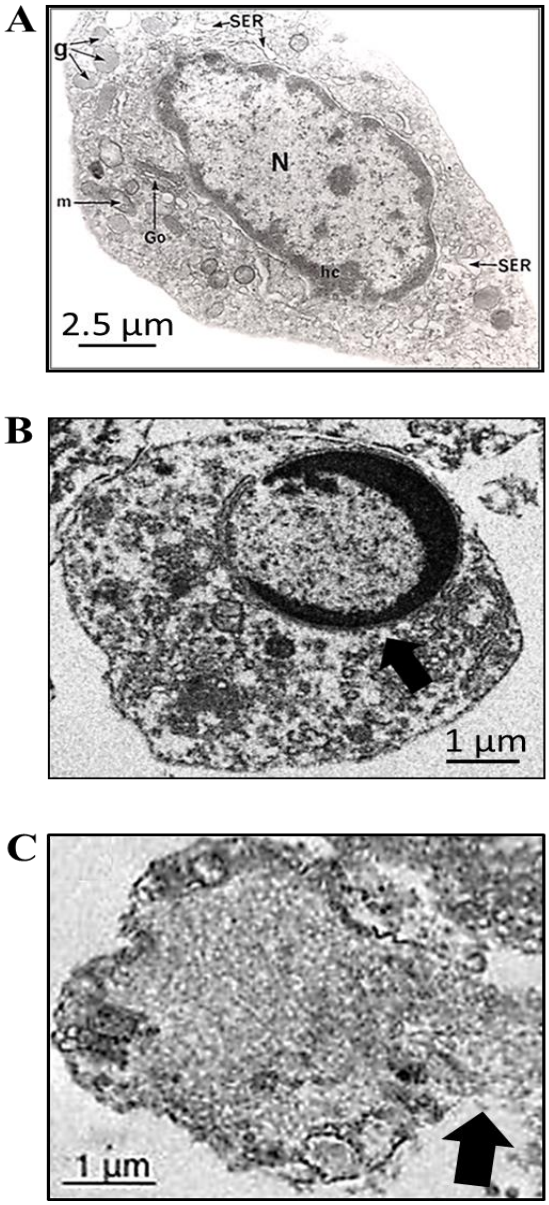

Figure 4.8. Transmission electron microscopy showing extracellular chromatin release from HCs *in vitro*. (**A**): Viable HC at 0 h: N- nucleus with intact membrane, rim of condensed heterochromatin (hc) at periphery; Go - Golgi body; m – mitochondrion; SER - smooth endoplasmic reticulum; g - cytoplasmic granules (Image courtesy of Dr Valerie J. Smith, St Andrews University). (**B**): Apoptotic HC displaying characteristic chromatin margination/crescent body formation (arrow), with intact nuclear and plasma membranes (image from Chapter 2, Figure 2.5, B); (**C**): HC exhibiting extracellular chromatin release, complete nuclear breakdown and swelling/mixing of the nuclear and cytoplasmic contents is clear, indicative of ETosis. Arrow indicates chromatin discharge from the cell at a breach point. Scale bars = 2.5 µm (**A**) or 1 µm (**B**, **C**).

4.3.5. Extracellular chromatin decoration

Immunocytochemical analyses to evaluate the decoration of the disgorged chromatin from HCs confirmed that it becomes associated with a protein recognised by a rabbit anti-human MPO antibody (Figure 4.9, A-D). This protein is likely to be PXN, a crustacean homologue of human MPO that is expressed by crustacean haemocytes involved in cell-to-cell adhesion (Johansson *et al*., 1995; Johansson, 1999; Schmidt *et al*., 2010). In the present study PXN was localised in a punctate fashion on extracellular DNA, where it was confirmed to be released from the peri-nuclear region of the HCs as the antibody did not co-localise with the nucleus in intact cells, (Figure 4.9, D). Additionally, actin did not co-localise with extracellular DNA (Figure 4.9, D), as was observed in NETs released from fathead minnow (Palic *et al*., 2007a). Crucially, histone H2A was liberated from the nuclei of HCs to the extracellular environment (Figure 4.9, E-H) and was demonstrated to co-localise with PXN on released extracellular chromatin (Figure 4.9, H). Importantly, no non-specific staining was detected on extracellular chromatin released from HCs (Appendix 7, A-D).

Figure 4.9.

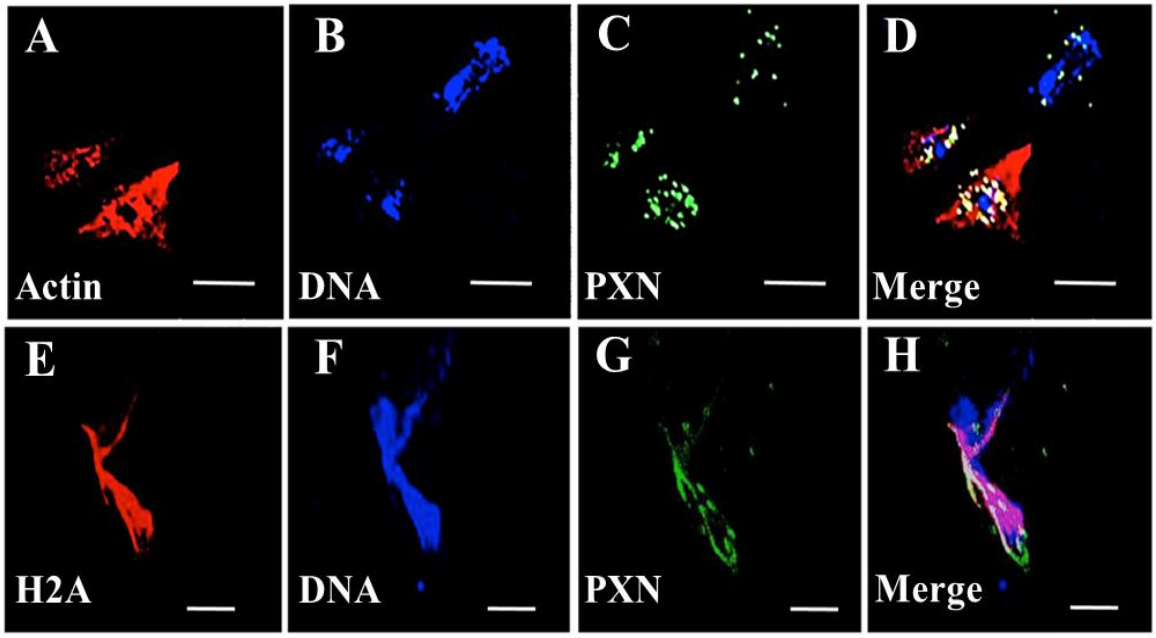

Figure 4.9. Immunocytochemical analysis of extracellular chromatin released from HCs *in vitro*. HCs after 24 h culture (10°C) with 0.1 µM PMA and examined by confocal microscopy. (**A-D**): Localisation of PXN on extracellular chromatin released from a HC. (**A**): F-actin in non-chromatin extruding HCs indicated by rhodamine phalloidin staining; (**B**): DNA revealed by Draq-5 (**C**): Localisation of PXN recognised by rabbit anti-human MPO antibody; (**D**): Merge of A-C. Note perinuclear localization of PXN in intact HCs (left and centre) compared to co-localization with extracellular DNA in ETotic HC (top right), scale bars = 25 µm. (**E-H**): Localisation of histone H2A and PXN on extracellular chromatin released from a HC. (**E**): Histone H2A revealed by mouse anti-H2A antibody; (**F**): DNA revealed by Draq-5 staining; (**G**): PXN revealed by rabbit anti-human MPO antibody; (**H**): Merge of E-G, scale bars = 20 µm.

4.3.6. Inhibition of extracellular chromatin release

The release of extracellular chromatin from crab HCs was dramatically reduced by pre-incubation with 2 µM DPI (<2%), 10 µM cyto D (<2%), or 1 µM Ro-31-8220 (<5%), prior to PMA treatments (Figure 4.10 and Figure 4.11, A, C, D). Percentages of extracellular chromatin release also remained low (<15%) after pre-incubation of HCs with 50 µM apocynin prior to PMA treatment (Figure 4.10), where small-scale diffuse release of chromatin was evident (Figure 4.11, B, arrows).

After 24 h culture, compared to the percentage of ETotic HCs treated with 0.1 µM PMA (63.4% ± 5.1% SEM), significant reductions (P<0.001; n=3) in the response were observed in HCs treated with PMA + DPI (1.3% ± 0.3% SEM), DPI alone (0.9% ± 0.5% SEM), PMA + apocynin (14.2% ± 4.1% SEM), apocynin alone (5.9% ± 4.1% SEM), PMA + cyto D (0.9% ± 0.3% SEM), cyto D alone (0.3% ± 0.1% SEM), PMA + Ro-31-8220 (3.6% ± 2.6% SEM) and Ro-31-8220 alone (4.6% ± 3.9% SEM) (Figure 4.10 and Figure 4.11, A-D). Percentages of viability remained high in HCs co-incubated with PMA + Ro-31-8220, as evidenced by the low number of Sytox Green stained HCs (Figure 4.11, D). This high rate of viability was obtained because Ro-31-8220 inhibits PKC, which is the major mechanism of the chemical stimulator PMA (a PKC activator). Therefore, Ro-31-8220 sequesters the cytotoxic effect that PMA has upon crab HCs. These results taken together demonstrate that the release of chromatin from crab HCs involves similar processes as those used by mammalian cells.

Figure 4.10.

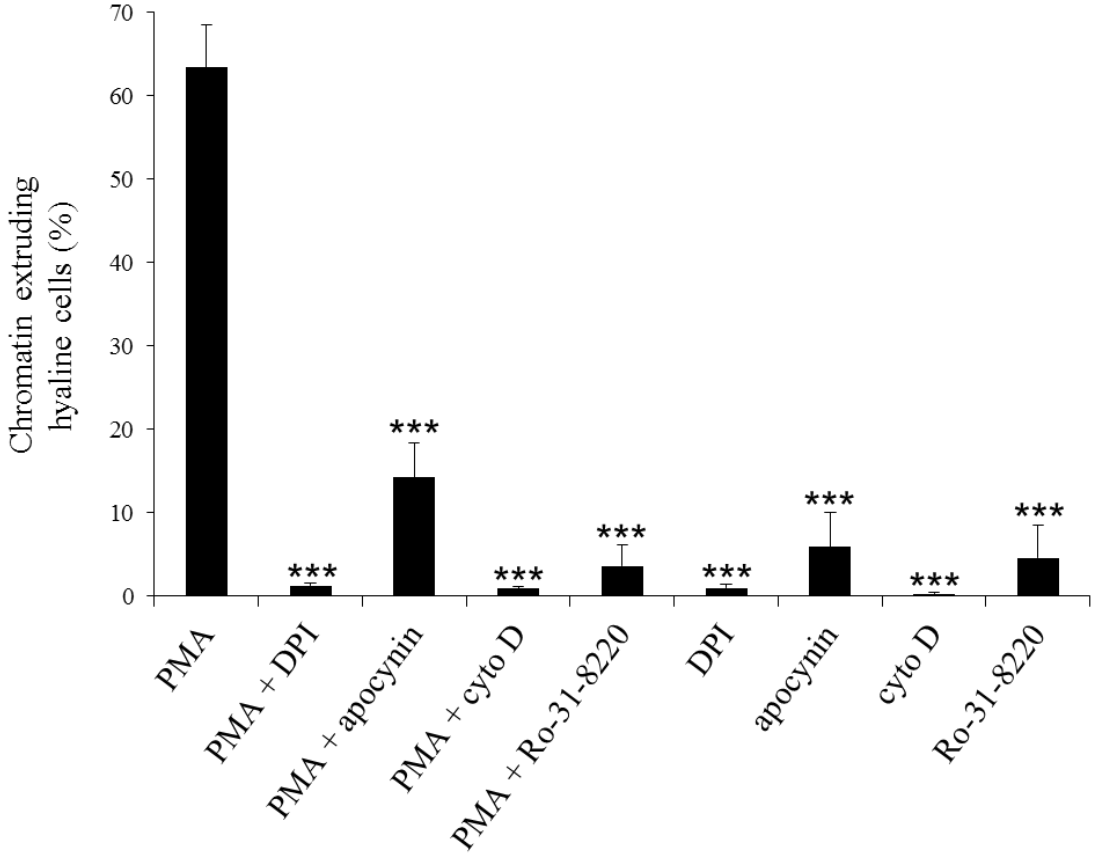

Figure 4.10. Inhibition of extracellular chromatin release from *C. maenas* HCs *in vitro*. Percentage of chromatin extruding HCs after 24 h culture (10°C) with different combinations of 0.1 µM PMA ± 2 µM DPI, 50 µM apocynin, 10 µM cyto D or 1 µM Ro-31-8220. Data are expressed as means ± SEM, n=5 (PMA only treatment) or n=3 (all other treatments), with a different crab used on each occasion**.** Statistical analysis was performed upon arc sine transformed data using one-way ANOVA with a Student Newman-Keuls multiple comparison *post hoc* test. *** $P<0.001$ *vs.* chromatin extruding HCs treated with PMA only.

Figure 4.11.

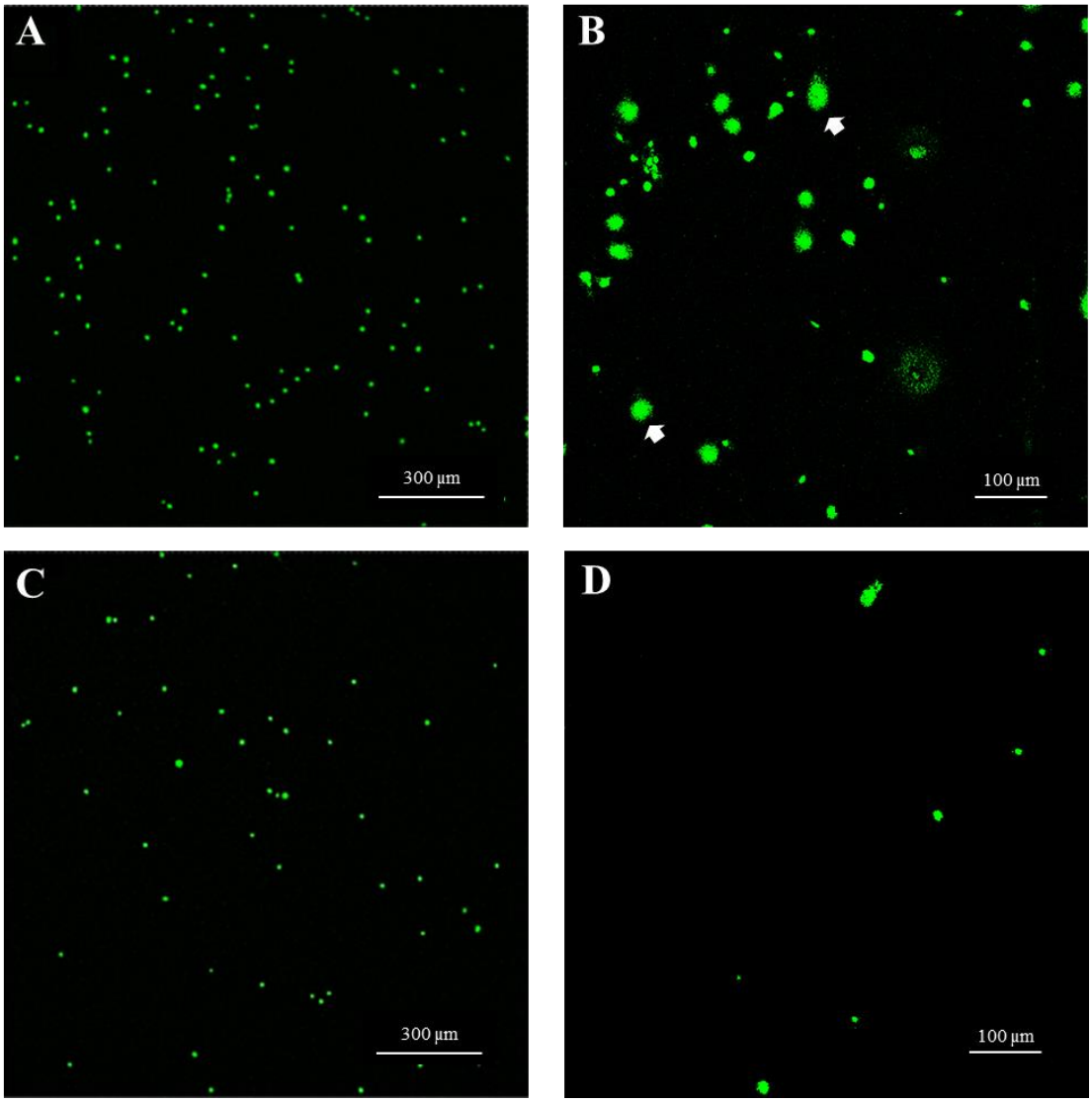

Figure 4.11. Representative confocal images after 24 h culture showing the inhibition of extracellular chromatin release in HCs *in vitro* by Sytox Green staining. (**A-D**): Efficient inhibition (**A, C, D** especially) of extracellular chromatin release after pre-treatment of HCs with various pharmalogical inhibitors of ETosis. (**A**): 0.1 µm PMA + 2 µm DPI; (**B**): 0.1 µm PMA + 50 µm apocynin. Note there is small-scale evidence of extracellular chromatin release in the form of swollen 'puff-ball-like' nuclei (white arrows). (**C**): 0.1 µm PMA + 10 µM cyto D; (**D**): 0.1 µm PMA + 1 µM Ro-31-8220. Note the high viability as evidenced by the small proportion of Sytox Green stained HCs (**D**). All images representative of n=3 experiments. Scale bars = 300 µm (**A, C**) or 100 µm (**B, D**).

4.4. Discussion

The experiments performed in this chapter successfully characterised and quantified ETotic cell death (*in vitro*) in phagocytic HCs from the crab, *C. maenas*, using the PKC activator PMA as the simulator. The present study demonstrated that monolayer cultures of crab HCs treated with PMA extruded ETs similar in morphology to mammalian NETs. For human NETs, diffuse forms are more common after *in vitro* culture (Gray *et al*., 2013), with a maximal rate of 15-20% achieved after 4 h culture (37°C) with 10 nM PMA (Fuchs *et al*., 2007). During the present study, both diffuse and spread ET morphologies were released from crab HCs *in vitro*, with spread ETs more frequently observed at later timepoints, where a maximum rate of ca. 63% ETosis was achieved from HCs after 24 h culture (10°C) with 100 nM PMA. A low level of ETosis would be expected to occur in control (untreated) HCs as the process is part of an innate immune response. Therefore, like apoptotic cell death, ETotic cell death would also be occurring under normal physiological conditions. Apart from the considerable evolutionary distance between crabs and humans, the ten-fold higher concentration of PMA that was used for ETosis stimulation in crab HCs may explain the higher levels obtained compared to human neutrophils. Additionally, the low culture temperature for crab HCs compared with that for mammalian neutrophils may also help explain the longer time observed for maximal levels of ETosis in crab HCs, as virtually all cellular processes will be slower at lower temperatures. Certainly arrest of neutrophil apoptosis can be achieved by incubating neutrophils at 15°C for a period of 20 h (Pryde *et al*., 2000). Interestingly, Kawata *et al*. (2014) claim that NET-like structures can be induced by cold shocking human promyelocytic leukemia cells (HL60) at 4°C for 1 h, then transferring the cells to normal culturing temperature (37°C) for 5 h. This finding may represent a PMA-independent method of inducing ETosis. However, although characteristic markers of ETosis were detected on extruded chromatin from HL60 cells after cold-shock, such as neutrophil elastase and histone H3 (Kawata *et al*., 2014), no mechanism was revealed, and follow up studies have failed to emerge. Therefore it remains uncertain whether this cold-shock effect in HL60 cells represents genuine ETosis.

Electron microscopy revealed that although ETs released from crab HCs appear similar in ultrastructural morphology to mammalian NETs, both the globular domains and smooth fibres of crab ETs are marginally larger than those described for human NETs (Brinkmann *et al*., 2004). However, although chromatin is similar in its dimensions across all animal taxa, at the ultrastructural level, differences in measurements may easily be introduced due to sample processing procedures, as well as the type of microscopy and analysis software used.

In the present study immunocytochemical analysis revealed that crab HCs released ETs that are decorated with histone H2A, similar to NETs. Histones are highly conserved nuclear proteins with powerful antimicrobial activities (Hirsch, 1958), and ETosis is the only known mechanism by which they are exposed to infective agents. Indeed, histone decoration of chromatin is a diagnostic feature of ETosis in mammals (Fuchs *et al*., 2007), with core histones H2A, H2B, H3 and H4 the most abundant proteins accounting for 70% of all NET-associated proteins (Urban *et al*., 2009).

With regard to the mechanism of extracellular chromatin release from crab HCs, it was demonstrated during this study that HCs do in fact undergo ETotic cell death via the same pathways used by NETs. This was revealed by potent inhibition of PMA-induced ETosis in crab HCs after pre-incubation with various inhibitors, including DPI, apocynin, Ro-31-8220 and cytochalasin D. DPI inhibits flavoprotein oxidoreductases (including NADPH oxidase) while apocynin inhibits the assembly of NADPH oxidase (Drummond *et al*., 2011). Ro-31-8220 is a pan protein kinase C inhibitor (Beltman *et al*., 1996), that inhibits generation of ROS upstream of NADPH oxidase activation, and cytochalasin D prevents actin polymerization required for phagocytosis (May *et al*., 1998). These agents also inhibit ETosis by mammalian neutrophils (Fuchs *et al*., 2007; Neeli *et al*., 2009; Azevedo *et al*., 2012; Gray *et al*., 2013) because NADPH oxidase and the cytoskeleton have crucial and overlapping roles in the process. NADPH oxidase is needed for decondensation of chromatin prior to its discharge, while the cytoskeleton is required for NADPH oxidase assembly (Neeli *et al*., 2009). Actin filamentation is also necessary for positioning the nucleus close to the plasma membrane and for rupture of the cell, hence the inhibitory effect of cytochalasin D, which also impairs histone citrullination (Neeli *et*

al., 2009). Inhibition of PKC occurs upstream of NADPH oxidase generation and Ro-31-8220 inhibits generation of ROS in human NETs (Gray *et al*., 2013). Therefore, it was clearly established that crab HCs are capable of undergoing vertebrate-type ETosis.

Apocynin was the least effective inhibitor in blocking ETosis in HCs. Indeed, a recent study comparing the pharmacology of chemically distinct NADPH oxidase inhibitors observed that apocynin can interfere with ROS detection and varies considerably in efficacy and potency, whereas DPI abolished NADPH oxidase-mediated ROS formation (Wind *et al*., 2010). Furthermore, only partial inhibition of NET release was observed (~40-50%) after pre-treatment of neutrophils with apocynin, prior to stimulation with α-synuclein or A25T amyloid fibrils (Azevedo *et al*., 2012). This is in stark contrast to DPI, which abrogates the release of PMA-induced NETs (Fuchs *et al*., 2007). With this in mind, it is perhaps unsurprising that pre-treatment of crab HCs with apocynin resulted in least efficient inhibition of PMA-induced ETosis.

This chapter reports the successful characterisation and quantification of ETosis in *C. maenas* HCs *in vitro*, and represents the first definitive demonstration of this cell death process in any invertebrate. Crucially, this study showed that extracellular chromatin released from crab HCs is decorated with histone H2A, is dependent upon activation of PKC and NADPH oxidase, as well as requiring structural re-organisation of the cytoskeleton, all four of which are hallmark features of ETosis in vertebrates. However, chemically-induced ETosis (via PMA) will differ substantially to ETotic responses mounted against microbial pathogens during innate immune defence, especially *in vivo*. Therefore, the next step was to implicate the possible role(s) of ETosis during host immune defence in the crab (Chapter 5).

Chapter 5

Role of ETosis during host immune defence

5.1. Introduction

In mammals, ETosis is not confined to neutrophils and has also been shown to occur in eosinophils, monocytes, macrophages and mast cells (von Köckritz-Blickwede *et al*., 2008; Webster *et al*., 2010; Aulik *et al*., 2012; Ueki *et al*., 2013). Cell-to-cell cooperation during host defence is well established in crustaceans (Smith and Ratcliffe, 1980a), for review see Smith, (2010). Therefore, having established that HCs of the crab undergo ETosis (Chapter 4), it also needs to be established whether or not the remaining haemocyte types of the crab (SGCs, GCs and ProHs) undergo similar-style ETosis.

ETotic responses are typically mounted against microbial pathogens during innate immune defence. Certainly LPS and bacteria are known to induce NETs in mammals, where bacteria such as *S. aureus* are trapped and killed by NETs (Fuchs *et al*., 2007). Therefore, non-self agents that the crab would naturally be exposed to deserve to be tested for their ability to stimulate ETosis. Hence, the non-self agents LPS, and the marine Gram-negative bacterium, *L. anguillarum*, which were previously considered for investigation of apoptosis (Chapter 3), also deserved to be considered for investigation of ETosis.

Encapsulation is a key process through which bacteria and other non-self materials are cleared from the haemocoel of arthropods (Smith and Ratcliffe, 1980a, 1980b; Cerenius and Söderhäll, 2004). During encapsulation in the crab, the HCs, SGCs and GCs all participate, where they work in concert to form layers of haemocytes around foreign material (Smith and Ratcliffe, 1980a). As these layers accumulate, the capsule forms and eventually the encapsulated matrix material blackens due to the deposition of melanin. The capsules frequently lodge in the haemal sinuses, typically the gill filaments, and are cast along with the gills during ecdysis (Smith and Ratcliffe, 1980a, 1980b; Smith *et al*., 1984). In *C. maenas*, the phagocytic uptake of bacteria by HCs is relatively low, ca. 15-20 % *in vitro* (Söderhäll *et al*., 1986) but *in vivo*, approximately 94 % of injected bacteria (*Bacillus cereus* and *Moraxella sp*) are removed from the circulation within the first hour post-injection, mainly to the gills where they become

sequestered in haemocyte capsules (Smith and Ratcliffe, 1980a; White and Ratcliffe, 1982). In crab, entrapped bacteria are killed within the capsules (White *et al*., 1985), with AMPs and other antimicrobial factors from the SGC and GCs playing a large part in this (Smith, 2010).

It has been assumed that the haemocytes forming the capsule die by necrosis. However, no studies have been carried out to ascertain what the form of cell death might be. For animals in lower taxa, especially those with an open circulatory system, the externalization of chromatin during ETosis may be a powerful way to prevent infectious agents gaining entry to the body cavity. Furthermore, externalised chromatin could play a pivotal role in the encapsulation of foreign materials by the haemocytes. Therefore it was hypothesised that chromatin released during ETosis participates in immune defence of the crab, not only by ensnaring microorganisms and externalising adhesion proteins, but crucially by providing the scaffold upon which intact haemocytes assemble during encapsulation. The study in this chapter set out to investigate the role of ETosis during host defence in the shore crab, *C. maenas*.

Specifically, the objectives of this chapter are:

1. To establish whether or not other haemocyte types of the crab (SGCs, GCs and ProHs) undergo extracellular chromatin release following activation of PKC.

2. To determine if separated HCs release extracellular chromatin following treatment with various non-self agents, and to determine if this release is dependent upon activation of NADPH-oxidase.

3. To determine if externalised chromatin released during ETosis participates in encapsulation reactions *in vivo*.

5.2. Materials and methods

5.2.1. Separation of haemocyte populations

C. maenas specimens were collected and maintained as described in Chapter 2 (Section 2.2.2). Haemolymph was sampled from crabs as described above (Chapter 2, Section 2.2.3) and separated HCs, GCs and ProHs were obtained as described in Chapter 3 (Section 3.2.1). To obtain enriched SGCs, density gradient centrifugation was used as above and the HC band was removed. Next, the underlying SGCs were harvested, leaving approximately 1 cm of cell suspension/Percoll above the GC band. The SGC suspension was diluted 10x in sterile filtered 3.2% NaCl and washed by centrifugation for 5 min at 500 x g (4°C). The supernatant was removed and the SGCs resuspended in 10 mL sterile filtered 3.2% NaCl plus MAC and washed by centrifugation for a second time, after which they were counted and used for *in vitro* experiments.

5.2.2. Preparation of monolayer haemocyte cultures

Approximately 1 mL of 3 x 10^4 mL^{-1} HCs, GCs, SGCs or ProHs resuspended in ML-15 (Chapter 2, Section 2.2.3) were prepared in 24-well flat bottomed culture plates as described above (Chapter 4, Section 4.2.2). One crab was sampled per experimental run with triplicate monolayer cultures set up per treatment per timepoint.

5.2.3. Extracellular chromatin release assays *in vitro*

5.2.3.1. Different haemocyte types

Monolayer cultures of separated HCs, GCs, SGCs or ProHs (3 x 10^4/well) were treated with 0.1 µM PMA and cultured for 24 h (10°C) in ML-15 as described above (Chapter 4, Section 4.2.3). The cells were then stained for 20 min (protected from light) with a final concentration of 1 µM Sytox Green and extracellular chromatin release detected and quantified as above (Chapter 4, Section 4.2.3). For each haemocyte type, one crab was sampled per experimental run with triplicate monolayer cultures set up per treatment.

For further assessment of the different haemocyte types after PMA treatment, samples from suspension cultures set up as described above Chapter 2, Section 2.2.4) were taken for cyto-centrifugation. Approximately 5 mL of separated, HCs, SGCs, GCs (5×10^5 mL^{-1}) or ProHs (2.5×10^5 mL^{-1}) resuspended in ML-15 (Chapter 2, Section 2.2.3) were treated with a final concentration of 0.1 µM PMA and cultured for 24 h (10°C). Subsequently, cyto-centrifuge preparations were made (either 1×10^5 HCs, SGCs and GCs or 5×10^4 ProHs/cyto-centrifuge preparation) as described above (Chapter 2, Section 2.2.5.1). After mounting slides in DePeX mounting medium, haemocytes were visualised using a Zeiss Axioskop light microscope (Carl Zeiss Microscopy Ltd, Cambridge, UK) and images captured using QCapturePro software.

5.2.3.2. LPS and Listonella anguillarum (non-self agents)

To test whether non-self agents could stimulate ETosis, HC monolayer cultures were treated with LPS (from *Escherichia coli* serotype 0111:B4) at 0.1 µg mL^{-1}, or a washed viable suspension of *L. anguillarum* (ATCC 43305) at 3×10^5 mL^{-1}. For all experiments involving *L. anguillarum*, ML-15 without 1% Pen/Strep was used. Controls received ML-15 only and all samples were cultured for 24 h (10°C). The cells were then stained with Sytox Green as above (Section 5.2.3.1) and extracellular chromatin release detected and quantified as above (Chapter 4, Section 4.2.3). For LPS or *L. anguillarum*, one crab was sampled per experimental run with triplicate monolayer cultures set up per treatment.

5.2.4. Inhibition of extracellular chromatin release *in vitro*

Monolayer cultures of HCs were incubated for 1 h (10°C) with the NADPH-oxidase inhibitor, DPI (2 µM final concentration) as described above (Chapter 4, Section 4.2.7), before addition of either LPS (0.1 µg mL^{-1} final concentration) or *L. anguillarum* (3×10^5 mL^{-1}) and incubation for 24 h (10°C) as above (Chapter 4, Section 4.2.7). Controls consisted of LPS or *L. anguillarum*-activated HCs minus DPI and HCs plus DPI. Chromatin release was detected and quantified as above (Chapter 4, Section 4.2.3).

5.2.5. Entrapment of *L. anguillarum* by extracellular chromatin traps *in vitro*

To investigate whether extracellular chromatin traps released from HCs were capable of ensnaring *L. anguillarum*, monolayer cultures of HCs were set up as described above (Chapter 4, Section 4.2.2). Next, HCs were treated with viable *L. anguillarum* at a final concentration of 3 x 10^4 mL^{-1} (lower concentration of bacteria to minimise bacterial clumping) and cultured for 24 h (10°C). After culture, HCs were stained with Sytox Green and extracellular chromatin release detected as described above (Chapter 4, Section 4.2.3).

Scanning electron microscopy was also used to visualise entrapped bacteria. Washed suspensions of 3 x 10^4 mL^{-1} viable *L. anguillarum* were added to monolayer cultures of HCs (3 x 10^4 mL^{-1}) set up on 10 mm diameter circular glass coverslips in the plate wells, and left for 24 h (10°C) to induce chromatin release (Chapter 4, Section 4.2.5). Controls received equal volumes of ML-15 only. HC monolayer cultures were then processed for scanning electron microscopy as above (Chapter 4, Section 4.2.5). The cells were examined using a Quanta™ 3D FEGFEI scanning electron microscope (FEI, Cambridge, UK).

5.2.6. Stimulation of extracellular chromatin release *in vivo*

To induce encapsulation *in vivo*, crabs received 100 µL injections of 20 µg mL^{-1} LPS (as above) in sterile filtered 3.2% NaCl, using the injection procedure described by Smith and Ratcliffe, (1980a). The dose represents a final concentration of ca. 0.1 µg mL^{-1} LPS within the haemocoel (for crabs with carapace widths between 60-90 mm and assuming a 20 mL total blood volume). The use of LPS mimics infection without the risk of pathology. Control crabs received 100 µL injections of sterile filtered 3.2% NaCl instead of LPS. Prior to injection, the area was swabbed with 96% ethanol. Briefly, injections were made into the unsclerotised membrane between the carapace and the last pereiopod using a 26G ⅜" needle and 1 mL syringe. Control and LPS injected crabs were kept separately in the aquarium in tanks (100 cm x 50 cm) containing aerated seawater (~32‰) at a temperature of 12 ± 2°C.

After 1, 3 or 24 h, control and LPS injected crabs were sacrificed by injection of 4 mL of 4% PFA in 2% NaCl using a 23G 1.25" sterile needle and a 5 mL syringe. The gills were excised from each crab as these organs are the primary site for the localisation and clearance of foreign material in the shore crab (Smith and Ratcliffe, 1980a). Gills from each timepoint were then fixed immediately with 20 mL fixative (4% PFA made up in 2% NaCl).

Gill tissue was processed at the Histology Unit of Queen's Medical Research Institute (Edinburgh University). Briefly, gills were embedded in paraffin wax and 4 µm thick sections were cut using a using a Leica RM2235 microtome (Leica Microsystems, Milton Keynes, UK). Gill sections on sterile glass slides were de-waxed by 2 x 5 min submersions in xylene then rehydrated through descending grades of ethanol (for 20 sec each), specifically 2x submersions in 100% ethanol then subsequent submersion in 95%, 80% and 70% ethanol respectively. The sections were then submerged in PBS until staining.

Haematoxylin and eosin (H and E) staining was used to visualize capsule formation and structure. The sections were first stained with haematoxylin (5 min) then washed in tap water. Next, they were submerged in acid/ethanol (0.3% HCl in 70% ethanol, pH 4.6) then washed as before. The sections were then submerged in Scott's tap water (23 mM $NaHCO_3$, 166 mM $MgSO_4$ dissolved in 5 L distilled water, pH 8) for 20-30 sec, washed in tap water then stained with eosin (5-10 sec) before a final wash in tap water. The sections were then dehydrated through ascending grades of ethanol (for 20 sec each), specifically submersions in 70%, 80%, 95% and 2x 100% ethanol respectively, then subjected to 2 x 5 min submersions in xylene. Lastly, 24 x 60 mm glass coverslips were mounted onto the slides using pertex mounting medium (Leica). The sections were then examined using a Zeiss Axioskop light microscope (Carl Zeiss Microscopy Ltd, Cambridge, UK) and images captured using QCapturePro software.

To visualise DNA, other gill sections were stained with 300 µL of 300 nM DAPI (Invitrogen) for 1 h at room temperature in a humid chamber (protected from light). Control sections were left unstained to assess levels of auto fluorescence emitted by gill tissue, and received 300 µL of PBS instead of DAPI. Following 3x 5 min washes in PBS, 24 x 60 mm glass coverslips (Leica Microsystems, Milton Keynes, UK) were mounted using ProLong Gold antifade mounting media (Invitrogen). After ca. 12 h, the sections were examined for DAPI stained extracellular chromatin (emission 461 nm, excitation 375 nm) using a Zeiss Axioskop 2 fluorescence microscope (Carl Zeiss Microscopy Ltd, Cambridge, UK) with QCapturePro software.

Immunohistochemistry was used to detect the presence of PXN and H2A in the haemocyte clumps. The gill sections were incubated for 30 min with 1 mg mL^{-1} sodium borohydride to reduce auto-fluorescence then received 3x5 min washes in PBS. Slides were then incubated for 1 h in blocking solution (3% BSA in PBS). Next, slides were incubated overnight at 4°C with primary antibodies diluted 1:200 in 3% BSA, specifically polyclonal rabbit anti-human MPO Ig (DAKO) or monoclonal mouse anti-H2A IgG1 (New England Biolabs) used to recognise PXN and H2A respectively, as described for immunocytochemistry (Chapter 4, Section 4.2.6.). Slides were then washed as before. Next, slides were incubated for 2 h (at room temperature) in the dark with fluorescently conjugated secondary antibodies diluted 1:300 in 3% BSA, specifically goat anti-rabbit Alexa Fluor 488 (Molecular Probes) (excitation 495 nm; emission 519 nm) to label PXN or goat anti-mouse Alexa Fluor 594 (Invitrogen) (excitation 590 nm; emission 617 nm) to label H2A, again as described for immunocytochemistry (Chapter 4, Section 4.2.6.). Slides were washed as before and further incubated for 1 h (at room temperature) in the dark with a final concentration of 5 µM TO-PRO-3 iodide (Invitrogen) (excitation 642 nm; emission 661 nm) to stain both extracellular and intracellular DNA. Lastly, slides were washed as above, submerged for 5 sec in millipore water, and then mounted with 24 x 60 mm coverslips using ProLong Gold antifade mounting media (Invitrogen). Slides were then examined using a DMIRE2 TCS2 confocal microscope (Leica Microsystems, Milton Keynes, UK). Controls to assess levels of auto-fluorescence and non-specific staining were carried out as previously described for immunocytochemistry (Chapter 4, Section 4.2.6.).

5.2.7. ETosis in encapsulation reactions *in vitro*

Additional *in vitro* experiments were performed using the NADPH-oxidase inhibitor DPI and DNAse-1. An *in vitro* approach was used because of the likely toxicity of these reagents *in vivo*. Haemolymph was removed from the crabs as above (Chapter 2, Section 2.2.3) and unseparated haemocytes diluted in MAC (1:1) were centrifuged (500 x g, 5 min, 4°C), resuspended in ML-15 (Chapter 2, Section 2.2.3), and adjusted to a final concentration of 1 x 10^6 mL^{-1}. Experimental samples received PMA (final concentration 0.1 µM) while controls received an equal volume of ML-15. Further suspension cultures were set up as above (Chapter 2, Section 2.2.4) in which haemocytes were pre-incubated with DPI (4 µM for 1 h) or DNAse-1 (200 U mL^{-1} for 15 min) at 10°C before the addition of PMA, as above. Higher concentrations of DPI and DNAse-1 were used in these experiments because of the greater number of haemocytes in the samples likely to undergo ETosis, compared to separated haemocyte cell types in culture. Controls received the same concentration of DPI or DNAse-1, but were given ML-15 instead of PMA.

All tubes were incubated at 10°C with 200 µL sub-samples (2 x 10^5 mL^{-1}) aspirated, after gentle mixing, at 1 h, 3 h or 24 h for cyto-centrifugation as described above (Chapter 2, Section 2.2.5.1). Two sets of slides were prepared for each timepoint and each treatment. One was air dried, fixed in absolute methanol, then subjected to Diff-Quik™ staining and mounted using DePeX before examination using a Zeiss Axioskop light microscope (Carl Zeiss Microscopy Ltd, Cambridge, UK). Images were captured using QCapturePro software. The second slide was fixed in 2.5% glutaraldehyde in 3.2% NaCl, washed 2x in PBS and stained with 1 µM Sytox Green (20 min). Extracellular chromatin was detected by confocal microscopy as described above (Chapter 4, Section 4.2.3). Clump size (μm^2 $x10^3$) and frequency, i.e. number per field of view (FoV) were calculated and quantified from representative Diff-Quik™ stained images (100x total mag). A clump was defined as a closely packed aggregation of 20 or more haemocytes. The image analysis software ImageJ™ was used to measure clump area and count clump numbers (from 6 comparable FoV). One crab was sampled per experiment.

5.2.8. Statistical analyses

All values were calculated as mean ± SEM. Percentage values were arc sine transformed and haemocyte clump size (area in μm^2 $x10^3$) or haemocyte clump frequency (number per FoV) values log transformed before statistical analysis. Statistical differences were then determined as described in Chapter 2 (Section 2.2.7). Significance was accepted at $P<0.05$.

5.3. Results

5.3.1. Extracellular chromatin release from other haemocyte types

Of the three other haemocyte types in *C. maenas*, only the SGCs exhibited extracellular chromatin release (0.1 µM PMA, 24 h) in a similar fashion to HCs (Figure 5.1 and Figure 5.2, A, B). Chromatin extrusion was not observed from either the GCs or the ProHs (Figure 5.1 and Figure 5.2, C, D). Compared to the GCs and ProHs, significantly more cells extruded chromatin ($P<0.001$; n=3) in the SGC population (50.8% ± 3.8% SEM) (Figure 5.1), with <5% in control SGCs. Cyto-centrifuge preparations revealed that released chromatin from SGCs tended to form diffuse 'puff-ball'-like shapes (Figure 5.2, F) rather than the spread 'comet'-like strands of chromatin commonly observed from HCs (Figure 5.2, E).

Figure 5.1.

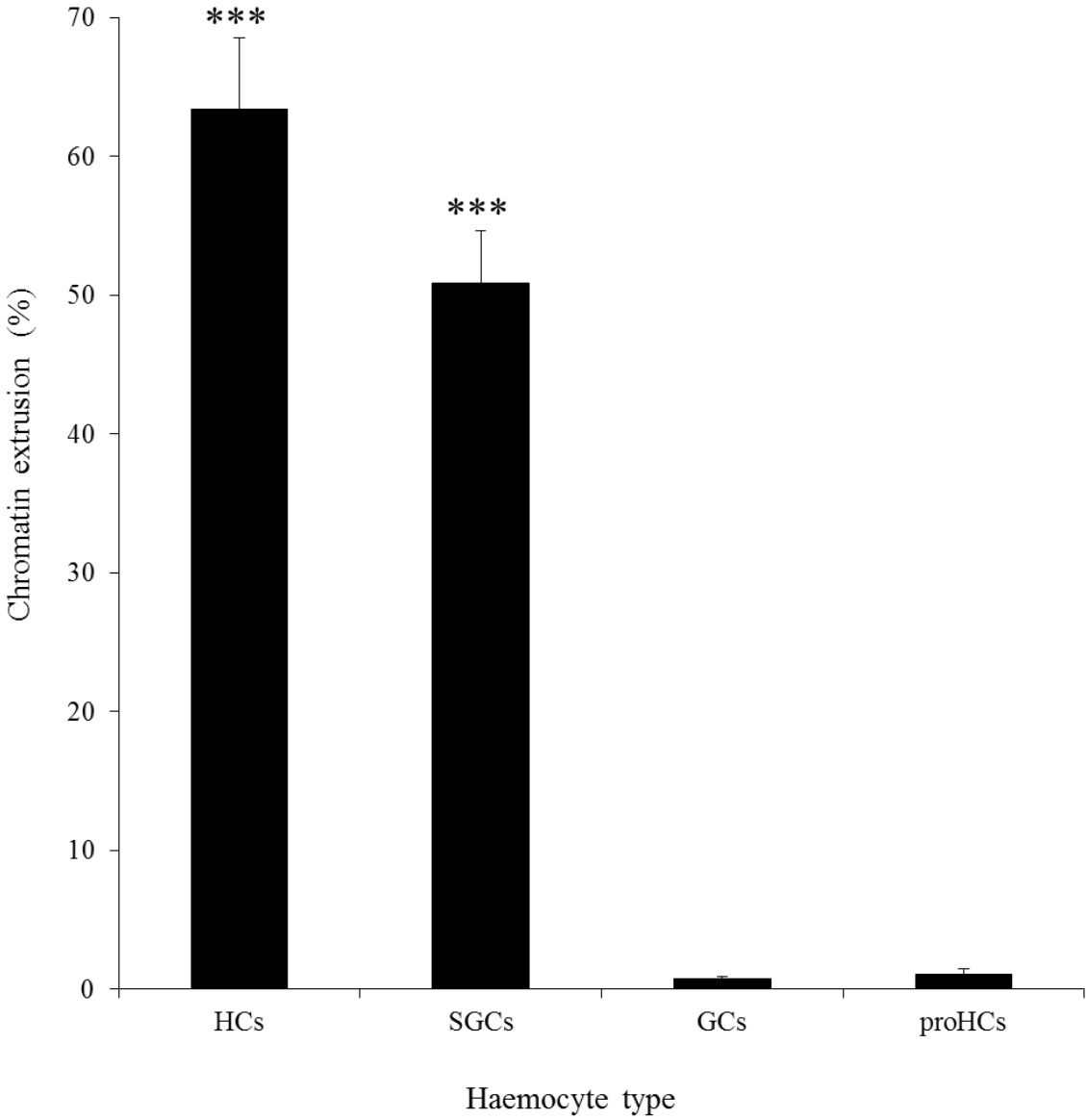

Figure 5.1. Rates of chromatin extrusion *in vitro* in different haemocyte types after PMA treatment. Percentage of chromatin extruding HCs, SGCs, GCs and ProHs after 24 h culture (10°C) with 0.1 µM PMA. Data expressed as means ± SEM, n=5 (HCs) or n=3 (all other haemocyte types), with a different crab used on each occasion. Data for HCs from Chapter 4, Figure 4.3. Statistical analysis was performed upon arc sine transformed data using one-way ANOVA with a Student Newman-Keuls multiple comparison *post hoc* test. *** $P<0.001$ *vs.* chromatin extruding GCs or ProHs.

Figure 5.2.

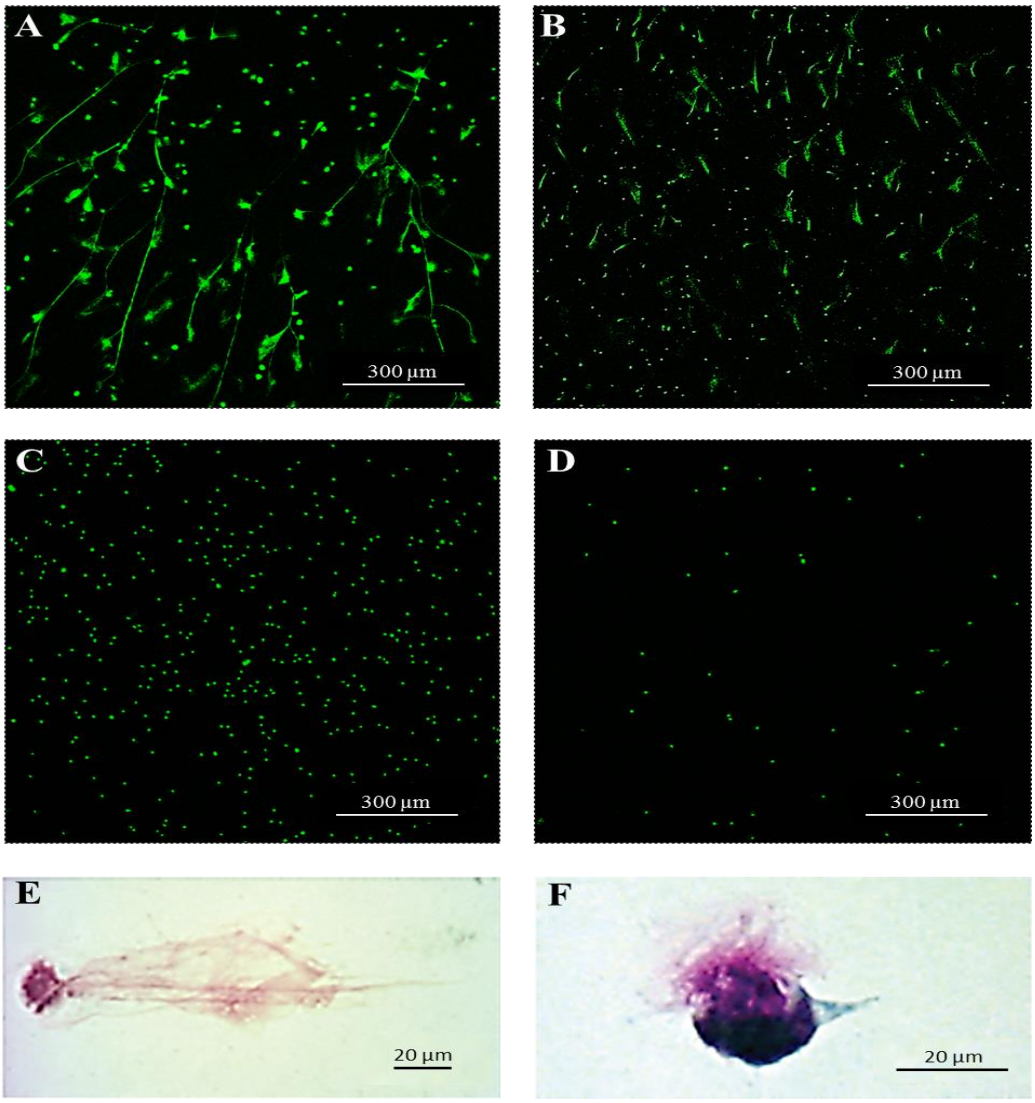

Figure 5.2. Morphological examination of extracellular chromatin release *in vitro* in different haemocyte type of *C. maenas*. (**A-D**): Representative confocal images of Sytox Green stained HCs (**A**), SGCs (**B**), GCs (**C**) and ProHs (**D**) after 24 h culture with 0.1 µM PMA. Note that there is better survival of ProHs (**D**) than all other haemocyte types, whereas GCs show the poorest survival as revealed by the large number of positively stained non-chromatin extruding nuclei (**C**). Images representative of n=5 (HCs) or n=3 experiments (all other haemocyte types). Scale bars = 300 µm. (**E-F**): Diff-Quik™ stained cyto-centrifuge preparations showing spread 'comet-like' extracellular release of nuclear material from a HC (**E**) and diffuse 'puff-ball-like' nuclear release from a SGC (**F**) after 24 h suspension culture with 0.1 µM PMA. Images captured at 1000x total mag, scale bars = 20 µm (images **E** and **F** courtesy of Dr Valerie J. Smith, St Andrews University).

5.3.2. ETosis following stimulation with LPS or *L. anguillarum*

Significantly higher rates ($P<0.001$; n=3) of ETosis were recorded from HCs after 24 h culture with *L. anguillarum* (33.6% ± 1.8% SEM) and LPS (31.5% ± 4.2% SEM) (Figure 5.3, A- C) compared with control values (<5%). These values are lower than those observed with PMA over the same culturing time (63.4% ± 5.1% SEM), but confirm that the process occurs after exposure of HCs to non-self agents. Crucially, after 24 h, no chromatin extrusion was observed from crab HCs which had been incubated with the NADPH oxidase inhibitor DPI prior to treatment with *L. anguillarum* or LPS (Figure 5.3, A, D, E). A significant reduction ($P<0.001$; n=3) in chromatin extrusion was observed from HCs treated with *L. anguillarum* + DPI (1.5% ± 0.7% SEM) and LPS + DPI (0.4% ± 0.2% SEM) (Figure 5.3, A). Representative confocal images of these treatments showed little evidence of chromatin release (Figure 5.3, D, E).

The bacteria became closely associated with the chromatin strands (Figure 5.4, A, B) in a similar way to the entrapment of bacteria by ETotic neutrophils (Fuchs *et al*., 2007). As the HCs and bacteria were stained with the vital DNA stain Sytox Green, viable cells could be distinguished from dead ones or those with extruded chromatin. Bacteria trapped on the extruded chromatin are dead, as evidenced by Sytox Green staining (Figure 5.4, A). The dark grey dots in the background of the phase contrast image (Figure 5.4, B) are definitely bacteria, and are clearly much more numerous than Sytox Green stained bacteria in the corresponding confocal fluorescence image (Figure 5.4, A). Therefore, only a relatively small proportion of non-entrapped bacteria are dead and the majority of bacteria not ensnared by the extracellular chromatin were still viable. Scanning electron microscopy further confirmed the efficient entrapment of bacteria by extracellular chromatin released from HCs (Figure 5.4, C, D).

Figure 5.3.

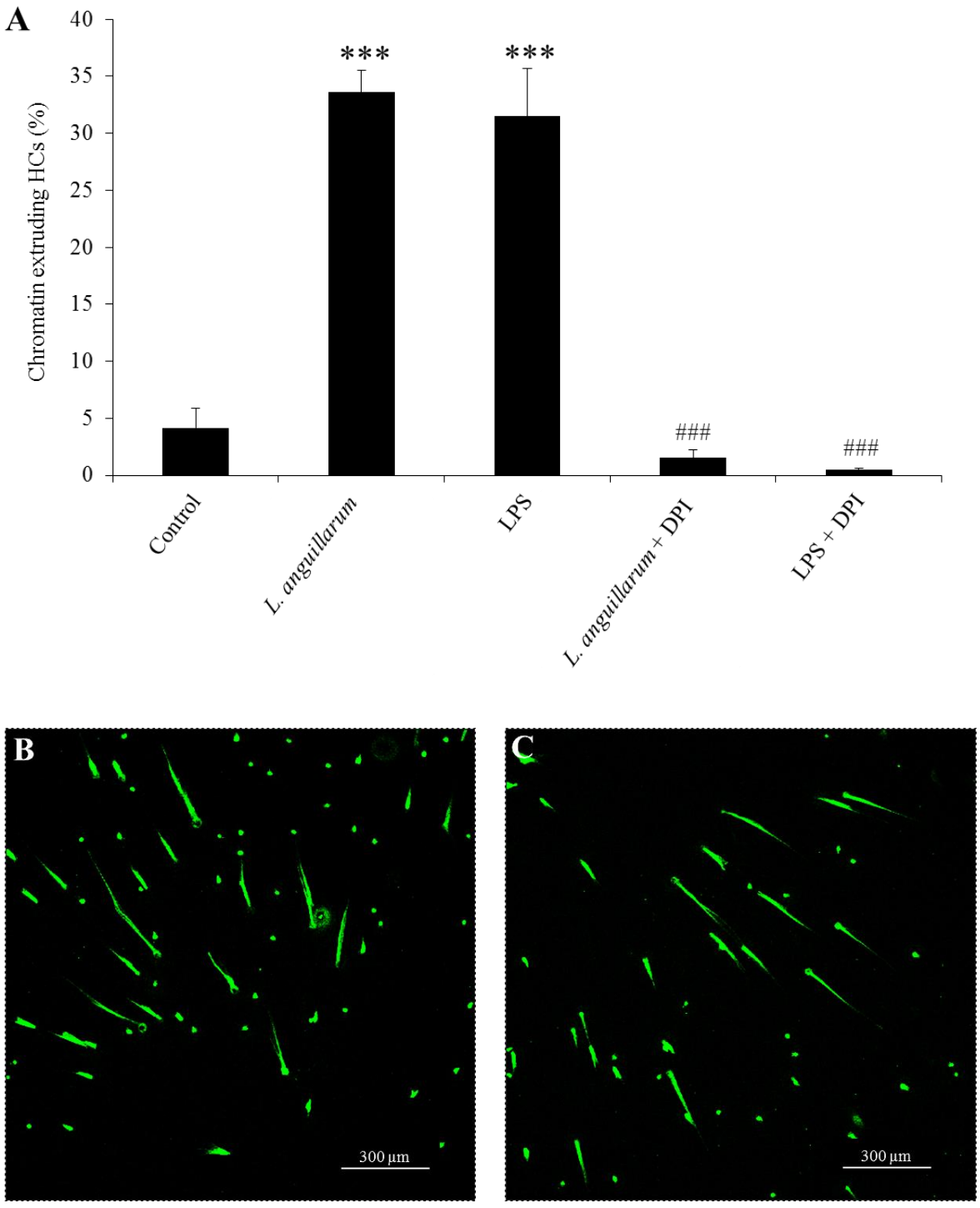
A
Chromatin extruding HCs (%)
40
35
30
25
20
15
10
5
0
***
***
###
###
Control
L. anguillarum
LPS
L. anguillarum + DPI
LPS + DPI
B
300 µm
C
300 µm

Figure 5.3 continued.

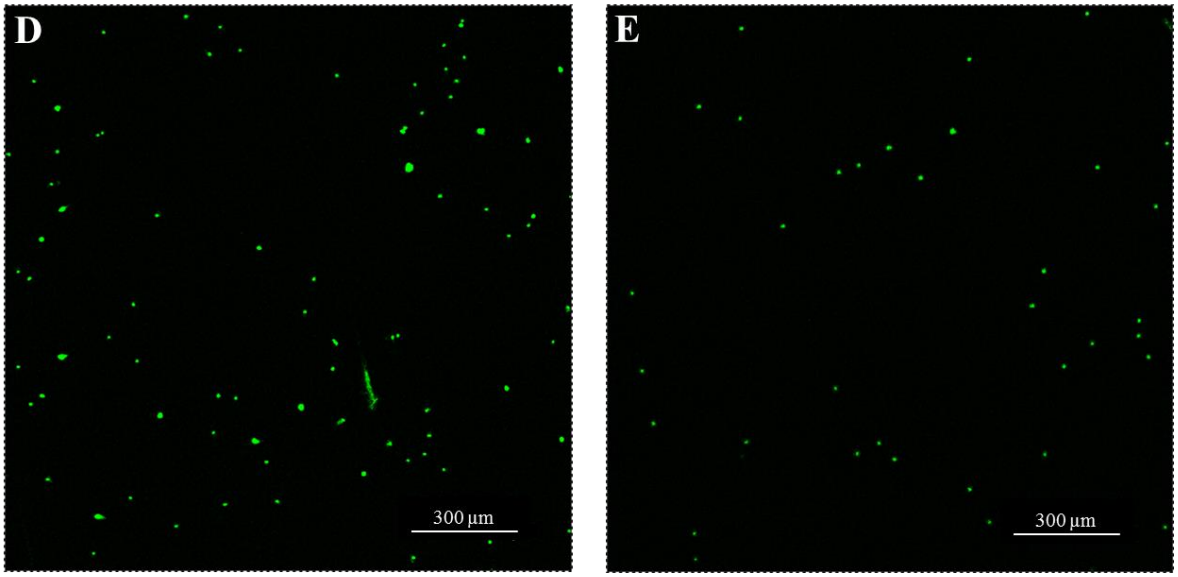

Figure 5.3. Stimulation/inhibition of chromatin extrusion in HCs *in vitro*.
(**A**): Percentage of chromatin extruding HCs after 24 h culture (10°C) with 3 x 10^5 mL^{-1} viable *L. anguillarum* or 0.1 µg mL^{-1} LPS, all ± 2 µM DPI. Data expressed as means ± SEM, n=5 (control) or n=3 (all other treatments), with a different crab used on each occasion**.** Data for control (untreated) HCs from Chapter 4, Figure 4.3. Statistical analysis was performed upon arc sine transformed data using one-way ANOVA with a Student Newman-Keuls multiple comparison *post hoc* test. *** $P<0.001$ *vs*. control (untreated) HCs; ### $P<0.001$ *vs.* matching treatment without DPI. (**B-E**): Representative confocal images of Sytox Green stained HCs after 24 h culture. (**B-C**): HCs exhibit typical spread 'comet-like' extracellular chromatin release after treatment with *L. anguillarum* (**B**) or LPS (**C**); (**D-E**): Inhibition of extracellular chromatin release from HCs cultured in the presence of *L. anguillarum* + DPI (**D**) and LPS + DPI (**E**). Images representative of n=3 experiments. Scale bars = 300 µm.

Figure 5.4.

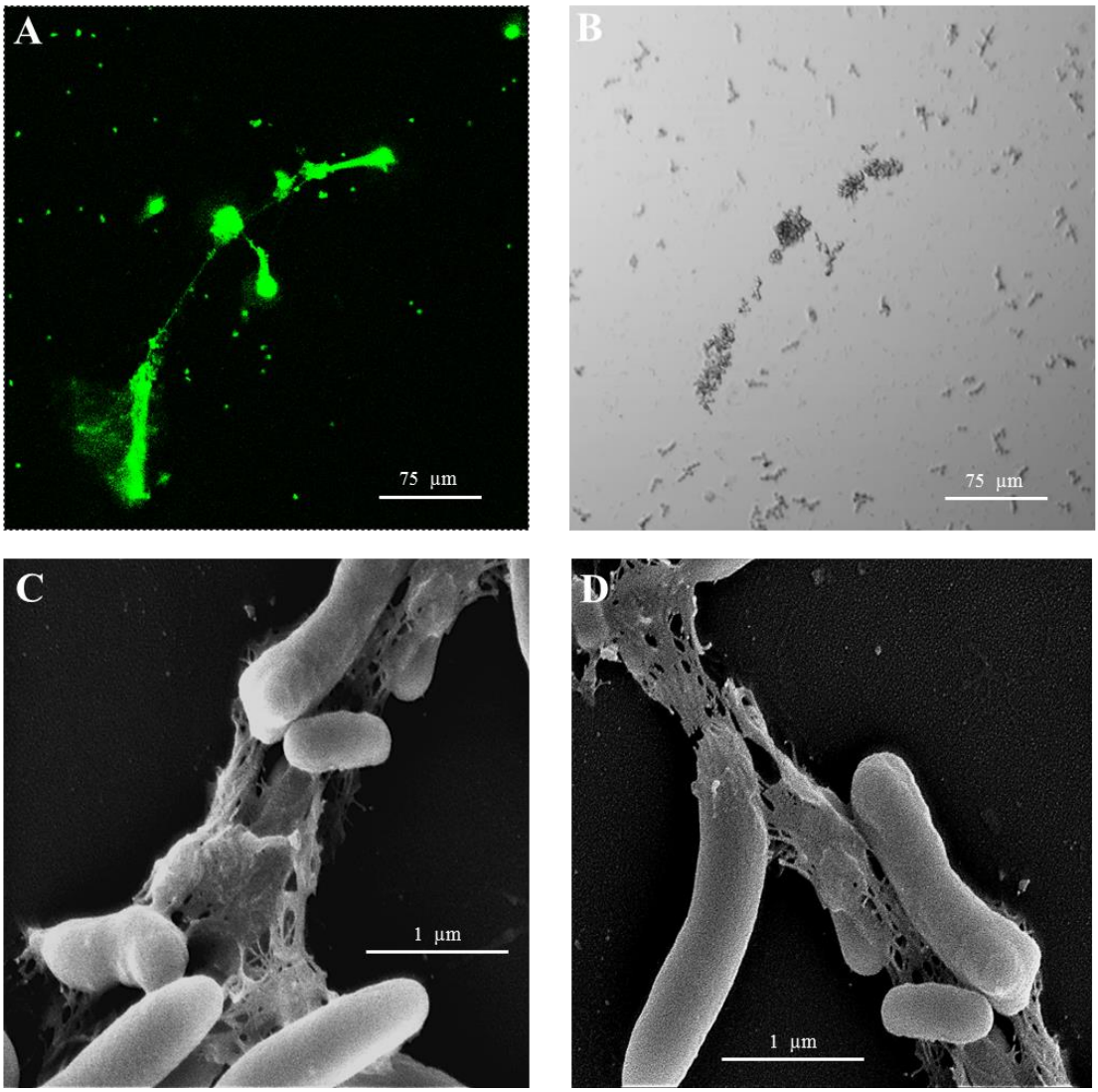

Figure 5.4. Extracellular chromatin released from HCs successfully traps bacteria *in vitro*. Trapped bacteria in extracellular chromatin traps released from HCs after 24 h culture (10°C) with 3 x 10^4 mL^{-1} viable *L. anguillarum*. (**A-B**): Confocal images of the same field of view showing successful ensnarement of *L. anguillarum* along strands of extracellular chromatin released from HCs, scale bars = 75 µm. (**A**): Sytox Green stained extracellular chromatin release. Background stained small dots are bacteria. (**B**): Phase contrast transmission image of the same field of view showing bacterial aggregation at the same localities as extracellular chromatin release (refer to **A)**. (**C and D**): Scanning electron microscopy of *L. anguillarum* caught in extracellular chromatin traps released from HCs, scale bars = 1 µm.

5.3.3. Participation of ETosis in encapsulation reactions *in vivo*

Haematoxylin and eosin staining confirmed that within 24 h post LPS injection, haemocyte capsules develop and lodge within the gill lamellae (Figure 5.5, A-D) in a similar way to that reported with bacteria (Smith and Ratcliffe, 1980a) or β-1,3-glucans (Smith *et al*., 1984). DAPI staining further revealed that ETotic haemocytes are present in the blood 1 h post LPS injection (Figure 5.5, E). By 3 h post LPS injection, the haemocytes are aggregated into loose clumps clearly associated with extracellular chromatin (Figure 5.5, F, I), and at 24 h, extracellular chromatin is conspicuously suffused throughout the core of fully formed haemocyte clumps (Figure 5.5, G, J), which are granuloma-like in appearance (Figure 5.5, C, G, J). In control crabs, there was no clump formation following saline injection (Figure 5.5, D), nor was any extracellular chromatin evident (Figure 5.5, H). Epibionts were evident on the external (seawater) surface of the lower lamella surface (Figure 5.5, H, arrow). In unstained gill sections, only the outer lining of the gill lamellae auto-fluoresced at the DAPI emission wavelength (Appendix 8, A, B).

Immunohistochemistry confirmed that a protein recognised by an anti-human MPO antibody is discernible within haemocyte clumps 3 h post injection of LPS (Figure 5.6, G-I). This protein is likely to be the MPO homologue PXN and was located mainly in the outer regions and interspersed between intact cells (Figure 5.6, I). Extracellular H2A is also present and co-localises with extracellular DNA within the haemocyte clumps 3 h post injection of LPS (Figure 5.6, J-L). These proteins appear to have been released from the haemocytes prior to cell clumping as at 1 h post LPS injection, extracellular PXN and H2A were visible within the lumen of the gill lamellae (Figure 5.6, A-F), with H2A, at this time, often co-localised with DNA (Figure 5.6, F). Neither PXN nor H2A were seen extracellular to the haemocytes or the gill tissue of control crabs 1 or 3 h post injection of saline. By 24 h, the haemocyte clumps were so densely compacted that visualisation of individual elements was no longer possible. Auto-fluorescence was observed on the outer gill lining, as confirmed from unstained control sections (Appendix 9, A-C). Apart from auto-fluorescence, no non-specific staining was observed in control sections (Appendix 9, D-F).

Figure 5.5.

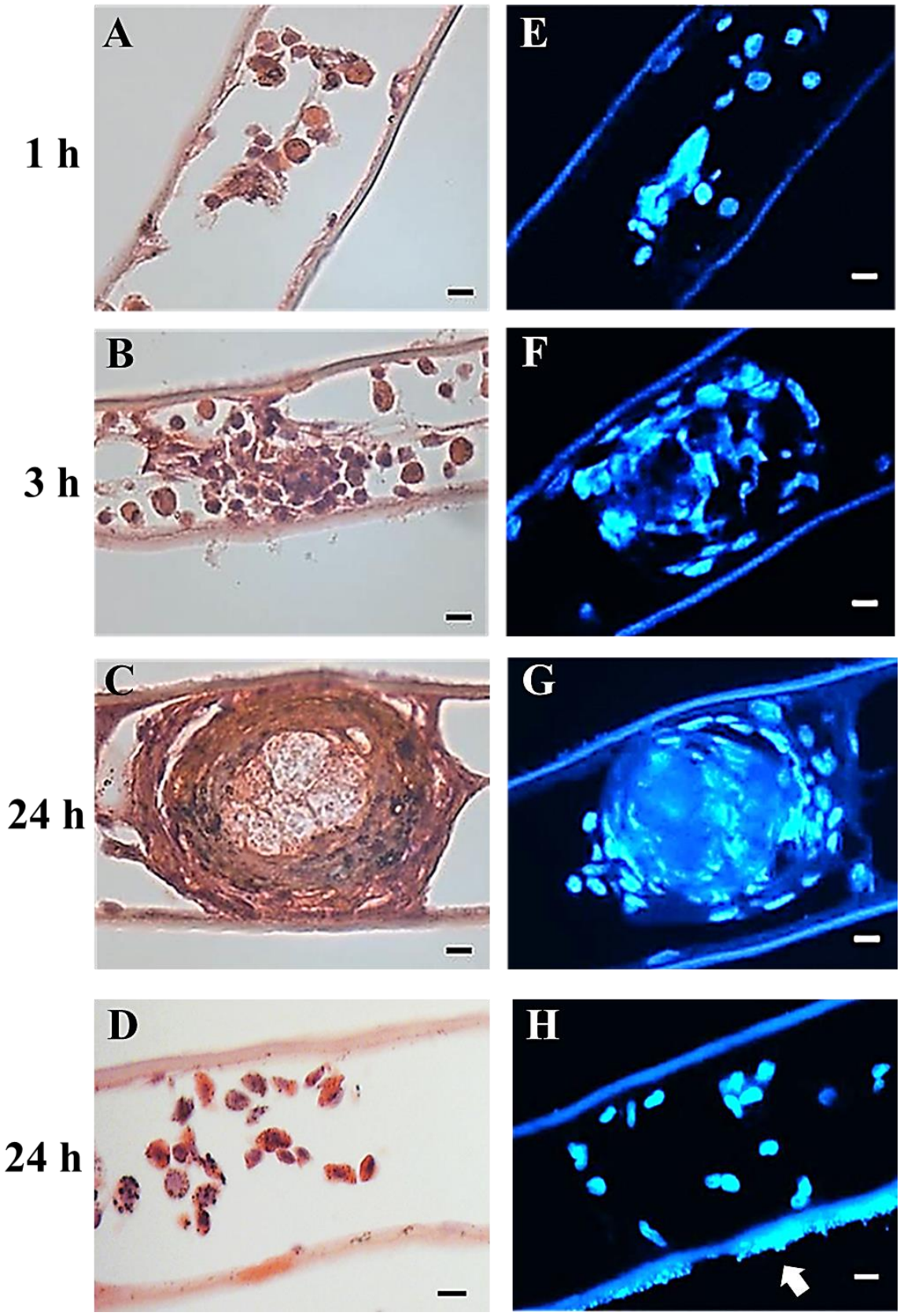

Figure 5.5 continued.

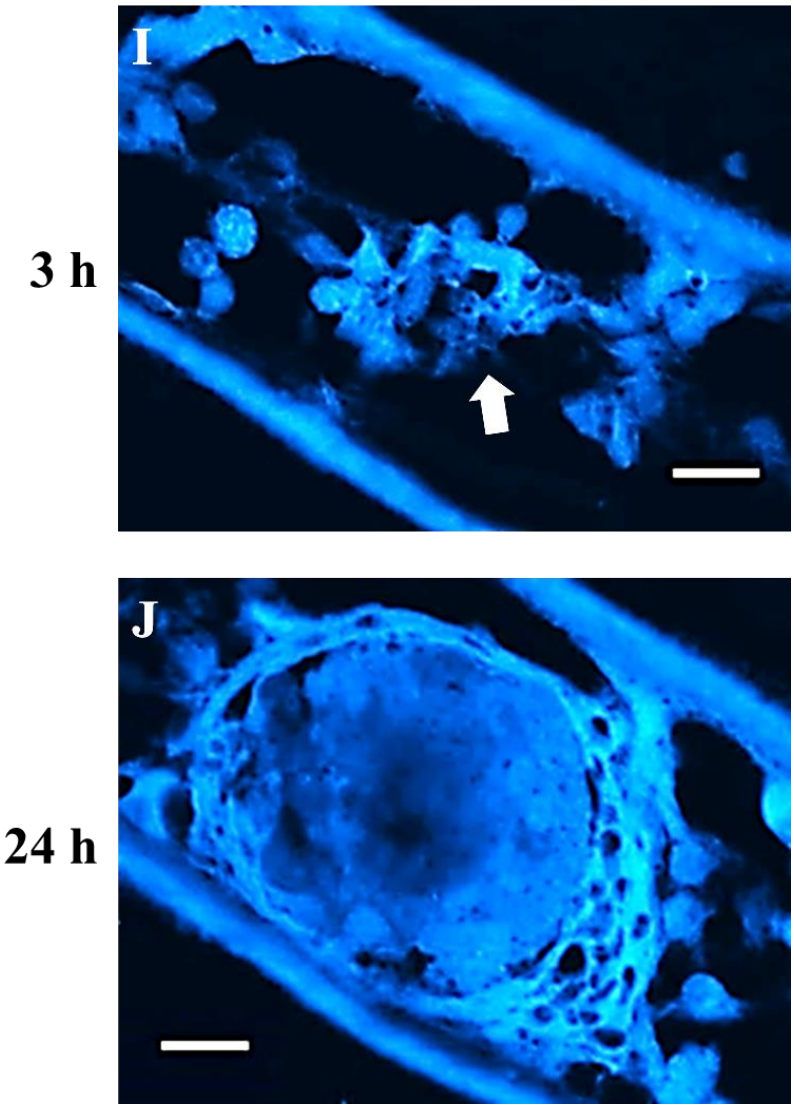

Figure 5.5. ***In vivo*** **demonstration of extracellular chromatin release and association of extracellular chromatin with haemocyte capsules.** Paraffin wax sections of gill lamellae stained with haematoxylin and eosin (**A-D**) or DAPI (**E-H**) at 1, 3 or 24 h post injection of 20 µg mL^{-1} LPS or saline (control). 1 h post LPS injection (**A** & **E**); 3h post LPS injection (**B** & **F**): 24 h post LPS injection (**C** & **G**); 24 h post saline injection (**D** & **H**): Epibionts are evident on the external (seawater) surface of the lower lamella surface (**H**, arrow). Neither haemocyte clumping, nor evidence of extracellular chromatin/basophilic material, are apparent. (**I-J**): High magnification of DAPI stained extracellular chromatin during early capsule development at 3 h (**I**, arrow) and a fully formed capsule at 24 h (**J**) post LPS injection. Images captured at 400x total mag (**A-H**) or 1000x total mag (**I-J**), all scale bars = 20 µm.

Figure 5.6.

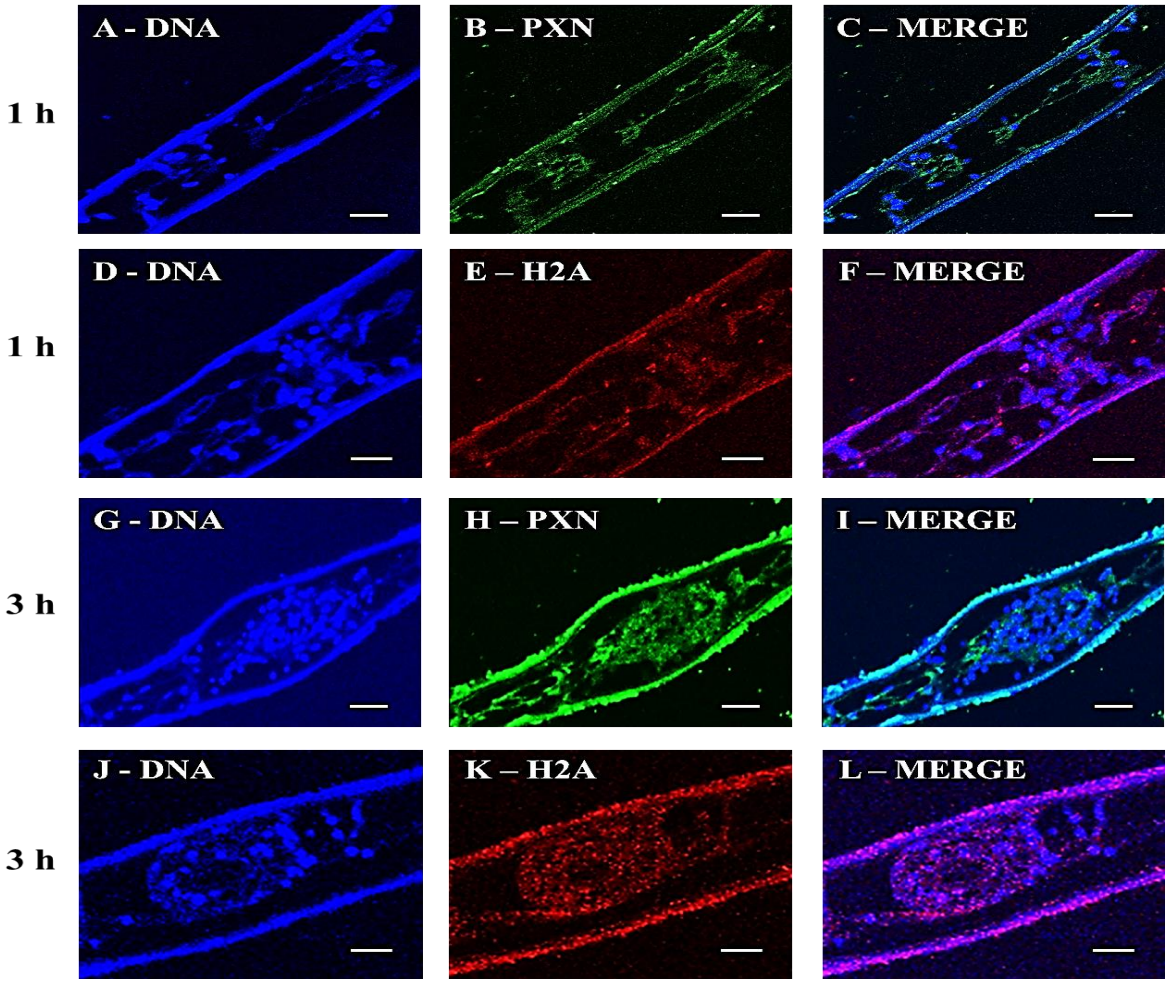

Figure 5.6. ***In vivo*** **ETosis: Immunohistochemical analysis revealing the distribution of DNA, PXN and H2A during the early stages of encapsulation.** Paraffin wax sections of gill lamellae excised from crabs 1 h and 3 h post injection of 20 µg mL^{-1} LPS. To-PRO-3 iodide was used to stain intra-cellular and extracellular DNA, PXN visualised with rabbit anti-human MPO antibody and H2A visualised with mouse anti-H2A antibody. (**A-F**): Early haemocyte clumps formed at 1 h post LPS injection at different regions of the gill. (**A**) DNA; (**B**): PXN; (**C**): Merge of images **A** and **B**. (**D**): DNA; (**E**): H2A; (**F**): Merge of images **D** and **E** showing that there is some co-localisation of H2A with some extracellular DNA (magenta) during early haemocyte clump formation. (**G-L**): Haemocyte clumps formed at 3 h post LPS treatment at different regions of the gill. (**G**): DNA; (**H**): PXN; (**I**): Merge of images **G** and **H**, note the mostly extracellular location of PXN (**I**). (**J**): DNA; (**K**): H2A; (**L**): Merge of images **J** and **K**, in places H2A can be seen co-localising with intra- and extra-cellular DNA (magenta) within the mid-formed haemocyte clump (**L**). Scale bars = 20 µm.

5.3.4. ETosis in encapsulation reactions *in vitro*

Diff-Quik™ stained cyto-centrifuge preparations revealed that distinct haemocyte clumps developed over 24 h in the presence of PMA (0.1 µM), (Figure 5.7, A-D). At 1 h, the haemocyte clumps were loose, varied in size and were few in number (Figure 5.7, A and Figure 5.8, A, B). However, Sytox Green staining did reveal ETotic haemocytes were present within these loose aggregations (Figure 5.7, E). By 3 h, the haemocyte clumps were more developed (Figure 5.7, B) and significantly more numerous ($P<0.001$; n=3) compared to the number of clumps observed at 1 h (Figure 5.8, B), with extracellular chromatin evident within and around the structures when stained with Sytox Green (Figure 5.7, F). By 24 h, the haemocyte clumps were substantially larger, but significantly less numerous ($P<0.001$; n=3) compared with the number of haemocyte clumps obtained at 3 h (Figure 5.8, B). At 24 h, haemocyte clumps contained high numbers of heavily compacted haemocytes (Figure 5.7, C, D, G, H), most probably arising from coalescence of smaller clumps. Certainly long strings of haemocytes were seen attaching to some of the extracellular complexes (Figure 5.7, G, H) and strands of basophilic material emanating between the attaching and aggregating haemocytes were also visible (Figure 5.7, D). This material is likely to be of nuclear origin as similar strands were also discernable on Sytox Green stained cyto-centrifuge preparations at the 24 h timepoint (Figure 5.7, H).

Importantly, inclusion of DPI or DNAse-1 in the PMA-stimulated mixed haemocyte cultures substantially affected the formation of haemocyte clumps (Figure 5.8, A, B and Figure 5.9, A-F). At 1 h, haemocyte clumps were too few in number and variable in size to assess statistically the impact of these reagents. However, in mixed haemocyte cultures treated with DNAse-1, significantly smaller and fewer ($P<0.001$; n=3) haemocyte clumps were observed at 3 h compared to PMA-only treated haemocytes (Figure 5.8, A, B). Those haemocyte clumps that did form in the presence of DNAse-1 at 3 h were loosely packed and contained very few stands of basophilic material (Figure 5.9, A). At 24 h, significantly smaller ($P<0.001$; n=3) haemocyte associations formed in DNAse-1 treated haemocytes compared to PMA-only treated haemocytes (Figure 5.8, A). At this timepoint it was clear that DNAse-1 treated haemocyte clumps lacked

cohesiveness (Figure 5.9, B) and displayed little evidence of association with Sytox Green stained extracellular chromatin (Figure 5.9, C).

Similar trends were observed in mixed haemocytes cultured with DPI. Compared to PMA-only treated mixed haemocyte cultures at 3 h, the clumps were significantly smaller and fewer in number ($P<0.05$; n=3) in the presence of DPI (Figure 5.8, A, B). At 3 h, haemocyte clumps formed in the presence of DPI contained little evidence of extracellular basophilic material (Figure 5.9, D), similar to those observed in the presence of DNAse-1 at the same timepoint (Figure 5.9, A). Compared to PMA-only treated haemocyte cultures at 24 h, clumps were also significantly smaller ($P<0.001$; n=3) in the presence of DPI (Figure 5.8, A) and significantly fewer ($P<0.05$; n=3) in number (Figure 5.8, B). Neither DPI nor DNAse-1 stimulated haemocyte clumping on their own. However, after 24 h, DPI-treated mixed haemocyte cultures tended to show more evidence of degranulation from SGCs and GCs (Figure 5.9, E, arrows) than mixed haemocyte cultures not exposed to this agent. Crucially, after 24 h there was a distinct lack of Sytox Green stained extracellular chromatin in haemocyte cultures treated with DPI (Figure 5.9, F).

Without these reagents, significantly high percentages ($P<0.001$; n=3) of viable washed mixed haemocytes remained after 24 h suspension culture (80.2% ± 2.4% SEM), compared to the total percentage of intact dead cells at the same timepoint, as determined from flow cytometry analysis (Figure 5.10, A). Furthermore, after 24 h, mixed haemocytes remained un-clotted (Figure 5.10, B) with no evidence of Sytox Green stained extracellular material (Figure 5.10, C). Overall, these results clearly show that over a 24 h time period, extracellular chromatin released from crab haemocytes is involved in the initiation and development of haemocyte clumps during encapsulation.

Figure 5.7.

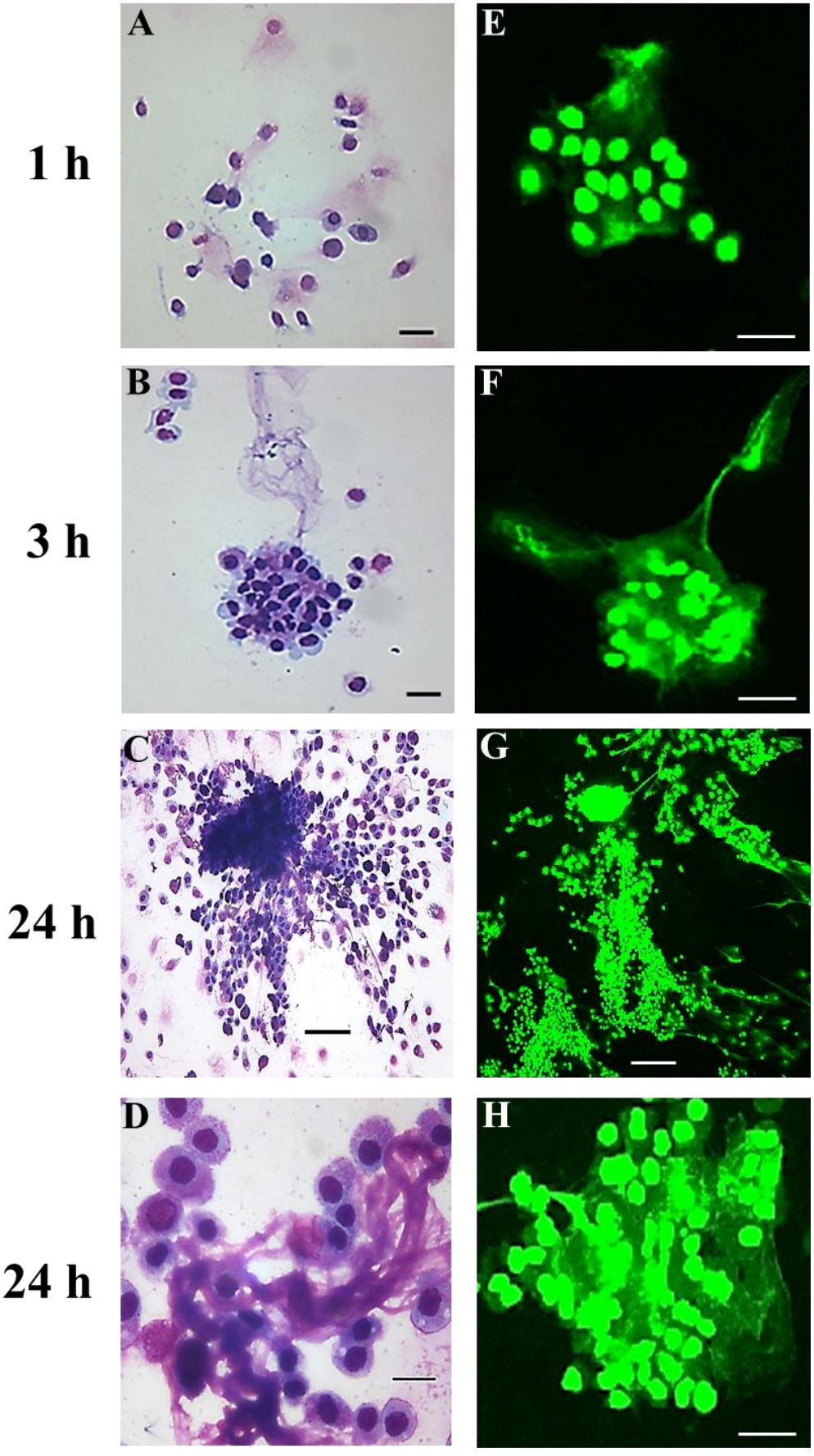

Figure 5.7. ETosis in encapsulation reactions *in vitro*. Suspension cultures of mixed haemocytes were treated with 0.1 µM PMA and cultured for 1, 3 and 24 h (10°C). (**A-D**): Cyto-centrifuge preparations of mixed haemocytes stained with Diff-Quik™ after 1 h (**A**), 3 h (**B**) and 24 h (**C** and **D**), where detail of a clump showing extruded material permeating intact haemocytes (**D**). (**E-H**): Cyto-centrifuge preparations of mixed haemocytes stained with Sytox Green). (**E**): ETosis in a small clump can be seen after 1 h; (**F**): Clump showing intact haemocytes entrapped by extracellular chromatin after 3 h; (**G**): Large haemocyte clumps showing strands of extracellular chromatin after 24 h; (**H**): Detail of a haemocyte clump at a different region after 24 h. The extracellular chromatin is suffused throughout the haemocyte matrix (**H**). Scale bars = 20 µm (**A, B, D**), 50 µm (**E, F, H**) or 100 µm (**C** and **G**). Images representative of n=3 experiments.

Figure 5.8.

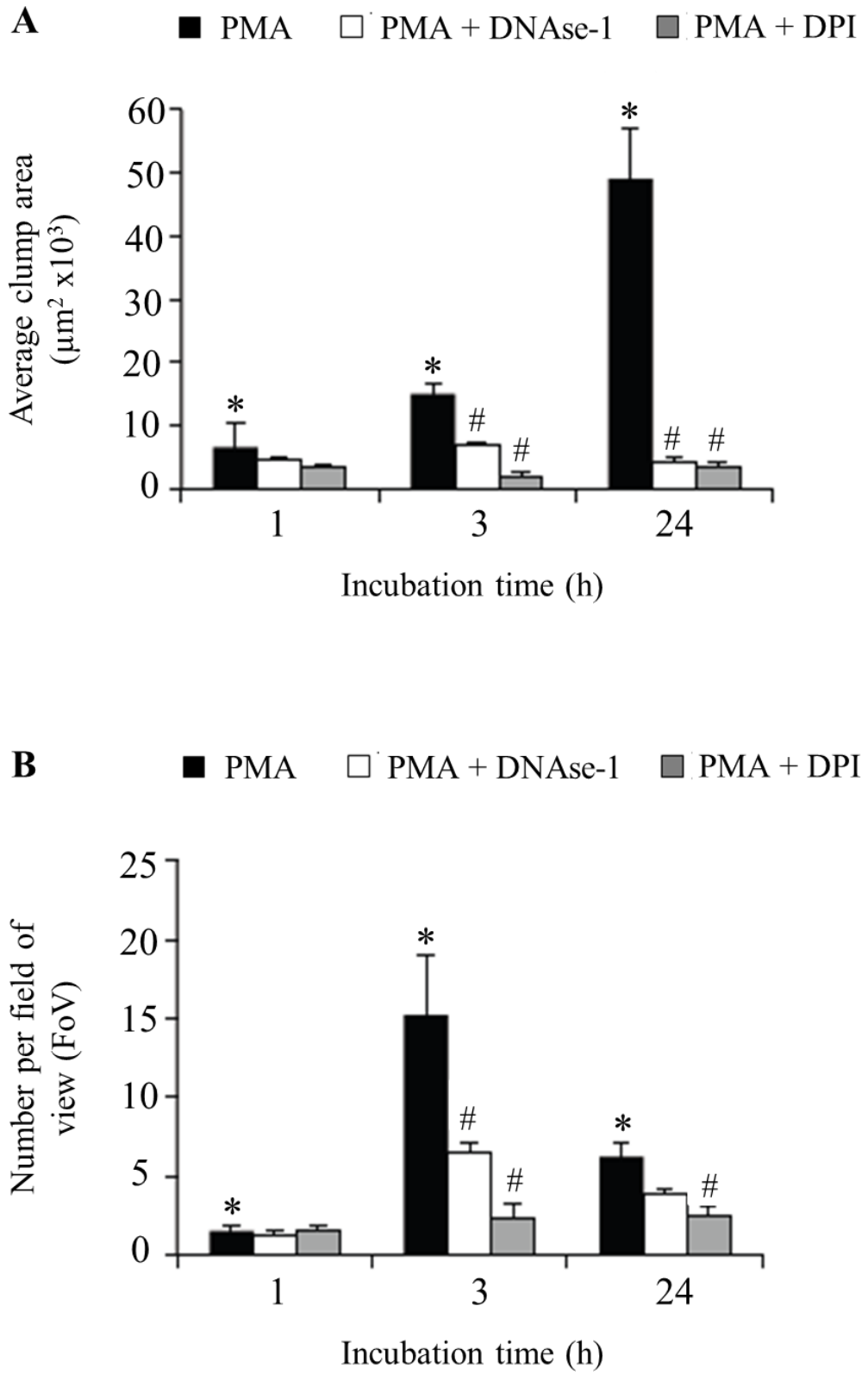
A
PMA
PMA + DNAse-1
PMA + DPI
Average clump area (µm² x10³)
60
50
40
30
20
10
0
*
*
*
#
#
#
#
1
3
24
Incubation time (h)
B
PMA
PMA + DNAse-1
PMA + DPI
Number per field of view (FoV)
25
20
15
10
5
0
*
*
*
#
#
#
1
3
24
Incubation time (h)

Figure 5.8. Quantification of haemocyte clump size and frequency during suspension culture *in vitro*. Haemocytes were treated with 0.1 µM PMA, 0.1 µM PMA + 200 U mL^{-1} DNAse-1 or 0.1 µM PMA + 4 µM DPI and cultured for 1, 3 and 24 h (10°C). (**A-B**): Quantification of mixed haemocyte clump size and frequency. All values are expressed as mean ± SEM, and the experiment repeated three times in total with a different crab used on each occasion. Values are mean ± SEM of one representative experiment from the three independent experiments. Statistical analysis was performed upon log transformed data using one-way ANOVA with a Student Newman-Keuls multiple comparison *post hoc* test. There were insufficient clumps at 1 h for statistical analysis. Significant differences between PMA-only treatments over time denoted by *. Significant differences between PMA-only and PMA + DNAse-1 or PMA + DPI within a single time-point denoted by #. (**A**): Clump size measured as area in $\mu m^2 \times 10^3$, n=6-52 clumps. PMA 1 h vs PMA 24 h = $P<0.01$; PMA 3 h vs PMA 24 h and PMA vs PMA + DNAse-1 both = $P<0.001$; PMA vs PMA + DPI = $P<0.05$. (**B**): Number of haemocyte clumps per FoV, n=6 FoV. PMA 1 h vs PMA 24 h = $P<0.01$; PMA 1 h vs PMA 3 h and PMA 3 h vs PMA 24 h = $P<0.001$; PMA vs PMA + DNAse-1 = $P<0.001$; PMA vs PMA+DPI = $P<0.05$. Data collation, figure production and statistical analysis courtesy of Dr Elisabeth A. Dyrynda (Heriot Watt University).

Figure 5.9.

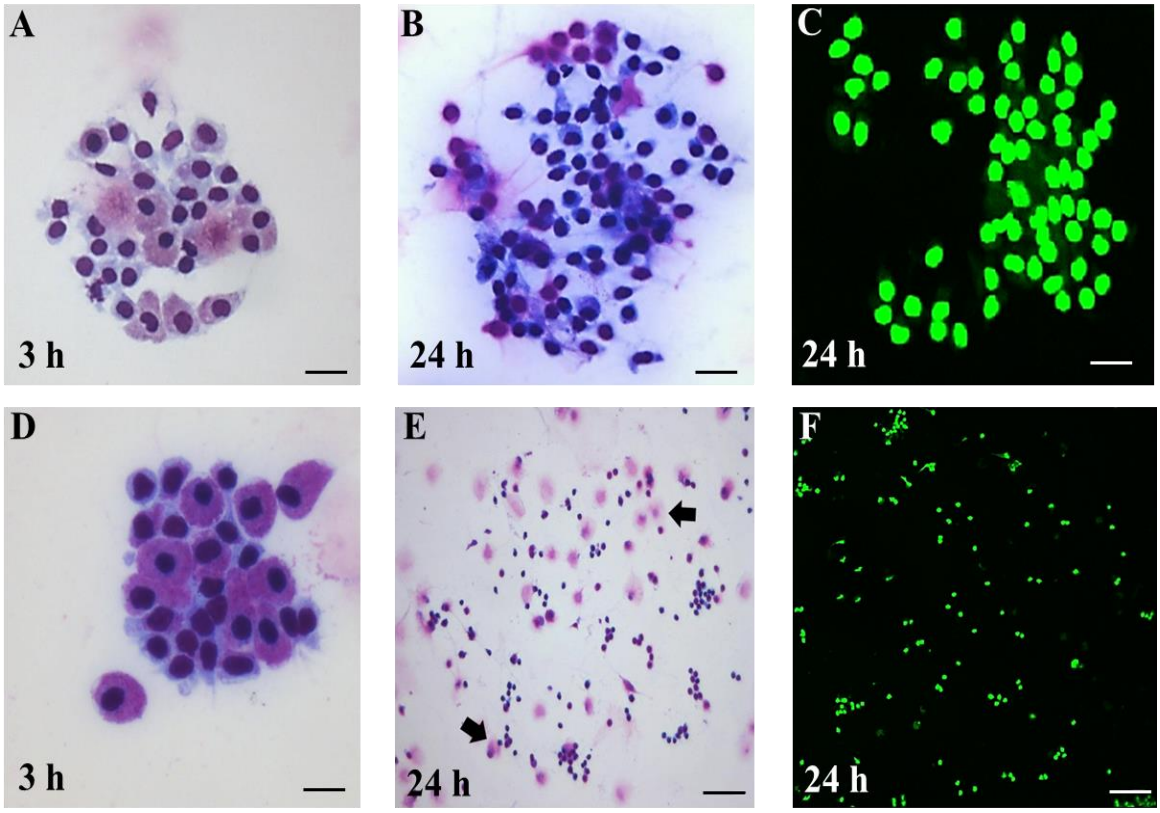

Figure 5.9. Impairment of extracellular chromatin release affects the formation of haemocyte clumps during suspension culture *in vitro*. (**A-C**): Cyto-centrifuge preparations of mixed haemocytes treated with 0.1 µM PMA + 200 U mL^{-1} DNAse-1. (**A-B**): Diff-Quik™ stained cyto-centrifuge preparations. (**A**): A small loose haemocyte clump at 3 h. Compare with Figure 5.7, images **B** and **F**. (**B**): Haemocyte clump at 24 h. Compare with Figure 5.7, images **C** and **D**. (**C**): Sytox Green stained haemocyte clump at 24 h, note the distinct lack of extracellular chromatin. Compare with Figure 5.7, images **G** and **H**. (**D-F**): Cyto-centrifuge preparations of mixed haemocytes treated with 0.1 µM PMA + 4 µM DPI. (**D-E**): Diff-Quik™ stained cyto-centrifuge preparations. (**D**): Small haemocyte clump at 3 h. Compare with Figure 5.7, images **B** and **F.** (**E**): 24 h, arrows indicate degranulated haemocytes. Compare with Figure 5.7, image **C**. (**F**): Sytox Green stained haemocytes at 24 h. Compare with Figure 5.7, images **G** and **H**. Images representative of n=3 experiments, scale bars = 20 µm (**A-D**) or 200 µm (**E** and **F**).

Figure 5.10.

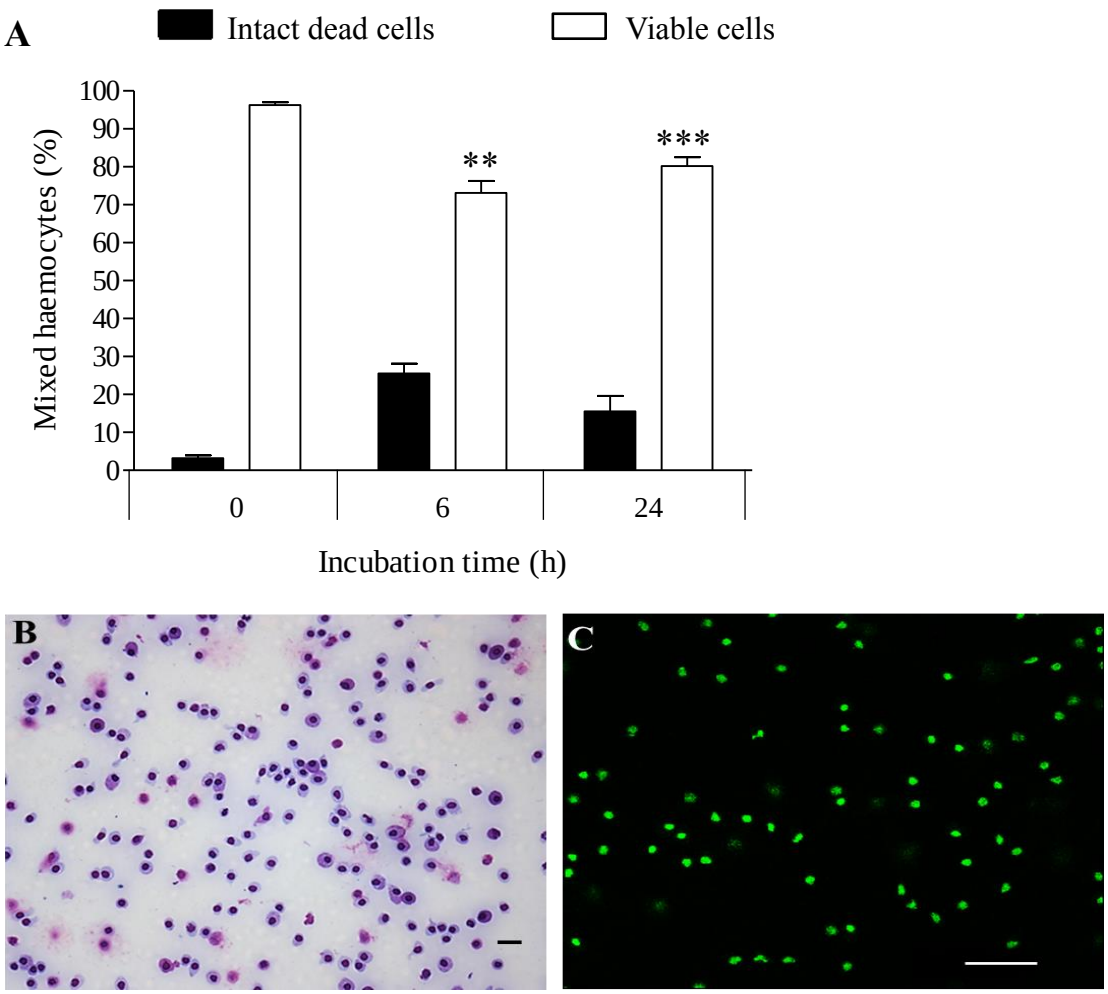

Figure 5.10. Viability of mixed haemocytes during *in vitro* suspension culture. (**A**): Viability in control haemocytes after 6 and 24 h culture (10°C) assessed by flow cytometry via bovine lactadherin-FITC and PI staining. Values for early apoptosis and late apoptosis/necrosis were combined to give rates of intact dead cells (data from Chapter 3, Figure 3.3). Data are expressed as means ± SEM, n=3, with a different crab used on each occasion. Statistical analysis was performed upon arc sine transformed data using one-way ANOVA with a Student Newman-Keuls multiple comparison *post hoc* test. *** $P<0.001$ *vs*. intact dead cells at 24 h; ** $P<0.01$ *vs.* intact dead cells at 6 h. (**B-C**): Cyto-centrifuge preparations of un-clotted control haemocytes after 24 h culture, stained with either Diff-Quik™ (**B**) or Sytox Green (**C**), images representative of n=3 experiments. (**B**): Light microscopy image captured at 200x total magnification, scale bar = 20 µm. (**C**): Confocal microscopy image captured 200x total magnification, scale bar = 50 µm.

5.4. Discussion

The present study has shown that different cell types *in vitro* vary in their capability to produce extracellular traps. Both crab HC and SGC populations are able to undergo ETotic-style chromatin release, in contrast to the GCs and ProHs, which did not show the response. Certainly GCs of the crab are unable to undergo a respiratory burst via activation of NADPH oxidase (Bell and Smith, 1993). The ProHs are known to be highly proliferative, (Roulston and Smith, 2011) which may explain why they do not undergo ETosis. By maintaining high levels of proliferation, consequent survival of ProHs would ensure that cell population dynamics are maintained. Certainly, after culture with PMA ProHs exhibited the highest levels of viability out of all haemocyte types. With regard to the SGCs it remains unclear whether they are capable of a NADPH oxidase-dependent respiratory burst (Bell and Smith, 1993), but certainly the SGCs are known to degranulate and lyse quickly in the presence of bacteria or LPS (Smith and Ratcliffe, 1980a; Smith and Söderhäll, 1983b; Söderhäll *et al*., 1986). Additionally, the SGCs as well as the GCs do co-operate with the HCs in the encapsulation of micro-organisms *in vivo* (Smith and Ratcliffe, 1980a), and both show antimicrobial activity, in contrast to crab HCs, which do not (Chisholm and Smith, 1992).

As bacteria and LPS were both shown to induce extracellular trap formation *in vitro*, this suggests a valid role for ETosis in host defence of the crab when the animal is exposed to such non-self agents. The percentages of ETotic HCs after stimulation with either bacteria or LPS were almost half (~30-35%) compared to those observed when HCs were stimulated with PMA (63%). PMA is a powerful activator of cell functions, even at very low nanomolarity (DeChatelet et al., 1996; Takei *et al*., 1996; Dekker et al., 2000), therefore its potency and effectiveness may help explain the high rate of ETosis exhibited by HCs in the present study. In contrast, human neutrophils stimulated for 3 h with *S. aureus* resulted in a greater generation of NETs (~35%) compared to PMA (~15-20%) over the same time period, whereas LPS induced NETs less efficiently than bacteria (Fuchs *et al*., 2007). As crabs would routinely be exposed to LPS and *L. anguillarum* in the wild, the lower rates of ETosis achieved with these non-self agents may represent a more biologically realistic response for this species.

Furthermore, in terms of immune defence, it would be disadvantageous for the crab to disable high numbers of HCs via ETosis, bearing in mind HCs comprise ca. 80% of the haemocyte population in *C. maenas* (Smith and Ratcliffe, 1978).

Scanning electron microscopy revealed that extracellular chromatin released from HCs ensnared *L. anguillarum* in a very similar fashion to the entrapment of *S. aureus*, *S. typhimunium* and *S. flexneri* by NETs (Brinkmann *et al*., 2004). Observations at fluorescence microscopy level in *Galleria mellonella* (wax moth) showed that granular haemocytes extrude fibrillar 'net-like' structures that are capable of entrapping FITC-labelled bacteria (Altincicek *et al*., 2008). However, no mechanism behind the release of these 'net-like' structures was explained and the structures had only a limited ability to trap bacteria. More reports are emerging detailing how pathogenic bacteria are able to escape NETs, by a variety of different mechanisms. These include polysaccharide capsule formation which causes electrochemical repulsion of AMPs via addition a of a positive charge to the bacterial cell surface (Wartha *et al*., 2007), biofilm formation (Hong *et al*., 2009; Thornton *et al*., 2013), NET inhibition/degradation by nucleases (Berends *et al*., 2010) and DNAse generation (Buchanan *et al*., 2006), or by inhibition of ROS formation via catalase generation and subsequent degradation of hydrogen peroxide to water and oxygen (Lögters *et al*., 2009; reviewed by Arazna *et al*., 2013). Interestingly, with regard to nucleases, it has recently been discovered that Lundep, an endonuclease from the salivary glands of the sand fly, *Lutzomyia longipalpis*, can destroy NETs and increase *Leishmania* parasite survival in neutrophils (Chagas *et al*., 2014).

One of the main functions of an immune system is to prevent the spread of microbes. Haemocyte encapsulation in the crab has been previously shown to do this very effectively. The bacteria, *Bacillus cereus* and *Moraxella sp*., are killed within haemocyte capsules, with the bacteria clearly contained as neither species re-entered the circulation within the experimental period of 4 days (White *et al*., 1985). The results from this chapter show that extracellular chromatin is clearly associated with the formation and development of haemocyte capsules and thus has a role in defence *in*

vivo. Immunohistochemistry revealed that extracellular chromatin released during ETosis assists in the aggregation of circulating haemocytes which become joined to each other. This process is assisted by the cell-adhesion protein, PXN, which is released from the haemocytes most probably through the mechanism previously described by Söderhäll (1982), i.e. via PRRs such as βGBP, LGBP and PGBP that have bound to their respective PAMPs, thus resulting in subsequent activation of the prophenoloxidase activating system. This apparent early release of PXN appears to occur very quickly and is likely to help haemocytes that either migrate into the area or flow by passively to stick together. Therefore, PXN assists to hold the developing structure firmly together. Whilst early stage encapsulation is occurring, small-scale ETosis is slowly starting at 1 h, with a subsequent increase in ETosis at 3 h through to 24 h. The extracellular chromatin meshes not only serve to trap infectious agents, they also appear to provide the scaffold upon which the haemocyte clumps develop, most likely by trapping passing or nearby circulating haemocytes. Furthermore, the extracellular co-localisation of H2A and chromatin at both 1 h and 3 h strongly suggests that *in vivo* the chromatin strands deliver histones and presumably other antimicrobial factors to assist in the killing of infectious agents. The externalisation of histones and chromatin in the extracellular space would further present 'damage' signals to the immune system consistent with the Danger Model (Seong and Matzinger, 2004). As the SGCs and GCs are involved during encapsulation in the crab (Smith and Ratcliffe, 1980a), AMPs released during degranulation from these haemocytes would likely assist to kill bacteria localised within the capsule matrix and in the close vicinity.

GC degranulation in the capsule would also release prophenoloxidase, which can add to ROS generation arising from by-products of activated phenoloxidase activity (Söderhäll *et al*., 2004). Additional ROS generation would aid the killing of infectious agents sufficiently contained within the haemocyte capsules and trapped on externalised chromatin. It has also been shown that haemocyanin isolated from crustacean haemolymph can generate ROS in response to microbial proteases and ligands *in vitro* (Jiang *et al*., 2007; reviewed by Coates and Nairn (2014)), thus it is plausible that haemocyanin (present in the circulating haemolymph) would also contribute to the killing of microbes within the capsule. Altincicek *et al*. (2008) reported that injection of

purified endogenous nucleic acids simultaneously with the pathogenic bacterium, *Photorhabdus luminescens*, in larvae of *G. mellonella* prolonged larval survival. The findings presented in this chapter strongly suggest that this enhanced survival may be attributable to trapping and killing of bacteria on the externally introduced chromatin.

This chapter demonstrates that extracellular chromatin released from ETotic haemocytes not only participates in defence by ensnaring microorganisms and externalising antibacterial histones (together with other haemocyte-derived defence factors), but crucially, provides the scaffold upon which intact haemocytes assemble during encapsulation. This finding changes the present view as to how capsules are initiated and formed in invertebrates (Chisholm and Smith, 1992).

Chapter 6

Demonstration of ETosis in other invertebrates

6.1. Introduction

To investigate if ETosis occurs more widely across invertebrate phyla, preliminary studies were also made on a distantly related protostome, the blue mussel, *Mytilus edulis*, and a cnidarian, the sea anemone, *Actinia equina*. These organisms were selected as their immune cells are known to be both phagocytic and capable of generating a respiratory burst, a defining characteristic of ETosis in mammals (Fuchs *et al*., 2007). In contrast to crab haemocytes, those of *M. edulis* display high rates of phagocytosis *in vitro* (>70%) (Wootton *et al*., 2003), with greatest uptake by the eosinophilic granular haemocytes, which also undergo a strong respiratory burst (Pipe *et al*., 1997). Sea anemones, whilst not possessing a dedicated, mesodermally-derived, coelomic immune system, nevertheless possess phagocytes that are known to undergo a respiratory burst (Hutton and Smith, 1996). Therefore, it was hypothesised that ETosis is an ancient process which predates the evolution of the coelom. The relative evolutionary positions of these organisms can be seen in Figure 6.1.

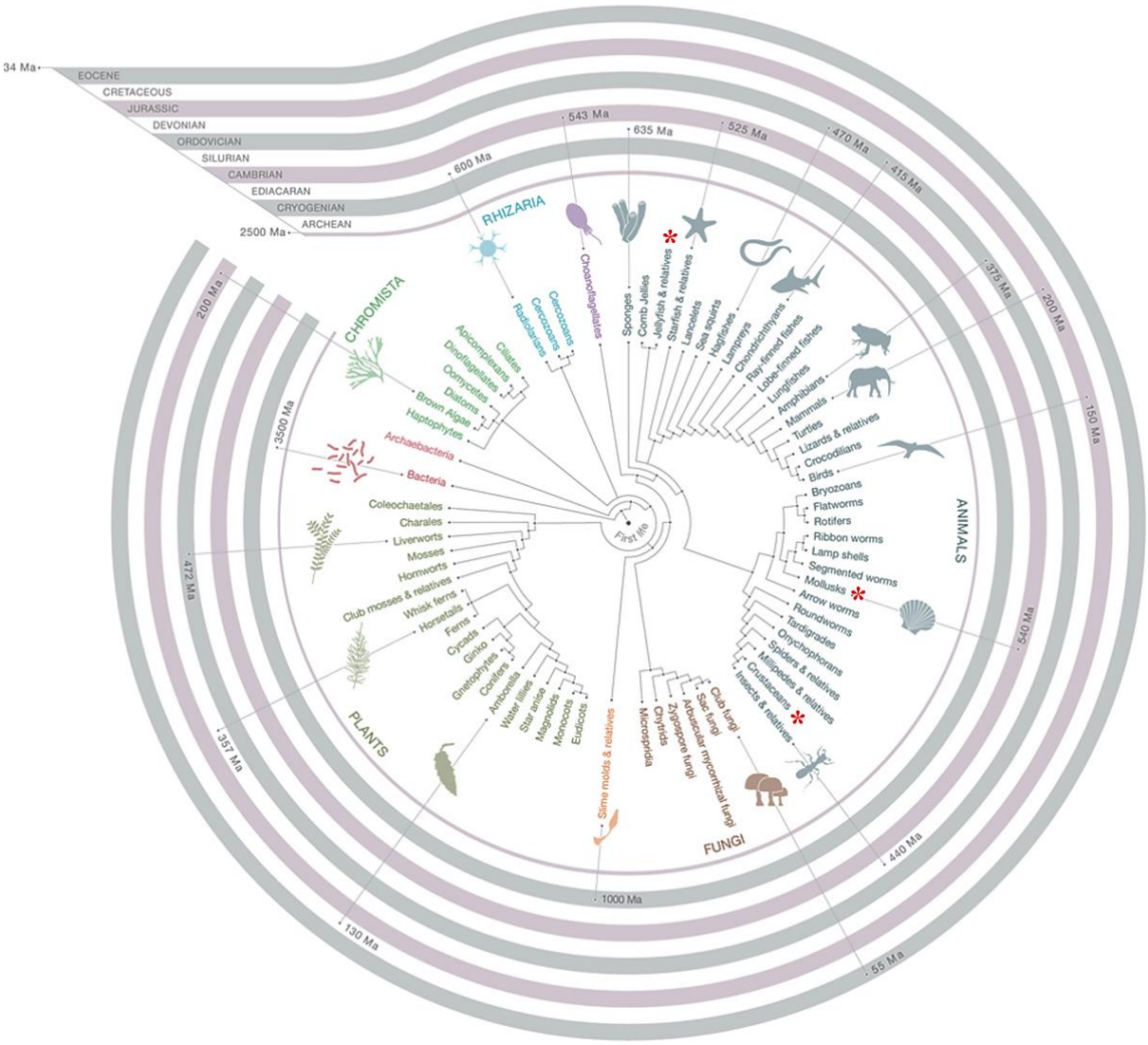

Figure 6.1. Charles Darwin's phylogenetic tree of life diagram (source: www.bbc.co.uk). *denotes relative evolutionary positions of crustaceans (which include the shore crab, *C. maenas*), molluscs (which include the blue mussel, *M. edulis*) and relatives of the jellyfish (which include the sea anemone, *A. equina*, within the phylum Cnidaria). Phylogenetic tree based on analyses of small sub-unit ribosomal ribonucleic acid (rRNA) sequences sampled from about 3,000 species from throughout the tree of life. Crustaceans and molluscs split from a common ancestor around 550 million years ago (Morris, 1997), whereas cnidarians arose over 600 million years ago (Ayala and Rzhetsky, 1998) with the origin of life ca. 4.5 billion years ago (Horowitz and Hubbard, 1974). Ma = mega-annum (a unit of time equal to one million years).

The study in this chapter set out to conventionally stimulate and inhibit ETosis in immune cells from *M. edulis* and *A. equina*, as previously demonstrated in HCs from *C. maenas* (Chapter 4).

Specifically, the objectives of this chapter are:

1. To determine if immune cells from *M. edulis* and *A. equina* release extracellular chromatin following activation of protein kinase C (PKC) and if so, whether it is reliant on NADPH-oxidase dependent ROS generation.

2. To quantify rates of extracellular chromatin release and inhibition from *M. edulis* and *A. equina* immune cells over various timepoints.

6.2. Materials and methods

6.2.1. Mussels and sea anemones

Mytilus edulis were collected from the causeway to Cramond Island, (Edinburgh, Scotland). *Actinia equina* were collected from rock pools at Milsey Bay (East Lothian, Scotland). Animals were maintained in tanks containing aerated seawater (~32‰) at a temperature of 12 ± 2°C. All animals were acclimated for 2 weeks and fed twice weekly with the marine green alga (*Tetraselmis suecica*). Only healthy adult animals with no external lesions or gross signs of disease were chosen for experimental purposes.

6.2.2. Haemolymph sampling from the mussel

Haemolymph was extracted according to the method of Wootton *et al*. (2003). Briefly, the valves of the mussel shell were prised apart. Using a 23G 1.25" needle and 1 mL syringe, 0.4 mL haemolymph was withdrawn from the posterior adductor muscle and into 0.6 mL of anticoagulant buffer (0.05 M Tris-HCl, 2% glucose, 2% NaCl, 0.5% EDTA; pH 7.6; Coles *et al*., 1995). The haemolymph was then centrifuged (5 min at 500 x g, 4°C), after which the supernatant was discarded and the haemocytes resuspended in ML-15 (Chapter 2, Section 2.2.3).

6.2.3. Collection of amoebocytes from the sea anemone

Amoebocytes (mesogleal cells) were obtained according to a modified procedure from Hutton and Smith, (1996). Briefly, from an incision in the centre of the pedal disc, the mesenteric filaments (located at the base of the coelenteron) were excised into 3.2% sterile filtered NaCl. The mesenteric filaments in homologous fluid drained from the coelenteron were teased apart using scissors and fine-pointed forceps and transferred into 3 mL sterile filtered 3.2% NaCl in a 15 mL Falcon tube. The mesenteric filaments/homologous fluid mixture was mixed further by repeated aspiration and kept at room temperature for ca. 15 min, with occasional shaking a mixing during this time. This process dissociated the amoebocytes from the filaments and resulted in a cloudy cell suspension being formed. The cell suspension was then harvested and centrifuged (5 min at 300 x g, 10°C) to sediment unwanted debris and the cell supernatant again harvested. The amoebocytes from the crude extracts were then resuspended in ML-15

(Chapter 2, Section 2.2.3). To enhance the cell preparation further, trypsin at a final concentration of 0.01% was added to the mesenteric filaments/homologous fluid mixture. The cell suspension was then centrifuged as above, harvested, and subjected to a second round of centrifugation at higher speed (5 min, 800 x g, 10°C). The supernatant was this time discarded and the pink cell pellet of enriched amoebocytes resuspended in ML-15 (Chapter 2, Section 2.2.3).

6.2.4. Cyto-centrifuge preparations

Cyto-centrifuge preparations of mussel and anemone cells were made and examined as described above (Chapter 2, Section 2.2.5.1). Briefly, after fixation/permeabilisation in absolute methanol for 1 min, mussel haemocytes were stained using Wright's stain (ca. 1.5 min) and sea anemone amoebocytes stained using Diff-Quik™.

6.2.5. Preparation of monolayer cell cultures

Monolayer cultures of approximately 1 mL of 3 x 10^4 mL^{-1} mussel haemocytes, or 1 mL of 1 x 10^4 mL^{-1} sea anemone amoebocytes resuspended in ML-15 were prepared in 24-well flat bottomed culture plates as described above (Chapter 4, Section 4.2.2). One mussel or sea anemone was sampled per experimental run with triplicate monolayer cultures set up per treatment per timepoint. Practical assistance with experiments was given by Ms Karen Nicol (Heriot Watt University) and Ms Charlotte Gibout (University Institute of Technology La Rochelle).

6.2.6. Extracellular chromatin release assays *in vitro*

Mussel haemocytes and sea anemone amoebocytes were stimulated with PMA, as described for crab HCs (Chapter 4, Section 4.2.3). For mussel haemocytes, extracellular chromatin release was induced using PMA at final concentrations of 0.1 µM, 25 µM and 50 µM in a final volume of 500 uL fresh ML-15 with the plates then incubated for 24-48 h (10°C). For the sea anemone cells, extracellular chromatin release was induced using PMA at a final concentration of 0.1 µM in a final volume of 500 uL fresh ML-15 incubated for 24 h (10°C). Afterwards, cells were stained, unfixed with 1 µM Sytox

Green, with visualisation and quantification of extracellular chromatin release carried out as described above (Chapter 4, Section 4.2.3).

To confirm the released material was of nuclear origin, DNAse-1 (100 U mL^{-1} final concentration) was added to monolayer cultures that had been previously stimulated with 0.1 µM PMA (24 h, 10°C). The cells were then stained, unfixed with 1 µM Sytox Green as above. Controls consisted of PMA-activated cells minus DNAse-1. For sea anemone amoebocytes, the incubation was 80 min at 15°C with changes recorded by confocal time-lapse photo microscopy as described above (Chapter 4, Section 4.2.3). Images were taken every 20 min and the image sequence then converted to video format (avi) using ImageJ™ (supplementary video 4).

6.2.7. Inhibition assays *in vitro*

Fresh monolayer cultures of mussel haemocytes were incubated for 1 h (10°C) with the NADPH-oxidase inhibitor, DPI (10 µM final concentration) as described above (Chapter 4, Section 4.2.7), before addition of PMA (50 µM final concentration) and incubation for 48 h (10°C) as above. Controls consisted of PMA-activated haemocytes minus DPI and haemocytes plus DPI. Monolayer cultures of sea anemone amoebocytes were incubated for 1 h (10°C) with DPI (2 µM), or the inhibitor of actin polymerization, cytochalasin D (10 µM) as described above (Chapter 4, Section 4.2.7), before addition of PMA (0.1 µM) and incubation for 24 h (10°C) as above. Controls consisted of PMA-activated amoebocytes minus DPI or cyto D and amoebocytes plus DPI or cyto D. Chromatin release was detected and quantified as above (Chapter 4, Section 4.2.3).

6.2.8. Statistical analyses

All values were calculated as mean ± SEM, with percentage values arc sine transformed before statistical analysis. Statistical differences were then determined as described in Chapter 2 (Section 2.2.7). Significance was accepted at $P<0.05$.

6.3. Results

6.3.1. Mussel haemocytes

Monolayer cultures of *M. edulis* haemocytes released Sytox Green-positive material after treatment with PMA, albeit at a lower abundance and requiring higher concentrations of PMA compared to crab HCs (Figure 6.2 and Figure 6.3). Within the mixed haemocyte population, the eosinophilic haemocytes were the cells predicted to undergo extracellular chromatin release (Figure 6.2, B, black arrow). After 24 h culture (10°C), a significantly higher proportion of *M. edulis* haemocytes treated with 0.1 µM PMA extruded chromatin (12.9% ± 1.9% SEM; $P<0.05$; n=3) compared to controls (2.9% ± 0.7% SEM) (Figure 6.2 and Figure 6.3, A). By increasing PMA concentration and incubation time, extracellular chromatin release from *M. edulis* haemocytes increased further (Figure 6.2, A). Values for chromatin extruding cells were significantly higher after 48 h culture with both 25 µM PMA (14.2% ± 3.4% SEM; $P<0.05$; n=3; Figure 6.2, A and Figure 6.3, B) and 50 µM PMA (27.4% ± 2.4% SEM; $P<0.05$; n=3; Figure 6.2, A and Figure 6.3, C and D), compared to control haemocytes (4.4% ± 4.0% SEM) (Figure 6.2, A and Figure 6.3, F). The spread 'comet-like' streaks of extracellular material released from *M. edulis* haemocytes (Figure 6.3, C, D) closely resembled those extruded from crab HCs and SGCs (Chapters 4 and 5). Crucially, after 48 h culture, rates of PMA-induced chromatin release were reduced by pre-treatment with DPI (Figure 6.2, A and Figure 6.3, E). Compared to PMA treated haemocytes, significant reductions ($P<0.05$; n=3) in rates of extracellular chromatin release were observed in haemocytes treated with PMA + DPI (8.9% ± 4.8% SEM) and DPI alone (5.6% ± 5.0% SEM) (Figure 6.2, A and Figure 6.3, E).

Figure 6.2.

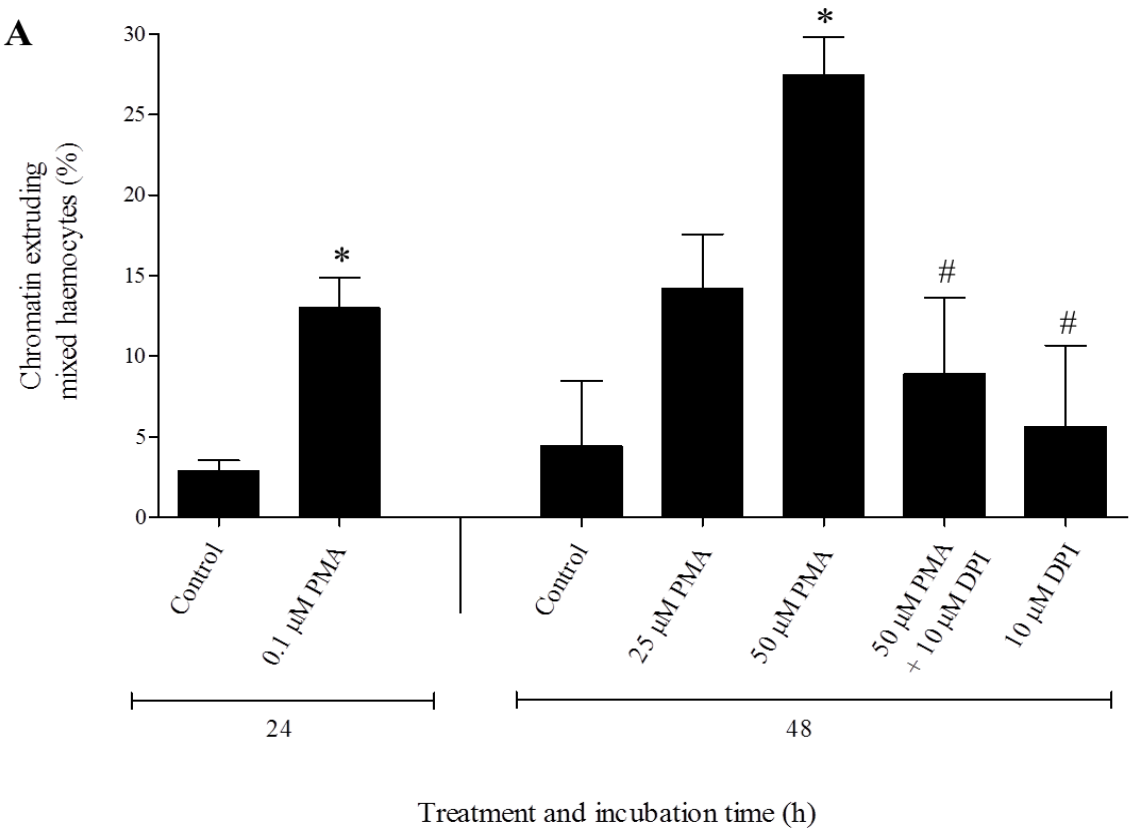
A
Chromatin extruding mixed haemocytes (%)
30
25
20
15
10
5
0
*
*
#
#
Control
0.1 µM PMA
Control
25 µM PMA
50 µM PMA
50 µM PMA + 10 µM DPI
10 µM DPI
24
48
Treatment and incubation time (h)

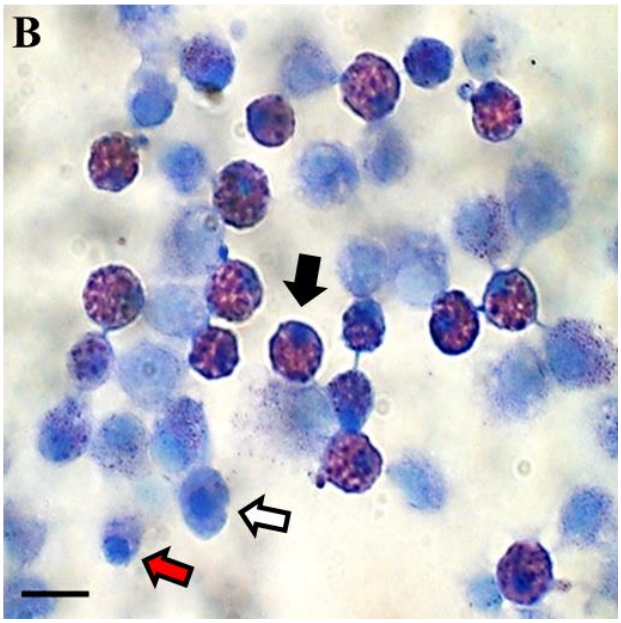
B

Figure 6.2. PMA-stimulated chromatin extrusion from *M. edulis* haemocytes *in vitro*. (**A**): Percentage of chromatin extruding haemocytes over 48 h culture (10°C) with.1, 25 and 50 µM PMA or 50 µM PMA ± 10 µM DPI. Data expressed as means ± SEM, n=3, with a different mussel used on each occasion**.** Statistical analysis was performed upon arc sine transformed data using one-way ANOVA with a Student Newman-Keuls multiple comparison *post hoc* test. **P*<0.05 *vs.* chromatin extruding control haemocytes at the corresponding timepoint; #*P*<0.05 *vs.* chromatin extruding haemocytes treated with 50 µM PMA only. (**B**): Wright's stained cyto-centrifuge preparation of mussel haemocytes (0 h), showing a hyaline haemocyte (red arrow), basophilic haemocyte (white arrow) and an eosinophilic haemocyte (black arrow). Practical assistance with experiments was provided by Ms Karen Nicol (Heriot-Watt University). Image captured at 400x total mag, scale bar = 20 µm.

Figure 6.3.

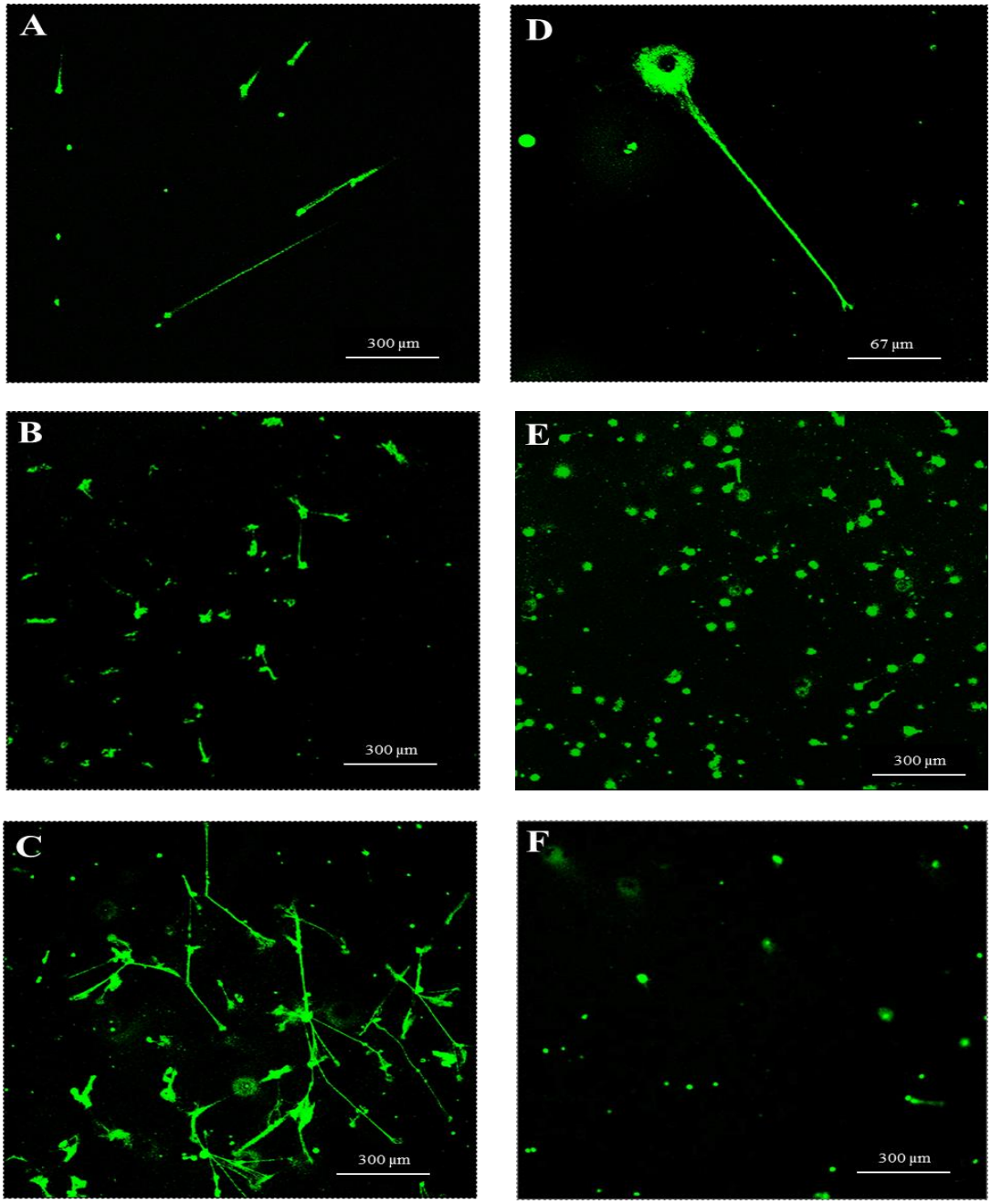

Figure 6.3. Representative confocal images of Sytox Green stained extracellular chromatin release from PMA-stimulated *M. edulis* haemocytes. (**A**): 0.1 µM PMA, 24 h; (**B**): 25 µM PMA, 48 h; (**C**): 50 µM PMA, 48 h, inter-connecting trands of extracellular chromatin can be seen; (**D**): 50 µM PMA, 48 h, an ETotic haemocyte displaying a spread 'comet-like' streak of extracellular chromatin; (**E**): 50 µM PMA + 10 µM DPI, 48 h; (**F**): Control 48 h. Images representative of n=3 experiments. Scale bars = 67 µm (**D**) or 300 µm (all other images).

6.3.2. Sea anemone amoebocytes

Remarkably, amoebocytes from the sea anemone also expelled Sytox Green-positive material after PMA treatment. Initially, crude extracts containing mesogleal cells were tested for chromatin release, within which the phagocytic haemocytes (Figure 6.4, A, black arrow) were the cells predicted to undergo extracellular chromatin release. Evidence of Sytox Green stained extracellular chromatin release was apparent in crude extracts where the chromatin formed short 'puff-ball' structures (Figure 6.4, B, C). However, crude extracts contained additional, uncategorized cells (Figure 6.4, A, white arrow) and a nematocyst (Figure 6.4, C, black arrow), as well as additional non-cellular material (Figure 6.4, C). Therefore, further treatment of the cell suspension was done with trypsin to enrich the amoebocytes and clean up the cell preparation.

After trypsin treatment, a higher proportion of phagocytic amoebocytes was observed compared to crude extracts (compare Figure 6.4, A, with Figure 6.5, B). However, similar to mussel haemocytes, a lower rate of extracellular chromatin release was exhibited by *A. equina* amoebocytes compared to crab HCs (Figure 6.5, A). Nonetheless, after 24 h culture (10°C), enriched mesogleal cells treated with 0.1 µM PMA displayed a significant increase in extracellular chromatin release (10.3% ± 1.8% SEM; $P<0.05$; n=3) compared to control (untreated) enriched mesogleal cells (2.8% ± 1.0% SEM) (Figure 6.5, A, Figure 6.6, A, B, C, F). Extracellular structures released from enriched mesogleal cells appeared as 'comet'-like streaks (Figure 6.6, A-C) and resembled ETs produced by crab HCs and SGCs (Chapters 4 and 5) as well as mussel haemocytes (Figure 6.3, A-D). Over the same incubation period, PMA-induced chromatin release from amoebocytes decreased with DPI or CytoD pre-treatment (Figure 6.5, A, Figure 6.6, D, E). Compared to PMA treated amoebocytes, significant reductions ($P<0.05$; n=3) in rates of extracellular chromatin release were observed in cells treated with PMA + DPI (3.0% ± 1.5% SEM) and PMA + cyto D (2.4% ± 1.3% SEM) (Figure 6.5, A, Figure 6.6, D, E).

Importantly, as the extracellular material released from the amoebocytes was successfully digested by DNAse-1 (Figure 6.7, A; supplementary video 4), the extruded material was confirmed to be composed of chromatin. Confocal time-lapse photo microscopy revealed

that extracellular chromatin released from enriched mesogleal cells was successfully digested over an 80 min time period (Figure 6.7, A; supplementary video 4), somewhat quicker as compared to digestion of extracellular chromatin released from crab HCs (Chapter 4, Figure 4.6, A; supplementary video 3). Over the same time period, the extracellular chromatin structures remained in amoebocyte cultures that did not receive DNAse-1 (Figure 6.7, B), a similar observation to that made for ETs released from crab HCs (Chapter 4, Figure 4.6, B).

Figure 6.4.

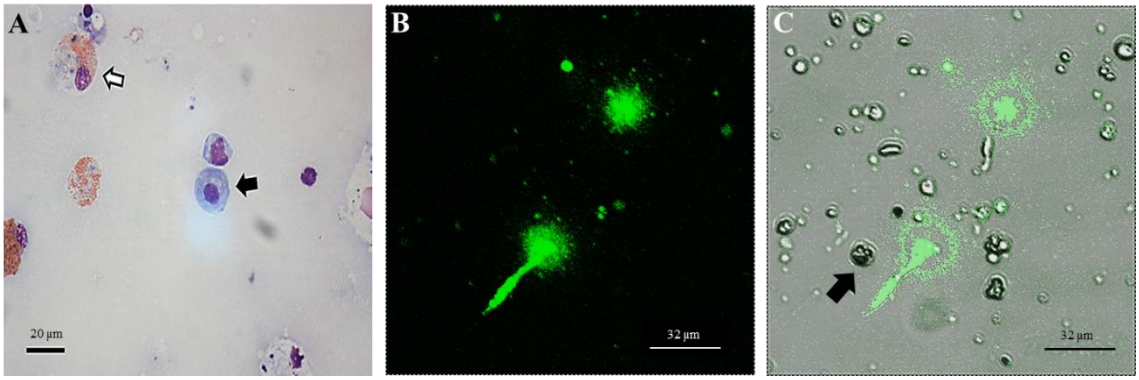

Figure 6.4. Morphology of *A. equina* crude mesogleal extracts and visualisation of extracellular chromatin release *in vitro*. (**A**): Diff-Quik™ stained cyto-centrifuge preparation of a fresh (0 h) crude mesogleal extract, showing an eosinophilic cell (white arrow) and a phagocytic cell (black arrow). The phagocytic cells bear strong resemblance to HCs from *C. maenas* and were the candidate cells for chromatin extrusion. Image captured at 400x total mag, scale bar = 20 µm. (**B-C**): Confocal images of Sytox Green stained crude mesogleal extracts (0.1 µM PMA, 24 h, 10°C) captured without phase contrast (**B**) or with phase contrast transmission overlay (**C**) at the same field of view, scale bars = 32 µm. Confocal images show diffuse 'puff-ball-like' and spread 'comet-like' chromatin extrusion from phagocytes. An un-fired nematocyst (stinging cell) is also visible (**C**, arrow).

Figure 6.5.

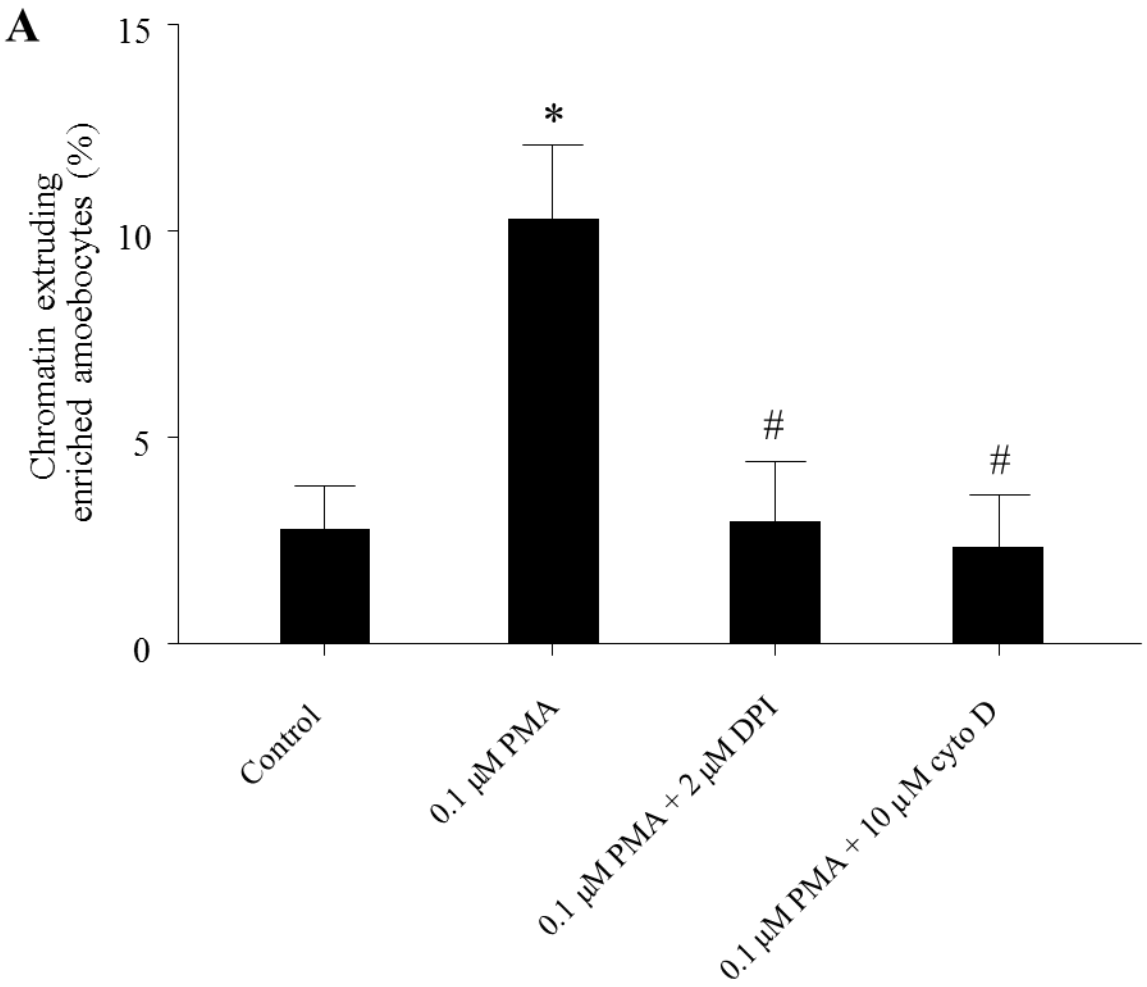
A
Chromatin extruding enriched amoebocytes (%)
15
10
5
0
*
#
#
Control
0.1 μM PMA
0.1 μM PMA + 2 μM DPI
0.1 μM PMA + 10 μM cyto D

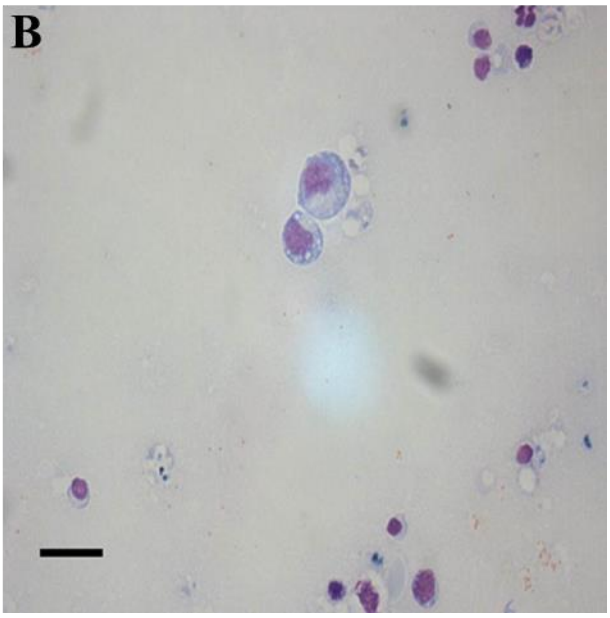
B

Figure 6.5. PMA-stimulated chromatin extrusion from *A. equina* enriched amoebocytes *in vitro*. (**A**): Percentage of chromatin extruding amoebocytes after 24 h culture (10°C) with 0.1 µM PMA, 0.1 µM PMA + 2 µM DPI or 0.1 µM PMA + 10 µM cyto D. Practical assistance with experiments was provided with assistance from Ms Charlotte Gibout (University Institute of Technology La Rochelle). Data expressed as means ± SEM, n=3, with a different sea anemone used on each occasion**.** Statistical analysis was performed upon arc sine transformed data using one-way ANOVA with a Student Newman-Keuls multiple comparison *post hoc* test. **P*<0.05 *vs.* chromatin extruding control amoebocytes; #*P*<0.05 *vs.* chromatin extruding amoebocytes treated with 0.1 µM PMA only. (**B**): Diff-Quik™ stained cyto-centrifuge preparation of a fresh (0 h) cell preparation, showing the enriched phagocytic amoebocytes. Image captured at 400x total mag, scale bar = 20 µm.

Figure 6.6.

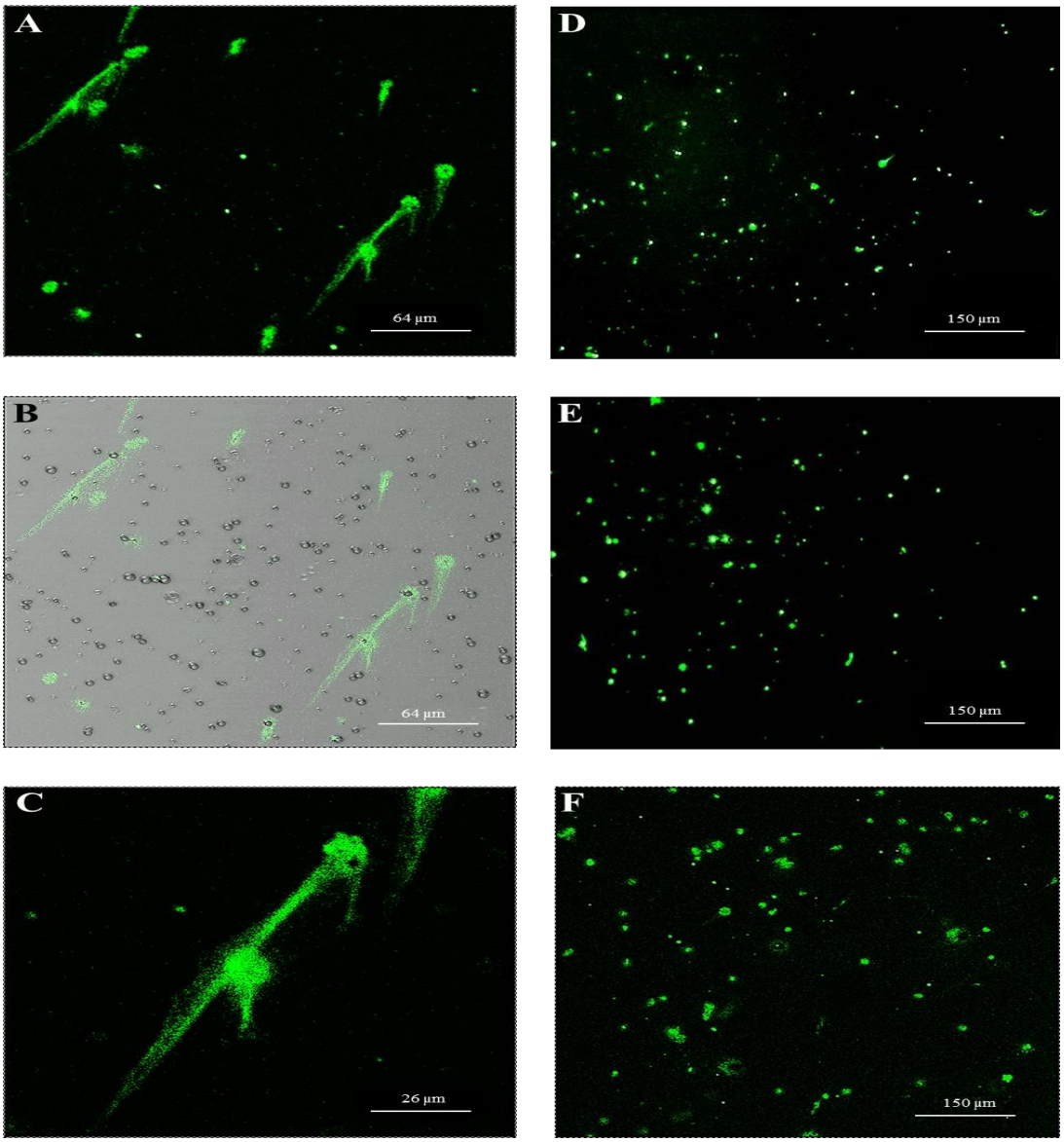

Figure 6.6. Representative confocal images of Sytox Green stained extracellular chromatin release from PMA-stimulated enriched *A. equina* amoebocytes. Amoebocytes were cultured for 24 h (10°C) with 0.1 µM PMA ± 2 µM DPI or 10 µM cyto D. (**A-B**): PMA treated amoebocytes (**A**) with phase contrast trasnmission overlay (**B**) at the same field of view. Spread 'comet-like' streaks of extracellular chromatin can be seen emanating from ETotic cells. (**C**): Enlarged region of image **A**, showing a spread 'comet-like' extracellular trap; (**D**): PMA + DPI; (**E**): PMA + cyto D; (**F**): Control amoebocytes. Images representative of n=3 experiments. Scale bars = 64 µm (**A** and **B**), 26 µm (**C**) or 150 µm (**D, E, F**).

Figure 6.7.

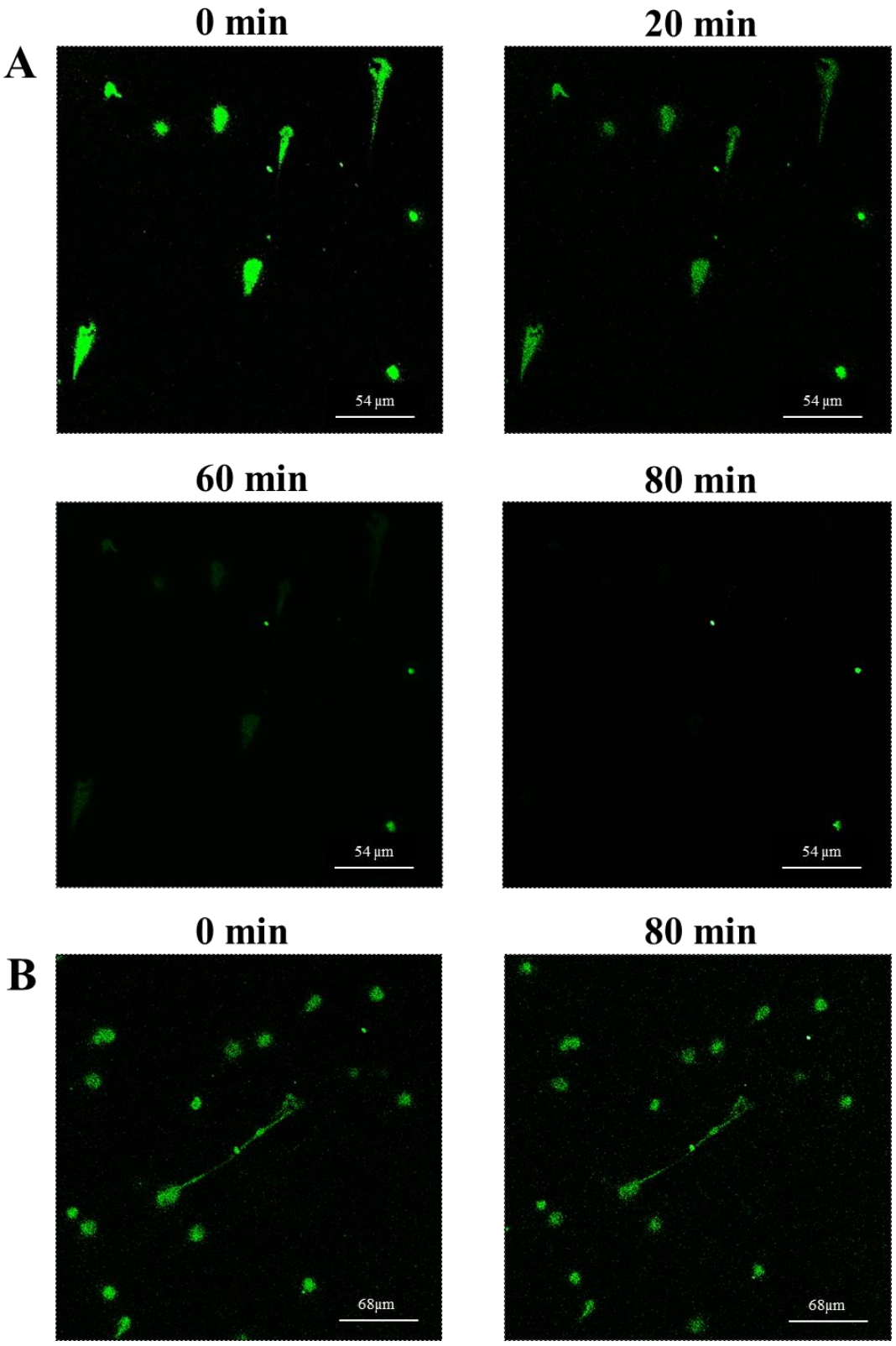
A
0 min
20 min
60 min
80 min
54 µm
54 µm
54 µm
54 µm
B
0 min
80 min
68µm
68µm

Figure 6.7. DNAse digestion of extracellular chromatin released from *A. equina* enriched amoebocytes *in vitro*. Confocal time-lapse photo microscopy of Sytox Green stained amoebocytes over an 80 min period. (**A**): Confocal images showing the digestion of extracellular chromatin 20, 60 and 80 min post addition of 100 U mL^{-1} DNAse-1 (refer to supplementary video 4); (**B**): Confocal images of control amoebocytes (no DNAse-1) taken at 0 and 80 min showing the released chromatin structures remain over the same time period. Scale bars = 54 µm (**A**) and 68 µm (**B**).

6.4. Discussion

Importantly, the findings from this preliminary study confirm that immune cells from other invertebrates are capable of ETotic-like chromatin release. The present study only considered mixed populations of cells. However, eosinophilic haemocytes of the mussel are strongly phagocytic and able to generate a respiratory burst (Pipe *et al*., 1997; Wootton *et al*., 2003). Additionally, sea anemones possess phagocytic amoebocytes that are also able to undergo a respiratory burst (Hutton and Smith, 1996). Therefore, as these cells possess the key characteristics of ETotic cells in mammals (Fuchs *et al*., 2007), it is highly likely that the ETotic-like response is performed by these cells. Certainly in the sea anemone the ETotic-like response was enhanced after enrichment of phagocytic amoebocytes by trypsin-digestion, which reduced mucus levels contained within homologous fluids. In terms of general morphology, ETs released from immune cells of the mussel and sea anemone bear strong resemblance to ETs produced by ETotic HCs and SGCs of the crab and NETs produced in mammals (Brinkmann *et al*., 2004). In the present study, diffuse and spread ETs were observed, both of which are established morphological terms used to describe the extracellular structures in mammals (Hakkim *et al*., 2011).

Albeit far from clear cut in comparison, the present study also indicates that the mechanisms of the ETotic-like responses exhibited by mussel and sea anemone immune cells are similar to ETosis performed by crab HCs (Chapter 4) and mammalian NETs. Chemical induction with PMA did induce extracellular chromatin release in mussel haemocytes and sea anemone amoebocytes which implies induction of the response via activation of PKC, with inhibition achieved by pre-treatment with the NADPH-oxidase inhibitor, DPI, similar to NETs (Fuchs *et al*., 2007). Additionally, pre-treatment of sea anemone enriched amoebocytes with the inhibitor of actin polymerization, cytochalasin D, also appeared to inhibit the ETotic-like response, as previously demonstrated in NETs (Neeli *et al*., 2009).

The lower rate of ETosis exhibited by mussel haemocytes combined with the requirement for a much greater concentration of PMA over a longer incubation time is not easily explained. However, this may be linked to the high rates of phagocytosis (>70%)

performed by bivalve haemocytes (Wootton *et al*., 2003), or simply that the conditions used to induce and measure ETosis have not yet been fully optimised for this organism. Phagocytic haemocytes are closely associated with food transport in bivalves (filter feeders), so it may be disadvantageous for mussels to disable high numbers of haemocytes via ETosis. Additionally, arthropods and molluscs are very distantly related, splitting from a common ancestor around 550 million years ago (Morris, 1997), with currently accepted phylogenetic analyses confirming their divergence into two super-phyla, specifically the Lophotrochozoans and the Ecdysozoans (Aguinaldo *et al*., 1997). Furthermore, extant species differ enormously in morphology, anatomy and life history.

Compared to crab HCs, much lower rates of ETosis were also exhibited from *A. equina* cells over the same incubation time and PMA concentration. However, as experiments with the mussel and sea anemone were both performed upon mixed populations of cells, it is likely that ETotic cells are at lower proportions than corresponding counts for isolated cell types. This may also help to explain the differences and greater variability of ETosis stimulation and inhibition exhibited by mussel haemocytes and sea anemone amoebocytes, compared to separated crab HCs. Although a separation method exists for *M. edulis* haemocytes (Pipe *et al*., 1997), in practice separations are often problematic. Haemolymph from several individuals must be pooled in order to obtain enough cells for successful separations, and reactions between cells from different individuals could also influence the variability of the procedure.

Having established that ETosis is integral to *in vivo* host defence in the crab (Chapter 5), it is reasonable to consider that ETosis is also involved in capsule formation by bivalves. It has been demonstrated that the edible cockle, *Cerastoderma edule*, can facilitate encapsulation responses in response to parasites *in vitro* and *in vivo* (Wootton *et al*., 2006). Similarly, cnidarian amoebocytes can aggregate and form melanised barriers *in vivo* in response to fungal hyphae (Mydlarz *et al*., 2008). Hence, it is conceivable that ETosis may be involved in such responses. It is also probable that high levels of mucus observed in anemones would aid localisation of extracellular chromatin and any microorganisms trapped on these ETs. Accordingly, the spread of invading pathogens

would be restricted and the infectious agents brought into close contact with antimicrobial factors produced by the surrounding tissues and/or mesogleal cells. Certainly AMPs such as aurelin are synthesised by the endoderm (innermost germ cell layer) of cnidarians (Ovchinnikova *et al*., 2006; Jung *et al*., 2009). Moreover, it is well established that amoebocytes of *A. equina* can generate and release extracellular ROS (Hutton and Smith, 1996), which would be capable of killing bacteria.

Cnidarians originated over 600 million years ago (Ayala and Rzhetsky, 1998), therefore, the findings from this preliminary study confirm that ETosis arose earlier in evolution than previously thought. Moreover, as members of the Cnidaria lack a and true circulatory system, extracellular chromatin release must be an ancient defence process that predates the development of an organised immune system within the mesoderm. In the pea plant, *Pisum sativum*, extracellular DNA in the root-cap slime has been demonstrated to confer protection against fungal infections (Wen *et al*., 2009). However, it is still to be established whether this extracellular DNA extrusion occurs in a controlled, NADPH-oxidase dependent manner, as observed during ETosis in animal immune cells. Additionally, because the chromatin was released from the root into the external environment (soil), rather than within the tissues of the plant itself, it remains unclear whether the extracellular DNA distribution is genuinely occurring as a result of ETosis. Therefore it is still unclear as to when ETosis first arose in eukaryotic evolution. Nonetheless, the findings from this preliminary study helps shed new light on how early multi-cellular animals may have defended themselves against prokaryotic competitors in their environment.

Chapter 7

General Discussion

7.1. General discussion

The present study used the shore crab, *C. maenas* as a model for the study of cell death processes in crustaceans, namely apoptosis and ETosis. The study confirmed that the key elements of apoptosis could be detected and quantified and that the pathways of the process were likely to be broadly similar to those of the mammalian system. Apoptosis was assessed in response to conditions and stimuli that the crab would normally experience and responses of the different haemocyte types in the crab were compared. The present research expanded beyond apoptosis to confirm that invertebrate haemocytes can form extracellular traps, and carried out detailed characterization of ETosis in the crab, including its role in host defence *in vivo*.

Chapter 2 compared a number of methods for detecting and quantifying apoptosis, and confirmed that its key characteristics were apparent in crab haemocytes. The use of mammalian apoptosis stimulators/inhibitors confirmed that the process in crab haemocytes was caspase-dependent and that it could be induced by the inhibition of NFκB and CDKs. Previous studies on apoptosis in invertebrate haemocytes have generally overlooked the pathways involved and have not attempted to investigate biochemical stimulation or inhibition. The present study is novel in that it assessed both early and late-stage apoptosis. A weakness in some earlier studies on crustaceans is that they have used only one or two assays that detect late-stage apoptosis, e.g. DNA fragmentation or TUNEL. Both of these can generate false positives from necrotic cells or from cells undergoing DNA repair or transcription. Given the differences between vertebrate and invertebrate systems, as well as amongst invertebrate taxa, it is important to validate apoptosis by using more than one method, and also to choose those which detect different aspects of the process.

The present study found that the majority of methods could be adapted successfully to studying apoptosis in a marine invertebrate, but not all were found to be suitable. The mitocapture assay is widely used in mammalian immunology, but was not successful in the present study. This reflects the difficulties that could arise in using kits optimized for mammalian cells and assuming that their immediate transfer to a novel species

(especially a marine one) will automatically be successful. Time and budget constraints did not allow further attempts to adapt the mitocapture assay, and also fed into the decision not to test/modify other kit assays such as the TUNEL assay. As the mitocapture assay relates to the intrinsic apoptosis pathway, optimizing this for crab is of interest, as most assays used to investigate invertebrate apoptosis relate to the extrinsic, receptor-mediated pathway. In the present study, flow cytometry with bovine lactadherin-FITC and PI staining was found to be the most effective and convenient method for routinely quantifying apoptosis in crab haemocytes. The method was rapid, reproducible and generated results relating to both the early and late stages. In contrast, unlike bovine lactadherin, AV binding of PS residues is calcium-dependent, therefore several EDTA-containing anticoagulant buffers normally used with haemocytes would need to be avoided using this method (so to avoid chelation of calcium).

In the light of recent knowledge regarding other forms of programmed cell death such as ETosis (reviewed in Chapter 1), it is plausible that standard assays for apoptosis are also recording these events. As ETotic cell death releases nuclear DNA to the extracellular environment, flow cytometry based assays using nuclear stains would also detect extracellular nuclear DNA. Therefore, when assessing apoptosis using established assays, it is possible some ETotic cells might be present within the late apoptotic/necrotic category, as they would have lost membrane integrity and be releasing nuclear DNA to the extracellular environment. Similarly, when using flow cytometry, some ETotic fragments might appear as B-lactadherin-FITC negative/PI-positive events, as these can represent either cellular debris or bare nuclei in the very late stages of necrosis (Zali *et al*., 2008; Wang *et al*., 2011b). Additionally, hypodiploid DNA (fragmented DNA) is indicative of late stage apoptosis and can contain DNA released from necrotic cells, therefore it may be that extracellular DNA released from ETotic haemocytes could also be contributing to the hypodiploid peak of DNA. While the study of Fuchs *et al*. (2007) stated that they could not detect fragmented DNA from ETotic neutrophils using the DNA ladder assay, the authors stated that variations in the experimental set-up, such as culture conditions, high/low serum levels etc could influence this.

The *in vitro* apoptosis investigations described in Chapter 3 provides insights into haemocyte responses to different life conditions, as well as differences amongst the haemocytes themselves. The significant differences in early and late apoptosis with temperature emphasizes that experimental conditions need to be consistent when comparing constitutive levels of apoptosis with those induced by experimental variants. The results from this chapter also found variations between cell types, with HCs showing significantly reduced numbers in culture with correspondingly higher levels of apoptotic death compared with GCs or ProHs. This could greatly alter the interpretation of results from other studies on crustacean apoptosis. Without differential cell counts, apparent experimental effects could relate to differing proportions of HCs or GCs rather than any effects on cell death processes. It was also observed that inducing haemocytopenia resulted in higher apoptosis values in the haemocytes. Numbers of circulating haemocytes can reduce dramatically during natural physiological processes such as the moult cycle or following infection (Smith and Ratcliffe, 1980b; Smith and Chisholm, 1994). Therefore, apoptosis might appear significantly higher during experimental studies, but again not represent a true reflection of the experimental effects.

Chapters 2 and 3 focussed on apoptosis, which for some time has been regarded as the only form of programmed cell death. While research in mammals has recently uncovered various different forms (see Chapter 1), none of these have been unequivocally demonstrated in any invertebrate. The characteristics of neutrophil ETosis described by Fuchs *et al*. (2007) and the similarities between mammalian and invertebrate phagocytes, made the study of ETosis in crab haemocytes a natural progression of the current research. Neutrophils and many invertebrate haemocytes both produce ROS (including H_2O_2) upon stimulation with PMA, bacteria or LPS, possess histones (including H2A), and contain granules within which are cationic AMPs and enzymes which are likely to decorate extracellular traps. The present study is the first to comprehensively show characterization and function of ETosis for any invertebrate. Extracellular traps from crab HCs were induced by a PKC activator, shown to be dependent on NADPH-activated ROS production, and the traps were also decorated with H2A and the crustacean homologue of MPO.

Whereas numerous inducers of mammalian ETosis have now been recorded, it is currently unknown which 'artificial' or 'natural' inducers could stimulate ETosis in crustaceans. Some studies have shown that nanoparticles or metal ions can induce ETosis in vertebrates (Haase *et al*., 2014), and investigations of these in invertebrates would also be of relevance to environmental contamination. The current study showed that LPS from *E. coli* induced ETs, although to a lesser degree than PMA. Other naturally occurring PAMPs that might generate ETs in *C. maenas* may include β-1,3-glucans such as laminarin and zymosan, which are known to activate *C. maenas* haemocytes (Smith and Söderhäll, 1983b). However, β-glucans are extremely diverse in terms of their molecular weight and conformation, which is linked to their immunostimulatory capabilities, and cellular responses to β-1,3- glucans compared with e.g. β-1,6-glucans or other glycans would not necessarily be the same (Smith *et al*., 1984). Interestingly, β-glucan protects NETs against degradation by *Aeromonas hydrophila* in *Cyprinus carpio* (common carp) (Brogden *et al*., 2012).

Numerous pathogens have now been shown to stimulate ETs from mammalian immune cells. The current study tested a mild, Gram-negative opportunistic pathogen, but was not able to extend these experiments further. It would be of interest in future research to compare examples of Gram-positive, mycobacteria or archean microorganisms, as representatives from all these groups exist in marine environments. With respect to the crab, *C. maenas* is an exceptionally robust species with few known natural pathogens. Among the most relevant to test against *C. maenas* HCs would be the bacterial pathogen, *Aerococcus viridian var. homari* (responsible for mortalities in the European lobster) and the dinoflagellate, *Hematodinium*, which causes fatalities in numerous commercially-important decapod crustaceans such as lobster, the edible crab and the Dublin Bay prawn (Hauton, 2012). As discussed in Chapter 5, bacteria can avoid capture and killing by neutrophil ETs via a variety of different mechanisms. It would be highly valuable to the shellfish industry to know if crustacean pathogens can evade ETs by similar strategies.

Although no natural viral pathogens are known to affect *C. maenas*, viral diseases are prevalent in crustacean aquaculture, most notably the white spot syndrome virus (WSSV)

which has plagued the global shrimp industry in recent decades (Escobedo-Bonilla *et al*., 2008). Such viruses cause mass mortalities and enormous economic losses, and therefore threaten the sustainability of the industry. Given that apoptosis is regarded generally as important in anti-viral defence, it is of fundamental importance to investigate this and other cell death pathways in crustaceans. Future work could therefore develop more detailed investigations of apoptotic and other cell death *in vitro* and *in vivo*, in response to viral infection in crustaceans.

While the early study by Fuchs *et al*. (2007) recorded bacterial killing by neutrophil ETs, later studies have raised questions over the mode of direct antimicrobial activity. Many studies assessed killing by incubation of pre-formed NETs with bacteria followed by diluting and plating to enumerate CFU (reviewed by Parker and Winterbourn, 2013). A common problem with this approach is that failure to release bacteria from the traps may have been interpreted as killing, therefore over-estimating it. Modified methods have demonstrated that NETs alone do not entirely kill microorganisms such as *Staphylococcus aureus*, *Candida albicans* or *Aspergillus fumigatus* (Bruns *et al*., 2010; Menegazzi *et al*., 2012; Parker *et al*., 2012). As a result, it has been suggested that the trapping of bacteria by ETs may be as important as killing.

During the present study, preliminary experiments gave no clear indications that *L. anguillarum* was being killed by ETs released from the HCs. This may have been because the assay was not sufficiently optimized, e.g. in terms of relative numbers of bacteria and HCs or incubation times. In crabs, the HCs have not been confirmed to contain AMPs (Sperstad *et al*., 2010), nor do their lysates show strong antibacterial activity (Chisholm and Smith, 1992). It is possible that antimicrobial killing by crab ETs comes from cooperation with the SGCs or GCs, via the release of the AMPs synthesized and stored in their granules (Brockton *et al*., 2007; Sperstad *et al*., 2010). Alternatively, the contribution of H_2O_2 from HC activation could aid in the killing of entrapped bacteria and this could be tested as part of future work. Bacterial killing by histones on the crab ETs could take place, although histones including H2A have been shown to lose potency at high salt concentrations (>0.3 M) (Fernandes *et al*., 2002). This suggests that histone-

mediated killing on crustacean ETs might vary between freshwater, brackish and marine species, and with the environment the crustacean experiences. The shore crab is extremely tolerant of a wide range of salinities (euryhaline) and it would be of interest to test how modes of antibacterial activity change under brackish/low salinity conditions.

Neutrophil functions are influenced by cytokines such as IL-8 and TNF and these two in particular are known to stimulate ETosis (Keshari *et al*., 2012). Cytokine-like regulators of the immune response in crustaceans or other invertebrates are largely unknown. However, the ProPO system of arthropods has numerous components that are involved in microbial recognition and regulation of the antimicrobial response. It would be of interest to investigate whether elements of the ProPO system such as glucans or LPS-binding proteins, α-macroglobulin or serpins could influence rates of ETosis. Possible regulators could originate from the plasma from haemocytes or be secreted into it from a tissue such as the hepatopancreas. As ETosis is a cell death process, it is possible that there may be some involvement of the astakines released from the haematopoietic tissue. Certainly, in crayfish, astakines have been demonstrated to stimulate haemocyte survival within the haematopoietic tissue itself (Watthanasurorot *et al*., 2011).

The signalling pathways that underlie the ETotic response are not known in either mammals or invertebrates. Standard experimental models, such as *D. melanogaster* and *D. rerio* should enlighten future studies in other species, including *C. maenas*. However, there may be subtle or more likely profound differences between ETotic responses in invertebrates and also vertebrates. Obvious differences in body complexity, presence/absence of adaptive immune components, and an open or closed circulatory system will no doubt attribute to differential ETotic responses observed in invertebrates and vertebrates.

In mammals, 24 proteins have been identified in association with NETs, including the histones H2A, H2B, H3 and H4 (nuclear proteins) and granule proteins such as elastase, MPO, lysozyme, cathepsin G and defensins (Urban *et al*., 2009). The present study shows that histone H2A and PXN decorate the ETs of *C. maenas*. There are likely to be

other proteins associated, but it was not possible to investigate this as part of the current study. The cytochemistry of haemocyte granules in crustaceans has not been well-characterized compared with other invertebrate taxa, but lysozyme, phosphatase, esterase and β-glucuronidase have all been localized in the granular haemocytes of shrimp (Hose *et al*., 1987; Sung & Sun 1999; Misra *et al*., 2004) and it is likely that GCs from other decapods are similar in content. Additional proteins that might decorate *C. maenas* ETs include the 6.5 kDa proline-rich AMP (Schnapp et al., 1996) and the 11.5 kDa cysteine-rich AMP carcinin (Relf *et al*., 1999; Brockton *et al*., 2007).

The present study showed that ET formation in the crab is part of *in vivo* defence, and that *in vitro* observations such as DNA extrusion, H2A and PXN localization are repeated *in vivo* as part of capsule formation. Future *in vitro* work on ETosis in invertebrates is likely to include characterization of ET proteins and it is probable that any identified would also be present *in vivo*. Although the results of the present *in vivo* work focussed on antimicrobial defence mechanisms, simulated by LPS injection, it is possible that ETosis plays a wider role in invertebrate physiology. As aggressive scavengers, crabs receive extensive wounds and frequently shed and re-grow damaged appendages. It would be of interest to investigate whether the scaffold provided by ETs in capsules also plays roles in wound repair or limb regeneration. Similarly, as animals which moult regularly, it is possible that ETosis could be involved in carapace formation and hardening.

Besides demonstrating the role of ETs in crustacean defence, the present study is also the first to show ETotic-like structures being generated from cells from different taxa. Remarkably, this included the anemone, *A. equina*, an acoelomate lacking a circulatory system. While the present study lacked the scope to repeat all the characterization in both species, naturally, this would need to be completed as part of future work. While ROS-dependency was demonstrated, follow-up work would need to demonstrate other key diagnostic features of ETosis. This ideally would include investigating the decoration of the extruded chromatin, more detailed study of the process in different cell types, and demonstration of ETotic responses *in vivo*. The decoration of ETs in the mussel is

particularly relevant, as mussel haemocytes contain elastase, cathepsin G, lysozyme and proteinases (Pipe, 1990) which have all been found in association with mammalian NETs (Urban *et al*., 2009). As discussed above (Chapter 6, Section 6.4) it is not easily explained why *M. edulis* haemocytes required far greater PMA concentrations and longer incubation periods to induce measurable levels of chromatin extrusion. While *A. equina* amoebocytes reacted at similar PMA concentrations and time conditions as crab HCs, their lower extrusion values are probably accounted for by the fact that the cells were much less enriched compared with crab HCs. By the nature of their body forms, size and ease of collection/maintenance, cnidarians are not an easy group to study in terms of immune defence. In order to optimize further work on ETosis in this group, it would be necessary to improve cell enrichment and characterization first.

A recent paper which emerged during the writing of this thesis found that ET-like structures could be induced in haemocytes of the Pacific oyster, *Crassostrea gigas*, by the bacteria, *Vibrio tasmaniensis* and *Brevibacterium stationis*, as well as zymosan (Poirier *et al*., 2014). Here, antimicrobial histones were also associated with ET-like structures, and these too were released from haemocytes in a ROS-dependent manner (Poirier *et al*., 2014). The oyster ET-like structures were capable of entrapping bacteria and *in vivo*, ETs together with antimicrobial histones were found consistently in gill tissue following injury and infection with *Vibrio* (Poirier *et al*., 2014). In common with the present study, PMA posed difficulties in stimulating the structures, with the authors concluding that the 'standard' concentration of PMA did not work on oyster cells. It is possible that if they had increased their concentrations/times that they might have observed chromatin release. The extensive literature on bivalve immunity has demonstrated many close similarities between oyster and mussel species, therefore it is probable that the characteristics of ETotic-like processes would be comparable. This further emphasizes the point that signalling pathways will not necessarily be identical across invertebrate taxa.

Although the evidence of ETotic-like events in sea anemone cells indicates the antiquity of the process in preceding the evolution of the coelom, genomic data is necessary to reveal the true phylogeny of ETosis. Superficially, there is commonality between ETosis

in different vertebrate and invertebrate species, but it is plausible that the process could have evolved separately more than once. At present, no genomic data exists regarding ETosis, although the use of models such as *Drosophila* will shed light on this in due course. If genetic data upholds the hypothesis that ETosis is an ancient process, then this could contribute to understanding some of its pathological effects in higher vertebrates. Their more complex vasculature together with an adaptive immune system suggests that externalized chromatin released could become problematic, thus implying that ETosis in higher vertebrates might be a double-edged sword. The benefits of ETosis in mammals include antimicrobial activity (von Kockritz-Blickwede and Nizet, 2009), the initiation and regulation of coagulation pathways (Iba *et al*., 2014), as well as anti-inflammatory activities (Farrera and Fadeel, 2013; Schauer *et al*., 2014). However, much of the medical literature implies that un-regulated or excessive ETosis is pro-inflammatory, where extruded ETotic material in the immediate extracellular environment becomes detrimental if not resolved, or evokes an adaptive response.

While haemocyte entrapment by externalized chromatin is essential for capsule development in invertebrates, in mammals, a similar assembly of leukocytes and platelets on DNA meshes can promote venous thrombosis (Brill *et al*., 2012; Fuchs *et al*., 2010, 2012). Moreover, it appears that NETs can also trap cancerous cells and enable their adhesion to healthy tissues, hence promoting metastasis (Cools-Lartigue *et al*., 2013). ETosis is further associated with chronic respiratory diseases such as cystic fibrosis, where extracellular chromatin leads to an increase in sputum viscosity that consequently aids microbial colonization and biofilm formation (Papayannopoulos *et al*., 2011; Young *et al*., 2011; Dubois *et al*., 2012). The majority of extracellular DNA found in the sputum of cystic fibrosis patients is NET derived, as the DNA-complexes are consistent with neutrophil ETosis and share a similar protein signature (Dwyer *et al*., 2014).

In mammals, the failure of NET clearance, coupled with inappropriate activation of adaptive immune responses is implicated in several autoimmune disease states, such as SLE (Lande *et al*., 2011) and rheumatoid arthritis (Khandpur *et al*., 2013). SLE is characterized by the production of auto-antibodies against immunogenic complexes of

self-DNA and neutrophil AMPs occurring through NETs (Lande *et al*., 2011). These complexes can pose further problems, with impairment of NET degeneration associated with glomerulonephritis, which blocks the filtering process in the kidney, lupus nephritis (kidney inflammation) and impairment of renal function (Hakkim *et al*., 2010). With regard to rheumatoid arthritis, Khandpur *et al*. (2013) found that the synovial fluid of affected joints and the rheumatoid nodules in skin contained a high number of NETs. In certain instances, auto-antibodies were also formed against citrullinated vimentin (an intermediate filament protein) on externalized chromatin released from ETotic neutrophils (Khandpur *et al*., 2013).

Evidently extracellular chromatin released during ETosis can become problematic. Therefore, ETosis investigations in lower vertebrates, such as fish and agnathans (jawless fish e.g. hagfish and lampreys), particularly at the gene level will become important in attempting to understand ETosis-associated pathologies in higher vertebrates. Agnathans were the first vertebrates known to arise over 500 million years ago (Shu *et al*., 1999) and do not possess true antibodies (instead they contain lymphocyte-like cells that produce functional analogues of immunoglobulins). Therefore, research on ETosis in such organisms will help reveal the true development of ETosis through vertebrate taxa. Currently, it remains unknown when ETosis first arose in eukaryotic evolution, thus it remains unclear how far down the evolutionary ladder it might be found. If successful demonstrations of ETosis in ancient invertebrate groups, as well as in early chordates can be achieved, these findings will contribute to answering fascinating questions. On a broad scale, they can address questions such as the evolutionary origins of programmed cell death, e.g. considering which of the various processes arose first (apoptosis or ETosis), and whether externalised chromatin is purely deployed for defence or serves additional beneficial purposes.

Appendices 1-9

Appendix 1.

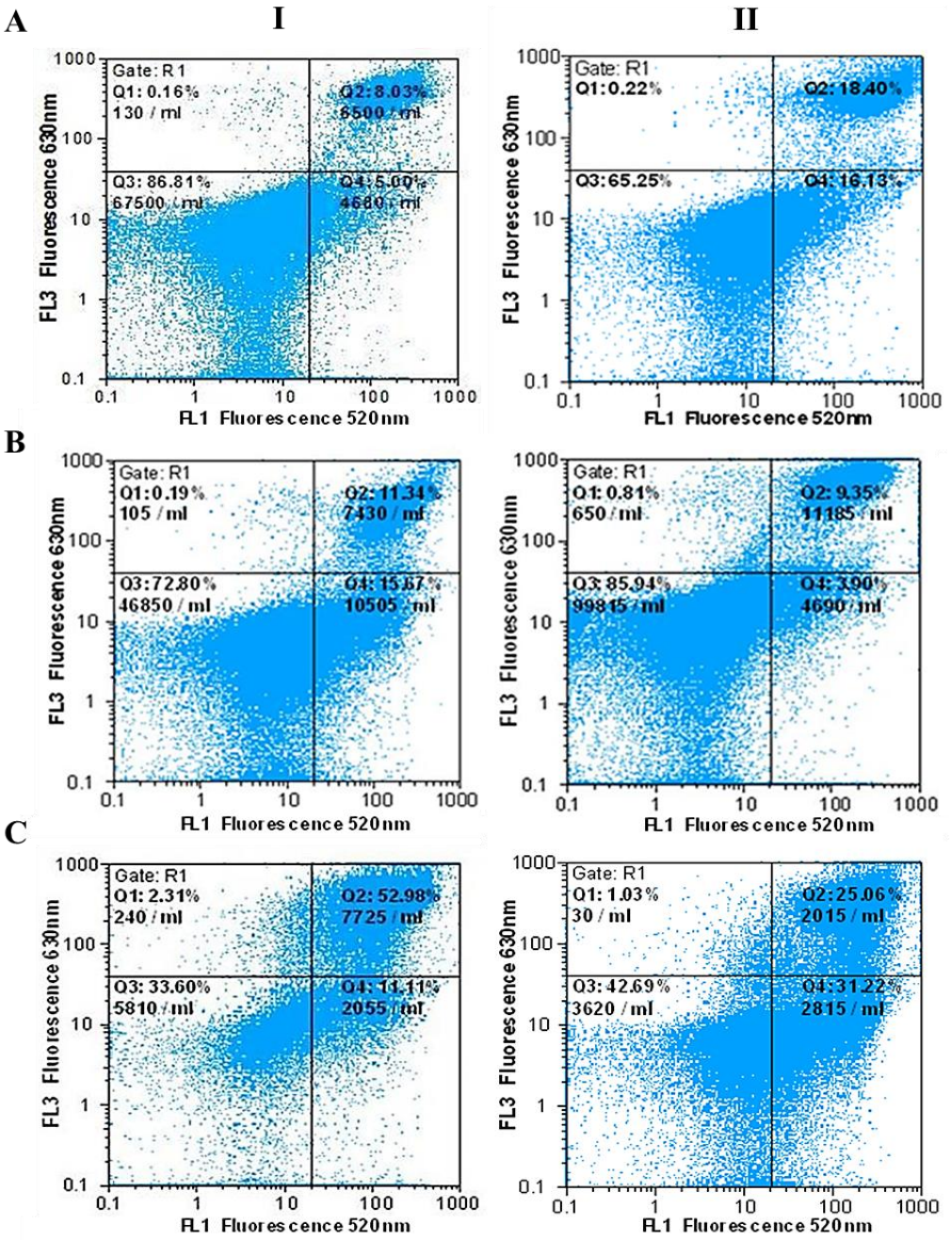

Appendix 1. Representative flow cytometry dotplots of *C. maenas* mixed haemocytes after suspension culture at different temperatures *in vitro*. (**A**-**C**): Proportions of viable, early apoptotic and late apoptotic/necrotic cells after 6 h (**I**) and 24 h culture (**II**) culture at 4°C (**A**), 10°C (**B**, control) or 20°C (**C**). Flow cytometry dotplots representative of n=3 experiments.

Appendix 2.

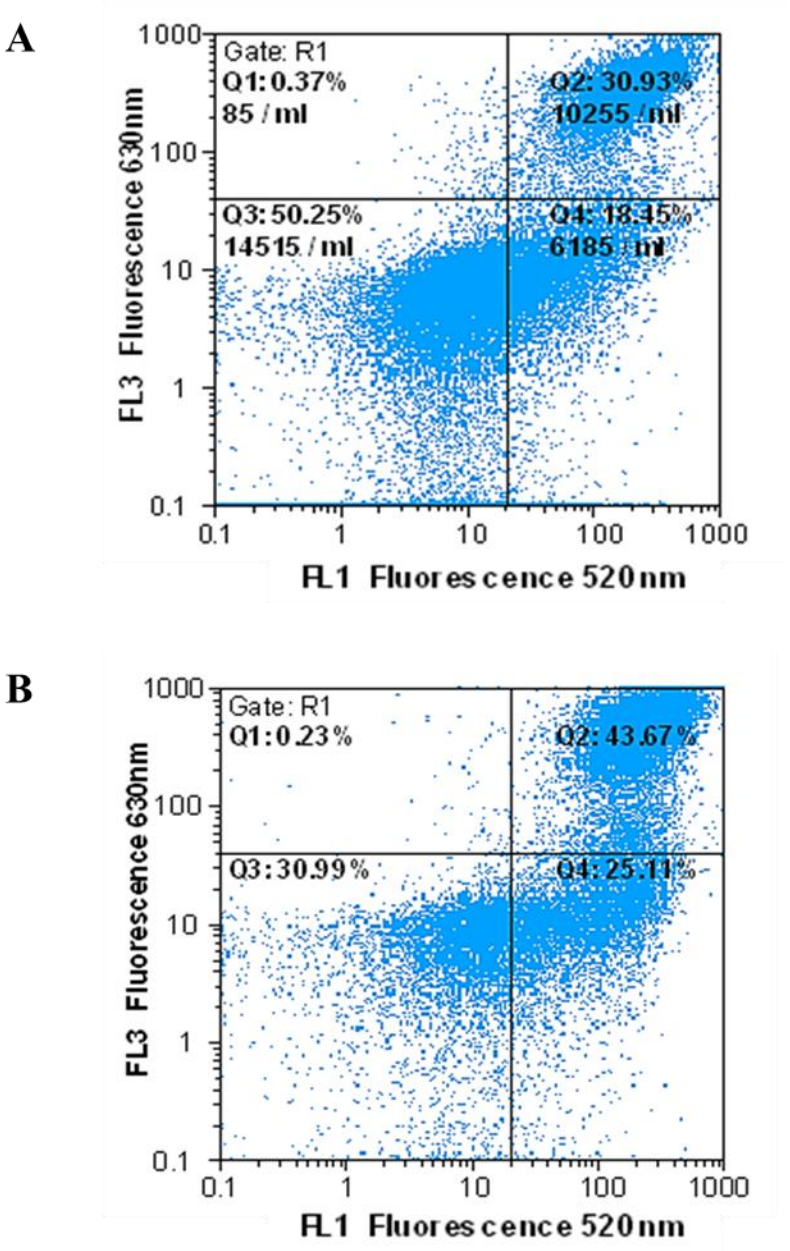

Appendix 2. Representative flow cytometry dotplots of mixed haemocytes after suspension culture *in vitro*, obtained from *C. maenas* individuals subject to repeated haemolymph sampling. (**A-B**): Proportions of viable, early apoptotic and late apoptotic/necrotic cells after 6 h (**A**) and 24 h culture (**B**) at 10°C. Flow cytometry dotplots representative of n=3 experiments.

Appendix 3.

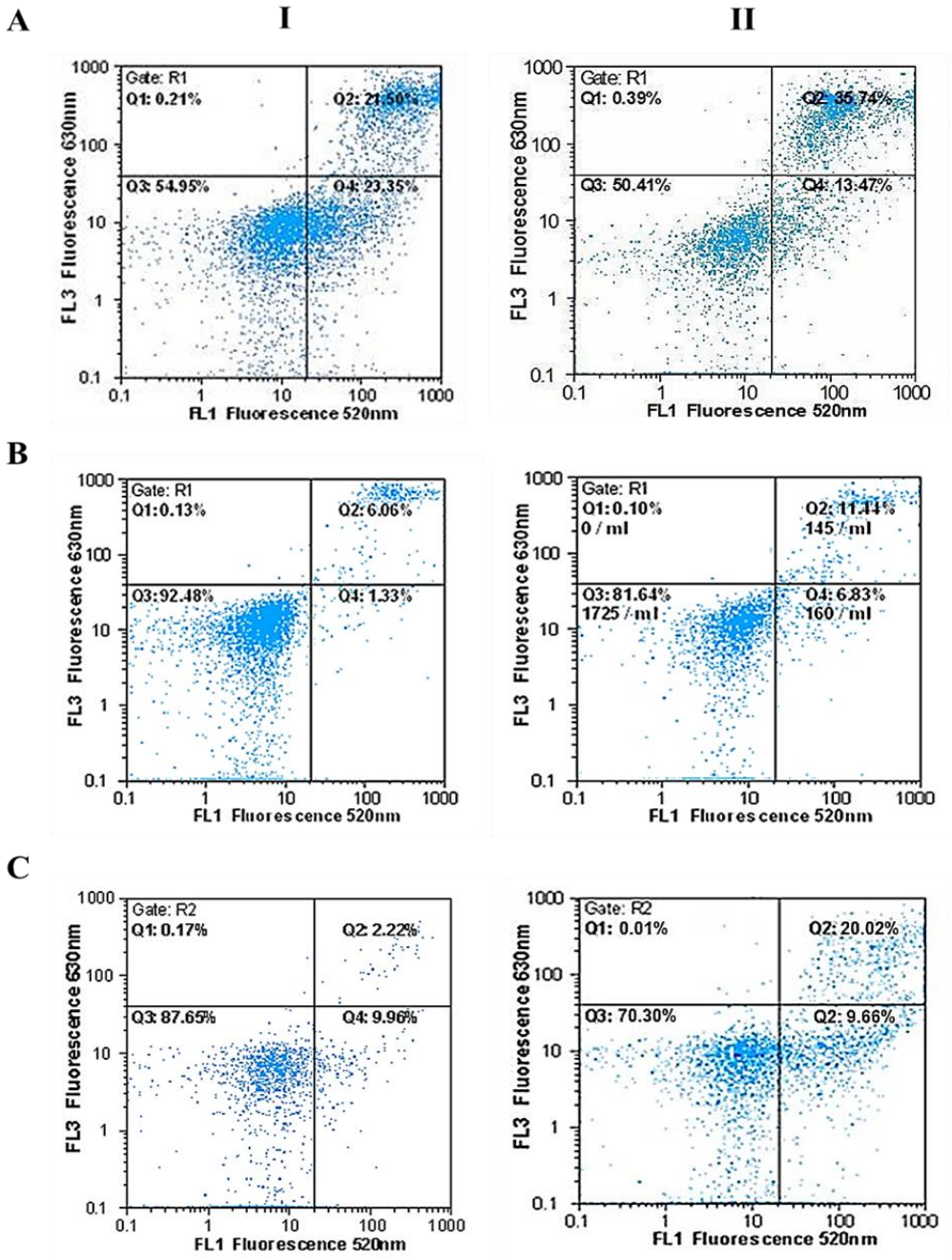

Appendix 3. Representative flow cytometry dotplots of *C. maenas* separated haemocytes after suspension culture *in vitro*. (**A-C**): Proportions of viable, early apoptotic and late apoptotic/necrotic HCs (**A**), GCs (**B**) or ProHs (**C**) after 6 h (**I**) and 24 h culture (**II**) at 10°C. Flow cytometry dotplots representative of n=3 experiments.

Appendix 4.

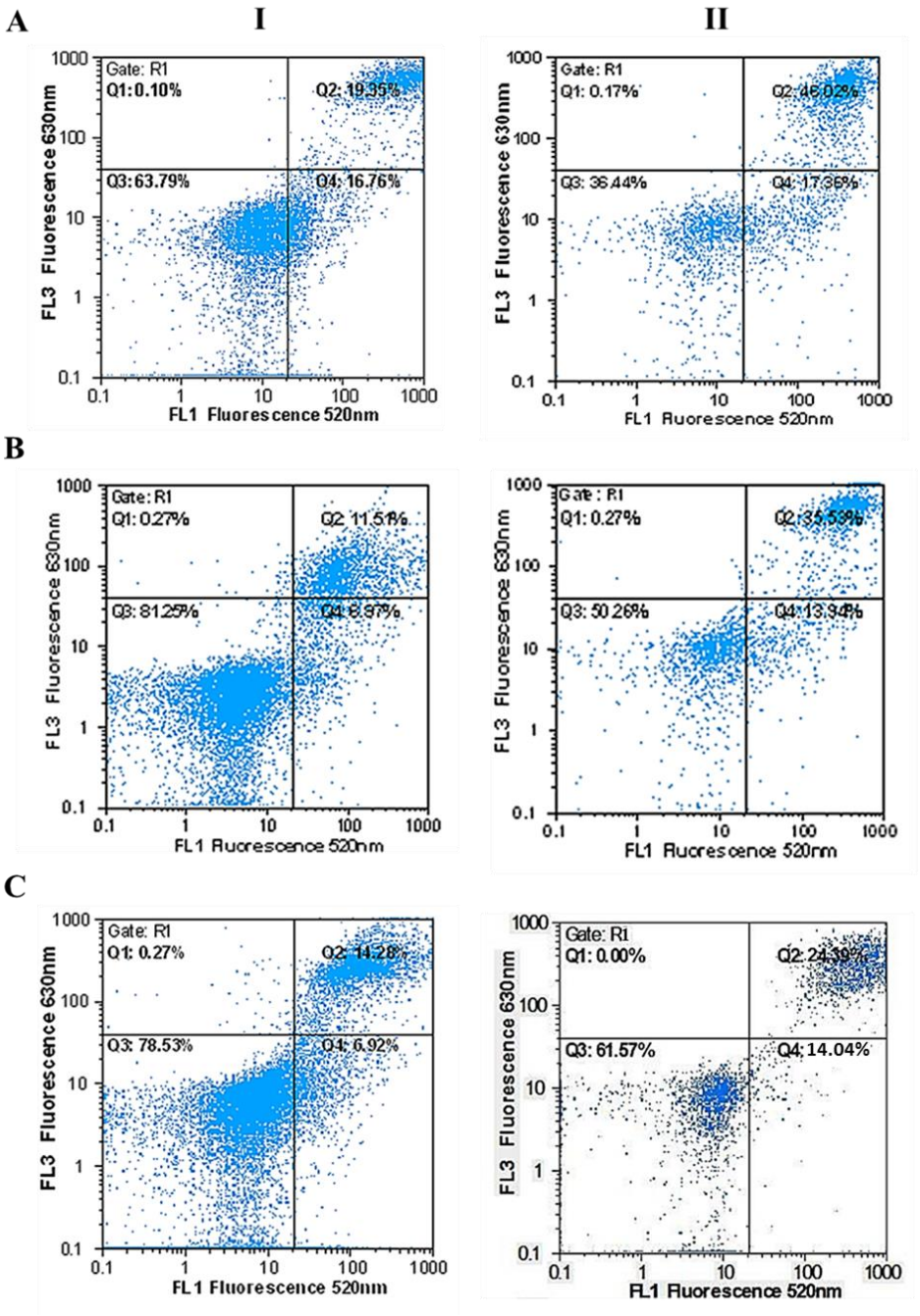

Appendix 4. Representative flow cytometry dotplots of *C. maenas* separated HCs after suspension culture with LPS *in vitro*. (**A-C**): Proportions of viable, early apoptotic and late apoptotic/necrotic untreated (control) HCs (**A**), 0.1 µg mL^{-1} LPS treated HCs (**B**) or 1 µg mL^{-1} LPS treated HCs (**C**) after 6 h (**I**) and 24 h culture (**II**) at 10°C. Flow cytometry dotplots representative of n=3 experiments.

Appendix 5.

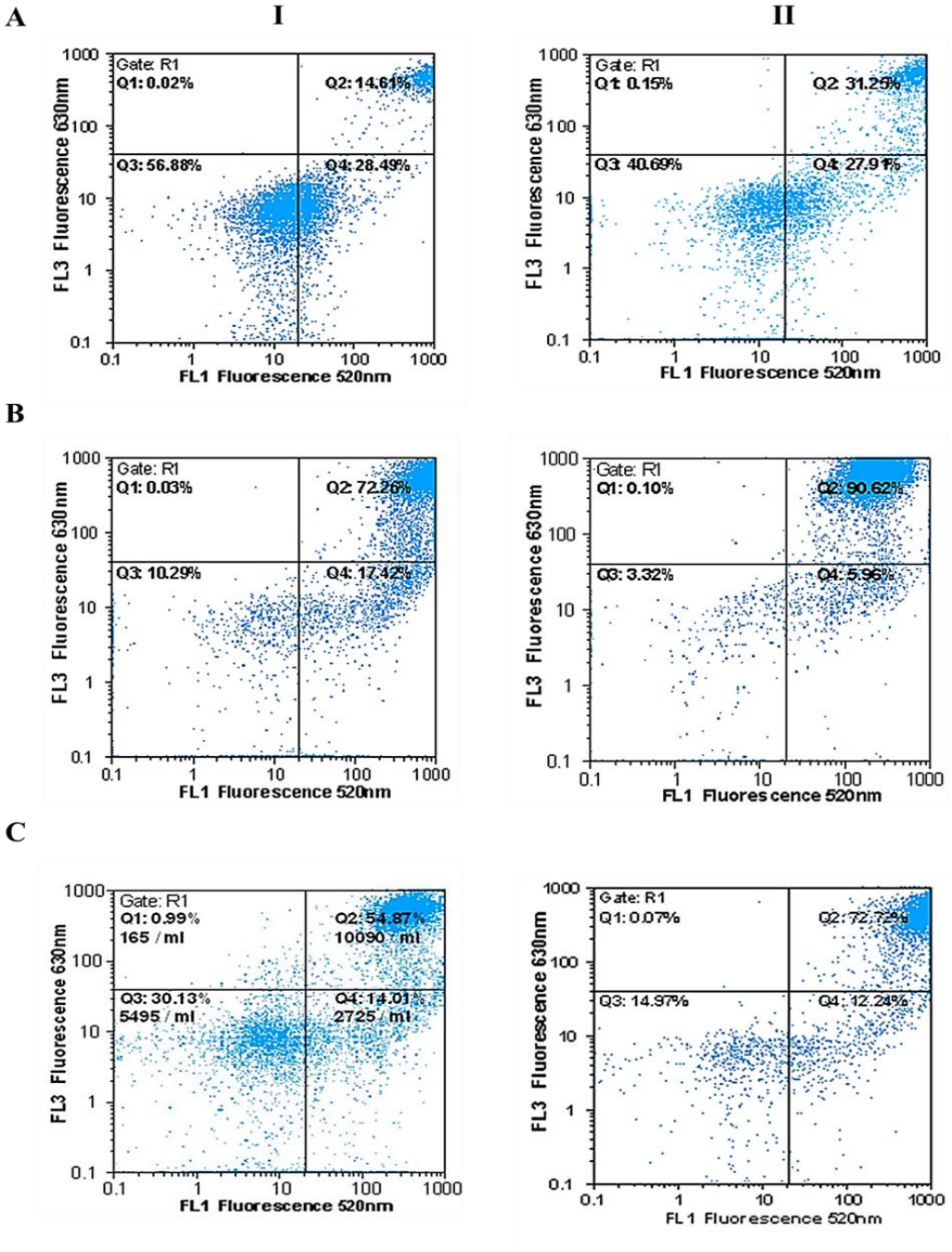

Appendix 5. Representative flow cytometry dotplots of *C. maenas* separated HCs after suspension culture with *Listonella anguillarum in vitro.* (**A**-**C**): Proportions of viable, early apoptotic and late apoptotic/necrotic untreated (control) HCs (**A**), HCs treated with 3 x 10^8 mL^{-1} viable *L. anguillarum* (**B**) or HCs treated with 3 x 10^8 mL^{-1} heat-killed *L. anguillarum* (**C**), after 6 h (**I**) and 24 h culture (**II**) at 10°C. Flow cytometry dotplots representative of n=5 (**A** and **B**) or n=3 experiments (**C**).

Appendix 6.

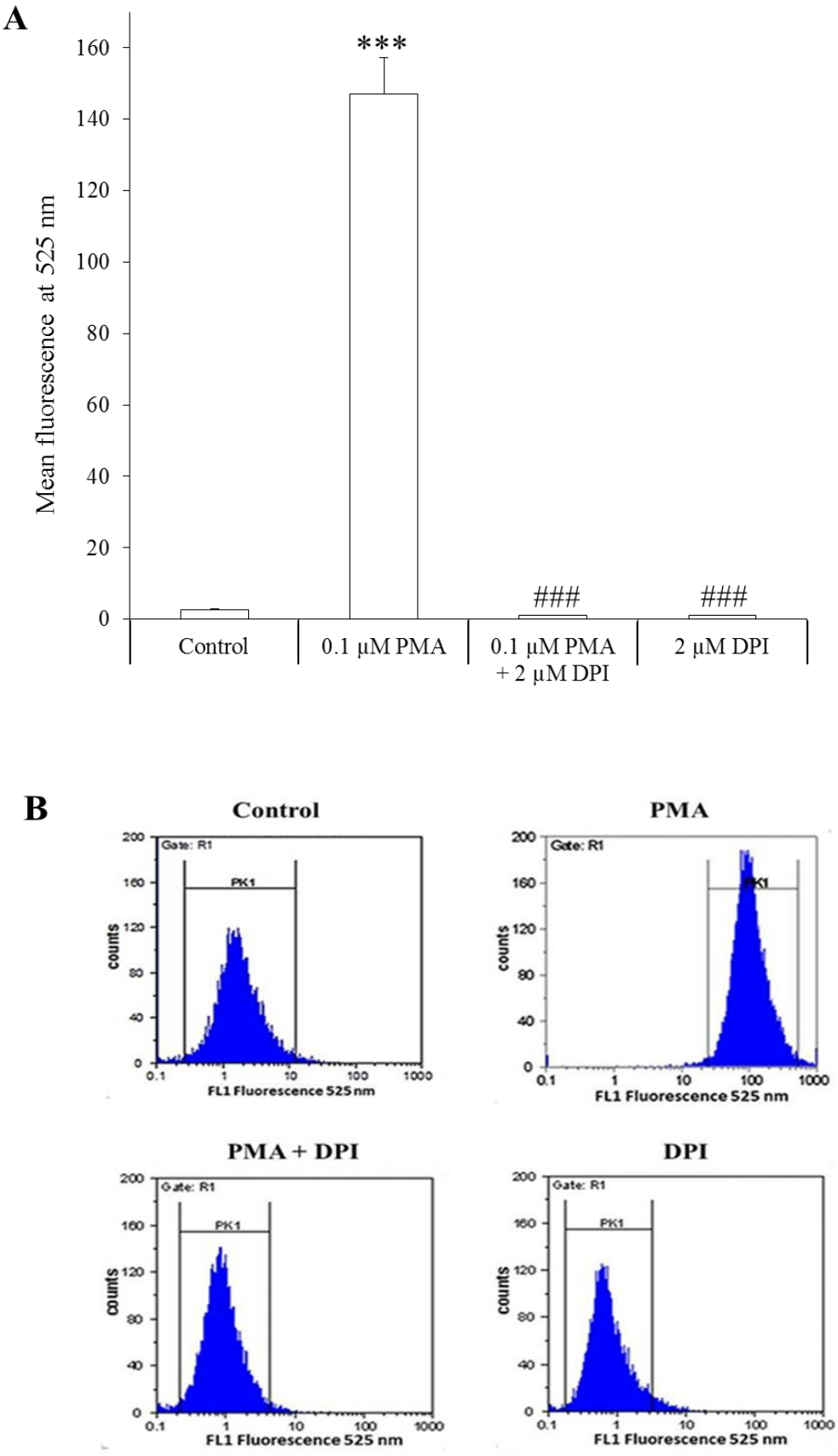
A
Mean fluorescence at 525 nm
160
140
120
100
80
60
40
20
0
***
###
###
Control
0.1 µM PMA
0.1 µM PMA + 2 µM DPI
2 µM DPI
B
Control
PMA
PMA + DPI
DPI
Gate: R1
PK1
counts
FL1 Fluorescence 525 nm
0.1
1
10
100
1000

Appendix 6 continued.

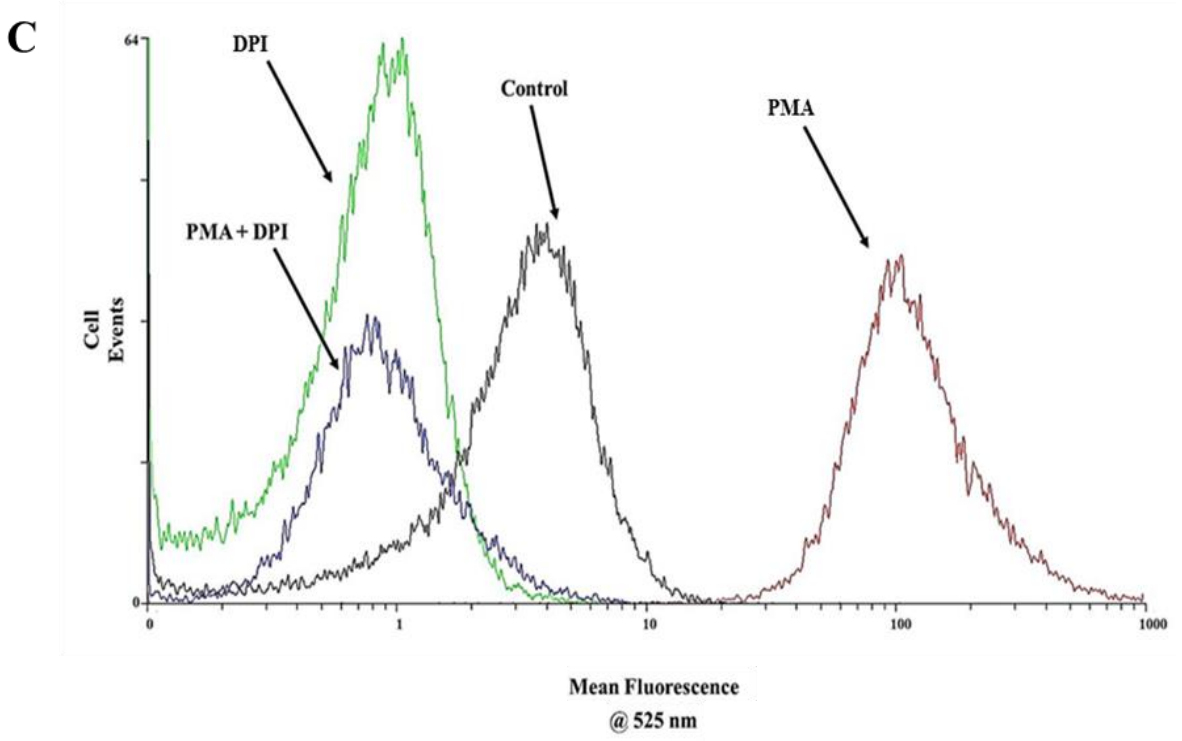

Appendix 6. Confirmation of ROS generation from *C. maenas* HCs *in vitro*.
(**A**): Mean fluorescence at 525 nm measured in HCs subject to the DHR 123 assay, via flow cytometry, after 24 h culture (10°C) with different combinations of 0.1 µM PMA and 2 µM DPI (NADPH-oxidase inhibitor).Control (untreated) HCs were cultured in ML-15 only. Data are expressed as means ± SEM, n=3, with a different crab used on each occasion**.** Statistical analysis was performed upon un-transformed data using one-way ANOVA with a Student Newman-Keuls multiple comparison *post hoc* test. *** $P<0.001$ vs. mean fluorescence emitted from control (untreated) HCs; ### $P<0.001$ *vs.* mean fluorescence emitted from 0.1 µM PMA only treated HCs. (**B**): Representative flow cytometry fluorescence histograms (at 525 nm) of control, PMA, PMA + DPI and DPI treated HCs. A large shift increase in fluoresce was observed in HCs treated with PMA indicative of ROS generation. No shift increases were observed in PMA + DPI and DPI treated HCs, indicating inhibition of ROS generation. Similarly, low basal levels of ROS generation were observed in control HCs; (**C**): Fluorescence histogram overlay of representative control, PMA, PMA + DPI and DPI treated HCs composed using WinMDI™.

Appendix 7.

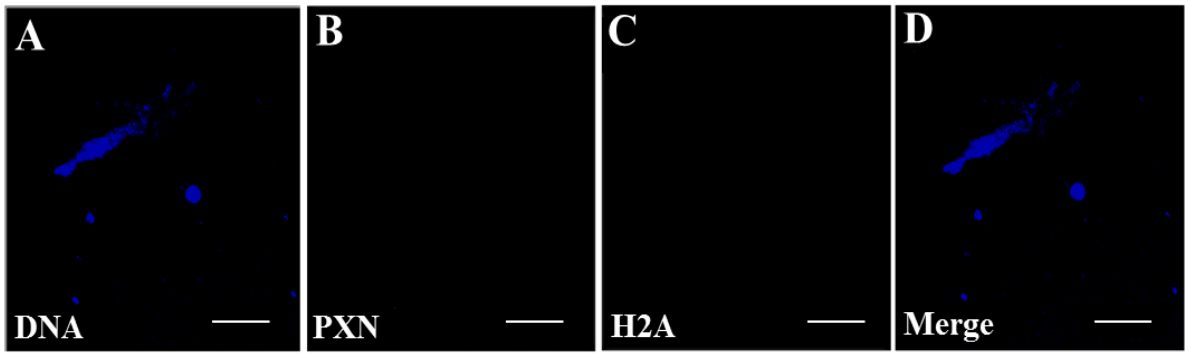

Appendix 7. Immunocytochemical analysis revealed no non-specific staining on extracellular chromatin released from *C. maenas* HCs *in vitro*. Immunocytochemistry was performed upon HCs after 24 h culture with 0.1 µM PMA using confocal microscopy without phase contrast transmission. Instead of primary antibodies 3% BSA was added, secondary antibodies were then added into the mix with Draq-5 DNA stain. (**A**): DNA revelaed by Draq-5 staining; (**B-C**): No un-specific staining was detected at the emission wavelengths for the detection of PXN (**B**) and H2A (**C**); (**D**): Merge of all three images showing no un-specific staining on extracellular chromatin released from a HC.
Scale bars = 25 µm.

Appendix 8.

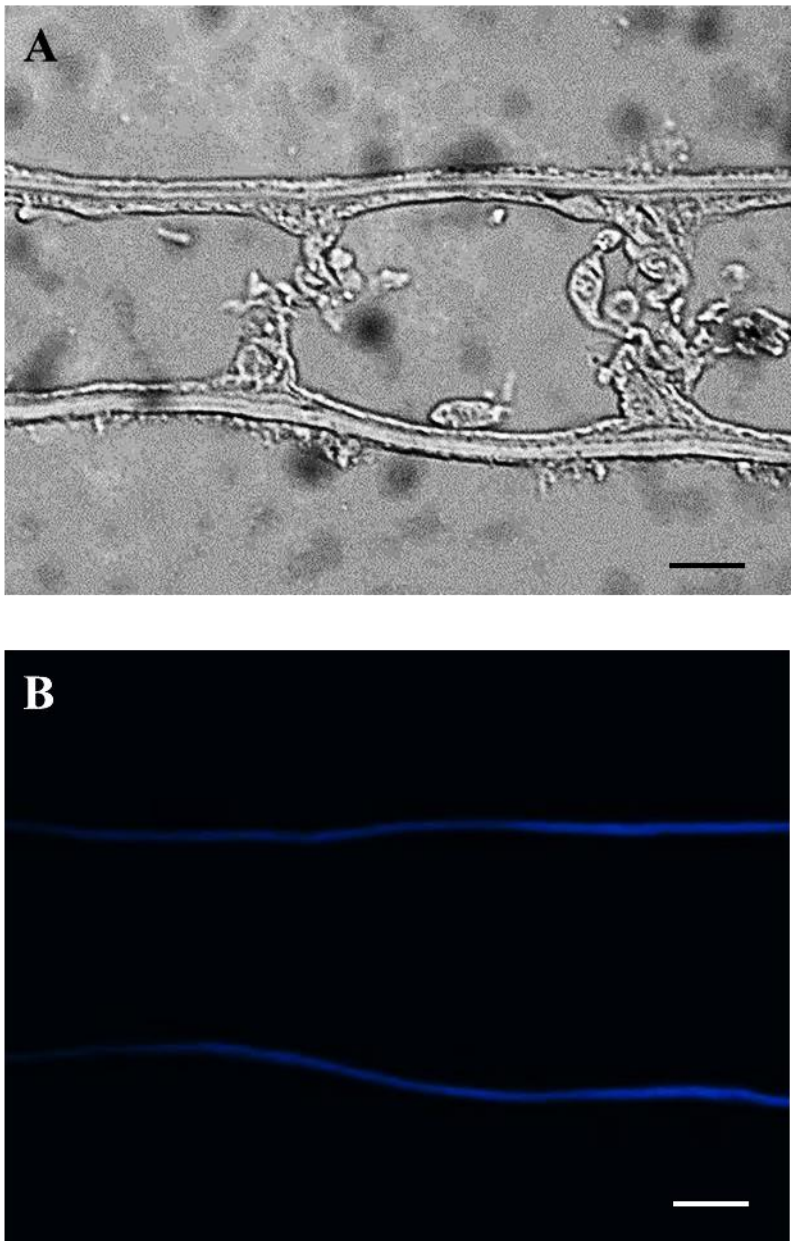

Appendix 8. *In vivo* assessment of auto-fluorescence from *C. maenas* gill tissue. Fluorescence microscopy analysis of paraffin wax sections of gill lamellae excised from a control crab 24 post saline injection. (**A**-**B**): Images of unstained gill lamellae taken with phase transmission (**A**) or without phase transmission (**B**) at the same field of view. The interior gill architecture can clearly be seen (**A**) but does not auto-fluoresce at the DAPI emission wavelength (**B**). Only the outer lining of the gill auto-fluoresces at the DAPI emission wavelength (**B**). Images taken at 400x total mag, scale bars = 20 µm.

Appendix 9.

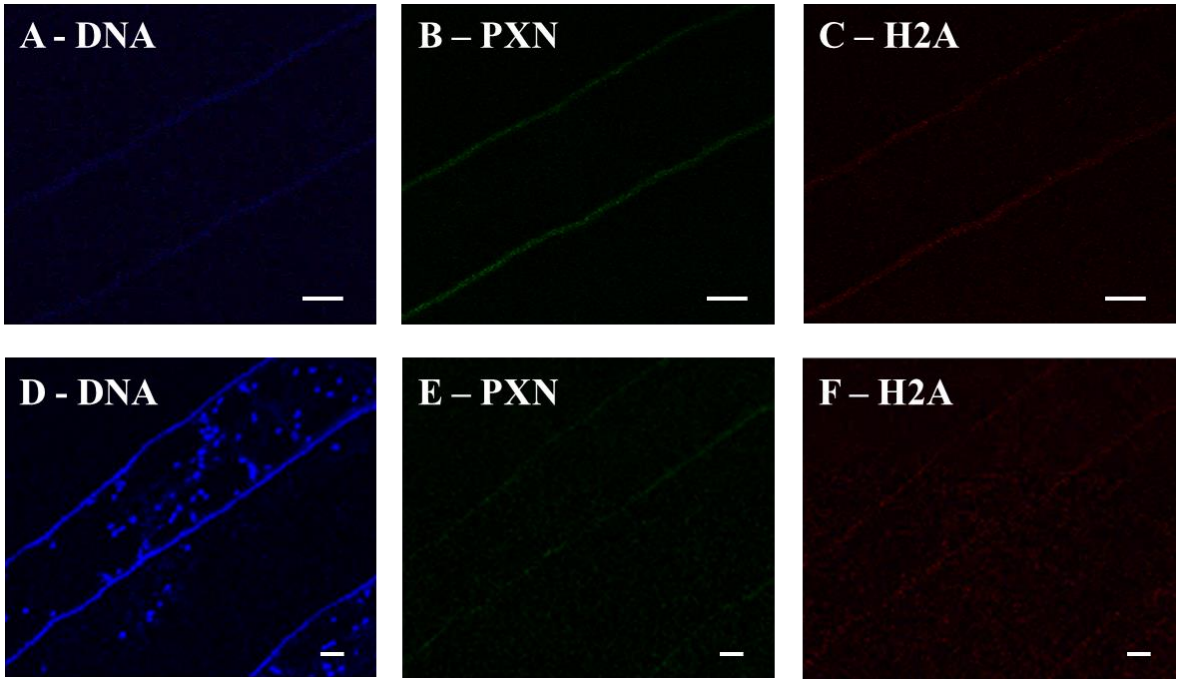

Appendix 9. *In vivo* immunohistochemical assessment of auto-fluorescence and non-specific staining in *C. maenas* gill tissue. Confocal microscopy analysis (without phase contrast transmission) of paraffin wax sections of gill lamellae excised from an experimental crab 1 h post injection of 20 µg mL^{-1} LPS. (**A-C**): Unstained control (received no stain at all) images which display the auto-fluorescence emitted from the outer gill lining at the emission wavelengths for detection of DNA (**A**), PXN (**B**) and H2A (**C**). (**D-F**) Secondary antibody control images (no primary antibodies but received secondary antibodies and TO-PRO-3 iodide DNA stain) at a different region of the gill which displays DNA staining of haemocytes within the gill, as well as a small proportion of extracellular DNA (**D**). Importantly, no non-specific staining was observed within the gill at the emission wavelengths for detection of PXN (**E**) and H2A (**F**). All scale bars = 20 µm.

Appendix 10:

Published Paper

nature COMMUNICATIONS

ARTICLE

Received 2 Dec 2013 | Accepted 8 Jul 2014 | Published 13 Aug 2014

DOI: 10.1038/ncomms5627 OPEN

Invertebrate extracellular phagocyte traps show that chromatin is an ancient defence weapon

Calum T. Robb[1,2], Elisabeth A. Dyrynda[1], Robert D. Gray[2], Adriano G. Rossi[2] & Valerie J. Smith[3]

Controlled release of chromatin from the nuclei of inflammatory cells is a process that entraps and kills microorganisms in the extracellular environment. Now termed ETosis, it is important for innate immunity in vertebrates. Paradoxically, however, in mammals, it can also contribute to certain pathologies. Here we show that ETosis occurs in several invertebrate species, including, remarkably, an acoelomate. Our findings reveal that the phenomenon is primordial and predates the evolution of the coelom. In invertebrates, the released chromatin participates in defence not only by ensnaring microorganisms and externalizing antibacterial histones together with other haemocyte-derived defence factors, but crucially, also provides the scaffold on which intact haemocytes assemble during encapsulation; a response that sequesters and kills potential pathogens infecting the body cavity. This insight into the early origin of ETosis identifies it as a very ancient process that helps explain some of its detrimental effects in mammals.

[1] Centre for Marine Biodiversity and Biotechnology, School of Life Sciences, Heriot Watt University, Edinburgh, Scotland EH14 4AS, UK. [2] Centre for Inflammation Research, Queen's Medical Research Institute, University of Edinburgh, Edinburgh, Scotland EH16 4TJ, UK. [3] Scottish Oceans Institute, School of Biology, University of St Andrews, St Andrews, Scotland KY16 8LB, UK. Correspondence and requests for materials should be addressed to V.J.S. (email: vjs1@st-andrews.ac.uk).

ETosis was first discovered in mammalian neutrophils[1] and is now known to occur in a variety of mammalian innate immune cells[2–5]. The phenomenon entails the expulsion of chromatin from the nucleus via reactive oxygen species (ROS) involvement and can be induced by various agents such as the protein kinase C activator, phorbol myristate acetate (PMA), H_2O_2 from the respiratory burst, lipopolysaccharide (LPS) or bacteria[6–8]. The discharged chromatin forms complex meshes that ensnare and kill bacteria, fungi, viruses and other parasites[7,9,10]. The process is now widely regarded as an important part of the mammalian inflammatory repertoire, but has also been implicated in a number of disease states, such as thrombosis, mastitis, appendicitis, preeclampsia, arthritis and promotion of cancer metastasis[11–13]. Although mainly described in mammalian systems, ETosis also occurs in chicken heterophils[14] and fish phagocytes[15]. However, the presence and role of ETosis in invertebrates has not been explored in detail, even though understanding the phylogeny of the process may help explain its varied effects in mammals.

As invertebrates depend on the innate activities of blood cells for defence and possess the key structures and protein homologues necessary to execute inflammation, we hypothesized that ETosis could be an important primordial defence strategy. For animals in lower taxa, especially those with an open circulatory system, we theorized that chromatin externalized by ETosis would represent a powerful way to contain infectious agents gaining entry into the body cavity and could play a role in the encapsulation of foreign materials by the haemocytes. For these studies, the shore crab, *Carcinus maenas,* was used as the main experimental animal because it possesses large populations of haemocytes that can be separated on Percoll and manipulated easily *in vitro*[16]. To investigate if ETosis occurs more widely across the invertebrates, comparative studies were also made on a distantly related protostome, the blue mussel, *Mytilus edulis*, and a cnidarian, specifically the sea anemone, *Actinia equina.* Mussel haemocytes are avidly phagocytic and display a strong respiratory burst[17,18]. Sea anemones, while not possessing a dedicated coelomic immune system, nevertheless, contain phagocytes within the mesoglea that are known to undergo a respiratory burst[19] and express ROS-relevant genes[20]. Therefore, we performed a study to ascertain if immune cells from these invertebrates exhibit ETosis.

The findings reported here confirm that invertebrate defence cells are indeed capable of ETosis and at least in crab, the process contributes to encapsulation reactions mounted against non-self agents. That an acoelomate invertebrate also undergoes an ETotic-type response shows for the first time that chromatin release is an ancient and evolutionary conserved mechanism.

Results

Characterization of chromatin release from crab haemocytes. Hyaline cells (HCs) were utilized for initial experiments, as among the four types of haemocyte in *C. maenas*, they are the only ones known to be both phagocytic and able to undergo a respiratory burst[21,22]. We found that treating preformed monolayers of isolated populations of crab HCs with PMA resulted in expulsion of material staining positively with Sytox Green (Fig. 1a–e). This reagent binds DNA but only permeates cells that have lost membrane integrity and thus reveals dead cells or exposed nucleic acid. Ejection of chromatin usually occurs between 2 and 24 h with the extruded material forming diffuse (puffball-like) structures (Fig. 1a,b), spread (comet-like) structures (Fig. 1c) or extended strands that interlink across cells (Fig. 1d,e), similar to the morphology of NETs produced by mammalian neutrophils[23]. Maximal expulsion of chromatin was achieved with 0.1 μM PMA over 24 h (Supplementary Fig. 1a,b), with 63.4 ± 5.1% s.e.m. of the haemocytes showing the phenomenon under these conditions. By contrast, the proportion was <5% in the controls. Importantly, DNAse-1 completely dissolved the material released from the HCs, confirming that it is chromatin (Supplementary Movie 1). Transmission electron microscopy revealed that nuclear membrane breakdown precedes chromatin release (Fig. 1f), as in neutrophils[6]. Moreover, there is no peripheral condensation of chromatin at the nuclear membrane, in contrast to healthy cells (Fig. 1g) or apoptotic cells (Fig. 1h; Supplementary Fig. 2a–d) Rather, scanning electron microscopy (SEM) showed that, unlike untreated haemocytes (Fig. 1i), extruded DNA forms a large extracellular complex mesh of strands (Fig. 1j) studded with small granules resembling globules (Fig. 1k). Thus expelled chromatin from crab haemocytes has a similar structure to mammalian NETs, although the smooth domains are *ca.* 26.0 nm (± 1.75 nm s.e.m.) in diameter while the globular domains are 47.8 nm (± 3.4 nm s.e.m.) in diameter, both of which are slightly larger than those previously determined for neutrophils[1]. Chromatin is similar in its dimensions across all animal taxa, but, at the ultrastructural level, differences in measurements may be introduced due to processing, type of microscopy and the analysis software used.

Immunocytochemical analyses to evaluate the decoration of the disgorged chromatin from HCs confirmed that it becomes associated with a protein recognized by an anti-myeloperoxidase antibody (Fig. 2a–d). This protein, peroxinectin (PXN), is a crustacean homologue of myeloperoxidase that is expressed by haemocytes involved in cell-to-cell adhesion[24,25]. In the present study, it was released from the perinuclear region of the HCs, as the antibody did not co-localize with the nucleus in intact cells (Fig. 2d). In addition, actin did not co-localize with the extracellular chromatin released from crab HCs (Fig. 2b,d) as was observed in NETs released from fathead minnow[15]. Crucially, we also demonstrate that histone H2A is liberated from the nuclei of the HCs to the extracellular environment (Fig. 2e–h). Non-specific staining was not apparent in any controls. Histones are highly conserved nuclear proteins with potent antibacterial properties[26]. ETosis is the only known mechanism by which they could be exposed to infective agents. Indeed decoration of chromatin NETs by histones is one of the characteristic features of the phenomenon for mammals[6].

The release of the extracellular chromatin by crab HCs was significantly reduced by diphenylene iodonium (DPI), apocynin, Ro-31-8220 and cytochalasin D (all $P<0.001$) (Fig. 3a). DPI inhibits flavoprotein oxidoreductases (including nicotinamide adenine dinucleotide phosphate (NADPH) oxidase) while apocynin inhibits the assembly of NADPH oxidase[27]. Ro-31-8220 is a pan protein kinase C inhibitor[28] that inhibits generation of ROS upstream of NADPH oxidase activation whereas cytochalasin D prevents actin polymerization[29]. These agents also inhibit ETosis by mammalian neutrophils[6,8,30,31], because NADPH oxidase and the cytoskeleton have crucial and overlapping roles in the process: NADPH oxidase is needed for decondensation of chromatin before its discharge, and the cytoskeleton is required for NADPH oxidase assembly[31]. Actin filamentation is also necessary for positioning the nucleus close to the plasma membrane and for rupture of the cell, hence the inhibitory effect of cytochalasin D, which also impairs histone citrullination[31]. Ro-31-8220 has been demonstrated to inhibit generation of ROS in human neutrophils[8]. It is therefore likely that chromatin release by crab HCs involves similar processes as those used by mammalian cells, so we conclude that the results taken together show that crab HCs are capable of undergoing vertebrate-type ETosis.

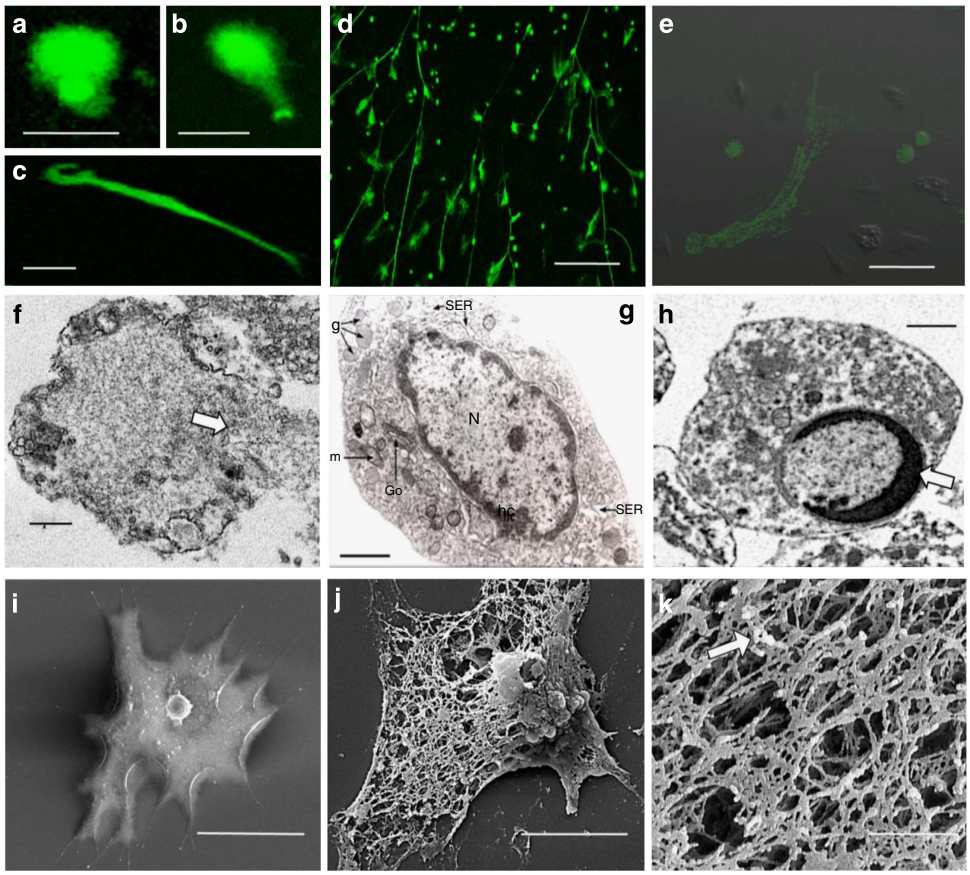

Figure 1 | Chromatin discharge by separated HCs from *C. maenas in vitro*. (**a**–**e**) Unfixed HCs in monolayer cultures stained with Sytox Green. (**a**,**b**) Diffuse extracellular chromatin at 3 h, 1.0 μM PMA. (**c**) Spread extracellular chromatin at 24 h, 0.1 μM PMA. (**a**–**c**) Scale bar, 30 μm. (**d**) Extended extracellular chromatin strands (24 h, 0.1 μM PMA). Scale bar, 300 μm. (**e**) Merged phase contrast and fluorescence images of an ETotic HC at 24 h (0.1 μM PMA). Also evident are viable cells and stained necrotic/late apoptotic cells with round stained nuclei. Scale bar, 50 μm. (**f**) TEM of a HC (24 h, 0.1 μM PMA) showing swelling of uncondensed chromatin, nuclear membrane breakdown and chromatin discharge from the cell at a breach point (arrow). (**g**) TEM of a control, unstimulated HC, N, nucleus with intact membrane and rim of condensed heterochromatin (hc) at the periphery. Go, Golgi body, g, granules, m, mitochondrion, SER, smooth endoplasmic reticulum. (**h**) TEM of an apoptotic HC showing an intact nuclear membrane with a thick, crescent shaped rim of condensed chromatin (arrow). (**f**–**h**) Scale bars, 1 μm. (**i**) SEM of control HC. Scale bar, 20 μm. (**j**) SEM of ETotic HC (24 h, 0.1 μM PMA). Scale bar, 5 μm. (**k**) SEM detail of extracellular chromatin released from a HC (24 h, 0.1 μM PMA). Arrow indicates granules studded on the extracellular mesh. Scale bar, 1 μm.

ETosis in crustacean host defence. To evaluate the role of chromatin release in crab host defence, additional *in vitro* experiments were performed using LPS or *Listonella anguillarum*, a mild bacterial pathogen of decapods, as the initiator. Both were found to significantly stimulate chromatin expulsion from the HCs within 24 h ($P<0.001$ compared with control) with no significant difference in the percentage of ETotic cells between treatment with LPS and the bacterium (Fig. 3a,b). With *L. anguillarum*, the bacteria become closely associated with the chromatin strands (Fig. 3c–e), in a similar way to the entrapment of bacteria by ETotic neutrophils[6]. The proportion of HCs induced by LPS or bacteria to extrude chromatin was found to be 31.0% (±4.2% s.e.m.) and 33.6% (±1.9% s.e.m.), respectively, after 24 h culture (10 °C) (Fig. 3b). These levels are lower than that achieved with PMA but perhaps reflect a more realistic level of response to natural infection. In both cases, the frequency of the responses were reduced to <2% by pretreatment with DPI ($P<0.001$).

Of the three other haemocyte types in *C. maenas*, only the semi-granular cells (SGCs) exhibited chromatin release 24 h after PMA treatment (0.1 μM) *in vitro* (Fig. 3f). Neither the prohaemocytes (immature haemocytes) nor the granular cells (GCs) showed the response (Fig. 3g,h). Curiously, there was better survival of prohaemocytes (Fig. 3g) than all other haemocyte types, whereas GCs showed the poorest survival as revealed by the large number of positively stained, non-chromatin extruding nuclei (Fig. 3h). The proportion of SGCs externalizing chromatin at this time was 50.8% (±3.8% s.e.m.), with <5% in the controls. In crab, the SGCs are known to degranulate and die in the presence of bacteria or LPS[32]. From the present study, it appears that the cells die through ETosis, although it remains unclear if SGCs are capable of a NADPH oxidase-dependent respiratory burst[22]. SGCs and GCs do, however, cooperate with the HCs in the encapsulation of microorganisms *in vivo*[33] and both show antimicrobial activity, in contrast to crab HCs, which do not[21].

Participation of ETosis in encapsulation reactions. Experiments to test the role of ETosis in encapsulation *in vivo* confirmed that 24 h following LPS injection, capsules formed and lodged within the gill lamellae (Fig. 4a–d) in a similar way to that reported previously with bacteria or β-1,3 glucans[33,34]. There is progression of haemocyte aggregation from 1 h post treatment, when intact haemocytes begin to associate (Fig. 4b),

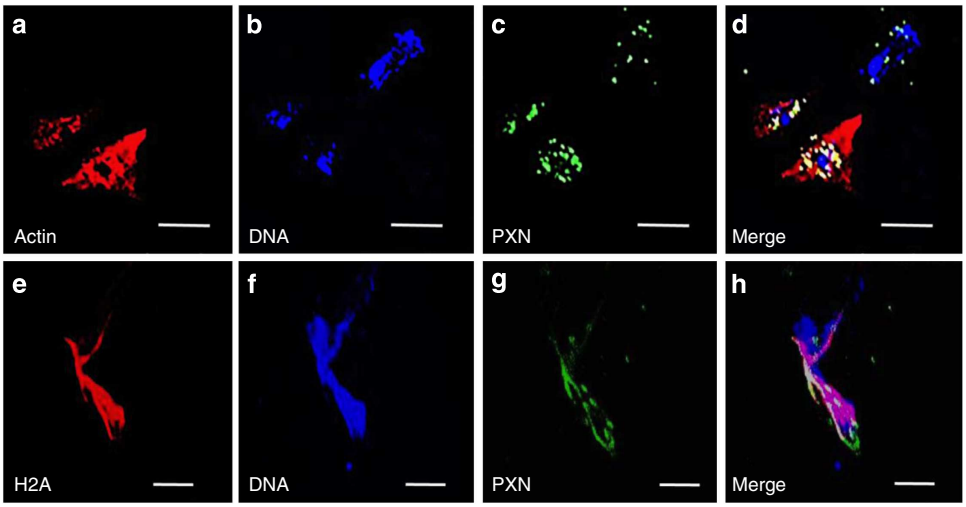

Figure 2 | Immunocytochemical analysis of chromatin released from HCs of *C. maenas in vitro*. (**a**–**d**) Localization of actin, DNA or PXN in an ETotic haemocyte (top right) and two non-ETotic haemocytes (bottom left), 24 h incubation with 0.1 μM PMA. (**a**) Actin shown by rhodamine phalloidin. (**b**) Visualization of DNA by Draq 5. (**c**) Localization of PXN, by anti-myeloperoxidase (MPO) antibody. (**d**) Merge of **a**–**c**. All scale bars, 25 μm. (**e**–**h**) Localization of histone H2A, DNA or PXN in a different ETotic cell. (**e**) Localization of H2A. (**f**) Visualization of DNA by Draq 5. (**g**) Localization of PXN, by anti-MPO antibody. (**h**) Merge of **e**–**g**. Note H2A co-localizes with extracellular DNA and PXN. All scale bars, 20 μm.

through coalescence into loose clumps at 3 h (Fig. 4c) and eventually development of fully formed, compact, structures after 24 h (Fig. 4d). Staining with 2-(4-amidinophenyl)-1H-indole-6-carboxamidine (DAPI) revealed that some haemocytes release chromatin within the first hour (Fig. 4f), but by 3 h, extracellular chromatin is much more in evidence, predominantly in the peripheral region of the clumps (Fig. 4g). By 24 h, chromatin is conspicuously diffused throughout the compacted cores of the capsules (Fig. 4h). Similar clumping was not apparent in the gills of the control crabs even after 24 h (Fig. 4a,e). Immunohistochemical analysis confirmed that at 1 h post LPS treatment, PXN is visible in the lumen of the gill filaments but is largely external to the cells (Fig. 4i,j). By contrast, some H2A does co-localize with extracellular nucleic acid (Fig. 4k,l). In the 3-h clumps, PXN is discernable within the clumps mainly in the outer regions and interspersed between intact cells (Fig. 4m,n). Co-localization of H2A with DNA, however, is more pronounced and occurs throughout the clump structure (Fig. 4o,p). Neither PXN nor H2A were seen extracellular to the haemocytes or the gill tissue of the sections from the controls. At 24 h, the capsules in the gills of experimental crabs were so densely compacted that visualization of individual elements was no longer possible. Autofluorescence was observed on the external surface (seawater side) of the gill lamellae, as confirmed from all unstained control sections. Moreover, apart from autofluorescence, non-specific staining was not seen in any of the immunohistochemical controls.

To further establish that ETosis plays a key part in the encapsulation response of crabs, additional assays were performed with PMA with or without DPI or DNAse-1. To avoid toxic effects of these reagents within the crab body, an *in vitro* approach was used. Washed unseparated haemocytes in suspension culture in ML-15 medium without these reagents were found to remain unclotted (Fig. 5a), with *ca.* 80% survival over 24 h (Supplementary Fig. 3). However, in the presence of PMA (0.1 μM), distinct haemocyte clumps, resembling capsules, developed over the 24 h incubation period (Fig. 5b–d). Confocal microscopy with Sytox Green staining revealed extracellular chromatin was present within these cell associations (Fig. 5e–h). At 1 h, the clumps were very loose with evidence of externalized chromatin within the haemocyte association (Fig. 5e). At this point, the cell aggregates varied considerably in size and were few in number (Fig. 5i,j). By 3 h, the clumps were larger with extracellular chromatin clearly evident within and around the constituent haemocytes (Fig. 5f), and were significantly more numerous compared with 1 h ($P<0.001$) (Fig. 5j). After 24 h, the clumps contained high numbers of highly compacted haemocytes (Fig. 5g,h). Long strings of haemocytes were seen attaching to some of the complexes (Fig. 5c) and strands of basophilic material were apparent emanating between the attaching and aggregated haemocytes (Fig. 5d). This material is likely to be of nuclear origin as similar strands were discernible on the Sytox Green stained preparations at this time point (Fig. 5g,h). By this time, the clumps were larger, but less numerous compared with those at 3 h ($P<0.001$) (Fig. 5i,j) probably from coalescence of smaller clumps.

Importantly, inclusion of DPI or DNAse-1 in the PMA-stimulated cultures substantially affected the formation of the haemocyte clumps, particularly after 3 and 24 h (Fig. 5k–n). At 1 h, clumps were too few and variable in size to assess statistically, but at 3 h, DPI significantly reduced the number of the clumps compared with the PMA only-treated cultures ($P<0.001$) (Fig. 5j). At 24 h, the clumps were also significantly smaller and fewer in number in the presence of DPI than without it ($P<0.001$; Fig. 5i,j). In the presence of DNAse, the clumps failed to form large compact structures at 3 h (Fig. 5l), and there were significantly fewer than in the PMA-stimulated cultures at this time ($P<0.001$) (Fig. 5j). Those that did form in the presence of DNAse-1 were loosely packed and contained very few strands of basophilic material (Fig. 5l). Crucially at 24 h, the haemocyte aggregates formed in the PMA + DNAse-1 mixtures lacked cohesiveness and evidence of extracellular chromatin (Fig. 5m,n). Neither DPI nor DNAse-1 stimulated haemocyte clumping on their own, although PMA + DPI-treated cultures tended to show more de-granulated cells than those not exposed to this reagent (Fig. 5k). Collectively, these results show that ETosis is involved in the initiation and development of capsule-like cell clumps over 24 h.

Chromatin release by defence cells from other invertebrates. Preliminary *in vitro* experiments were undertaken to assess if

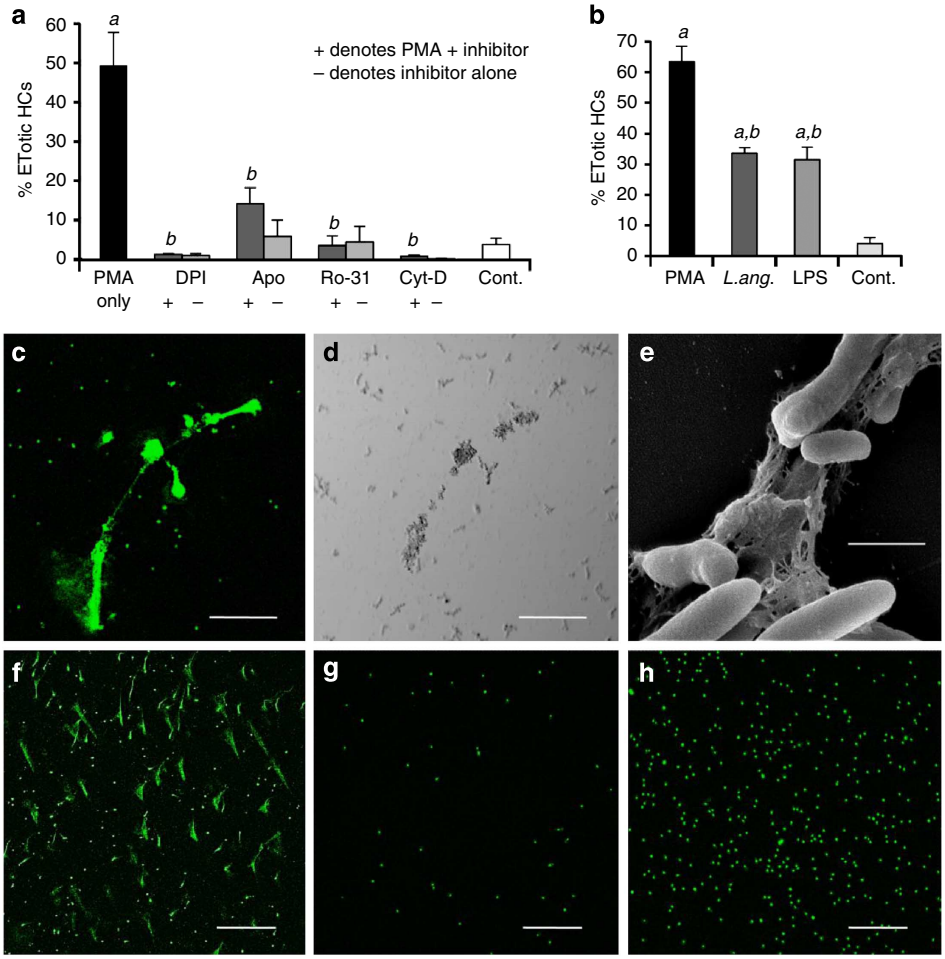

Figure 3 | Chromatin release in cellular defences of *C. maenas in vitro*. (**a**) Percentage of *C. maenas* HCs following PMA treatment (24 h, 0.1 μM) or PMA plus the inhibitors DPI (2 μM), apocynin (Apo) (50 μM), Ro-31-8220 (Ro-31) (1 μM), cytochalasin D (Cyt-D) (10 μM) or left untreated (Cont.). Values are mean ± s.e.m., $n=3$. Significant differences between PMA treatments and untreated controls denoted by *a*; Significant differences between PMA and PMA +/− inhibitor denoted by *b*. All *P* values are <0.001, one-way analysis of variance (ANOVA) with Student–Newman–Keuls (SNK) *post hoc* test. (**b**) Percentage of ETotic *C. maenas* HCs following treatment with PMA (0.1 μM), live *L. anguillarum* (3×10^5 ml^{-1}) or LPS (0.1 μg ml^{-1}) compared with controls. All cultures incubated at 10 °C for 24 h. Values are mean ± s.e.m., $n=3$. Significant differences between the control and PMA, LPS or *L. anguillarum* are indicated by *a*. Significant differences between PMA and LPS or *L. anguillarum* are indicated by *b*. All *P* values are <0.001, one-way ANOVA with SNK *post hoc* test. (**c**) Unfixed, ETotic HCs (24 h, *L. anguillarum* (3×10^4 ml^{-1}) stained with Sytox Green. Stained small dots in background are bacteria. (**d**) Phase contrast view of (**c**). (**c**,**d**) Scale bar, 75 μm. (**e**) SEM of chromatin released from an HC, trapping *L. anguillarum*. Scale bar, 1 μm. (**f**–**h**) Effect of PMA (24 h, 0.1 μM) on other haemocyte populations, stained with Sytox Green. (**f**) ETotic SGCs. (**g**) Non-ETotic prohaemocytes. (**h**) Non-ETotic GCs. (**f**–**h**) Scale bars, 300 μm.

haemocytes from a distantly related protostome and an acoelomate invertebrate release chromatin. Using PMA as the stimulus, Sytox Green-positive extracellular material was clearly observed with the mussel, *M. edulis* haemocytes (Fig. 6a–c), although at a lower frequency and only with much higher concentrations of PMA than that of crab HCs over a longer time (Fig. 6d). Only 27.0% (± 2.8 s.e.m.) of mussel haemocytes were ETotic, even with a PMA concentration of 50 μM over 48 h. The released material was digested completely by DNAse-1 and as the response is inhibited by DPI (Fig. 6d), we conclude that it is an ETotic phenomenon. Remarkably, cells extracted from the mesoglea of the sea anemone, *A. equina*, also expel DNAse-sensitive nuclear material after 24 h treatment with PMA (0.1 μM) (Fig. 6e–g, Supplementary Movie 2). In crude extracts, the chromatin formed short diffuse structures (Fig. 6e,f) but, after removal of mucus by trypsin digestion, the released chromatin resembled the spread structures similar to those produced by crab and mussel haemocytes (Fig. 6g). The percentage of enriched mesogleal cells showing this response was 10.3% (± 1.6% s.e.m.) (Fig. 6h). Pretreatment of the cells with DPI or cytochalasin D significantly reduced this extrusion of chromatin ($P<0.05$) (Fig. 6h) indicating that the process is very likely to be ETosis.

Discussion

Defence cells from protostome and acoelomate invertebrates can undergo NADPH oxidase or ROS-dependent ETosis, upholding our hypothesis that it represents a primordial cellular phenomenon. We propose that haemocytes that undergo such chromatin release are designated InEPTs (invertebrate extracellular phagocyte traps) to distinguish them from vertebrate ETotic cells. Here, we define a role for InEPTs in host defence of crab, showing induction by bacteria or LPS with the disgorged chromatin able to ensnare microorganisms. Crucially, chromatin released from InEPTs is clearly associated with the formation of haemocyte capsules that are stimulated to develop and lodge in the gill lamellae by injected LPS. Encapsulation is the major process through which bacteria or other non-self materials are cleared

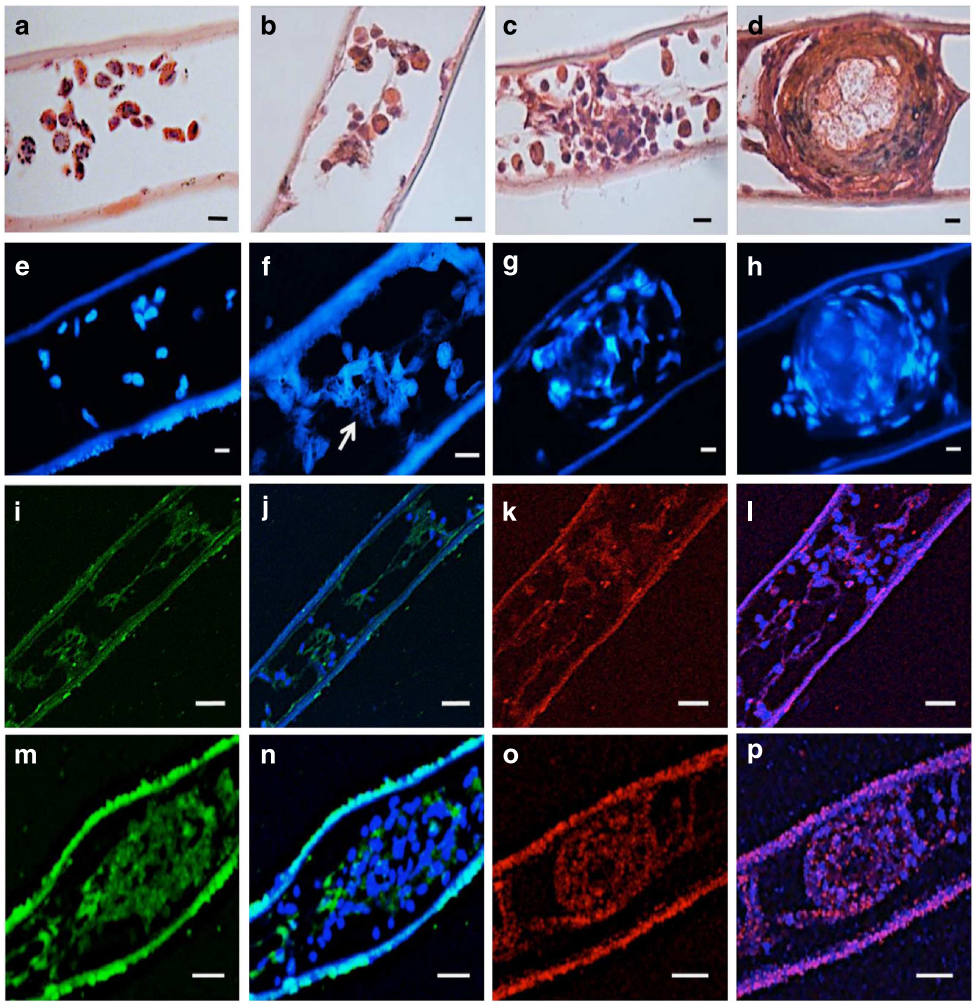

Figure 4 | *In vivo* role of ETosis during host defence in *C. maenas*. (**a**–**d**) Haematoxylin and eosin-stained paraffin wax sections of gill lamellae at various incubation periods after 100 µl injection of LPS (20 µg ml^{-1}) or saline. (**a**) Control, 24 h after injection of sterile saline. (**b**) Part of a gill lamella 1 h after LPS treatment. (**c**) Early capsule formed 3 h after LPS treatment. (**d**) Fully formed capsule 24 h after LPS injection. (**e**–**h**) 2-(4-amidinophenyl)-1H-indole-6-carboxamidine (DAPI)-stained paraffin wax sections of gill lamellae after 100 µl injection of LPS (20 µg ml^{-1}) or saline. (**e**) Control, saline treatment (24 h). Epibionts are evident on the external (seawater) surface of the lower lamella surface and there is no haemocyte clumping or externalized chromatin. (**f**) 1 h post LPS treatment showing ETotic cells within a gill lamella. Arrow indicates likely externalized chromatin. (**g**) Haemocyte clump 3 h post LPS treatment. (**h**) Fully formed capsule 24 h post LPS treatment. (**i**–**l**) Immunohistochemical staining of haemocyte aggregations formed at 1 h post LPS treatment. (**i**) PXN visualization with anti-MPO antibody. (**j**) Merge of **i** with same section stained with TO-PRO-3 iodide to reveal DNA. (**k**) Visualization of H2A in a different area of lamella. (**l**) Merge of **k** with same section stained with TO-PRO-3 iodide. (**m**–**p**) Immunohistochemical staining of a haemocyte clump 3 h post LPS treatment. (**m**) Visualization of PXN with anti-MPO antibody. (**n**) Merge of **m** with same section stained with TO-PRO-3 iodide. Note the mostly extracellular location of PXN. (**o**) Visualization of H2A in a different clump. (**p**) Merge of **o** with same section stained with TO-PRO-3 iodide. H2A co-localization is pronounced and occurs throughout clump structure. All scale bars, 20 µm.

from the haemocoel of arthropods[33,35]. In *C. maenas*, the phagocytic capability of HCs is relatively low at *ca.* 15–20% (ref. 32) but ~94% of injected bacteria are removed from the circulation within the first hour of infection, mainly to the gill lamellae where they become sequestered in haemocyte capsules[33,36]. It is known that in crab, entrapped bacteria are killed within such capsules[37], no doubt aided by antimicrobial peptides (AMPs) synthesized and stored in the SGCs and GCs[21,38]. In the present study, we show that chromatin of InEPTs enable the formation and development of these capsules by binding pathogens and facilitating assembly of other non-ETotic haemocytes to the scaffold. This finding radically changes the present view as to how capsules are initiated in invertebrates[21] and confirms the original proposal by Brinkmann and Zychlinsky[12] that chromatin is indeed an evolutionary ancient defence weapon. As revealed by the immunohistochemical analyses presented here, the chromatin aids the aggregation of haemocytes, which become bound to each other, with PXN released from the cells serving to hold the structure firmly together. In addition, the extruded chromatin serves to deliver histones and (likely) other antimicrobial proteins, thereby facilitating the killing of infectious agents caught in the meshes. The externalization of histones on chromatin would further present 'damage' signals to the immune system, consistent with the danger model[39].

A role for extracellular chromatin released by haemocytes actively participating in defence has not previously been demonstrated in any invertebrate. One study on the wax moth, *Galleria mellonella*, reported that injection of purified endogenous nucleic acids simultaneously with pathogenic bacteria prolonged

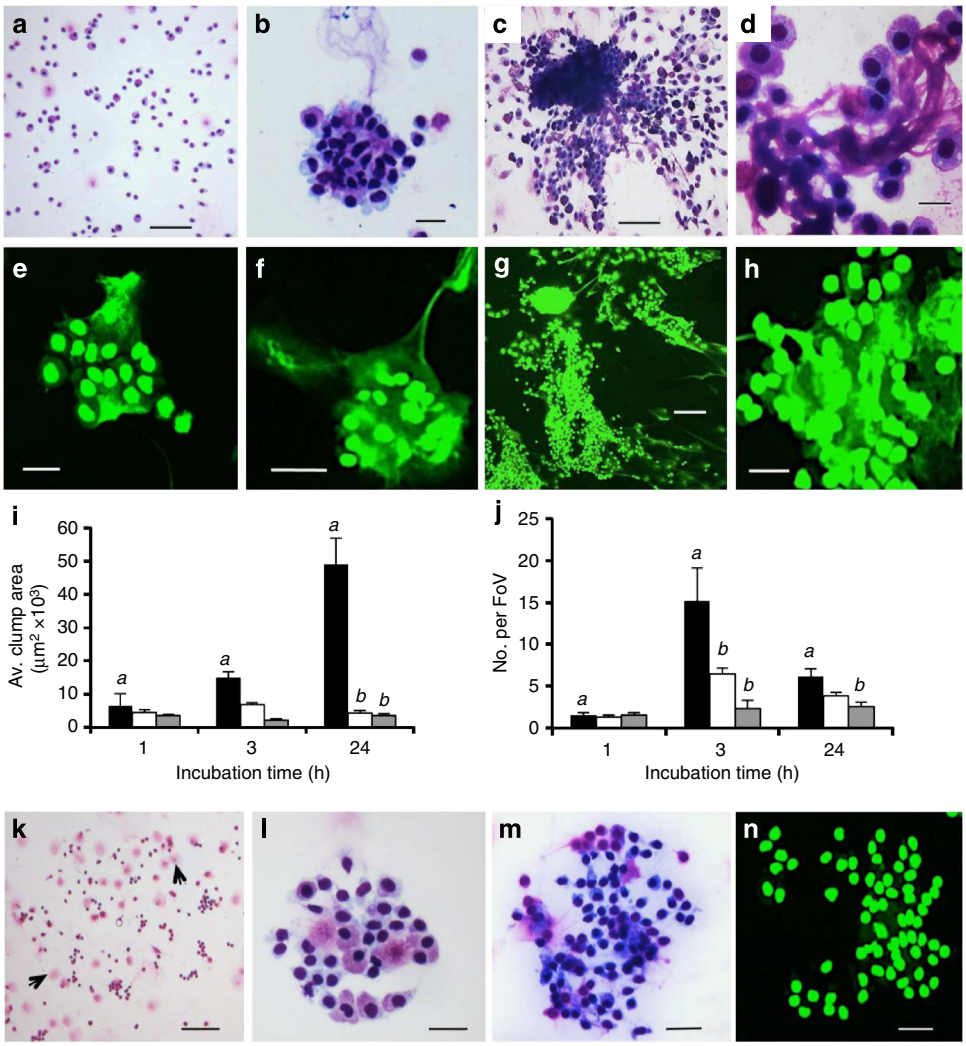

Figure 5 | ETosis during the formation of haemocyte clumps in suspension culture. (**a**–**d**) Diff-Quik stained cytocentrifuge preparations of unseparated *C. maenas* haemocytes. (**a**) 24 h, control (no PMA). Scale bar, 100 μm (**b**) 3 h, 0.1 μM PMA. Scale bar, 20 μm. (**c**) 24 h, 0.1 μM PMA. Scale bar, 100 μm. (**d**) Detail of clump (24 h) showing extruded material permeating intact cells. Scale bar, 20 μm. (**e**–**h**) Sytox Green stained cytocentrifuge preparations. (**e**) ETosis in small clump 1 h (0.1 μM PMA). (**f**) Clump showing intact haemocytes entrapped by extracellular chromatin (3 h 0.1 μM PMA). (**g**) 24 h, 0.1 μM PMA. Clump showing strands of chromatin. (**h**) Detail showing extracellular chromatin suffused through the cell matrix (24 h). Scale bars (**e**,**f**,**h**) 20 μm, (**g**) 100 μm. (**i**–**n**) Haemocyte clumps formed in PMA only, PMA + DPI or PMA + DNase. All incubations 10 °C. (**i**,**j**) solid columns = PMA only, open columns = PMA + DNAse-1, grey columns = PMA + DPI. Values are mean ± s.e.m. of one representative experiment from three independent experiments. Significant differences between PMA-only treatments over time denoted by *a*. Significant differences between PMA-only and PMA + DNAse or PMA + DPI within one time point indicated by *b*, one-way analysis of variance with Student–Newman–Keuls *post hoc* test. (**i**) Clump size. Values are mean ± s.e.m. ($n = 6$–52). PMA 1 h versus 24 h, $P < 0.01$; PMA 3 h versus 24 h and PMA versus PMA + DNAse-1, both $P < 0.001$; PMA versus PMA + DPI $P < 0.05$. (**j**) Number of haemocyte clumps (that is, >20 haemocytes in close contact). Values are mean number per field of view (FoV) ± s.e.m. ($n = 6$). PMA only 1 h versus 24 h, $P < 0.01$. PMA only 1 h versus 3 h, and 3 h versus 24 h, both $P < 0.001$. PMA versus PMA + DNAse, $P < 0.001$; PMA versus PMA + DPI $P < 0.05$. (**k**–**m**) Diff-Quik™ stained cytocentrifuge haemocyte preparations. (**k**) 24 h PMA + DPI. Compare with **c**. Arrows indicate degranulated cells. Scale bar, 200 μm. (**l**) Small, loose haemocyte clump, 3 h PMA + DNAse-1. Compare with **b**, **f**. Scale bar, 20 μm. (**m**) Haemocyte clump, 24 h PMA + DNAse-1. Compare with **c**,**d**. Scale bar, 40 μm. (**n**) Haemocyte clump, 24 h PMA + DNAse-1, Sytox Green stain. Compare with **g**,**h**. Scale bar, 20 μm.

larval survival[40]. The present findings suggest that the injected bacteria were not only killed by AMPs and other immune molecules but also trapped on the externally introduced chromatin and then confined within haemocyte nodules, and thus unable to establish a lethal infection.

As our preliminary experiments found ETotic-style chromatin release similarly occurs in *M. edulis* haemocytes, it is plausible to predict that the process is similarly involved in the development of capsules in bivalves. Certainly, molluscs mount encapsulation reactions to parasites[41]. The less frequent ETotic response by mussel haemocytes and the need for much higher PMA concentrations over a longer incubation time, reported here, is not easily explained, but may relate to the high level of phagocytosis exhibited by bivalves[17]. Phagocytes are closely associated with food transport in these filter feeders so it would be disadvantageous for such animals to disable many haemocytes in this way. Anthozoan cnidarians also display amoebocyte aggregation *in vivo* in response to encounters with fungal hyphae[42], so it is conceivable that chromatin is involved in this process. Mucus, especially within the mesoglea, probably serves to localize the chromatin and any microorganisms trapped on the meshes. Thus, the spread of invading pathogens or parasites

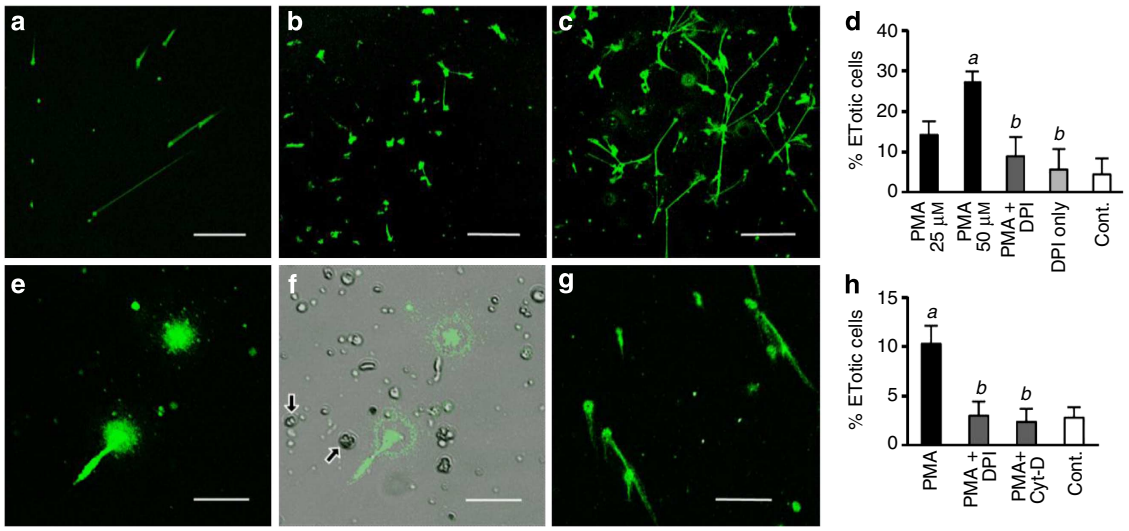

Figure 6 | PMA-stimulated chromatin release by defence cells from other invertebrate species *in vitro*. (**a**–**d**) Unfixed *M. edulis* haemocytes in monolayer culture (24–48 h at 10 °C), stained with Sytox Green. (**a**) 0.1 μM PMA, 24 h. (**b**) 25 μM PMA, 48 h. (**c**) 50 μM PMA, 48 h. (**a**–**c**) Scale bars, 300 μm. (**d**) Percentage of ETotic *M. edulis* haemocytes following PMA treatment (25 or 50 μM, 48 h), 50 μM PMA +/− 10 μM DPI or untreated (Cont.). Values means ± s.e.m., $n=3$. Significant differences between PMA and untreated haemocytes denoted by *a*. Significant differences between PMA and PMA +/− DPI denoted by *b*. In both cases, $P<0.05$, one-way analysis of variance (ANOVA) with Student–Newman–Keuls (SNK) *post hoc* test. (**e**–**g**) Chromatin release by mesogleal cells isolated from *A. equina* (24 h, 0.1 μM PMA, 10 °C). (**e**) Crude cell extract. (**f**) Merge of **e** with same phase contrast image. Arrows indicate cnidocytes. (**e**,**f**) Scale bars, 33 μm (**g**) Phagocyte-enriched mesogleal extract after trypsin digestion and differential centrifugation. Scale bar, 65 μm. (**h**) Percentage of ETotic cells enriched from the mesoglea of *A. equina* following treatment with PMA (24 h, 0.1 μM), PMA + 2 μM DPI, PMA + 10 μM cytochalasin D (Cyt-D) or left untreated (Cont.). Values are mean ± s.e.m., $n=3$. Significant differences between PMA and untreated cells are denoted by *a*. Significant differences between PMA, and PMA + DPI or PMA + Cyt-D are denoted by *b*. In both cases $P<0.05$, one-way ANOVA with SNK *post hoc* test.

would be stemmed and the infectious material would be brought into intimate contact with antimicrobial agents produced by the tissues or mesogleal cells. AMPs are synthesized by the endoderm of cnidarians[43,44] and amoebocytes of *A. equina* release extracellular ROS[19] capable of killing bacteria.

As members of the Cnidaria lack a coelom and true circulatory system, chromatin released through ETosis must be an ancient defence process that predates the development of an organized immune system within the mesoderm. In plants, extracellular DNA in root-cap slime of pea, *Pisum sativum*, confers protection against fungal infections[45], but whether the DNA is extruded in a controlled, NADPH oxidase or ROS-dependent manner, as in vertebrate immune cells, has yet to be established. Moreover, as the chromatin is discharged to the external environment (that is, the soil), rather than within the tissues, it is uncertain if the deployment of chromatin in pea root genuinely represents ETosis. Therefore, at present, it is unknown when ETosis arose in eukaryote evolution, but the present study sheds new light on how early multicellular animals might have protected themselves against prokaryote competitors in their environment.

Our findings also help to inform some of the pathological consequences associated with ETosis in higher vertebrates. We reveal a truly beneficial role for this process in animals without fully tubular vascular systems. For higher vertebrates, however, ETosis may be viewed as a double-edged sword: the trapping and killing of microorganisms is valuable but the ETotic material could become detrimental if it is not resolved or evokes an adaptive response. For instance, while entrapment of haemocytes by externalized chromatin is crucial for capsule development in invertebrates, in mammals, equivalent assembly of leucocytes and platelets on DNA meshes within blood vessels may lead to venous thrombosis[11,46,47]. Moreover, a recent paper has suggested that NETs can facilitate metastasis of tumours by trapping cancerous cells and enabling their adhesion to healthy tissues[13]. ETosis is further associated with chronic respiratory diseases, such as cystic fibrosis, where the externalized chromatin causes, among other effects, an increase in sputum viscosity that aids microbial colonization and biofilm formation[48–50].

In mammals, the lack of NETs clearance, together with inappropriate stimulation of an adaptive immune response, may occur in a number of autoimmune diseases; for example, systemic lupus erythematosis[51] and rheumatoid arthritis[52]. A characteristic of systemic lupus erythematosis is the production of auto-antibodies against immunogenic complexes of self-DNA and neutrophil AMPs arising from neutrophil ETosis[51]. Such complexes may pose an additional complication of glomerulonephritis occluding the kidney and impairing renal function[53]. In rheumatoid arthritis, NETs are abundant in the synovial fluid of affected joints and rheumatoid nodules in skin, with autoantibodies sometimes forming against citrullinated vimentin, an intermediate filament protein, externalized on the chromatin[52]. For invertebrates, the problem of autoimmunity is non-existent, as they do not synthesize antibodies and cannot mount antibody-mediated adaptive immune responses. As such, invertebrates facilitate the study of processes central to innate immunity in a non-biased environment (that is, one fully without the presence of clonally derived lymphocytes and their activities).

In conclusion, the InEPTs described here confirm that extracellular chromatin is a primordial defence process that effectively protects against infection and, accordingly, has been conserved through evolution. In higher animals, the advantages of externalized chromatin as an anti-infective strategy remain, but the more complex vasculature of vertebrates and the presence of an adaptive immune system mean that exposed chromatin can be problematic. The phylogenetic history of ETosis as a primitive host defence strategy accounts for its paradoxical effects in higher vertebrates.

Methods

Animals and reagents. Specimens were collected from the Forth Estuary, Scotland and kept in seawater (~32‰, 12 ± 2 °C) until use. Only healthy individuals, showing no signs of injury or infection were used. Unless otherwise specified, all reagents were purchased from Sigma Aldrich.

Preparation of monolayer cultures of crab haemocytes. Haemolymph (2 ml) was withdrawn from the unsclerotized membrane between the merus and the carpus of a cheliped of adult intermolt crabs (8.5 ± 1.0 cm carapace width) into a syringe containing 2 ml of anti-coagulant (0.5 M NaCl; 0.1 M glucose; 30 mM trisodium citrate; 26 mM citric acid (monohydrate); 10 mM ethylene diamine tetra-acetic acid (EDTA); pH 4.6)[16]. The haemocyte populations were separated by isopycnic density centrifugation (25,000*g*, 20 min, 4 °C) on preformed continuous 60% Percoll gradients in 3.2% NaCl[16]. HCs were obtained from the top band, SGCs from the middle band with GCs from the bottom band[16]. Prohaemocytes, normally at very low levels in the haemolymph of crabs, were recruited into the circulation by prebleeding (2 ml) 24 h before collection at the second bleed[54]. They were then isolated by two-step separation, first on 60% Percoll as above and, second on a preformed continuous 40% Percoll gradient in 3.2% NaCl[54]. After washing in 0.22 μm filtered 3.2% NaCl, each of the separated cell populations were re-suspended in modified L-15 medium (ML-15) made by supplementing single-strength medium with 0.4 M NaCl and a penicillin/streptomycin mix (100 U per 100 μg ml^{-1}). The haemocytes were cultured in flat-bottomed 24-well plates to allow for cell attachment (1 h, 10 °C) with triplicate cultures of *ca.* 3×10^4 cells made for each animal. A minimum of three animals was used in each experiment.

Assay of chromatin release by crab haemocytes *in vitro*. ETosis by crab haemocytes was induced with phorbol-12-myristate 13-acetate (PMA) at final concentrations 0.01–1.0 μM. Controls received equal volumes of medium only. The plates were incubated at 10 °C for 1–24 h before staining, unfixed, for 20 min with 1 μM Sytox Green (Invitrogen) and visualization with a Leica (DMIRE2) TCS2 confocal microscope (excitation 504 nm; emission 523 nm). Using a combination of fluorescence and phase contrast microscopy, the percentages of viable, chromatin extruding or non-ETotic dead cells were calculated from a minimum of 300 cells from a minimum of three fields of view from replicate experiments using the image analysis software, ImageJ (National Institutes of Health, USA). In judging ETotic cells, no distinction was made between diffuse or spread forms of chromatin. To confirm that the released material was of nuclear origin, DNAse-1 (Fermentek) (100 U ml^{-1} final concentration) was added to HC cultures that been treated with 0.1 μM PMA 24 h previously and then stained, unfixed, with Sytox Green (20 min). The cultures were incubated (10 °C) with changes recorded by live time-lapse photo-microscopy.

Chromatin decoration *in vitro*. Immunocytochemistry was used to investigate decoration of the chromatin from crab HCs with H2A and PXN. The primary antibodies were mouse anti-H2A IgG1 (New England Biolabs) or rabbit anti-human myeloperoxidase IgG (Dako), an antibody that recognizes PXN, both at a dilution of 1:200 in phosphate-buffered saline (PBS) supplemented with 3% bovine serum albumin (BSA). The secondary antibodies were Alexa Fluor 594F(ab)$_2$ goat anti-mouse IgG (excitation 590 nm; emission 617 nm) or Alexa Fluor 488 goat anti-rabbit IgG (excitation 495 nm; emission 519 nm) (both from Invitrogen) to detect H2A and PXN, respectively. Both secondary antibodies were diluted 1:300 in PBS supplemented with 3% BSA.

Monolayer cultures of HCs were stimulated with 0.1 μM PMA, as above, except that the cells were cultured on glass coverslips laid in the plate wells, rather than directly on the well surface. After 24 h, the culture medium was removed and the cells fixed with 4% paraformaldehyde in 2% NaCl (30 min). The cells were washed three times with PBS, permeabilized with 0.1% Triton X-100 (5 min) and washed thrice again with PBS before blocking in 3% BSA v/v in PBS for 1 h. The haemocytes were then incubated for 1.5 h with the primary antibodies and, after further three washes in PBS, the slides were incubated (1.5 h) with the secondary antibodies. Controls included haemocytes without primary and secondary antibodies, haemocytes incubated only with secondary antibodies and haemocytes treated with mouse or rabbit sera instead of primary antibodies. For each control, 3% BSA in PBS was substituted for the relevant antibody solution(s). DNA and actin were localized, respectively, with 5 μM Draq 5 (excitation 647 nm; emission 681 nm) (Biostatus) or 0.15 μM rhodamine phalloidin (excitation 540 nm; emission 565 nm) (Invitrogen) plus the secondary antibodies. The haemocytes were finally washed three times with PBS and mounted onto sterile glass slides with Vectashield (Vector Laboratories) before examination by confocal microscopy, as above.

Electron microscopy. Material was fixed (2 h) in 2.5% glutaraldehyde, in 0.1 M sodium cacodylate (CAC), pH 7.2 then washed in PBS and dehydrated through a graded series of ethanols. For SEM, the material was critical point dried (3 h), sputter coated with gold and visualized with a Quanta 3D FEG–FEI microscope (FEI UK). For transmission electron microscopy, fixed samples were washed in three changes of CAC, post fixed in 1% osmium tetroxide, in 0.1 M CAC, for 45 min and washed three times, as above, before dehydration in 50, 70, 90 and 100% normal grade acetone (10 min each). This was followed by two 10 min washes in Analar acetone and embedding in araldite. Ultrathin sections (60 nm thickness) were stained with uranyl acetate and lead citrate and viewed using a Phillips CM120 microscope (FEI UK). The diameters of globular and smooth domains of extracellular chromatin released from crab HCs were measured from high resolution SEM using ImageJ. The diameters of ~15 randomly selected domains were measured and the average diameter calculated (nm).

Inhibition of ETosis by crab HCs *in vitro*. Fresh HC monolayer cultures were incubated with either 2 μM diphenyleneiodonium, 50 μM apocynin (1-(4-hydroxy-3-methoxyphenyl) ethanone) (Calbiochem), 1 μM Ro-31-8220 (3-(3-(4-(1-methyl-1*H*-indol-3-yl)-2,5-dioxo-2,5-dihydro-1*H*-pyrrol-3-yl)-1*H*-indol-1-yl)propyl carbamimidothioate) or 10 μM cytochalasin D (all for 1 h, 10 °C) before addition of PMA, as above. Controls consisted of stimulated haemocytes minus inhibitor or non-stimulated haemocytes plus inhibitor. Chromatin release was detected and quantified as above.

Stimulation of ETosis with LPS or bacteria *in vitro*. Cultures of crab HCs were set up, as above, but treated with LPS from *Escherichia coli* serotype 0111:B4 (final concentration 0.1 μg ml^{-1}) or a washed suspension of the fish pathogen, *Listonella anguillarum* (ATCC 43305), (3×10^5 ml^{-1} final) instead of PMA. Controls received medium only. All cultures were incubated for 24 h (10 °C) then processed and visualized as above. Inhibition experiments were also performed with DPI, as above.

ETosis in the host defences of *C. maenas in vivo*. To ascertain if ETosis or released chromatin participates in encapsulation reactions, crabs were given injections of LPS (100 μl of 20 μg ml^{-1} LPS from *Escherichia coli* serotype 0111:B4 in sterile 3.2% NaCl). The injections were made through the unsclerotized membrane between the carapace and the coxa of the fourth pereiopod (walking leg)[33]. The dose given represents a final concentration of ~0.1 μg ml^{-1} within the haemocoel and mimics infection without the risk of pathology. It stimulates the formation of haemocyte capsules in the gills, the main site for the sequestration of non-self agents[33,36]. Control crabs were given 100 μl of 0.22 μm filtered sterile 3.2% NaCl instead of LPS. Both treatment groups were housed separately in the aquarium until sampling at 1, 3 or 24 h when they were killed. The gills were excised and fixed in 2.5% glutaraldehyde before processing and embedding in paraffin wax. Sections (4-μm thick) were cut and stained with 300 nM 2-(4-amidinophenyl)-1H-indole-6-carboxamidine (DAPI) (excitation 375 nm; emission 461 nm) (Invitrogen) or haemotoxylin and eosin and examined by confocal microscopy, as above, or with a Zeiss AxioSkop fluorescence microscope with QCapturePro software.

Immunohistochemistry was used to demonstrate the role of externalized chromatin in encapsulation reactions *in vivo*. The primary antibodies were the same as those used to study chromatin decoration *in vitro* and at the same dilution, described above. To induce the haemocytes to form capsules, crabs were given injections of LPS or, for controls, 3.2% NaCl, and processed as above except that gill tissue was fixed in paraformaldehyde plus 2% NaCl before embedding and sectioning. All sections were incubated for 30 min with 1 mg ml^{-1} sodium borohydride to reduce autofluorescence then washed three times in PBS for 5 min per wash. A blocking solution of 3% BSA in PBS was added to the sections for 1 h before overnight incubation at 4 °C with the primary antibodies as above. Sections were then washed three times and incubated for 2 h in the dark (4 °C) with secondary antibodies, as above. Sections were washed again three times and incubated for a further 1 h with 5 μM TO-PRO-3 iodide (excitation 642 nm; emission 661 nm) (Invitrogen) to stain both extracellular and intracellular DNA. Finally, sections were washed three times, submerged for 5 s in Millipore water and then mounted using ProLong Gold anti-fade mounting medium (Invitrogen). Immunohistochemical controls paralleled those specified for the chromatin decoration *in vitro* above. Slides were examined using a confocal microscope as above.

ETosis by crab haemocytes in suspension culture. Unseparated haemocytes diluted in anticoagulant (above) were centrifuged (500*g*, 5 min, 4 °C) and re-suspended in ML-15 in sterile 15 ml tubes to give a concentration of 1×10^6 ml^{-1}. The experimental tubes received PMA (final concentration 0.1 μM) while the controls were given the same volume of ML-15. All tubes were incubated at 10 °C with subsamples (200 μl) aspirated, after gentle mixing, at 1, 3 or 24 h for cytocentrifugation in a Shandon Cytospin 3 at 7*g* (250 r.p.m.) for 3 min. Two sets of slides were prepared for each time and each treatment. One was air-dried, fixed with methanol (1 min) and stained with Diff-Quik (Gamidor) (red, then blue: 1.5 min each), before air-drying, mounting in DePex (30 min) and examination by light microscopy as above. The other was fixed in 2.5% glutaraldehyde in 3.2% NaCl, stained with 1 μM Sytox Green (20 min) and examined with the Zeiss AxioSkop microscope as above.

To confirm the role of chromatin in encapsulation *in vitro*, further sets of cultures were set up in which the haemocytes were pre-incubated with either DPI (4 μM for 1 h) or DNAse-1 (200 u ml^{-1} for 15 min) before the addition of PMA, as above. Higher concentrations of DPI and DNAse-1 were used here because of the greater number of (unseparated) haemocytes present in the suspension cultures

compared to those in the single-population monolayer cultures. Controls received DPI or DNAse-1, but were given 3.2% NaCl instead of PMA. The tubes were then incubated, sampled and processed for light microscopy, as above. To assess clump size and frequency, images were recorded as above. To make a clear distinction between controls and treated cells, clumps were defined as a closely packed aggregation of 20 or more cells. The image analysis software ImageJ was used to measure clump numbers and areas (μm^2) from a minimum of six fields of view ($\times 100$ magnification) per experiment. The experiment was repeated three times.

Chromatin release by defence cells from other invertebrates. Mussel haemolymph (0.4 ml) was withdrawn from the adductor muscle of each animal into a syringe containing an equal volume of 0.05 M Tris–HCl buffer, pH 7.6, supplemented with 2% glucose, 2% NaCl and 0.5% EDTA[17]. The haemocytes were counted immediately and 3×10^4 ml^{-1} were seeded into wells of a plastic 24-well plate, as above. Mesogleal cells were extracted from *A. equina* by excising the mesenteric filaments, mixing them with an equal volume of homologous fluid drained from the coelenteron and then vigorously pipetted to dissociate the amoebocytes[19]. Digests were performed with 0.01% trypsin in 0.4 M NaCl (10 min, 10 °C), centrifuged (300*g*, 5 min, 10 °C) and the supernatant re-centrifuged as before. Panning was used to further enrich the phagocytes leaving *ca.* 1×10^4 ml^{-1} per well. Cells from both species were incubated at 10 °C and then assayed for chromatin release by confocal microscopy following PMA treatment and staining with Sytox Green, as above.

Statistical analysis. Data were tested for normality using the Kolmogorov–Smirnov test and tested for significance using one-way analysis of variance with a Student–Newman–Keuls *post hoc* test. Where appropriate, data were log or arc sine transformed before analysis. Probability values of $P < 0.05$ were regarded as statistically significant.

References

1. Brinkmann, V. *et al.* Neutrophil extracellular traps kill bacteria. *Science* **303,** 1532–1535 (2004).
2. von Kockritz-Blickwede, M. *et al.* Phagocytosis independent antimicrobial activity of mast cells by means of extracellular trap formation. *Blood* **111,** 3070–3080 (2008).
3. Yousefi, S. *et al.* Catapult-like release of mitochondrial DNA by eosinophils contributes to antibacterial defense. *Nat. Med.* **14,** 949–953 (2008).
4. Webster, S. J. *et al.* Distinct cell death programs in monocytes regulate innate responses following challenge with common causes of invasive bacterial disease. *J. Immunol.* **185,** 2968–2979 (2010).
5. Aulik, N. A., Hellenbrand, K. M. & Czuprynski, C. J. *Mannheimia haemolytica* and its leukotoxin causes macrophage extracellular trap 2 (MET) formation by bovine macrophages. *Infect. Immun.* **80,** 1923–1933 (2012).
6. Fuchs, T. A. *et al.* Novel cell death program leads to neutrophil extracellular traps. *J. Cell Biol.* **176,** 231–241 (2007).
7. Papayannopoulos, V. & Zychlinsky, A. NETs: a new strategy for using old weapons. *Trends Immunol.* **30,** 513–521 (2009).
8. Gray, R. D. *et al.* Activation of conventional protein kinase C (PKC) is critical in the generation of human neutrophil extracellular traps. *J. Inflamm.* **10,** 10–12 (2013).
9. von Kockritz-Blickwede, M. & Nizet, V. Innate immunity turned inside-out: antimicrobial defence by phagocyte extracellular traps. *J. Mol. Med.* **87,** 775–783 (2009).
10. Branzk, N. & Papayannopoulos, V. Molecular mechanisms regulating NETosis in infection and disease. *Semin. Immunopathol.* **35,** 513–530 (2013).
11. Fuchs, T. A. *et al.* Extracellular DNA traps promote thrombosis. *Proc. Natl Acad. Sci.* **107,** 15880–15885 (2010).
12. Brinkmann, V. & Zychlinsky, A. Neutrophil extracellular traps: is immunity the second function of chromatin? *J. Cell Biol.* **198,** 773–783 (2012).
13. Cools-Lartigue, J. *et al.* Neutrophil extracellular traps sequester circulating tumor cells and promote metastasis. *J. Clin. Invest.* **123,** 3446–3458 (2013).
14. Chuammitri, P. *et al.* Chicken heterophil extracellular traps (HETs): Novel defense mechanism of chicken heterophils. *Vet. Immunol. Immunopathol.* **129,** 126–131 (2009).
15. Palic, D., Ostojic, J., Andreasen, J. B. & Roth, J. A. Fish cast NETs: neutrophil extracellular traps are released from fish neutrophils. *Dev. Comp. Immunol.* **31,** 805–816 (2007).
16. Söderhäll, K. & Smith, V. J. Separation of the haemocyte populations of *Carcinus maenas* and other marine decapods, and prophenoloxidase distribution. *Dev. Comp. Immunol.* **7,** 229–239 (1983).
17. Wootton, E. C., Dyrynda, E. A. & Ratcliffe, N. A. Bivalve immunity: comparisons between the marine mussel (*Mytilus edulis*) the edible cockle (*Cerastoderma edule*) and the razor-shell (*Ensis siliqua*). *Fish Shellfish Immunol.* **15,** 195–210 (2003).
18. Arumugam, M., Romestand, B., Torreilles, J. & Roch, P. *In vitro* production of superoxide and nitric oxide (as nitrite and nitrate) by *Mytilus galloprovincialis* haemocytes upon incubation with PMA or laminarin or during yeast phagocytosis. *Eur. J. Cell Biol.* **79,** 513–519 (2000).
19. Hutton, D. M. C. & Smith, V. J. Antibacterial properties of isolated amoebocytes from the sea anemone *Actinia equine, in vitro*. *Biol. Bull.* **191,** 441–451 (1996).
20. Kawahara, T. & Lambeth, D. Molecular evolution of Phox-related regulatory subunits for NADPH oxidase enzymes. *BMC Evol. Biol.* **7,** 178 (2007).
21. Chisholm, J. R. S. & Smith, V. J. Antibacterial activity in the haemocytes of the shore crab, *Carcinus maenas* (L.). *J. Mar. Biol. Assoc. UK* **72,** 529–542 (1992).
22. Bell, K. L. & Smith, V. J. *In vitro* superoxide production by the hyaline cells of the shore crab, *Carcinus maenas* (L.). *Dev. Comp. Immunol.* **17,** 211–219 (1993).
23. Hakkim, A. *et al.* Activation of the Raf-MEK-ERK pathway is required for neutrophil extracellular trap formation. *Nat. Chem. Bio.* **7,** 75–77 (2011).
24. Johansson, M. W. Cell adhesion molecules in invertebrate immunity. *Dev. Comp. Immunol.* **23,** 303–315 (1999).
25. Schmidt, O., Söderhäll, K., Theopold, U. & Faye, I. Role of adhesion in arthropod immune recognition. *Ann. Rev. Entomol.* **55,** 485–504 (2010).
26. Hirsch, J. G. Bactericidal action of histone. *J. Exp. Med.* **108,** 925–944 (1958).
27. Drummond, G. R., Selemis, S., Griedling, K. K. & Sobey, C. G. Combating oxidative stress in vascular disease: NADPH oxidases as therapeutic targets. *Nat. Rev. Drug Discov.* **10,** 453–471 (2011).
28. Beltman, J., McCormick, F. & Cook, S. J. Selective protein kinase C inhibitor, Ro-131-8220, inhibits mitogen-activated protein kinase pgosphatase-1 (MKP-1) expression, induces c-Jun expression, and activates Jun N-terminal kinase. *J. Biol. Chem.* **271,** 27018–27024 (1996).
29. May, J. A. *et al.* GPIIb-IIIa antagonists cause rapid disaggregation of platelets pre-treated with cytochalasin D. Evidence that the stability of platelet aggregates depends on normal cytoskeletal assembly. *Platelets* **9,** 227–232 (1998).
30. Azvedo, E. P. *et al.* Amyloid fibrils trigger the release of neutrophil extracellular traps (NETs) causing fibril fragmentation by NET-associated elastase. *J. Biol. Chem.* **287,** 37206–37218 (2012).
31. Neeli, I., Dwivedi, N., Khan, S. & Radic, M. Regulation of extracellular chromatin release from neutrophils. *J. Innate Immunol.* **1,** 194–201 (2009).
32. Söderhäll, K., Smith, V. J. & Johansson, M. Exocytosis and phagocytosis by isolated haemocyte populations of crustaceans: evidence for cell co-operation in the cellular defence reactions. *Cell Tiss. Res.* **245,** 43–49 (1986).
33. Smith, V. J. & Ratcliffe, N. A. Cellular defense reactions of the shore crab, *Carcinus maenas* (L.): *in vivo* haemocytic and histopathological responses to injected *bacteria*. *J. Invertebr. Pathol.* **35,** 65–74 (1980).
34. Smith, V. J., Söderhäll, K. & Hamilton, M. B 1,3-glucan induced cellular defence reactions in the shore crab, *Carcinus maenas*. *Comp. Biochem. Physiol.* **77A,** 635–639 (1984).
35. Cerenius, L. & Söderhäll, K. The prophenoloxidase-activating system in invertebrates. *Immunol. Rev.* **198,** 116–126 (2004).
36. White, K. N. & Ratcliffe, N. A. The segregation and elimination of radio and fluorescent-labelled marine bacteria from the haemolymph of the shore crab, *Carcinus maenas*. *J. mar. biol. Ass. UK* **62,** 819–833 (1982).
37. White, K. N., Ratcliffe, N. A. & Rosa, M. The antibacterial activity of hemocyte clumps in the gills of the shore crab, *Carcinus maenas*. *J. Mar. Biol. Assoc. UK* **65,** 857–870 (1985).
38. Sperstad, S. V., Smith, V. J. & Stensvåg, K. Expression of antimicrobial peptides from *Hyas araneus* hemocytes following bacterial challenge *in vitro*. *Dev. Comp. Immunol.* **34,** 618–624 (2010).
39. Seong, S. Y. & Matzinger, P. Hydrophobicity: an ancient damage-associated molecular pattern that initiates innate immune response. *Nat. Rev. Immunol.* **4,** 469–478 (2004).
40. Altincicek, B. *et al.* Host-derived extracellular nucleic acids enhance innate immune responses, induce coagulation and prolong survival upon infection in insects. *J. Immunol.* **181,** 2705–2712 (2008).
41. Wootton, E. C., Dyrynda, E. A. & Ratcliife, N. A. Interaction between non-specific electrostatic forces and humoral factors in haemocyte attachment and encapsulation in the edible cockle *Cerastoderma edule*. *J. Exp. Biol.* **209,** 1326–1335 (2006).
42. Mydlarz, L. D., Holthouse, S. F., Peters, E. C. & Harvell, C. D. Cellular responses in sea fan corals: granular amoebocytes react to pathogen and climate stressors. *PLoS ONE* **3,** e1811 (2008).
43. Jung, S. *et al.* Hydramacin-1, structure and antibacterial activity of a protein from the basal metazoan Hydra. *J. Biol. Chem.* **284,** 1896–1905 (2009).
44. Ovchinnikova, T. V. *et al.* Aurelin, a novel antimicrobial peptide from jellyfish, *Aurelia aurita,* with structural features of defensins and channel-blocking toxins. *Biochem. Biophys. Res. Comm.* **348,** 514–523 (2006).
45. Wen, F., White, G. J., Van Etten, H. D., Xiong, Z. & Hawes, M. C. Extracellular DNA Is required for root tip resistance to fungal infection. *Plant Physiol.* **151,** 820–829 (2009).
46. Fuchs, T. A. *et al.* Neutrophil extracellular trap (NET) impact on deep vein thrombosis. *Arterioscler. Thromb. Vasc. Biol.* **32,** 1777–1783 (2012).

47. Brill, A. *et al.* Neutrophil extracellular traps promote deep vein thrombosis in mice. *J. Thromb. Haemost.* **10,** 136–144 (2012).
48. Young, R. L. *et al.* Neutrophil extracellular trap (NET)-mediated killing of *Pseudomonas aeruginosa*: evidence of acquired resistance within the CF airway, independent of CFTR. *PLoS ONE* **6,** e23637 (2011).
49. Papayannopoulos, V. *et al.* Neutrophil elastase enhances sputum solubilization in cystic fibrosis patients receiving DNAse therapy. *PLoS ONE* **6,** e28526 (2011).
50. Dubois, A. V. *et al.* Influence of DNA on the activities and inhibition of neutrophil serine proteases in cystic fibrosis sputum. *Am. J. Respir. Cell. Mol. Biol.* **47,** 80–86 (2012).
51. Lande, R. *et al.* Neutrophils activate plasmacytoid dendritic cells by releasing self-DNA-peptide complexes in systemic lupus erythematosus. *Sci. Transl. Med.* **3,** 73ra19 (2011).
52. Khandpur, R. *et al.* NETs are a source of citrullinated autoantigens and stimulate inflammatory responses in rheumatoid arthritis. *Sci. Transl. Med.* **5,** 178ra40 (2013).
53. Hakkim, A. *et al.* Impairment of neutrophil extracellular trap degradation is associated with lupus nephritis. *Proc. Natl Acad. Sci.* **107,** 9813–9821 (2010).
54. Roulston, C. & Smith, V. J. Isolation and *in vitro* characterization of prohaemocytes from the spider crab, *Hyas araneus*. *Dev. Comp. Immunol.* **35,** 537–544 (2011).

Acknowledgements

We would like to thank Professor Steve Chapman and the School of Life Sciences (HWU) for the Principal's Sports Award and a PhD Scholarship to CTR. RDG is funded by a Wellcome Trust fellowship (WT093767). We acknowledge funding from the Medical Research Council, UK (G0601481 and MR/K013386/1) for A.G.R. We are grateful to Dr Steve Euston and Dr David Brown (HWU) and Stephen Mitchell (EU) for help with microscopy. The technical support given by James Buchanan (HWU), Stephen Mitchell (EU), Melanie McMillan (EU) and Duncan Humphries (EU) is also acknowledged.

Author contributions

V.J.S. conceived the project and designed the experiments with E.A.D., A.G.R. and C.T.R. The experimental work was performed primarily by C.T.R. Advice, intellectual input, facilities and reagents were provided by V.J.S., E.A.D., A.G.R. and R.D.G. The data were analyzed by E.A.D., C.T.R. and V.J.S. V.J.S. wrote the paper and all authors contributed equally to its revision.

Additional information

Supplementary Information accompanies this paper at http://www.nature.com/naturecommunications

Competing financial interests: The authors declare no competing financial interests.

Reprints and permission information is available online at http://npg.nature.com/reprintsandpermissions/

How to cite this article: Robb, C. T. *et al.* Invertebrate extracellular phagocyte traps show that chromatin is an ancient defence weapon. *Nat. Commun.* 5:4627 doi: 10.1038/ncomms5627 (2014).

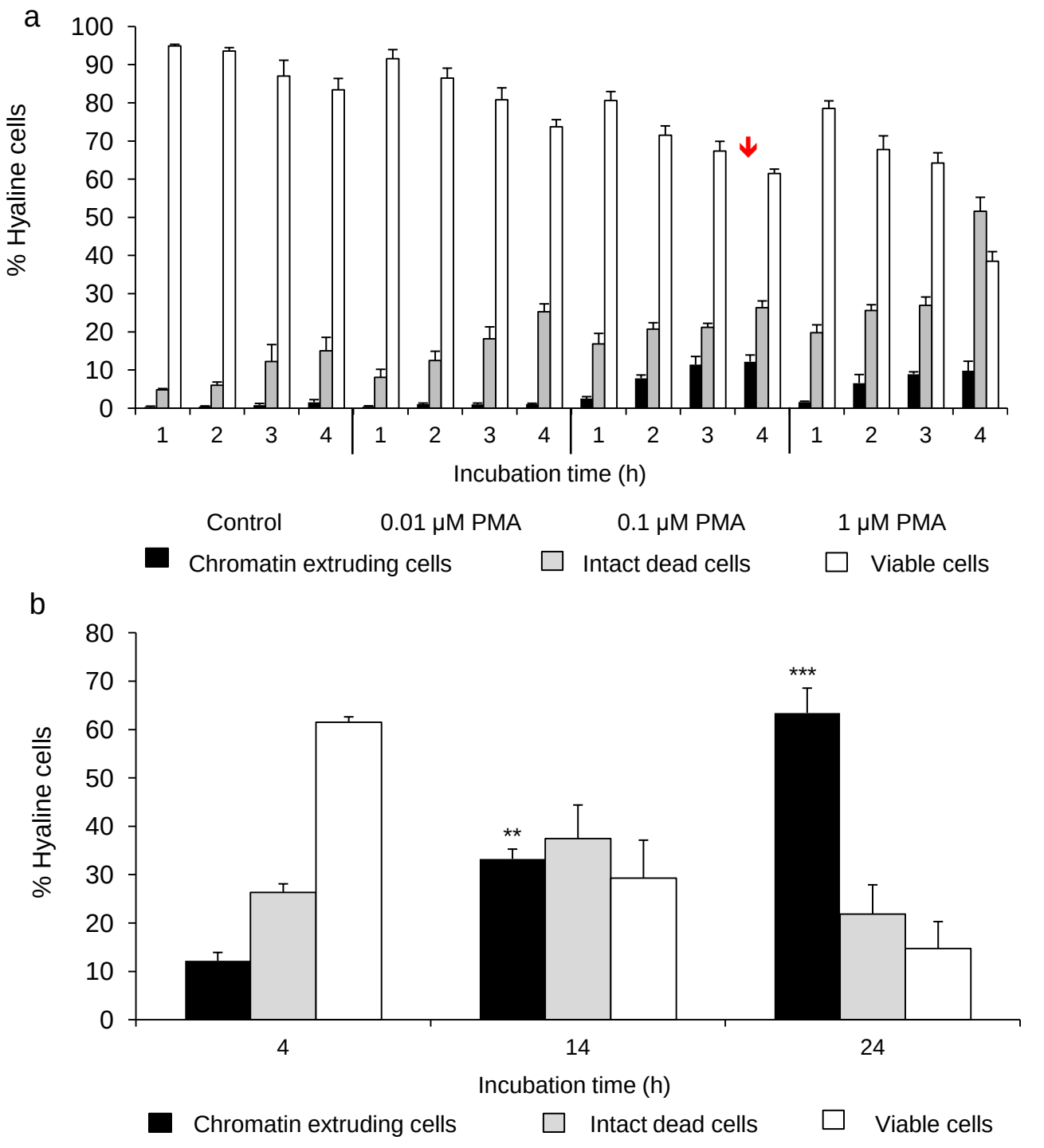

Supplementary Figure 1. Effect of PMA on separated hyaline cells (HC) from crab *in vitro.* Concentration-time analysis of the effect of PMA on separated HCs from *C. maenas* cultured in ML-15 medium. **(a)** Percentage of chromatin-extruding haemocytes with different concentrations of PMA over 4 h, as determined by confocal microscopy. Arrow indicates the optimal concentration (0.1 µM) of PMA for chromatin extrusion combined with overall lower value of non-ETotic cell death. **(b)** Percentage of chromatin-extruding cells over 24 h with 0.1 µM PMA, showing significant differences (one-way ANOVA with Student-Newman-Keuls *post hoc* test) between chromatin-extruding haemocytes at 14 and 24 h compared to 4 h. ** represents $P<0.01$; *** represents $P<0.001$. Values for (a) and (b) are means ± s.e.m. ($n = 3$).

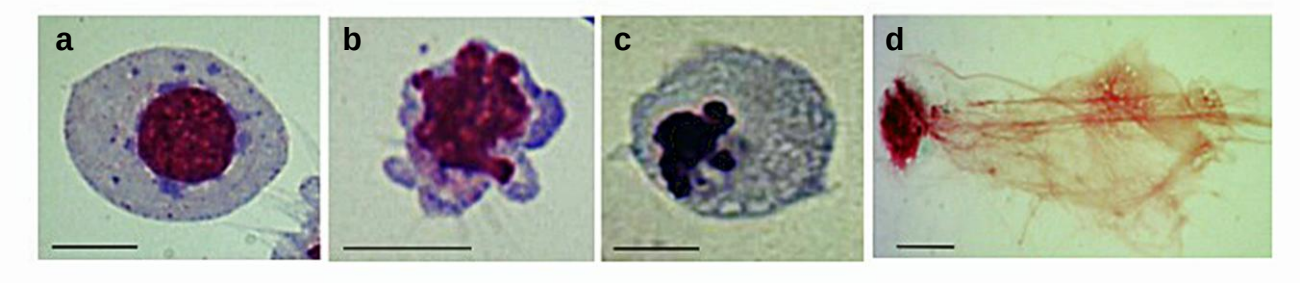

Supplementary Figure 2. Morphological appearance of crab hyaline cells during apoptosis compared to ETosis as revealed by cytocentrifugation. (a) Control, viable haemocyte with intact plasma and nuclear membranes. (b-c) Apoptotic HCs cultured for 24 h at 10 ^{o}C in ML-15 medium containing 10 μM of the cyclin-dependent-kinase inhibitor, R-roscovitine (Calbiochem), an inducer of apoptosis[1] **(b)** Membrane blebbing **(c)** Condensed nucleus showing karyorrhexis. **(d)** ETotic cell with extruded chromatin after treatment with 0.1 μM PMA (24 h). All cytocentrifuge preparations were stained with DiffQuik™. Scale bars (a-c) 10 μm, (d) 20 μm.

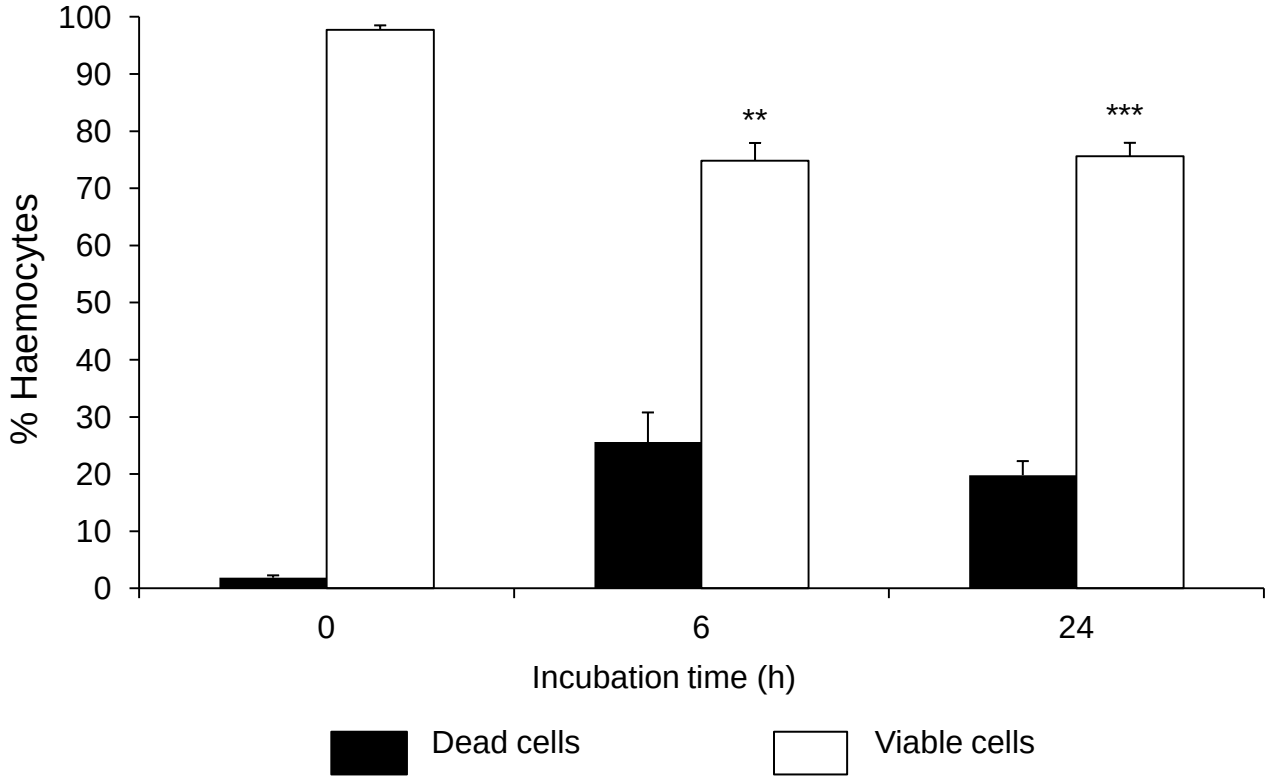

Supplementary Figure 3. Viability of *C. maenas* haemocytes in suspension culture. Washed unseparated *C. maenas* haemocytes cultured in suspension in ML-15 medium at 10 °C and analysed by flow cytometry at 0, 6 and 24 h. The haemocytes were stained with bovine lactadherin-FITC and propidium iodide. *** $P<0.001$ viable versus dead cells at 24 h, ** $P<0.01$ viable versus dead cells at 6 h. Significance calculated by one-way ANOVA with a Student-Neumann-Keuls *post-hoc* test. Values are means ± s.e.m. ($n = 3$).

Supplementary reference

1. Rossi, A.G. *et al*, Cyclin-dependent kinase inhibitors enhance the resolution of inflammation by promoting inflammatory cell apoptosis. *Nat. Med.* **12**, 1056-1064 (2006).

References

Abrams, J.M., White, K., Fessler, L.I., Steller, H. (1993). Programmed cell death during *Drosophila* embryogenesis. *Development* **117**, 29–43.

Aguinaldo, A.M.A., Turbeville, J.M., Linford, L.S., Rivera, M.C., Garey, J.R., Raff, R.A., Lake, J.A. (1997). Evidence for a clade of nematodes, arthropods and other moulting animals. *Nature* **387**, 489–493.

Alessandri, A.L., Duffin, R., Leitch, A.E., Lucas, C.D., Sheldrake, T.A., Dorward, D.A., Hirani, N., Pinho, V., de Sousa, L.P., Teixeira, M.M., Lyons, J.F., Haslett, C., Rossi, A.G. (2011). Induction of Eosinophil Apoptosis by the Cyclin-Dependent Kinase Inhibitor AT7519 Promotes the Resolution of Eosinophil-Dominant Allergic Inflammation. *PLoS ONE* **6**.

Alnemri, E.S., Livingston, D.J., Nicholson, D.W., Salvesen, G., Thornberry, N.A., Wong, W.W., Yuan, J. (1996). Human ICE/CED-3 protease nomenclature. *Cell* **87**, 171.

Altincicek, B., Stotzel, S., Wygrecka, M., Preissner, K.T., Vilcinskas, A. (2008). Host-derived extracellular nucleic acids enhance innate immune responses, induce coagulation, and prolong survival upon infection in insects. *J Immunol* **181**, 2705–12.

Amparyup, P., Kondo, H., Hirono, I., Aoki, T., Tassanakajon, A. (2008). Molecular cloning, genomic organization and recombinant expression of a crustin-like antimicrobial peptide from black tiger shrimp Penaeus monodon. *Mol Immunol*. **45**, 1085–93.

Andrabi, S.A., Dawson, T.M., Dawson, V.L. (2008). Mitochondrial and nuclear cross talk in cell death: parthanatos. *Ann. N. Y. Acad. Sci*. **1147**, 233–241.

Aoshiba, K., Nakajima, Y., Yasui, S., Tamaoki, J., Nagai, A. (1999). Red blood cells inhibit apoptosis of human neutrophils. *Blood* **93**, 4006–4010.

Arazna, M., Pruchniak, M.P., Demkow, U. (2013). Neutrophil extracellular traps in bacterial infections: strategies for escaping from killing. *Respir Physiol Neurobiol* **187**, 74–77.

Aulik, N.A., Hellenbrand, K.M., Czuprynski, C.J. (2012). Mannheimia haemolytica and its leukotoxin cause macrophage extracellular trap formation by bovine macrophages. *Infect Immun* **80**, 1923–33.

Ayala, F.J. and Rzhetsky, A. (1998). Origin of the metazoan phyla: molecular clocks confirm paleontological estimates. *Proc. Natl. Acad. Sci. U.S.A* **95**, 606–611.

Azevedo, E.P.C., Guimarães-Costa, A.B., Torezani, G.S., Braga, C.A., Palhano, F.L., Kelly, J.W., Saraiva, E.M., Foguel, D. (2012). Amyloid fibrils trigger the release of neutrophil extracellular traps (NETs), causing fibril fragmentation by NET-associated elastase. *J. Biol. Chem* **287**, 37206–37218.

Barreiro, R., Luker, G., Herndon, J., Ferguson, T.A. (2004). Termination of Antigen-Specific Immunity by CD95 Ligand (Fas Ligand) and IL-10. *The Journal of Immunology* **173**, 1519–1525.

Bartlett, T.C., Cuthbertson, B.J., Shepard, E.F., Chapman, R.W., Gross, P.S., Warr, G.W. (2002). Crustins, homologues of an 11.5-kDa antibacterial peptide, from two species of penaeid shrimp, *Litopenaeus vannamei* and *Litopenaeus setiferus*. *Mar. Biotechnol* **4**, 278–293.

Bauriedel, G., Hutter, R., Welsch, U., Bach, R., Sievert, H., Luderitz, B. (1999). Role of smooth muscle cell death in advanced coronary primary lesions: implications for plaque instability. *Cardiovasc Res* **41**, 480–8.

Bayne, C.J. (1990). Phagocytosis and Non-Self Recognition in Invertebrates. *BioScience* **40**, 723–731.

Beiter, K., Wartha, F., Albiger, B., Normark, S., Zychlinsky, A., Henriques-Normark, B. (2006). An endonuclease allows Streptococcus pneumoniae to escape from neutrophil extracellular traps. *Curr. Biol* **16**, 401–407.

Beiter, T., Fragasso, A., Hudemann, J., Schild, M., Steinacker, J.M., Mooren, F.C., Niess, A.M. (2014). Neutrophils release extracellular DNA traps in response to exercise. *J. Appl. Physiol* **3**, 325-33.

Bell, K.L. (1994). Studies on Phagocytosis in the Shore Crab "*Carcinus Maenas*" (Crustacea, Decapoda), University of St Andrews PhD thesis.

Bell, K.L. and Smith, V.J. (1993). In vitro superoxide production by hyaline cells of the shore crab *Carcinus maenas* (L.). *Dev Comp Immunol* **17**, 211–9.

Beltman, J., McCormick, F., Cook, S.J. (1996). The selective protein kinase C inhibitor, Ro-31-8220, inhibits mitogen-activated protein kinase phosphatase-1 (MKP-1) expression, induces c-Jun expression, and activates Jun N-terminal kinase. *J. Biol. Chem* **271**, 27018–27024.

Berends, E.T.M., Horswill, A.R., Haste, N.M., Monestier, M., Nizet, V., von Köckritz-Blickwede, M. (2010). Nuclease expression by Staphylococcus aureus facilitates escape from neutrophil extracellular traps. *J Innate Immun* **2**, 576–586.

Bianchi, M., Niemiec, M.J., Siler, U., Urban, C.F., Reichenbach, J. (2011). Restoration of anti-Aspergillus defense by neutrophil extracellular traps in human chronic granulomatous disease after gene therapy is calprotectin-dependent. *J Allergy Clin Immunol* **127**, 1243–52.

Bidla, G., Dushay, M.S., Theopold, U. (2007). Crystal cell rupture after injury in Drosophila requires the JNK pathway, small GTPases and the TNF homolog Eiger. *J Cell Sci* **120**, 1209–15.

Bosmann, M., Grailer, J.J., Ruemmler, R., Russkamp, N.F., Zetoune, F.S., Sarma, J.V., Standiford, T.J., Ward, P.A. (2013). Extracellular histones are essential effectors of C5aR- and C5L2-mediated tissue damage and inflammation in acute lung injury. *FASEB J* **27**, 5010–5021.

Bottjer, D.J. (2005). The early evolution of animals. *Sci. Am* **293**, 42–47.

Boudreau, N., Sympson, C.J., Werb, Z., Bissell, M.J. (1995). Suppression of ICE and apoptosis in mammary epithelial cells by extracellular matrix. *Science* **267**, 891–3.

Branzk, N., Lubojemska, A., Hardison, S.E., Wang, Q., Gutierrez, M.G., Brown, G.D., Papayannopoulos, V. (2014). Neutrophils sense microbe size and selectively release neutrophil extracellular traps in response to large pathogens. *Nat. Immunol.*

Bréa, D., Meurens, F., Dubois, A.V., Gaillard, J., Chevaleyre, C., Jourdan, M.L., Winter, N., Arbeille, B., Si-Tahar, M., Gauthier, F., Attucci, S. (2012). The pig as a model for investigating the role of neutrophil serine proteases in human inflammatory lung diseases. *Biochem. J* **447**, 363–370.

Brill, A., Fuchs, T.A., Savchenko, A.S., Thomas, G.M., Martinod, K., De Meyer, S.F., Bhandari, A.A., Wagner, D.D. (2012). Neutrophil extracellular traps promote deep vein thrombosis in mice. *J. Thromb. Haemost* **10**, 136–144.

Brinkmann, V., Reichard, U., Goosmann, C., Fauler, B., Uhlemann, Y., Weiss, D.S., Weinrauch, Y., Zychlinsky, A. (2004). Neutrophil extracellular traps kill bacteria. *Science* **303**, 1532–5.

Brinkmann, V. and Zychlinsky, A. (2012). Neutrophil extracellular traps: is immunity the second function of chromatin? *J Cell Biol* **198**, 773–83.

Brockton, V., Hammond, J.A., Smith, V.J. (2007). Gene characterisation, isoforms and recombinant expression of carcinin, an antibacterial protein from the shore crab, *Carcinus maenas. Mol. Immunol* **44**, 943–949.

Brockton, V. and Smith, V.J. (2008). Crustin expression following bacterial injection and temperature change in the shore crab, *Carcinus maenas*. *Dev Comp Immunol* **32**, 1027–33.

Brogden, G., von Köckritz-Blickwede, M., Adamek, M., Reuner, F., Jung-Schroers, V., Naim, H.Y., Steinhagen, D. (2012). β-Glucan protects neutrophil extracellular traps against degradation by Aeromonas hydrophila in carp (*Cyprinus carpio*). *Fish & Shellfish Immunology* **33**, 1060–1064.

Bruns, S., Kniemeyer, O., Hasenberg, M., Aimanianda, V., Nietzsche, S., Thywissen, A., Jeron, A., Latge, J.P., Brakhage, A.A., Gunzer, M. (2010). Production of extracellular traps against *Aspergillus fumigatus in vitro* and in infected lung tissue is dependent on invading neutrophils and influenced by hydrophobin RodA. *PLoS Pathog* **6**.

Buchanan, J.T., Simpson, A.J., Aziz, R.K., Liu, G.Y., Kristian, S.A., Kotb, M., Feramisco, J., Nizet, V. (2006). DNase expression allows the pathogen group A *Streptococcus* to escape killing in neutrophil extracellular traps. *Curr. Biol* **16**, 396–400.

Burhans, W.C., Weinberger, M., Marchetti, M.A., Ramachandran, L., D'Urso, G., Huberman, J.A. (2003). Apoptosis-like yeast cell death in response to DNA damage and replication defects. *Mutat Res* **532**, 227–43.

Capinera, J.L. (2008). Encyclopedia of Entomology. Springer Science & Business Media.

Caserta, T.M., Smith, A.N., Gultice, A.D., Reedy, M.A., Brown, T.L. (2003). Q-VD-OPh, a broad spectrum caspase inhibitor with potent antiapoptotic properties. *Apoptosis* **8**, 345–352.

Center for History and New Media, n.d. Zotero Quick Start Guide [WWW Document]. URL http://zotero.org/support/quick_start_guide

Cerenius, L. and Söderhäll, K. (2004). The prophenoloxidase-activating system in invertebrates. *Immunol. Rev* **198**, 116–126.

Chagas, A.C., Oliveira, F., Debrabant, A., Valenzuela, J.G., Ribeiro, J.M.C., Calvo, E. (2014). Lundep, a Sand Fly Salivary Endonuclease Increases *Leishmania* Parasite Survival in Neutrophils and Inhibits XIIa Contact Activation in Human Plasma. *PLoS Pathog* **10**.

Chang, C.C., Yeh, M.S., Lin, H.K., Cheng, W. (2008). The effect of *Vibrio alginolyticus* infection on caspase-3 expression and activity in white shrimp *Litopenaeus vannamei*. *Fish Shellfish Immunol* **25**, 672–8.

Chang, C.C., Yeh, M.S., Cheng, W. (2009). Cold shock-induced norepinephrine triggers apoptosis of haemocytes via caspase-3 in the white shrimp, *Litopenaeus vannamei*. *Fish Shellfish Immunol* **27**, 695–700.

Chaurio, R., Janko, C., Muñoz, L., Frey, B., Herrmann, M., Gaipl, U. (2009). Phospholipids: Key Players in Apoptosis and Immune Regulation. *Molecules* **14**, 4892–4914.

Chen, G., Zhang, D., Fuchs, T.A., Manwani, D., Wagner, D.D., Frenette, P.S. (2014). Heme-induced neutrophil extracellular traps contribute to the pathogenesis of sickle cell disease. *Blood* **123**, 3818–3827.

Chen, L.M., Kaniga, K., Galan, J.E. (1996). Salmonella spp. are cytotoxic for cultured macrophages. *Mol Microbiol* **21**, 1101–15.

Cheng, W., Liu, C.H., Tsai, C.H., Chen, J.C. (2005). Molecular cloning and characterisation of a pattern recognition molecule, lipopolysaccharide- and beta-1,3-glucan binding protein (LGBP) from the white shrimp *Litopenaeus vannamei*. *Fish Shellfish Immunol* **18**, 297–310.

Chiruvella, K.K., Kari, V., Choudhary, B., Nambiar, M., Ghanta, R.G., Raghavan, S.C. (2008). Methyl angolensate, a natural tetranortriterpenoid induces intrinsic apoptotic pathway in leukemic cells. *FEBS Lett* **582**, 4066–76.

Chisholm, J.R.S. and Smith, V.J. (1992). Antibacterial activity in the haemocytes of the shore crab, *Carcinus maenas*. *Journal of the Marine Biological Association of the United Kingdom* **72**, 529–542.

Chisholm, J.R.S. and Smith, V.J. (1994). Variation of antibacterial activity in the haemocytes of the shore crab, *Carcinus maenas*, with temperature. *Journal of the Marine Biological Association of the United Kingdom* **74**, 979–982.

Chuammitri, P., Ostojic, J., Andreasen, C.B., Redmond, S.B., Lamont, S.J., Palic, D. (2009). Chicken heterophil extracellular traps (HETs): novel defense mechanism of chicken heterophils. *Vet Immunol Immunopathol* **129**, 126–31.

Cikala, M., Wilm, B., Hobmayer, E., Bottger, A., David, C.N. (1999). Identification of caspases and apoptosis in the simple metazoan Hydra. *Curr Biol* **9**, 959–62.

Clark, S.R., Ma, A.C., Tavener, S.A., McDonald, B., Goodarzi, Z., Kelly, M.M., Patel, K.D., Chakrabarti, S., McAvoy, E., Sinclair, G.D., Keys, E.M., Allen-Vercoe, E., Devinney, R., Doig, C.J., Green, F.H., Kubes, P. (2007). Platelet TLR4 activates neutrophil extracellular traps to ensnare bacteria in septic blood. *Nat Med* **13**, 463–9.

Coates, C.J. and Nairn, J. (2014). Diverse immune functions of hemocyanins. *Developmental & Comparative Immunology* **45**, 43–55.

Cohen, A.N., Carlton, J.T., Fountain, M.C. (1995). Introduction, dispersal and potential impacts of the green crab *Carcinus maenas* in San Francisco Bay, California. *Marine Biology* **122**, 225–237.

Coles, J.A., Farley, S.R., Pipe, R.K. (1995). Alteration of the immune response of the common marine mussel *Mytilus edulis* resulting from exposure to cadmium. *Diseases of Aquatic Organisms* **22**, 59–65.

Colotta, F., Re, F., Polentarutti, N., Sozzani, S., Mantovani, A. (1992). Modulation of granulocyte survival and programmed cell death by cytokines and bacterial products. *Blood* **80**, 2012–20.

Conradt, B. and Horvitz, H.R. (1999). The TRA-1A sex determination protein of *C. elegans* regulates sexually dimorphic cell deaths by repressing the egl-1 cell death activator gene. *Cell* **98**, 317–27.

Cookson, B.T. and Brennan, M.A. (2001). Pro-inflammatory programmed cell death. *Trends Microbiol* **9**, 113–4.

Cools-Lartigue, J., Spicer, J., McDonald, B., Gowing, S., Chow, S., Giannias, B., Bourdeau, F., Kubes, P., Ferri, L. (2013). Neutrophil extracellular traps sequester circulating tumor cells and promote metastasis. *J Clin Invest* **1**.

Danial, N.N. and Korsmeyer, S.J. (2004). Cell Death: Critical Control Points. *Cell* **116**, 205–219.

Darzynkiewicz, Z., Huang, X., Okafuji, M., King, M.A. (2004). Cytometric methods to detect apoptosis. *Methods Cell Biol* **75**, 307–41.

Darzynkiewicz, Z., Juan, G., Li, X., Gorczyca, W., Murakami, T., Traganos, F. (1997). Cytometry in cell necrobiology: analysis of apoptosis and accidental cell death (necrosis). *Cytometry* **27**, 1–20.

Dasgupta, S.K., Guchhait, P., Thiagarajan, P. (2006). Lactadherin binding and phosphatidylserine expression on cell surface-comparison with annexin A5. *Transl Res* **148**, 19–25.

DeChatelet, L.R., Shirley, P.S., Johnston, R.B., Jr. (1976). Effect of phorbol myristate acetate on the oxidative metabolism of human polymorphonuclear leukocytes. *Blood* **47**, 545–554.

De Guise, S., Morsey, B., Maratea, J., Goedken, M., Sidor, I., Atherton, J. (2005). Development of assays to evaluate cellular immune function in the American lobster (*Homarus americanus*). *Journal of Shellfish Research* **24**, 705–711.

De Jong, J.S., van Diest, P.J., van der Valk, P., Baak, J.P. (2001). Expression of growth factors, growth factor receptors and apoptosis related proteins in invasive breast cancer: relation to apoptotic rate. *Breast Cancer Res Treat* **66**, 201–8.

Dekker, L.V., Leitges, M., Altschuler, G., Mistry, N., McDermott, A., Roes, J., Segal, A.W. (2000). Protein kinase C-beta contributes to NADPH oxidase activation in neutrophils. *Biochem J* **347**, 285–289.

Deter, R.L. and De Duve, C. (1967). Influence of glucagon, an inducer of cellular autophagy, on some physical properties of rat liver lysosomes. *J. Cell Biol* **33**, 437–449.

Deveraux, Q.L. and Reed, J.C. (1999). IAP family proteins--suppressors of apoptosis. *Genes Dev* **13**, 239–52.

Dixon, S.J., Lemberg, K.M., Lamprecht, M.R., Skouta, R., Zaitsev, E.M., Gleason, C.E., Patel, D.N., Bauer, A.J., Cantley, A.M., Yang, W.S., Morrison III, B., Stockwell, B.R. (2012). Ferroptosis: An Iron-Dependent Form of Nonapoptotic Cell Death. *Cell* **149**, 1060–1072.

Dockrell, D.H., Marriott, H.M., Prince, L.R., Ridger, V.C., Ince, P.G., Hellewell, P.G., Whyte, M.K. (2003). Alveolar macrophage apoptosis contributes to pneumococcal clearance in a resolving model of pulmonary infection. *J Immunol* **171**, 5380–8.

Doitsh, G., Galloway, N.L.K., Geng, X., Yang, Z., Monroe, K.M., Zepeda, O., Hunt, P.W., Hatano, H., Sowinski, S., Muñoz-Arias, I., Greene, W.C. (2014). Cell death by pyroptosis drives CD4 T-cell depletion in HIV-1 infection. *Nature* **505**, 509–514.

Dorward, D.A., Lucas, C.D., Alessandri, A.L., Marwick, J.A., Rossi, F., Dransfield, I., Haslett, C., Dhaliwal, K., Rossi, A.G. (2013). Technical Advance: Autofluorescence-based sorting: rapid and nonperturbing isolation of ultrapure neutrophils to determine cytokine production. *J Leukoc Biol* **94**, 193–202.

Dransfield, I., Buckle, A.M., Savill, J.S., McDowall, A., Haslett, C., Hogg, N. (1994). Neutrophil apoptosis is associated with a reduction in CD16 (Fc gamma RIII) expression. *J Immunol* **153**, 1254–63.

Drummond, G.R., Selemidis, S., Griendling, K.K., Sobey, C.G. (2011). Combating oxidative stress in vascular disease: NADPH oxidases as therapeutic targets. *Nat Rev Drug Discov* **10**, 453–471.

Dubois, A.V., Gauthier, A., Bréa, D., Varaigne, F., Diot, P., Gauthier, F., Attucci, S. (2012). Influence of DNA on the activities and inhibition of neutrophil serine proteases in cystic fibrosis sputum. *Am. J. Respir. Cell Mol. Biol* **47**, 80–86.

Dubrez-Daloz, L., Dupoux, A., Cartier, J. (2008). IAPs: more than just inhibitors of apoptosis proteins. *Cell Cycle* **7**, 1036–46..

Dunn, S.R., Phillips, W.S., Spatafora, J.W., Green, D.R., Weis, V.M. (2006). Highly conserved caspase and Bcl-2 homologues from the sea anemone *Aiptasia pallida*: lower metazoans as models for the study of apoptosis evolution. *J Mol Evol* **63**, 95–107.

Dwyer, M., Shan, Q., D'Ortona, S., Maurer, R., Mitchell, R., Olesen, H., Thiel, S., Huebner, J., Gadjeva, M. (2014). Cystic Fibrosis Sputum DNA Has NETosis Characteristics and Neutrophil Extracellular Trap Release Is Regulated by Macrophage Migration-Inhibitory Factor. *J Innate Immun*.

Ekert, P.G. and Vaux, D.L. (1997). Apoptosis and the immune system. *Br Med Bull* **53**, 591–603.

Elmore, S. (2007). Apoptosis: A Review of Programmed Cell Death. *Toxicologic Pathology* **35**, 495–516.

Ermert, D., Urban, C.F., Laube, B., Goosmann, C., Zychlinsky, A., Brinkmann, V. (2009). Mouse neutrophil extracellular traps in microbial infections. *J Innate Immun* **1**, 181–93.

Escobedo-Bonilla, C.M., Alday-Sanz, V., Wille, M., Sorgeloos, P., Pensaert, M.B., Nauwynck, H.J. (2008). A review on the morphology, molecular characterization, morphogenesis and pathogenesis of white spot syndrome virus. *J Fish Dis* **31**, 1–18.

Farrera, C., Bhattacharya, K., Lazzaretto, B., Andón, F.T., Hultenby, K., Kotchey, G.P., Star, A., Fadeel, B. (2014). Extracellular entrapment and degradation of single-walled carbon nanotubes. *Nanoscale*.

Farrera, C. and Fadeel, B. (2013). Macrophage clearance of neutrophil extracellular traps is a silent process. *J. Immunol* **191**, 2647–2656.

Fernandes, J.M.O., Kemp, G.D., Molle, M.G., Smith, V.J. (2002). Anti-microbial properties of histone H2A from skin secretions of rainbow trout, *Oncorhynchus mykiss*. *Biochemical Journal* **368**, 611-620.

Fink, S.L. and Cookson, B.T. (2005). Apoptosis, pyroptosis, and necrosis: mechanistic description of dead and dying eukaryotic cells. *Infect Immun* **73**, 1907–16.

Frantz, S., Ducharme, A., Sawyer, D., Rohde, L.E., Kobzik, L., Fukazawa, R., Tracey, D., Allen, H., Lee, R.T., Kelly, R.A. (2003). Targeted deletion of caspase-1 reduces early mortality and left ventricular dilatation following myocardial infarction. *J Mol Cell Cardiol* **35**, 685–94.

Frisch, S.M. and Francis, H. (1994). Disruption of epithelial cell-matrix interactions induces apoptosis. *J Cell Biol* **124**, 619–26.

Fuchs, T.A., Abed, U., Goosmann, C., Hurwitz, R., Schulze, I., Wahn, V., Weinrauch, Y., Brinkmann, V., Zychlinsky, A. (2007). Novel cell death program leads to neutrophil extracellular traps. *J Cell Biol* **176**, 231–41.

Fuchs, T.A., Brill, A., Duerschmied, D., Schatzberg, D., Monestier, M., Myers, D.D., Jr., Wrobleski, S.K., Wakefield, T.W., Hartwig, J.H., Wagner, D.D. (2010). Extracellular DNA traps promote thrombosis. *Proc Natl Acad Sci U S A* **107**, 15880–5.

Fuchs, T.A., Brill, A., Wagner, D.D. (2012). Neutrophil extracellular trap (NET) impact on deep vein thrombosis. *Arterioscler. Thromb. Vasc. Biol* **32**, 1777–1783.

Fulda, S. and Vucic, D. (2012). Targeting IAP proteins for therapeutic intervention in cancer. *Nat Rev Drug Discov* **11**, 109–24.

Galvão, A., Rebordão, M.R., Szóstek, A.Z., J. Skarzynski, D., Ferreira-Dias, G. (2012). Cytokines and neutrophil extracellular traps in the equine endometrium: friends or foes? *Pferdeheilkunde* **1**, 4-7.

Gandin, V., Pellei, M., Tisato, F., Porchia, M., Santini, C., Marzano, C. (2012). A novel copper complex induces paraptosis in colon cancer cells via the activation of ER stress signalling. *Journal of Cellular and Molecular Medicine* **16**, 142–151.

Gavrieli, Y., Sherman, Y., Ben-Sasson, S.A. (1992). Identification of programmed cell death in situ via specific labeling of nuclear DNA fragmentation. *J Cell Biol* **119**, 493–501.

Ghavami, S., Hashemi, M., Ande, S.R., Yeganeh, B., Xiao, W., Eshraghi, M., Bus, C.J., Kadkhoda, K., Wiechec, E., Halayko, A.J., Los, M. (2009). Apoptosis and cancer: mutations within caspase genes. *J Med Genet* **46**, 497–510.

Giomi, F. and Portner, H.O. (2013). A role for haemolymph oxygen capacity in heat tolerance of eurythermal crabs. *Front Physiol* **4**.

Graidist, P., Fujise, K., Wanna, W., Sritunyalucksana, K., Phongdara, A. (2006). Establishing a role for shrimp fortilin in preventing cell death. *Aquaculture* **255**, 157–164.

Granja, C.B., Aranguren, L.F., Vidal, O.M., Aragon, L., Salazar, M. (2003). Does hyperthermia increase apoptosis in white spot syndrome virus (WSSV)-infected *Litopenaeus vannamei*? *Dis Aquat Organ* **54**, 73–8.

Gray, R.D., Lucas, C.D., Mackellar, A., Li, F., Hiersemenzel, K., Haslett, C., Davidson, D.J., Rossi, A.G. (2013). Activation of conventional protein kinase C (PKC) is critical in the generation of human neutrophil extracellular traps. *J Inflamm* **10**.

Griffith, T.S. and Ferguson, T.A. (2011). Cell Death in the Maintenance and Abrogation of Tolerance: The Five Ws of Dying Cells. *Immunity* **35**, 456–466.

Guicciardi, M.E. and Gores, G.J. (2009). Life and death by death receptors. *Faseb J.* **23**, 1625–37.

Guimarães-Costa, A.B., Souza-Vieira, T.S., Paletta-Silva, R., Freitas-Mesquita, A.L., Meyer-Fernandes, J.R., Saraiva, E.M. (2014). 3'-Nucleotidase/nuclease activity allows *Leishmania* parasites to escape killing by neutrophil extracellular traps. *Infect. Immun* **4**, 1732-40.

Guo, H., Xian, J.A., Li, B., Ye, C.X., Wang, A.L., Miao, Y.T., Liao, S.A. (2013). Gene expression of apoptosis-related genes, stress protein and antioxidant enzymes in hemocytes of white shrimp *Litopenaeus vannamei* under nitrite stress. *Comp Biochem Physiol C Toxicol Pharmacol* **157**, 366–71.

Haase, H., Fahmi, A., Mahltig, B. (2014). Impact of silver nanoparticles and silver ions on innate immune cells. *J Biomed Nanotechnol* **10**, 1146–1156.

Hacker, G. (2000). The morphology of apoptosis. *Cell Tissue Res* **301**, 5–17.

Hakkim, A., Fürnrohr, B.G., Amann, K., Laube, B., Abed, U.A., Brinkmann, V., Herrmann, M., Voll, R.E., Zychlinsky, A. (2010). Impairment of neutrophil extracellular trap degradation is associated with lupus nephritis. *Proc. Natl. Acad. Sci. U.S.A* **107**, 9813–9818.

Hakkim, A., Fuchs, T.A., Martinez, N.E., Hess, S., Prinz, H., Zychlinsky, A., Waldmann, H. (2011). Activation of the Raf-MEK-ERK pathway is required for neutrophil extracellular trap formation. *Nat Chem Biol* **7**, 75–77.

Hall, P.A., Coates, P.J., Ansari, B., Hopwood, D. (1994). Regulation of cell number in the mammalian gastrointestinal tract: the importance of apoptosis. *J Cell Sci* **107**, 3569–77.

Hammond, J.A. and Smith, V.J. (2002). Lipopolysaccharide induces DNA-synthesis in a sub-population of hemocytes from the swimming crab, *Liocarcinus depurator*. *Dev Comp Immunol* **26**, 227–36.

Hauton, C., Brockton, V., Smith, V.J. (2006). Cloning of a crustin-like, single whey-acidic-domain, antibacterial peptide from the haemocytes of the European lobster, *Homarus gammarus*, and its response to infection with bacteria. *Mol Immunol* **43**, 1490–6.

Hauton, C., Williams, J.A., Hawkins, L.E. (1997). The effects of a live *in vivo* pathogenic infection on aspects of the immunocompetence of the common shore crab, *Carcinus maenas* (L.). *Journal of Experimental Marine Biology and Ecology* **211**, 115–128.

Hauton, C. (2012). The scope of the crustacean immune system for disease control. *J. Invertebr. Pathol* **110**, 251–260.

Hazeldine, J., Harris, P., Chapple, I.L., Grant, M., Greenwood, H., Livesey, A., Sapey, E., Lord, J.M. (2014). Impaired neutrophil extracellular trap formation: a novel defect in the innate immune system of aged individuals. *Aging Cell* **13**, 690-698.

Hemmers, S., Teijaro, J.R., Arandjelovic, S., Mowen, K.A. (2011). PAD4-Mediated Neutrophil Extracellular Trap Formation Is Not Required for Immunity against Influenza Infection. *PLoS ONE* **6**.

Henderson, L.M. and Chappell, J.B. (1993). Dihydrorhodamine 123: a fluorescent probe for superoxide generation? *European Journal of Biochemistry* **217**, 973–980.

Hengartner, M.O.and Horvitz, H.R. (1994). *C. elegans* cell survival gene ced-9 encodes a functional homolog of the mammalian proto-oncogene bcl-2. *Cell* **76**, 665–76.

Her, E., Frazer, J., Austen, K.F., Owen, W.F., Jr. (1991). Eosinophil hematopoietins antagonize the programmed cell death of eosinophils. Cytokine and glucocorticoid effects on eosinophils maintained by endothelial cell-conditioned medium. *J Clin Invest* **88**, 1982–7.

Hermosilla, C., Caro, T.M., Silva, L.M.R., Ruiz, A., Taubert, A. (2014). The intriguing host innate immune response: novel anti-parasitic defence by neutrophil extracellular traps. *Parasitology* **11**, 1489-98.

Hernroth, B., Sköld, H.N., Wiklander, K., Jutfelt, F., Baden, S. (2012). Simulated climate change causes immune suppression and protein damage in the crustacean *Nephrops norvegicus*. *Fish & Shellfish Immunology* **33**, 1095–1101.

Hirsch, J.G. (1958). Bactericidal action of histone. *J Exp Med* **108**, 925–944.

Homburg, C.H., de Haas, M., von dem Borne, A.E., Verhoeven, A.J., Reutelingsperger, C.P., Roos, D. (1995). Human neutrophils lose their surface Fc gamma RIII and acquire Annexin V binding sites during apoptosis *in vitro*. *Blood* **85**, 532–40.

Hong, W., Juneau, R.A., Pang, B., Swords, W.E. (2009). Survival of bacterial biofilms within neutrophil extracellular traps promotes nontypeable Haemophilus influenzae persistence in the chinchilla model for otitis media. *J Innate Immun* **1**, 215–224.

Horowitz, N.H. and Hubbard, J.S. (1974). The Origin of Life. *Annual Review of Genetics* **8**, 393–410.

Hose, J.E., Martin, G.G., Nguyen, V.A., Lucas, J., Rosenstein, T. (1987). Cytochemical Features of Shrimp Hemocytes. *Biol Bull* **173**, 178–187.

Hose, J.E., Martin, G.G., Tiu, S., McKrell, N. (1992). Patterns of hemocyte production and release throughout the molt cycle in the penaeid shrimp *Sicyonia ingentis*. *Biological Bulletin* **183**, 185–199.

Hou, C.C. and Yang, W.X. (2013). Characterization and expression pattern of p53 during spermatogenesis in the Chinese mitten crab *Eriocheir sinensis*. *Mol Biol Rep* **40**, 1043–1051.

Hsu, J.P., Huang, C., Liao, C.M., Hsuan, S.L., Hung, H.H., Chien, M.S. (2005). Engulfed pathogen-induced apoptosis in haemocytes of giant freshwater prawn, *Macrobrachium rosenbergii*. *J. Fish Dis* **28**, 729–735.

Hutton, D. and Smith, V.J. (1996). Antibacterial properties of isolated amoebocytes from the sea anemone *Actinia equina*. *Biol Bull* **191**, 441–451.

Iba, T., Miki, T., Hashiguchi, N., Tabe, Y., Nagaoka, I. (2014). Is the neutrophil a "prima donna" in the procoagulant process during sepsis? *Crit Care* **18**, 230.

Iwanaga, S. and Lee, B.L. (2005). Recent advances in the innate immunity of invertebrate animals. *J Biochem Mol Biol* **38**, 128–50.

Janeway, C.A. Jr. and Medzhitov, R. (2002). Innate immune recognition. *Annu Rev Immunol* **20**, 197–216.

Janeway C.A. Jr., T.P., Walport M and Shlomchik M. (2001). Immunobiology: The Immune System in Health and Disease., 5th edition. Garland Science, New York.

Jiang, N., Tan, N.S., Ho, B., Ding, J.L. (2007). Respiratory protein–generated reactive oxygen species as an antimicrobial strategy. *Nat Immunol* **8**, 1114–1122.

Jin, X.K., Li, W.W., He, L., Lu, W., Chen, L.L., Wang, Y., Jiang, H., Wang, Q. (2011). Molecular cloning, characterization and expression analysis of two apoptosis genes, caspase and nm23, involved in the antibacterial response in Chinese mitten crab, *Eriocheir sinensis*. *Fish & Shellfish Immunology* **30**, 263–272.

Ji, P.F., Yao, C.L., Wang, Z.Y. (2009). Immune response and gene expression in shrimp (Litopenaeus vannamei) hemocytes and hepatopancreas against some pathogen-associated molecular patterns. *Fish Shellfish Immunol* **27**, 563–70.

Jiravanichpaisal, P., Lee, S.Y., Kim, Y.A., Andren, T., Soderhall, I. (2007). Antibacterial peptides in hemocytes and hematopoietic tissue from freshwater crayfish *Pacifastacus leniusculus*: characterization and expression pattern. *Dev Comp Immunol* **31**, 441–55.

Johansson, M.W. (1999). Cell adhesion molecules in invertebrate immunity. *Dev. Comp. Immunol* **23**, 303–315.

Johansson, M.W., Lind, M.I., Holmblad, T., Thornqvist, P.O., Soderhall, K. (1995). Peroxinectin, a novel cell adhesion protein from crayfish blood. *Biochem Biophys Res Commun* **216**, 1079–87.

Johnson, N.G., Burnett, L.E., Burnett, K.G. (2011). Properties of bacteria that trigger hemocytopenia in the Atlantic blue crab, *Callinectes sapidus*. *Biol Bull* **221**, 164–75.

Jung, S., Dingley, A.J., Augustin, R., Anton-Erxleben, F., Stanisak, M., Gelhaus, C., Gutsmann, T., Hammer, M.U., Podschun, R., Bonvin, A.M.J.J., Leippe, M., Bosch, T.C.G., Grötzinger, J. (2009). Hydramacin-1, structure and antibacterial activity of a protein from the basal metazoan Hydra. *J. Biol. Chem* **284**, 1896–1905.

Jurisicova, A., Varmuza, S., Casper, R.F. (1996). Programmed cell death and human embryo fragmentation. *Mol Hum Reprod* **2**, 93–8.

Kaczanowski, S., Sajid, M., Reece, S.E. (2011). Evolution of apoptosis-like programmed cell death in unicellular protozoan parasites. *Parasit Vectors* **4**.

Kam, P.C. and Ferch, N.I. (2000). Apoptosis: mechanisms and clinical implications. *Anaesthesia* **55**, 1081–93.

Kawakami, T., He, J., Morita, H., Yokoyama, K., Kaji, H., Tanaka, C., Suemori, S., Tohyama, K., Tohyama, Y. (2014). Rab27a Is Essential for the Formation of Neutrophil Extracellular Traps (NETs) in Neutrophil-Like Differentiated HL60 Cells. *PLoS ONE* **9**.

Kawata, J., Kikuchi, M., Saitoh, H. (2014). Genomic DNAs in a human leukemia cell line unfold after cold shock, with formation of neutrophil extracellular trap-like structures. *Biotechnol. Lett* **36**, 241–250.

Kerr, J.F., Wyllie, A.H., Currie, A.R. (1972). Apoptosis: a basic biological phenomenon with wide-ranging implications in tissue kinetics. *Br J Cancer* **26**, 239–57.

Keshari, R.S., Jyoti, A., Dubey, M., Kothari, N., Kohli, M., Bogra, J., Barthwal, M.K., Dikshit, M. (2012). Cytokines induced neutrophil extracellular traps formation: implication for the inflammatory disease condition. *PLoS One* **7**.

Khandpur, R., Carmona-Rivera, C., Vivekanandan-Giri, A., Gizinski, A., Yalavarthi, S., Knight, J.S., Friday, S., Li, S., Patel, R.M., Subramanian, V., Thompson, P., Chen, P., Fox, D.A., Pennathur, S., Kaplan, M.J. (2013). NETs are a source of citrullinated autoantigens and stimulate inflammatory responses in rheumatoid arthritis. *Sci Transl Med* **5**.

Khanobdee, K., Soowannayan, C., Flegel, T.W., Ubol, S., Withyachumnarnkul, B. (2002). Evidence for apoptosis correlated with mortality in the giant black tiger shrimp *Penaeus monodon* infected with yellow head virus. *Dis Aquat Organ* **48**, 79–90.

Kim, Y.N., Koo, K.H., Sung, J.Y., Yun, U.J., Kim, H. (2012). Anoikis resistance: an essential prerequisite for tumor metastasis. *Int J Cell Biol*.

Kolodgie, F.D., Narula, J., Burke, A.P., Haider, N., Farb, A., Hui-Liang, Y., Smialek, J., Virmani, R. (2000). Localization of apoptotic macrophages at the site of plaque rupture in sudden coronary death. *Am J Pathol* **157**, 1259–68.

Koopman, G., Reutelingsperger, C.P., Kuijten, G.A., Keehnen, R.M., Pals, S.T., van Oers, M.H. (1994). Annexin V for flow cytometric detection of phosphatidylserine expression on B cells undergoing apoptosis. *Blood* **84**, 1415–20.

Kuhnel, F., Zender, L., Paul, Y., Tietze, M.K., Trautwein, C., Manns, M., Kubicka, S. (2000). NFkappaB mediates apoptosis through transcriptional activation of Fas (CD95) in adenoviral hepatitis. *J Biol Chem* **275**, 6421–7.

Kumar, S. (2007). Caspase function in programmed cell death. *Cell Death Differ* **14**, 32–43.

Kumar, S. and Doumanis, J. (2000). The fly caspases. *Cell Death Differ* **7**, 1039–44.

Kurosaka, K., Takahashi, M., Watanabe, N., Kobayashi, Y. (2003). Silent cleanup of very early apoptotic cells by macrophages. *J Immunol* **171**, 4672–9.

Lacoste, A., De Cian, M.C., Cueff, A., Poulet, S.A. (2001). Noradrenaline and alpha-adrenergic signalling induce the hsp70 gene promoter in mollusc immune cells. *J Cell Sci* **114**, 3557–64.

Lamkanfi, M., Declercq, W., Kalai, M., Saelens, X., Vandenabeele, P. (2002). Alice in caspase land. A phylogenetic analysis of caspases from worm to man. *Cell Death Differ* **9**, 358–61.

Lande, R., Ganguly, D., Facchinetti, V., Frasca, L., Conrad, C., Gregorio, J., Meller, S., Chamilos, G., Sebasigari, R., Riccieri, V., Bassett, R., Amuro, H., Fukuhara, S., Ito, T., Liu, Y.-J., Gilliet, M. (2011). Neutrophils activate plasmacytoid dendritic cells by releasing self-DNA-peptide complexes in systemic lupus erythematosus. *Sci Transl Med* **3**.

Lee, A., Whyte, M.K., Haslett, C. (1993). Inhibition of apoptosis and prolongation of neutrophil functional longevity by inflammatory mediators. *J Leukoc Biol* **54**, 283–8.

Lee, S.H., Meng, X.W., Flatten, K.S., Loegering, D.A., Kaufmann, S.H. (2013). Phosphatidylserine exposure during apoptosis reflects bidirectional trafficking between plasma membrane and cytoplasm. *Cell Death Differ* **20**, 64–76.

Leitch, A.E., Riley, N.A., Sheldrake, T.A., Festa, M., Fox, S., Duffin, R., Haslett, C., Rossi, A.G. (2010). The cyclin-dependent kinase inhibitor R-roscovitine down-regulates Mcl-1 to override pro-inflammatory signalling and drive neutrophil apoptosis. *Eur J Immunol* **40**, 1127–38.

Leitch, A.E., Lucas, C.D., Marwick, J.A., Duffin, R., Haslett, C., Rossi, A.G. (2012). Cyclin-dependent kinases 7 and 9 specifically regulate neutrophil transcription and their inhibition drives apoptosis to promote resolution of inflammation. *Cell Death Differ* **19**, 1950–61.

Leu, J.H., Kuo, Y.C., Kou, G.H., Lo, C.F. (2008). Molecular cloning and characterization of an inhibitor of apoptosis protein (IAP) from the tiger shrimp, *Penaeus monodon*. *Dev Comp Immunol* **32**, 121–33.

Leu, J.H., Chen, Y.C., Chen, L.L., Chen, K.Y., Huang, H.T., Ho, J.M., Lo, C.F. (2012). Litopenaeus vannamei inhibitor of apoptosis protein 1 (LvIAP1) is essential for shrimp survival. *Dev Comp Immunol* **38**, 78–87.

Levi-Schaffer, F., Temkin, V., Malamud, V., Feld, S., Zilberman, Y. (1998). Mast Cells Enhance Eosinophil Survival In Vitro: Role of TNF-α and Granulocyte-Macrophage Colony-Stimulating Factor. *J Immunol* **160**, 5554–5562.

Li, F., Zhang, D., Fujise, K. (2001). Characterization of fortilin, a novel antiapoptotic protein. *J Biol Chem* **276**, 47542–9.

Lin, X. and Soderhall, I. (2011). Crustacean hematopoiesis and the astakine cytokines. *Blood* **117**, 6417–24.

Lippolis, J.D., Reinhardt, T.A., Goff, J.P., Horst, R.L. (2006). Neutrophil extracellular trap formation by bovine neutrophils is not inhibited by milk. *Vet Immunol Immunopathol* **113**, 248–55.

Liu, H., Chen, R., Zhang, Q., Peng, H., Wang, K. (2011). Differential gene expression profile from haematopoietic tissue stem cells of red claw crayfish, *Cherax quadricarinatus*, in response to WSSV infection. *Developmental & Comparative Immunology* **35**, 716–724.

Liu, H., Wang, Y., Zhang, Y., Song, Q., Di, C., Chen, G., Tang, J., Ma, D. (1999). TFAR19, a novel apoptosis-related gene cloned from human leukemia cell line TF-1, could enhance apoptosis of some tumor cells induced by growth factor withdrawal. *Biochem Biophys Res Commun* **254**, 203–10.

Liu, Q.A. and Hengartner, M.O. (1999). The molecular mechanism of programmed cell death in *C. elegans*. *Ann N Y Acad Sci* **887**, 92–104.

Li, W.W., Jin, X.K., He, L., Jiang, H., Xie, Y.N., Wang, Q. (2010a). Molecular cloning, characterization and expression analysis of cathepsin C gene involved in the antibacterial response in Chinese mitten crab, *Eriocheir sinensis*. *Dev Comp Immunol* **34**, 1170-4.

Li, W.W., Jin, X.K., He, L., Jiang, H., Gong, Y.N., Xie, Y.N., Wang, Q. (2010b). Molecular cloning, characterization, expression and activity analysis of cathepsin L in Chinese mitten crab, *Eriocheir sinensis*. *Fish & Shellfish Immunology* **29**, 1010–1018.

Locksley, R.M., Killeen, N., Lenardo, M.J. (2001). The TNF and TNF receptor superfamilies: integrating mammalian biology. *Cell* **104**, 487–501.

Lögters, T., Margraf, S., Altrichter, J., Cinatl, J., Mitzner, S., Windolf, J., Scholz, M. (2009). The clinical value of neutrophil extracellular traps. *Med. Microbiol. Immunol* **198**, 211–219.

Lorenzon, S., de Guarrini, S., Smith, V.J., Ferrero, E.A. (1999). Effects of LPS injection on circulating haemocytes in crustaceans *in vivo*. *Fish & Shellfish Immunology* **9**, 31–50.

Lowe, S.W. and Lin, A.W. (2000). Apoptosis in cancer. *Carcinogenesis* **21**, 485–495.

Lucas, C.D., Allen, K.C., Dorward, D.A., Hoodless, L.J., Melrose, L.A., Marwick, J.A., Tucker, C.S., Haslett, C., Duffin, R., Rossi, A.G. (2013). Flavones induce neutrophil apoptosis by down-regulation of Mcl-1 via a proteasomal-dependent pathway. *Faseb J* **27**, 1084–94.

Luo, L., Zhang, S., Wang, Y., Rahman, M., Syk, I., Zhang, E., Thorlacius, H. (2014). Proinflammatory role of neutrophil extracellular traps in abdominal sepsis. *Am. J. Physiol. Lung Cell Mol. Physiol* **307**, 586–596.

Ma, A.C. and Kubes, P. (2008). Platelets, neutrophils, and neutrophil extracellular traps (NETs) in sepsis. *J Thromb Haemost* **6**, 415–20.

Majno, G., Gattuta, M., Thompson, T.E. (1960). Cellular death and necrosis: Chemical, physical and morphologic changes in rat liver. *Virchows Arch. path Anat* **333**, 421–465.

Majno, G. and Joris, I. (1995). Apoptosis, oncosis, and necrosis. An overview of cell death. *The American journal of pathology* **146**, 3–15.

Marivin, A., Berthelet, J., Plenchette, S., Dubrez, L. (2012). The Inhibitor of Apoptosis (IAPs) in Adaptive Response to Cellular Stress. *Cells* **1**, 711–737.

Martin, S.J., Reutelingsperger, C.P., McGahon, A.J., Rader, J.A., van Schie, R.C., LaFace, D.M., Green, D.R. (1995). Early redistribution of plasma membrane phosphatidylserine is a general feature of apoptosis regardless of the initiating stimulus: inhibition by overexpression of Bcl-2 and Abl. *J Exp Med* **182**, 1545–56.

May, J.A., Ratan, H., Glenn, J.R., Lösche, W., Spangenberg, P., Heptinstall, S. (1998). GPIIb-IIIa antagonists cause rapid disaggregation of platelets pre-treated with cytochalasin D. Evidence that the stability of platelet aggregates depends on normal cytoskeletal assembly. *Platelets* **9**, 227–232.

McFall, A., Ulku, A., Lambert, Q.T., Kusa, A., Rogers-Graham, K., Der, C.J. (2001). Oncogenic Ras blocks anoikis by activation of a novel effector pathway independent of phosphatidylinositol 3-kinase. *Mol Cell Biol* **21**, 5488–99.

Medzhitov, R., Janeway, C.A., Jr., 2002. Decoding the patterns of self and nonself by the innate immune system. Science. **296**, 298–300.

Menegazzi, R., Decleva, E., Dri, P. (2012). Killing by neutrophil extracellular traps: fact or folklore? *Blood* **119**, 1214–1216.

Menegazzo, L., Ciciliot, S., Poncina, N., Mazzucato, M., Persano, M., Bonora, B., Albiero, M., Vigili de Kreutzenberg, S., Avogaro, A., Fadini, G.P. (2014). NETosis is induced by high glucose and associated with type 2 diabetes. *Acta Diabetol*.

Menze, M.A., Fortner, G., Nag, S., Hand, S.C. (2010). Mechanisms of apoptosis in Crustacea: What conditions induce versus suppress cell death? *Apoptosis* **15**, 293–312.

Misra, C.K., Das, B.K., Pradhan, J., Pattnaik, P., Sethi, S.N., Mukherjee, S.C. (2004). Changes in lysosomal enzyme activity and protection against Vibrio infection in *Macrobrachium rosenbergii* (De Man) post larvae after bath immunostimulation with β-glucan. *Fish & Shellfish Immunology* **17**, 389–395.

Molthathong, S., Buaklin, A., Senapin, S., Klinbunga, S., Rojtinnakorn, J., Flegel, T.W. (2008a). Up-regulation of ribophorin I after yellow head virus (YHV) challenge in black tiger shrimp *Penaeus monodon*. *Fish Shellfish Immunol* **25**, 40–6.

Molthathong, S., Senapin, S., Klinbunga, S., Puanglarp, N., Rojtinnakorn, J., Flegel, T.W. (2008b). Down-regulation of defender against apoptotic death (DAD1) after yellow head virus (YHV) challenge in black tiger shrimp *Penaeus monodon*. *Fish Shellfish Immunol* **24**, 173–9.

Morris, S.C. (1997). Molecular clocks: Defusing the Cambrian "explosion"? *Current Biology* **7**.

Mpoke, S.S. and Wolfe, J. (1997). Differential staining of apoptotic nuclei in living cells: application to macronuclear elimination in Tetrahymena. *J Histochem Cytochem* **45**, 675–83.

Murray, J., Barbara, J.A., Dunkley, S.A., Lopez, A.F., Van Ostade, X., Condliffe, A.M., Dransfield, I., Haslett, C., Chilvers, E.R. (1997). Regulation of neutrophil apoptosis by tumor necrosis factor-alpha: requirement for TNFR55 and TNFR75 for induction of apoptosis *in vitro*. *Blood* **90**, 2772–83.

Mydlarz, L.D., Holthouse, S.F., Peters, E.C., Harvell, C.D. (2008). Cellular Responses in Sea Fan Corals: Granular Amoebocytes React to Pathogen and Climate Stressors. *PLoS ONE* **3**.

Nagata, S. (2005). DNA degradation in development and programmed cell death. Annu Rev Immunol **23**, 853–75.

Narasaraju, T., Yang, E., Samy, R.P., Ng, H.H., Poh, W.P., Liew, A.A., Phoon, M.C., van Rooijen, N., Chow, V.T. (2011). Excessive neutrophils and neutrophil extracellular traps contribute to acute lung injury of influenza pneumonitis. *Am. J. Pathol* **179**, 199–210.

Neeli, I., Dwivedi, N., Khan, S., Radic, M. (2009). Regulation of extracellular chromatin release from neutrophils. *J Innate Immun* **1**, 194–201.

Neeli, I. and Radic, M. (2012). Knotting the NETs: Analyzing histone modifications in neutrophil extracellular traps. *Arthritis Research & Therapy* **14**, 115.

Neumann, A., Völlger, L., Berends, E.T.M., Molhoek, E.M., Stapels, D.A.C., Midon, M., Friães, A., Pingoud, A., Rooijakkers, S.H.M., Gallo, R.L., Mörgelin, M., Nizet, V., Naim, H.Y., von Köckritz-Blickwede, M. (2014). Novel Role of the Antimicrobial Peptide LL-37 in the Protection of Neutrophil Extracellular Traps against Degradation by Bacterial Nucleases. *J Innate Immun* **6**.

Newcomb-Fernandez, J.K., Zhao, X., Pike, B.R., Wang, K.K., Kampfl, A., Beer, R., DeFord, S.M., Hayes, R.L. (2001). Concurrent assessment of calpain and caspase-3 activation after oxygen-glucose deprivation in primary septo-hippocampal cultures. *J Cereb Blood Flow Metab* **21**, 1281–94.

Nicoletti, I., Migliorati, G., Pagliacci, M.C., Grignani, F., Riccardi, C. (1991). A rapid and simple method for measuring thymocyte apoptosis by propidium iodide staining and flow cytometry. *J Immunol Methods* **139**, 271–9.

Ogawa, Y., Nishioka, A., Kobayashi, T., Kariya, S., Hamasato, S., Saibara, T., Seguchi, H., Yoshida, S. (2001). Radiation-induced apoptosis of human peripheral T cells: Analyses with cDNA expression arrays and mitochondrial membrane potential assay. *International Journal of Molecular Medicine* **7**, 603-7.

Oklu, R., Stone, J.R., Albadawi, H., Watkins, M.T. (2014). Extracellular Traps in Lipid-Rich Lesions of Carotid Atherosclerotic Plaques: Implications for Lipoprotein Retention and Lesion Progression. *Journal of Vascular and Interventional Radiology* **25**, 631–634.

Ottonello, L., Frumento, G., Arduino, N., Bertolotto, M., Dapino, P., Mancini, M., Dallegri, F. (2002). Differential regulation of spontaneous and immune complex-induced neutrophil apoptosis by proinflammatory cytokines. Role of oxidants, Bax and caspase-3. *J Leukoc Biol* **72**, 125–32.

Ovchinnikova, T.V., Balandin, S.V., Aleshina, G.M., Tagaev, A.A., Leonova, Y.F., Krasnodembsky, E.D., Men'shenin, A.V., Kokryakov, V.N. (2006). Aurelin, a novel antimicrobial peptide from jellyfish *Aurelia aurita* with structural features of defensins and channel-blocking toxins. *Biochem. Biophys. Res. Commun* **348**, 514–523.

Oweson, C.A., Baden, S.P., Hernroth, B.E. (2006). Manganese induced apoptosis in haematopoietic cells of *Nephrops norvegicus* (L.). *Aquat Toxicol* **77**, 322–8.

Palic, D., Ostojic, J., Andreasen, C.B., Roth, J.A. (2007a). Fish cast NETs: neutrophil extracellular traps are released from fish neutrophils. *Dev Comp Immunol* **31**, 805–16.

Palic, D., Andreasen, C.B., Ostojic, J., Tell, R.M., Roth, J.A. (2007b). Zebrafish (Danio rerio) whole kidney assays to measure neutrophil extracellular trap release and degranulation of primary granules. *J Immunol Methods* **319**, 87–97.

Pan, D., He, N., Yang, Z., Liu, H., Xu, X. (2005). Differential gene expression profile in hepatopancreas of WSSV-resistant shrimp (*Penaeus japonicus*) by suppression subtractive hybridization. *Dev Comp Immunol* **29**, 103–12.

Papayannopoulos, V. and Zychlinsky, A. (2009). NETs: a new strategy for using old weapons. *Trends Immunol* **30**, 513–21.

Papayannopoulos, V., Metzler, K.D., Hakkim, A., Zychlinsky, A. (2010). Neutrophil elastase and myeloperoxidase regulate the formation of neutrophil extracellular traps. *J Cell Biol* **191**, 677–91.

Papayannopoulos, V., Staab, D., Zychlinsky, A. (2011). Neutrophil Elastase Enhances Sputum Solubilization in Cystic Fibrosis Patients Receiving DNase Therapy. *PLoS ONE* **6**.

Parihar, M.S., Nazarewicz, R.R., Kincaid, E., Bringold, U., Ghafourifar, P. (2008). Association of mitochondrial nitric oxide synthase activity with respiratory chain complex *I. Biochem Biophys Res Commun* **366**, 23–8.

Parish, I.A., Rao, S., Smyth, G.K., Juelich, T., Denyer, G.S., Davey, G.M., Strasser, A., Heath, W.R. (2009). The molecular signature of CD8+ T cells undergoing deletional tolerance. *Blood* **113**, 4575–4585.

Parker, H., Albrett, A.M., Kettle, A.J., Winterbourn, C.C. (2012). Myeloperoxidase associated with neutrophil extracellular traps is active and mediates bacterial killing in the presence of hydrogen peroxide. *J. Leukoc. Biol* **91**, 369–376.

Parker, H. and Winterbourn, C.C. (2013). Reactive oxidants and myeloperoxidase and their involvement in neutrophil extracellular traps. *Front Immunol* **3**.

Pellegrini, M., Belz, G., Bouillet, P., Strasser, A. (2003). Shutdown of an acute T cell immune response to viral infection is mediated by the proapoptotic Bcl-2 homology 3-only protein Bim. *Proceedings of the National Academy of Sciences* **100**, 14175–14180.

Penaloza, C., Lin, L., Lockshin, R.A., Zakeri, Z. (2006). Cell death in development: shaping the embryo. *Histochemistry and Cell Biology* **126**, 149–158.

Perazzolo, L.M. and Barracco, M.A. (1997). The prophenoloxidase activating system of the shrimp *Penaeus paulensis* and associated factors. *Dev Comp Immunol* **21**, 385–95.

Phillipson, M. and Kubes, P. (2011). The neutrophil in vascular inflammation. *Nat. Med* **17**, 1381–1390.

Phongdara, A., Wanna, W., Chotigeat, W. (2006). Molecular cloning and expression of caspase from white shrimp Penaeus merguiensis. *Aquaculture* **252**, 114–120.

Pijanowski, L., Golbach, L., Kolaczkowska, E., Scheer, M., Verburg-van Kemenade, B.M., Chadzinska, M. (2013). Carp neutrophilic granulocytes form extracellular traps via ROS-dependent and independent pathways. *Fish Shellfish Immunol* **34**, 1244–52.

Pilsczek, F.H., Salina, D., Poon, K.K.H., Fahey, C., Yipp, B.G., Sibley, C.D., Robbins, S.M., Green, F.H.Y., Surette, M.G., Sugai, M., Bowden, M.G., Hussain, M., Zhang, K., Kubes, P. (2010). A Novel Mechanism of Rapid Nuclear Neutrophil Extracellular Trap Formation in Response to *Staphylococcus aureus*. *The Journal of Immunology* **185**, 7413–7425.

Pipe, R.K. (1990). Hydrolytic enzymes associated with the granular haemocytes of the marine mussel *Mytilus edulis*. *Histochem. J* **22**, 595–603.

Pipe, R.K., Farley, S.R., Coles, J.A. (1997). The separation and characterisation of haemocytes from the mussel *Mytilus edulis*. *Cell Tissue Res* **289**, 537–545.

Poirier, A.C., Schmitt, P., Rosa, R.D., Vanhove, A.S., Kieffer-Jaquinod, S., Rubio, T.P., Charrière, G.M., Destoumieux-Garzón, D. (2014). Antimicrobial histones and DNA traps in invertebrate immunity: evidences in Crassostrea gigas. *J. Biol. Chem* **289**, 24821-24831.

Polakowska, R.R., Piacentini, M., Bartlett, R., Goldsmith, L.A., Haake, A.R. (1994). Apoptosis in human skin development: morphogenesis, periderm, and stem cells. Dev Dyn **199**, 176–88.

Pryde, J.G., Walker, A., Rossi, A.G., Hannah, S., Haslett, C. (2000). Temperature-dependent arrest of neutrophil apoptosis. Failure of Bax insertion into mitochondria at 15 degrees C prevents the release of cytochrome c. *J Biol Chem* **275**, 33574-84.

Qiu, L., Jiang, S., Huang, J., Wang, W., Zhang, D., Wu, Q., Yang, K. (2008). Molecular cloning and mRNA expression of cathepsin C gene in black tiger shrimp (*Penaeus monodon*). *Comparative Biochemistry and Physiology Part A: Molecular & Integrative Physiology* **150**, 320–325.

Rada, B., Jendrysik, M.A., Pang, L., Hayes, C.P., Yoo, D., Park, J.J., Moskowitz, S.M., Malech, H.L., Leto, T.L. (2013). Pyocyanin-Enhanced Neutrophil Extracellular Trap Formation Requires the NADPH Oxidase. *PLoS ONE* **8**.

Raff, M.C. (1992). Social controls on cell survival and cell death. *Nature* **356**, 397–400.

Rajesh, S., Kiruthika, J., Ponniah, A.G., Shekhar, M.S. (2012). Identification, cloning and expression analysis of Catechol-O-methyltransferase (COMT) gene from shrimp, *Penaeus monodon* and its relevance to salinity stress. *Fish Shellfish Immunol* **32**, 693–9.

Ratcliffe, N.A. and Rowley, A.F. (1979). Role of hemocytes in defense against biological agents. Insect haemocytes, development, forms, functions and techniques. Cambridge University Press, New York, NY, 331-414.

Rattanachai, A., Hirono, I., Ohira, T., Takahashi, Y., Aoki, T. (2004). Cloning of kuruma prawn *Marsupenaeus japonicus* crustin-like peptide cDNA and analysis of its expression. *Fisheries Science* **70**, 765–771.

Relf, J.M., Chisholm, J.R.S., Kemp, G.D., Smith, V.J. (1999). Purification and characterization of a cysteine-rich 11.5-kDa antibacterial protein from the granular haemocytes of the shore crab, *Carcinus maenas*. *European Journal of Biochemistry* **264**, 350–357.

Remijsen, Q., Kuijpers, T.W., Wirawan, E., Lippens, S., Vandenabeele, P., Vanden Berghe, T. (2011). Dying for a cause: NETosis, mechanisms behind an antimicrobial cell death modality. *Cell Death Differ* **18**, 581–8.

Renehan, A.G., Booth, C., Potten, C.S. (2001). What is apoptosis, and why is it important? *Bmj* **322**, 1536–8.

Rengpipat, S., Rukpratanporn, S., Piyatiratitivorakul, S., Menasaveta, P. (2000). Immunity enhancement in black tiger shrimp (*Penaeus monodon*) by a probiont bacterium (*Bacillus* S11). *Aquaculture* **191**, 271–288.

Renshaw, S.A., Timmons, S.J., Eaton, V., Usher, L.R., Akil, M., Bingle, C.D., Whyte, M.K. (2000). Inflammatory neutrophils retain susceptibility to apoptosis mediated via the Fas death receptor. *J Leukoc Biol* **67**, 662–8.

Reynolds, E.S. (1963). The use of lead citrate at high pH as an electron-opaque stain in electron microscopy. *J Cell Biol* **17**, 208–12.

Riccardi, C. and Nicoletti, I. (2006). Analysis of apoptosis by propidium iodide staining and flow cytometry. *Nat Protoc* **1**, 1458–61.

Robertson, A.J., Croce, J., Carbonneau, S., Voronina, E., Miranda, E., McClay, D.R., Coffman, J.A. (2006). The genomic underpinnings of apoptosis in *Strongylocentrotus purpuratus*. *Dev Biol* **300**, 321–34.

Rock, K.L. and Kono, H. (2008). The inflammatory response to cell death. *Annual review of pathology* **3**, 99–126.

Rodriguez, J., Boulo, V., Mialhe, E., Bachere, E. (1995). Characterisation of shrimp haemocytes and plasma components by monoclonal antibodies. *J Cell Sci* **108**, 1043–50.

Romero, A., Estevez-Calvar, N., Dios, S., Figueras, A., Novoa, B. (2011). New insights into the apoptotic process in mollusks: characterization of caspase genes in *Mytilus galloprovincialis*. *PLoS One* **6**.

Rossi, A.G., Sawatzky, D.A., Walker, A., Ward, C., Sheldrake, T.A., Riley, N.A., Caldicott, A., Martinez-Losa, M., Walker, T.R., Duffin, R., Gray, M., Crescenzi, E., Martin, M.C., Brady, H.J., Savill, J.S., Dransfield, I., Haslett, C. (2006). Cyclin-dependent kinase inhibitors enhance the resolution of inflammation by promoting inflammatory cell apoptosis. *Nat Med* **12**, 1056–64.

Roulston, C. and Smith, V.J. (2011). Isolation and in vitro characterisation of prohaemocytes from the spider crab, *Hyas araneus* (L.). *Dev Comp Immunol* **35**, 537–44.

Sahtout, A.H., Hassan, M.D., Shariff, M. (2001). DNA fragmentation, an indicator of apoptosis, in cultured black tiger shrimp Penaeus monodon infected with white spot syndrome virus (WSSV). *Dis Aquat Organ* **44**, 155–9.

Sahul Hameed, A.S., Sarathi, M., Sudhakaran, R., Balasubramanian, G., Syed Musthaq, S. (2006). Quantitative assessment of apoptotic hemocytes in white spot syndrome virus (WSSV)-infected penaeid shrimp, *Penaeus monodon* and *Penaeus indicus*, by flow cytometric analysis. *Aquaculture* **256**, 111–120.

Saitoh, T., Komano, J., Saitoh, Y., Misawa, T., Takahama, M., Kozaki, T., Uehata, T., Iwasaki, H., Omori, H., Yamaoka, S., Yamamoto, N., Akira, S. (2012). Neutrophil extracellular traps mediate a host defense response to human immunodeficiency virus-1. *Cell Host Microbe* **12**, 109–16.

Sakamaki, K. and Satou, Y. (2009). Caspases: evolutionary aspects of their functions in vertebrates. *J Fish Biol*. **74**, 727–53.

Sangsuriya, P., Rojtinnakorn, J., Senapin, S., Flegel, T.W. (2007). Characterization and tissue expression of apoptosis-related ALG-2 interacting protein Alix/AIP1 from the black tiger shrimp Penaeus monodon. *Fish Shellfish Immunol* **23**, 485–92.

Savill, J. and Fadok, V. (2000). Corpse clearance defines the meaning of cell death. *Nature* **407**, 784–8.

Savill, J.S., Wyllie, A.H., Henson, J.E., Walport, M.J., Henson, P.M., Haslett, C. (1989). Macrophage phagocytosis of aging neutrophils in inflammation. Programmed cell death in the neutrophil leads to its recognition by macrophages. *J. Clin. Invest* **83**, 865–875.

Schauer, C., Janko, C., Munoz, L.E., Zhao, Y., Kienhöfer, D., Frey, B., Lell, M., Manger, B., Rech, J., Naschberger, E., Holmdahl, R., Krenn, V., Harrer, T., Jeremic, I., Bilyy, R., Schett, G., Hoffmann, M., Herrmann, M. (2014). Aggregated neutrophil extracellular traps limit inflammation by degrading cytokines and chemokines. *Nat. Med* **20**, 511-517.

Schmidt, O., Söderhäll, K., Theopold, U., Faye, I. (2010). Role of adhesion in arthropod immune recognition. *Annu. Rev. Entomol* **55**, 485–504.

Schnapp, D., Kemp, G.D., Smith, V.J. (1996). Purification and characterization of a proline-rich antibacterial peptide, with sequence similarity to bactenecin-7, from the haemocytes of the shore crab, *Carcinus maenas*. *Eur J Biochem* **240**, 532–9.

Schulze-Bergkamen, H. and Krammer, P.H. (2004). Apoptosis in cancer--implications for therapy. *Semin Oncol* **31**, 90–119.

Seong, S.Y. and Matzinger, P. (2004). Hydrophobicity: an ancient damage-associated molecular pattern that initiates innate immune responses. *Nat Rev Immunol* **4**, 469–478.

Sequeira, T.V., Lobo-Da-Cunha, M., Baldaia, A., Arala-Chaves, L.M. (1995). Flow Cytometric Analysis of Molt-Related Changes in Hemocyte Type in Male and Female *Penaeus japonicus*. *Biol Bull* **189**.

Shaham, S. (1998). Identification of multiple *Caenorhabditis elegans* caspases and their potential roles in proteolytic cascades. *J Biol Chem* **273**, 35109–17.

Shi, J., Shi, Y., Waehrens, L.N., Rasmussen, J.T., Heegaard, C.W., Gilbert, G.E. (2006). Lactadherin detects early phosphatidylserine exposure on immortalized leukemia cells undergoing programmed cell death. *Cytometry A* **69**, 1193–201.

Shu, D.G., Luo, H.L., Conway Morris, S., Zhang, X.L., Hu, S.X., Chen, L., Han, J., Zhu, M., Li, Y., Chen, L.Z. (1999). Lower Cambrian vertebrates from south China. *Nature* **402**, 42–46.

Silva, L.M.R., Muñoz Caro, T., Gerstberger, R., Vila-Viçosa, M.J.M., Cortes, H.C.E., Hermosilla, C., Taubert, A. (2014). The apicomplexan parasite *Eimeria arloingi* induces caprine neutrophil extracellular traps. *Parasitol. Res* **113**, 2797-2807.

Singh, N. (2007). Apoptosis in health and disease and modulation of apoptosis for therapy: An overview. *Indian journal of clinical biochemistry* **22**, 6–16.

Smith, V.J. and Ratcliffe, N.A. (1978). Host Defence Reactions of the Shore Crab, *Carcinus Maenas* (L.), in Vitro. *Journal of the Marine Biological Association of the United Kingdom* **58**, 367–379.

Smith, V.J. and Ratcliffe, N.A. (1980a). Cellular defense reactions of the shore crab, *Carcinus maenas*: in vivo hemocytic and histopathological responses to injected bacteria. *Journal of Invertebrate Pathology* **35**, 65–74.

Smith, V.J. and Ratcliffe, N.A. (1980b). Host Defence Reactions of the Shore Crab, *Carcinus Maenas* (L.): Clearance and Distribution of Injected Test Particles. *Journal of the Marine Biological Association of the United Kingdom* **60**, 89–102.

Smith, V.J. and Soderhall, K. (1983a). Induction of degranulation and lysis of haemocytes in the freshwater crayfish, *Astacus astacus* by components of the prophenoloxidase activating system *in vitro*. *Cell Tissue Res* **233**, 295–303.

Smith, V.J. and Söderhäll, K. (1983b). β-l,3 glucan activation of crustacean haemocytes *in vitro* and *in vivo*. *Biol Bull* **164**, 299–314.

Smith, V.J., Söderhäll, K., Hamilton, M. (1984). β-1,3 glucan induced cellular defence reactions in the shore crab, Carcinus *maenas*. *Comparative Biochemistry and Physiology Part A: Physiology* **77**, 635–639.

Smith, V.J. and Soderhall, K. (1991). A comparison of phenoloxidase activity in the blood of marine invertebrates. *Dev Comp Immunol* **15**, 251–61.

Smith, V.J. and Chisholm, J.R.S. (1992). Non-cellular immunity in crustaceans. *Fish & Shellfish Immunology* **2**, 1–31.

Smith, V.J. and Chisholm, J.R. (2001). Antimicrobial proteins in crustaceans. *Adv Exp Med Biol* **484**, 95–112.

Smith, V.J., Brown, J.H., Hauton, C. (2003). Immunostimulation in crustaceans: does it really protect against infection? *Fish & Shellfish Immunology* **15**, 71–90.

Smith, V.J., Fernandes, J.M., Kemp, G.D., Hauton, C. (2008). Crustins: enigmatic WAP domain-containing antibacterial proteins from crustaceans. *Dev Comp Immunol* **32**, 758–72.

Smith, V.J., Roulston, C. & Dyrynda, E. A. (2010). The Shrimp Book: The Shrimp Immune System, 1st ed. Nottingham University Press, Nottingham UK.

Smith, V.J. (2010). Immunology of Invertebrates: Cellular, in Encyclopaedia of Life Sciences (ELS) On-line Library. John Wiley & Sons, Ltd.

Söderhäll, I., Bangyeekhun, E., Mayo, S., Söderhäll, K. (2003). Hemocyte production and maturation in an invertebrate animal; proliferation and gene expression in hematopoietic stem cells *of Pacifastacus leniusculus*. *Developmental & Comparative Immunology* **27**, 661–672.

Söderhäll, K. (1982). Prophenoloxidase activating system and melanization - a recognition mechanism of arthropods? A review. *Dev. Comp. Immunol* **6**, 601–611.

Soderhall, K., Cerenius, L., Johansson, M.W. (1994). The prophenoloxidase activating system and its role in invertebrate defence. *Ann N Y Acad Sci* **712**, 155–61.

Soderhall, K. and Smith, V.J. (1983). Separation of the haemocyte populations of Carcinus maenas and other marine decapods, and prophenoloxidase distribution. *Dev Comp Immunol* **7**, 229–39.

Söderhäll, K., Smith, V., Johansson, M. (1986). Exocytosis and uptake of bacteria by isolated haemocyte populations of two crustaceans: evidence for cellular co-operation in the defence reactions of arthropods. *Cell Tissue Res* **245**, 43–49.

Sperandio, S., de Belle, I., Bredesen, D.E. (2000). An alternative, nonapoptotic form of programmed cell death. *Proceedings of the National Academy of Sciences* **97**, 14376–14381.

Sperstad, S.V., Haug, T., Paulsen, V., Rode, T.M., Strandskog, G., Solem, S.T., Styrvold, O.B., Stensvag, K. (2009a). Characterization of crustins from the hemocytes of the spider crab, *Hyas araneus*, and the red king crab, *Paralithodes camtschaticus*. *Dev Comp Immunol* **33**, 583–91.

Sperstad, S.V., Haug, T., Vasskog, T., Stensvag, K. (2009b). Hyastatin, a glycine-rich multi-domain antimicrobial peptide isolated from the spider crab (*Hyas araneus*) hemocytes. *Mol Immunol* **46**, 2604–12.

Sperstad, S.V., Smith, V.J., Stensvag, K. (2010). Expression of antimicrobial peptides from *Hyas araneus* haemocytes following bacterial challenge *in vitro*. Dev Comp *Immunol* **34**, 618–24.

Srinivasula, S.M and Ashwell, J.D. (2008). IAPs: what's in a name? *Mol Cell* **30**, 123–35.

Sritunyalucksana, K., Wongsuebsantati, K., Johansson, M.W., Soderhall, K. (2001). Peroxinectin, a cell adhesive protein associated with the proPO system from the black tiger shrimp, *Penaeus monodon*. *Dev Comp Immunol* **25**, 353–63.

Steinberg, B.E. and Grinstein, S. (2007). Unconventional roles of the NADPH oxidase: signalling, ion homeostasis, and cell death. *Sci STKE*.

Stensvag, K., Haug, T., Sperstad, S.V., Rekdal, O., Indrevoll, B., Styrvold, O.B. (2008). Arasin 1, a proline-arginine-rich antimicrobial peptide isolated from the spider crab, *Hyas araneus*. *Dev Comp Immunol* **32**, 275–85.

Stern, M., Meagher, L., Savill, J., Haslett, C. (1992). Apoptosis in human eosinophils. Programmed cell death in the eosinophil leads to phagocytosis by macrophages and is modulated by IL-5. *J Immunol* **148**, 3543–9.

Sung, H. H. and Sun, R. (1999). Intrahaemocytic activity of lysosomal enzymes in *Penaeus monodon* and *Macrobrachium rosenbergii*. *Fish Shellfish Immunol* **9**, 505-508.

Supungul, P., Klinbunga, S., Pichyangkura, R., Hirono, I., Aoki, T., Tassanakajon, A. (2004). Antimicrobial peptides discovered in the black tiger shrimp *Penaeus monodon* using the EST approach. *Dis Aquat Organ* **61**, 123–35.

Tait, J. and Gunn, J.D. (1918). The Blood of *Astacus Fluviatilis*: A Study in Crustacean Blood, with Special Reference to Coagulation and Phagocytosis. *Exp Physiol* **12**, 35–80.

Tait, S.W. and Green, D.R. (2010). Mitochondria and cell death: outer membrane permeabilization and beyond. *Nat Rev Mol Cell Biol* **11**, 621–32.

Takanaski, S., Nonaka, R., Xing, Z., O'Byrne, P., Dolovich, J., Jordana, M. (1994). Interleukin 10 inhibits lipopolysaccharide-induced survival and cytokine production by human peripheral blood eosinophils. *J Exp Med* **180**, 711–5.

Takei, H., Araki, A., Watanabe, H., Ichinose, A., Sendo, F. (1996). Rapid killing of human neutrophils by the potent activator phorbol 12-myristate 13-acetate (PMA) accompanied by changes different from typical apoptosis or necrosis. *J. Leukoc. Biol* **59**, 229–240.

Terahara, K., Takahashi, K.G., Mori, K. (2005). Pacific oyster hemocytes undergo apoptosis following cell-adhesion mediated by integrin-like molecules. *Comp Biochem Physiol A Mol Integr Physiol* **141**, 215–22.

Terajima, D., Shida, K., Takada, N., Kasuya, A., Rokhsar, D., Satoh, N., Satake, M., Wang, H.G. (2003). Identification of candidate genes encoding the core components of the cell death machinery in the *Ciona intestinalis* genome. *Cell Death Differ* **10**, 749–53.

Thammavongsa, V., Missiakas, D.M., Schneewind, O. (2013). *Staphylococcus aureus* Degrades Neutrophil Extracellular Traps to Promote Immune Cell Death. *Science* **342**, 863–866.

Thatte, U. and Dahanukar, S. (1997). Apoptosis: clinical relevance and pharmacological manipulation. *Drugs* **54**, 511–32.

Theopold, U., Schmidt, O., Söderhäll, K., Dushay, M.S. (2004). Coagulation in arthropods: defence, wound closure and healing. *Trends in Immunology* **25**, 289–294.

Thornqvist, P.O., Johansson, M.W., Soderhall, K. (1994). Opsonic activity of cell adhesion proteins and beta-1,3-glucan binding proteins from two crustaceans. *Dev Comp Immunol* **18**, 3–12.

Thornton, R.B., Wiertsema, S.P., Kirkham, L.A.S., Rigby, P.J., Vijayasekaran, S., Coates, H.L., Richmond, P.C. (2013). Neutrophil extracellular traps and bacterial biofilms in middle ear effusion of children with recurrent acute otitis media - a potential treatment target. *PLoS ONE* **8**.

Tidball, J.G., Albrecht, D.E., Lokensgard, B.E., Spencer, M.J. (1995). Apoptosis precedes necrosis of dystrophin-deficient muscle. *J Cell Sci* **108**, 2197–204.

Ueki, S., Melo, R.C.N., Ghiran, I., Spencer, L.A., Dvorak, A.M., Weller, P.F. (2013). Eosinophil extracellular DNA trap cell death mediates lytic release of free secretion-competent eosinophil granules in humans. *Blood* **121**, 2074–2083.

Urban, C.F., Reichard, U., Brinkmann, V., Zychlinsky, A. (2006). Neutrophil extracellular traps capture and kill *Candida albicans* yeast and hyphal forms. *Cell Microbiol* **8**, 668–76.

Urban, C.F., Ermert, D., Schmid, M., Abu-Abed, U., Goosmann, C., Nacken, W., Brinkmann, V., Jungblut, P.R., Zychlinsky, A. (2009). Neutrophil extracellular traps contain calprotectin, a cytosolic protein complex involved in host defense against *Candida albicans*. *PLoS Pathog* **5**.

Vargas-Albores, F., Gollas-Galván, T., Hernández-López, J. (2005). Functional characterization of *Farfantepenaeus californiensis*, *Litopenaeus vannamei* and *L. stylirostris* haemocyte separated using density gradient centrifugation. *Aquaculture Research* **36**, 352–360.

Vaux, D.L., Cory, S., Adams, J.M. (1988). Bcl-2 gene promotes haemopoietic cell survival and cooperates with c-myc to immortalize pre-B cells. *Nature* **335**, 440–2.

Venet, F., Pachot, A., Debard, A.L., Bohe, J., Bienvenu, J., Lepape, A., Powell, W.S., Monneret, G. (2006). Human CD4+CD25+ regulatory T lymphocytes inhibit lipopolysaccharide-induced monocyte survival through a Fas/Fas ligand-dependent mechanism. *J Immunol* **177**, 6540–7.

Vermes, I., Haanen, C., Steffens-Nakken, H., Reutelingsperger, C. (1995). A novel assay for apoptosis. Flow cytometric detection of phosphatidylserine expression on early apoptotic cells using fluorescein labelled Annexin V. *J Immunol Methods* **184**, 39–51.

Villanueva, E., Yalavarthi, S., Berthier, C.C., Hodgin, J.B., Khandpur, R., Lin, A.M., Rubin, C.J., Zhao, W., Olsen, S.H., Klinker, M., Shealy, D., Denny, M.F., Plumas, J., Chaperot, L., Kretzler, M., Bruce, A.T., Kaplan, M.J. (2011). Netting neutrophils induce endothelial damage, infiltrate tissues, and expose immunostimulatory molecules in systemic lupus erythematosus. *J Immunol* **187**, 538–52.

Vogt C. (1842). Untersuchungen uber die Entwicklungsgeschichte der Geburtshelerkroete. *(Alytes obstetricians),* Solothurn: Jent und Gassman, pp 130.

Von Köckritz-Blickwede, M., Goldmann, O., Thulin, P., Heinemann, K., Norrby-Teglund, A., Rohde, M., Medina, E. (2008). Phagocytosis-independent antimicrobial activity of mast cells by means of extracellular trap formation. *Blood* **111**, 3070–80.

Von Köckritz-Blickwede, M., Chow, O.A., Nizet, V. (2009). Fetal calf serum contains heat-stable nucleases that degrade neutrophil extracellular traps. *Blood* **114**, 5245–5246.

Von Köckritz-Blickwede, M. and Nizet, V. (2009). Innate immunity turned inside-out: antimicrobial defense by phagocyte extracellular traps. *J Mol Med* **87**, 775–783.

Wachter, B.D., Sartoris, F.J., Pörtner, H.O. (1997). The anaerobic endproduct lactate has a behavioural and metabolic signalling function in the shore crab. *J. Exp. Biol* **200**, 1015–1024.

Waehrens, L.N., Heegaard, C.W., Gilbert, G.E., Rasmussen, J.T. (2009). Bovine lactadherin as a calcium-independent imaging agent of phosphatidylserine expressed on the surface of apoptotic HeLa cells. *J Histochem Cytochem* **57**, 907–14.

Walker, N.I., Harmon, B.V., Gobé, G.C., Kerr, J.F. (1988). Patterns of cell death. *Methods and achievements in experimental pathology* **13**, 18–54.

Walton, A. and Smith, V.J. (1999). Primary culture of the hyaline haemocytes from marine decapods. *Fish & Shellfish Immunology* **9**, 181–194.

Wang, Z., Hu, L., Yi, G., Xu, H., Qi, Y., Yao, L. (2004). ORF390 of white spot syndrome virus genome is identified as a novel anti-apoptosis gene. *Biochemical and Biophysical Research Communications* **325**, 899–907.

Wang, L., Zhi, B., Wu, W., Zhang, X. (2008). Requirement for shrimp caspase in apoptosis against virus infection. *Developmental & Comparative Immunology* **32**, 706–715.

Wang, W. and Zhang, X. (2008). Comparison of antiviral efficiency of immune responses in shrimp. *Fish Shellfish Immunol* **25**, 522–7.

Wang, Y., Dawson, V.L., Dawson, T.M. (2009). Poly(ADP-ribose) signals to mitochondrial AIF: a key event in parthanatos. *Exp Neurol* **218**, 193–202.

Wang, Z., Wilhelmsson, C., Hyrsl, P., Loof, T.G., Dobes, P., Klupp, M., Loseva, O., Morgelin, M., Ikle, J., Cripps, R.M., Herwald, H., Theopold, U. (2010). Pathogen entrapment by transglutaminase - a conserved early innate immune mechanism. *PLoS Pathog* **6**.

Wang, Y., Li, J., Liu, P., Li, J., Zhang, Z., Chang, Z., He, Y., Liu, D. (2011a). The responsive expression of a caspase gene in Chinese shrimp *Fenneropenaeus chinensis* against pH stress. *Aquaculture Research* **42**, 1214–1230.

Wang, J.H., Zhou, Y.J., Bai, X., He, P. (2011b). Jolkinolide B from *Euphorbia fischeriana Steud* induces apoptosis in human leukemic U937 cells through PI3K/Akt and XIAP pathways. *Mol Cells* **32**, 451–7.

Ward, C., Chilvers, E.R., Lawson, M.F., Pryde, J.G., Fujihara, S., Farrow, S.N., Haslett, C., Rossi, A.G. (1999). NF-kappaB activation is a critical regulator of human granulocyte apoptosis *in vitro*. *J Biol Chem* **274**, 4309–18.

Ward, C., Murray, J., Clugston, A., Dransfield, I., Haslett, C., Rossi, A.G. (2005). Interleukin-10 inhibits lipopolysaccharide-induced survival and extracellular signal-regulated kinase activation in human neutrophils. *Eur J Immunol* **35**, 2728–37.

Wardini, A.B., Guimaraes-Costa, A.B., Nascimento, M.T., Nadaes, N.R., Danelli, M.G., Mazur, C., Benjamim, C.F., Saraiva, E.M., Pinto-da-Silva, L.H. (2010). Characterization of neutrophil extracellular traps in cats naturally infected with feline leukemia virus. *J Gen Virol* **91**, 259–64.

Wardle, D.J., Burgon, J., Sabroe, I., Bingle, C.D., Whyte, M.K., Renshaw, S.A. (2011). Effective caspase inhibition blocks neutrophil apoptosis and reveals Mcl-1 as both a regulator and a target of neutrophil caspase activation. *PLoS One* **6**.

Wartha, F., Beiter, K., Albiger, B., Fernebro, J., Zychlinsky, A., Normark, S., Henriques-Normark, B. (2007). Capsule and D-alanylated lipoteichoic acids protect Streptococcus pneumoniae against neutrophil extracellular traps. *Cell. Microbiol* **9**, 1162–1171.

Wartha, F. and Henriques-Normark, B. (2008). ETosis: a novel cell death pathway. *Sci Signal* **1**.

Watthanasurorot, A., Soderhall, K., Jiravanichpaisal, P., Soderhall, I. (2011). An ancient cytokine, astakine, mediates circadian regulation of invertebrate hematopoiesis. *Cell Mol Life Sci* **68**, 315–23.

Webster, S.J., Daigneault, M., Bewley, M.A., Preston, J.A., Marriott, H.M., Walmsley, S.R., Read, R.C., Whyte, M.K., Dockrell, D.H. (2010). Distinct cell death programs in monocytes regulate innate responses following challenge with common causes of invasive bacterial disease. *J Immunol* **185**, 2968–79.

Weill, M., Philips, A., Chourrout, D., Fort, P. (2005). The caspase family in urochordates: distinct evolutionary fates in ascidians and larvaceans. *Biol Cell* **97**, 857–66.

Wen, F., White, G.J., VanEtten, H.D., Xiong, Z., Hawes, M.C. (2009). Extracellular DNA is required for root tip resistance to fungal infection. *Plant Physiol* **151**, 820–9.

White, K. N. and Ratcliffe, N. A. (1982). The segregation and elimination of radio- and fluorescent-labelled marine bacteria from the haemolymph of the shore crab, *Carcinus maenas*. *J. mar. biol. Ass. UK* **62**, 819–833.

White, K.N., Ratcliffe, N.A., Rossa, M. (1985). The Antibacterial Activity of Haemocyte Clumps in the Gills of the Shore Crab, *Carcinus Maenas*. *Journal of the Marine Biological Association of the United Kingdom* **65**, 857–870.

Wiens, M., Krasko, A., Perovic, S., Muller, W.E. (2003). Caspase-mediated apoptosis in sponges: cloning and function of the phylogenetic oldest apoptotic proteases from Metazoa. *Biochim Biophys Acta* **1593**, 179–89.

Wind, S., Beuerlein, K., Eucker, T., Muller, H., Scheurer, P., Armitage, M., Ho, H., Schmidt, H., Wingler, K. (2010). Comparative pharmacology of chemically distinct NADPH oxidase inhibitors. *Br J Pharmacol* **161**, 885–898.

Wongprasert, K., Sangsuriya, P., Phongdara, A., Senapin, S. (2007). Cloning and characterization of a caspase gene from black tiger shrimp (*Penaeus monodon*)-infected with white spot syndrome virus (WSSV). *Journal of Biotechnology* **131**, 9–19.

Wootton, E.C., Dyrynda, E.A., Pipe, R.K., Ratcliffe, N.A. (2003). Comparisons of PAH-induced immunomodulation in three bivalve molluscs. *Aquat Toxicol* **65**, 13–25.

Wootton, E.C., Dyrynda, E.A., Ratcliffe, N.A. (2006). Interaction between non-specific electrostatic forces and humoral factors in haemocyte attachment and encapsulation in the edible cockle, *Cerastoderma edule*. *J Exp Biol* **209**, 1326–1335.

Wu, X.G., Xiong, H.T., Wang, Y.Z., Du, H.H. (2012). Evidence for cell apoptosis suppressing white spot syndrome virus replication in *Procambarus clarkii* at high temperature. *Dis Aquat Organ* **102**, 13–21.

Wyllie, A.H. (1980). Glucocorticoid-induced thymocyte apoptosis is associated with endogenous endonuclease activation. *Nature* **284**, 555–6.

Wyllie, A.H. (1987). Apoptosis: Cell death in tissue regulation. *The Journal of Pathology* **153**, 313–316.

Xian, J.A., Miao, Y.T., Li, B., Guo, H., Wang, A.L. (2013). Apoptosis of tiger shrimp (*Penaeus monodon*) haemocytes induced by *Escherichia coli* lipopolysaccharide. *Comp Biochem Physiol A Mol Integr Physiol* **164**, 301–6.

Xian, J.A., Wang, A.L., Hao, X.M., Miao, Y.T., Li, B., Ye, C.X., Liao, S.A. (2012). *In vitro* toxicity of nitrite on haemocytes of the tiger shrimp, *Penaeus monodon*, using flow cytometric analysis. *Comp Biochem Physiol C Toxicol Pharmacol* **156**, 75–9.

Xian, J.A., Wang, A.L., Tian, J.X., Huang, J.W., Ye, C.X., Wang, W.N., Sun, R.Y. (2009). Morphologic, physiological and immunological changes of haemocytes from *Litopenaeus vannamei* treated by lipopolysaccharide. *Aquaculture* **298**, 139–145.

Xian, J.A., Wang, A.L., Ye, C.X., Chen, X.D., Wang, W.N. (2010). Phagocytic activity, respiratory burst, cytoplasmic free-Ca2+ concentration and apoptotic cell ratio of haemocytes from the black tiger shrimp, *Penaeus monodon* under acute copper stress. *Comparative Biochemistry and Physiology Part C: Toxicology & Pharmacology* **152**, 182–188.

Shi, X.Z., Li, X.C.,Wang, S., Zhao, X.F., Wang, J.X. (2010). Transcriptome analysis of hemocytes and hepatopancreas in red swamp crayfish, *Procambarus clarkii*, challenged with white spot syndrome virus. *Invertebrate Survival Journal* **7**, 119-131.

Young, R.L., Malcolm, K.C., Kret, J.E., Caceres, S.M., Poch, K.R., Nichols, D.P., Taylor-Cousar, J.L., Saavedra, M.T., Randell, S.H., Vasil, M.L., Burns, J.L., Moskowitz, S.M., Nick, J.A. (2011). Neutrophil extracellular trap (NET)-mediated killing of *Pseudomonas aeruginosa*: evidence of acquired resistance within the CF airway, independent of CFTR. *PLoS ONE* **6**.

Yousefi, S., Gold, J.A., Andina, N., Lee, J.J., Kelly, A.M., Kozlowski, E., Schmid, I., Straumann, A., Reichenbach, J., Gleich, G.J., Simon, H.U. (2008). Catapult-like release of mitochondrial DNA by eosinophils contributes to antibacterial defense. *Nat Med* **14**, 949–53.

Yousefi, S., Mihalache, C., Kozlowski, E., Schmid, I., Simon, H.U. (2009). Viable neutrophils release mitochondrial DNA to form neutrophil extracellular traps. *Cell Death Differ* **16**, 1438–44.

Yu, Y. and Su, K. (2013). Neutrophil Extracellular Traps and Systemic Lupus Erythematosus. *J Clin Cell Immunol* **4**.

Zali, H., Rezaei-Tavirani, M., Kariminia, A., Yousefi, R., Shokrgozar, M.A. (2008). Evaluation of growth inhibitory and apoptosis inducing activity of human calprotectin on the human gastric cell line (AGS). *Iran Biomed J* **12**, 7–14.

Zasloff, M. (1992). Antibiotic peptides as mediators of innate immunity. *Curr Opin Immunol* **4**, 3–7.

Zawrotniak, M. and Rapala-Kozik, M. (2013). Neutrophil extracellular traps (NETs) - formation and implications. *Acta Biochim. Pol* **60**, 277–284.

Zhang, J., Li, F., Wang, Z., Xiang, J. (2007). Cloning and recombinant expression of a crustin-like gene from Chinese shrimp, *Fenneropenaeus chinensis*. *J Biotechnol* **127**, 605–14.

Zhang, J.S., Li, D.M., Ma, Y., He, N., Gu, Q., Wang, F.S., Jiang, S.Q., Chen, B.Q., Liu, J.R. (2013). gamma-Tocotrienol induces paraptosis-like cell death in human colon carcinoma SW620 cells. *PLoS One* **8**.

Ziegler, U. and Groscurth, P. (2004). Morphological features of cell death. *News Physiol Sci* **19**, 124–8.

Zong, W.X. and Thompson, C.B. (2006). Necrotic death as a cell fate. *Genes Dev* **20**, 1–15.